UNIVERSIDAD COMPLUTENSE DE MADRID

FACULTAD DE CIENCIAS FÍSICAS
Departamento de Física de la Tierra, Astronomía y Astrofísica I

TESIS DOCTORAL

Non-stationary ENSO influence on European and Mediterranean rainfall: dynamics and modulations

Influencia no estacionaria de ENSO en la precipitación europea y mediterránea : dinámica y modulaciones

MEMORIA PARA OPTAR AL GRADO DE DOCTOR

PRESENTADA POR

Jorge López Parages

Directora

Belén Rodríguez de Fonseca

Madrid, 2016

UNIVERSIDAD COMPLUTENSE DE MADRID

FACULTAD DE CIENCIAS FÍSICAS
DEPARTAMENTO DE FÍSICA DE LA TIERRA, ASTRONOMÍA Y ASTROFÍSICA I

Non-stationary ENSO influence on European and Mediterranean Rainfall: Dynamics and Modulations

Influencia no estacionaria de ENSO en la Precipitación Europea y Mediterránea: Dinámica y Modulaciones

Dirigida por:

Dra. Belén Rodríguez de Fonseca
Profesora Titular UCM

Memoria presentada por:

D. Jorge López Parages
para aspirar al grado de Doctor en Física
Madrid, Septiembre de 2015

Este trabajo ha sido financiado, principalmente, por el Ministerio de Ciencia e Innovación a través del Programa de ayudas FPI asociado al proyecto TRACS (CGL2009-10285). Han contribuido, también, los proyectos MOVAC (200800050084028), MULCLIVAR (CGL2012-38923-C02-01), y PREFACE (603521).

This work was mainly supported by the Spanish Ministry of Science and Innovation through the FPI Program associated with the TRACS project (CGL2009-10285). It has been also partially funded by the projects MOVAC (200800050084028), MULCLIVAR (CGL2012-38923-C02-01), and PREFACE (603521).

Science is the belief in the ignorance of experts

La ciencia es la convicción en la ignorancia de los expertos

Richard Phillips Feynman,

What is Science?, The Physics Teacher, vol.7, issue 6, p. 313-320

A mis padres

Agradecimientos

Resulta muy difícil sintetizar en pocas líneas la cantidad de personas que me han servido de apoyo durante todos estos años. No obstante, haré lo que buenamente pueda.

En primer lugar agradecer a mi directora de Tesis Belén Rodríguez de Fonseca por su guía durante este período. He aprendido mucho a tu lado Belén. A veces la toma de decisiones ha resultado complicada, en gran medida por la diferencia de caracteres que tenemos, pero sin duda pienso que nos complementamos muy bien, ¿no crees? Dejando a un lado tu gran valía como investigadora y tu ayuda en ese aspecto, me gustaría realzar aquí tu valor como persona. Eres una "tía estupenda". Estoy bastante seguro de que vamos a trabajar mucho juntos en el futuro, pero de lo que estoy convencido (y deseo) es de que seguiremos siendo buenos amigos.

También me gustaría dar las gracias a las personas del Departamento de Física de la Tierra, Astronomía y Astrofísica I (Geofísica y Meteorología) por tratarme tan bien todo este tiempo. Sólo tengo buenas palabras para todas ellas. Me gustaría, no obstante, resaltar especialmente a algunas.

Gracias a Salva y Lucía por ayudarnos de manera silenciosa a que nuestro día a día sea más fácil.

Gracias a Carlos Yagüe y Encarna Serrano. Tuve la suerte de ser alumno vuestro durante la carrera, y estos años he tenido aún más suerte al teneros como compañeros. Carlos, creo que si no fuera por ti aún andaría peleándome para que me dieran el título de máster. Gracias por estar siempre que se te necesita.

Gracias a Ana Negredo y Marisa Osete, dos grandes luchadoras. Gracias Ana por tu simpatía y alegría desbordantes. Puede que no te des cuentas pero tienes la capacidad de sacar una sonrisa a alguien incluso en los días más difíciles. Muchas gracias. Para mí, por encima de una compañera, eres una amiga.

Muchísimas gracias a las y los “veteranos” TROPEROS Irene, Javi G., Teresa, y Elsa, y no TROPEROS Álvaro, Blanca, Javi P., y Juan, que me acogieron estupendamente al llegar al departamento y siguen, hoy en día, dándome buenos consejos. Mil gracias. En especial a Tere y Elsa, con las que he podido compartir más tiempo. Es un gusto trabajar con vosotras. Sois encantadoras. También quiero agradecer a Luis Dinis y Luis Durán, que aunque no oficialmente, he sentido como compañeros durante este tiempo. Muchas gracias también a los dos.

A los no tan "veteranos” (aunque cada vez más) muchísimas gracias por todo. Muchas gracias Cahlo, Coumba, Ibrahima, Iñigo, Javi B., Jesús, Julián, Mariano, Marta A., Marta M., y Roberto. No podría imaginar mejores personas con las que disfrutar esta experiencia. Aunque espero mantener el contacto con todas y todos, os voy a echar seguro muchísimo de menos. Y también muchas gracias a los más nuevos. Gracias Ade, Antonio, Jon y Cristina por los buenos ratos juntos. Os he cogido mucho cariño en poco tiempo.

No me gustaría dejar de mencionar tampoco a los compañeros y compañeras del departamento de Física de la Tierra, Astronomía y Astrofísica II (Astrofísica y Física de la Atmósfera), los cuales siempre me han mostrado su cariño. Me acuerdo especialmente de Gabriel y Miguel. Gracias a los dos por vuestra compañía durante mi primera andadura en este mundillo de la investigación.

Also, I would like to thank all the people who helped me during my stays in Toulousse and Melbourne. They were certainly really enriching experiences for me.

Merci beaucoup Laurent Terray de me donner l’occasion de faire mon séjour á Toulousse. Et merci á tous mes collégues de CERFACS pour votre hospitalité.

Thanks a lot Dietmar Dommenget for giving me the opportunity to share those three months with you and your team; and sorry about my shortcomings as football player, which no doubt contributed to our loss in the final of the “Melbourne inter-center Championship 2013”;). Special thanks also to Claudia Frauen for being so patient with me and my doubts. And thanks to the citizens of Melbourne for showing me a striking new concept of barbecue!

También quiero dar las gracias a las personas que me han ayudado en mi labor docente estos años. Gracias Belén, Carlos, Fátima, Maurizio y Gregg. Poder dar clases con vosotras ha sido una gran experiencia para mí. Quiero acordarme también aquí del alumnado que he tenido este tiempo, el cual estoy seguro me ha aportado muchísimas cosas positivas también.

No quiero olvidar el hecho de que estos años en los que he desarrollado esta Tesis han sido años difíciles para la Universidad Pública. Quiero agradecer explícitamente a todas las personas luchadoras que me he ido encontrando por el camino. Gracias por vuestra dedicación y compromiso para cambiar las cosas. Lo que he aprendido de vosotras me ha hecho crecer sin duda como universitario.

Dejo para el final lo más importante en mi vida.

Empezando por los amigos que estuvieron, están, y sé que estarán siempre que se les necesita. Muchísimas gracias Alba, Alejandro, Andrés, David, Guille, Raquel, y Valerie por vuestra amistad todos estos años. Por tantos buenos momentos, y los que vendrán. Hago extensible este agradecimiento también a Edurne y Laurita. Con la primera sólo he podido compartir unas cañas veraniegas, y a la segunda aún no he tenido la suerte de conocerla. Pero seguro que en el futuro compartiremos también buenos momentos juntos.

También dar las gracias a mis muchas amistades "madrileñas". Sobre todo a Rocío, Riki, Fran, Celia, y David R. ¡Cuántos buenos ratos hemos pasado! Mil gracias también a Irene y Luis, a los cuales quiero como hermanos. Aunque suene un poco presuntuoso, creo que hoy soy un poco mejor persona que la que llegó hace años a Madrid desde Málaga y eso, en gran parte, es gracias a todos vosotros.

Quiero también agradecer su apoyo a mi nueva y numerosa familia madrileña con la que he compartido tantos buenos momentos. En especial a Juan y Bea por alimentarme tan bien estos años y, sobre todo, por quererme tanto. Y a Rosi, Ángel, Rodrigo y María por tantísimas muestras de cariño.

No tengo palabras para expresar mi agradecimiento a mi familia de Álcala de Henares con las que compartí mis primeros años fuera de Málaga. Gracias Cohy, Ángel, Marina y Paula. Todas las gracias que os dé son pocas. Gracias Cristina por tener siempre un abrazo y un beso para mí, me lo merezca o no. Aunque no te lo diga las veces que debiera, sabes que te quiero.

Un millón de gracias a mi hermana María, la cual me conoce tan bien que sabe lo que significa para mí sin necesidad de que yo se lo diga. Llevamos separados muchos años pero tú siempre has conseguido que te sienta cerca. Y gracias a Guti, al que también quiero como un hermano.

Mamá, Papá, es imposible daros las gracias como merecéis. Me limitaré a dedicaros esta Tesis por todo lo que habéis hecho por mí. Sois el ejemplo en el que me miro cuando estoy perdido.

Lucía, lo que ponga en estas líneas es una simple anécdota. Tú y yo lo sabemos. Eres la mejor compañera que puedo tener. Gracias por todo. Te quiero.

Me gustaría terminar estos agradecimientos acordándome de mi abuelo Enrique. Sin duda he querido mucho a mis abuelos y abuelas, pero él era especial. Los que hemos tenido la suerte de crecer a tu lado lo sabemos. Ya "crecidito" ¡cuánto hiciste por mí durante los años en Alcalá abuelo! Y después en las innumerables mudanzas de los cursos siguientes. Por eso y por todo lo demás muchas gracias. Nada me haría más feliz que compartir este día contigo. Allá donde estés, espero que nos sientas cerca.

Madrid, Octubre de 2015

Contents

Summary

Introduction

European and Mediterranean climate fluctuations are traditionally associated with atmospheric internal variability, with special attention to the North Atlantic Oscillation (NAO). However, external contributions related to sea surface temperatures (SSTs) can also play a noticeable role. In particular, a significant ENSO signature over the North Atlantic European (NAE) sector has been detected in previous works, even though it has not been unanimously accepted and diverging views exist (Brönnimann (2007) and papers therein). Furthermore, nowadays there is a growing evidence advocating for a non-stationary behavior of the tropospheric ENSO-NAE link, which could contribute for an improvement of the poor skill of current seasonal forecast system over Europe (Van Oldenborgh, 2005). Related to this, in this thesis the teleconnection between ENSO and the leading European-Mediterranean rainfall mode (hereinafter leading EMedR mode), and specifically its possible modulation by the multidecadal variability, is deeply analysed in late winter-early spring, which is considered the most appropriate season to study the ENSO influence over the NAE sector.

Objectives

The main objectives of this thesis are:

1. To detect the leading EMedR variability mode and its relation to ENSO in the observational record.

2. To analyse the physical mechanisms associated with this teleconnection and its evolution in time.

3. To evaluate the internal contribution, associated with the coupled ocean-atmosphere climate system, to the stationarity of the teleconnection.

4. To assess the ENSO-related impact over Europe and the Mediterranean region for distinct ENSO forcings and SST mean states.

Data and Methodology

Gridded data based on surface observations, *reanalysis*, and numerical simulations, are used in this thesis. The former are: ERSSTv3b, HadISST, and Delaware and GPCC precipitation. They are combined with the 20CR reanalysis and unforced long-term preindustrial control simulations from CMIP5 models. Finally, sensitivity experiments with the ACCESS model (AGCM) are performed.

Furthermore, familiar mathematical tools of climate variability are used: EOF, MCA, clustering analysis, regression and composites maps, etc.

Results

The results of this thesis, which are compiled in four scientific publications, are divided into the following parts:

1. **A non-stationary teleconnection between ENSO and the leading EMedR mode in the observational record (López-Parages and Rodríguez-Fonseca, 2012).** Sliding correlations between the principal component for the leading EMedR EOF and El Niño3.4 index have been made with a 21-yr window. In October-November-December (OND), a changing link in phase with the Pacific Decadal Oscillation (PDO) appears, obtaining only significant correlations for extreme phases. In February-March-April (FMA) a non-stationary link evolving in phase with the Atlantic Multidecadal Oscillation (AMO) is found. This AMO-like evolution is consistent with previous results (Mariotti et al., 2002; Sutton and Hodson, 2003; Knippertz et al., 2003). Under negative AMO phases, anomalous positive rainfall over central Europe, and anomalous negative rainfall over northern Scandinavia and the Mediterranean, are detected in relation to anomalous positive SSTs over the tropical Pacific. These periods are denoted as *P*. Under positive AMO phases the aforementioned link is almost the opposite, but noticeably weaker. These periods are denoted as *N*. Therefore, these results point to a changing teleconnection between ENSO and the leading EMedR mode and suggest a modulating role of natural variability.

2. **ENSO-Leading EMedR mode: An internal teleconnection of the ocean-atmosphere coupled system taking place in a non-stationary way (López-Parages et al. (2014), López-Parages et al. (2015a)).** This link is analysed in unforced long-term preindustrial control simulations from 18 different CMIP5 models. A changing teleconnection, consistent with observations, is found. It responds to statistically significant variations in jet streams at multidecadal timescales. These changes seem to be forced by the underlying SST. Consequently, depending on the ocean mean state spatial configuration, ENSO-related Rossby waves are either efficiently or not efficiently propagated from the tropical Pacific to the NAE sector. Then, only for *P* decades, an ENSO signature is detected on the leading EMedR mode. These results confirm that the non-stationary teleconnection can be modulated by the internal variability of the ocean-atmosphere coupled system. Thus, the following hypothesis is posed: *a common ENSO forcing produces distinct responses over the NAE sector depending on the ocean background state.*

3. **ENSO-Leading EMedR mode: A non-stationary link modulated by the SST mean state (López-Parages et al., 2015b).** A set of experiments, in which diverse SST ENSO configurations are prescribed under different SST mean states, is performed. The results demonstrate how the remote impact of both warm and cold ENSO events on the NAE climate could be noticeably different depending on the SST background state. In particular, SST mean state can modulate two distinct mechanisms associated with ENSO events: (1) the thermally driven direct circulation (Walker and Hadley cells) connecting the Atlantic and Pacific basins, and (2) the Rossby wave propagation from the tropical Pacific to the North Atlantic. The former explains an enhanced impact of Central Niñas on the Azores high pressures system during those decades in which a *P*-like SST mean state occurs. The latter explains a reinforced impact of Eastern Niños on EMedR under the same SST background state. This result is consistent with those identified in observations and CMIP5 models, and demonstrates how the teleconnection can be modulated by the multidecadal SST variability.

Conclusions

The main findings from this PhD thesis are:

1. The leading variability mode of the EMedR at interannual timescales, in OND and FMA, is related to El Niño in a non-stationary way in the observational record.

2. The non-stationary teleconnection identified in FMA can be reproduced by internal variability of the ocean-atmosphere coupled system.

3. The absence of stationarity in the aforementioned link can be explained by multidecadal changes of jet streams forced by the ocean.

4. Sensitivity experiments with the ACCESS model demonstrate how the ENSO impact on the leading EMedR mode in FMA can be modulated by the SST mean state variability. This modulation occurs, however, in a distinct way depending on the phase, amplitude, and spatial pattern of the SST ENSO forcing.

5. Extratropical jet streams play a key role for tropical-extratropical teleconnections. According to our results, if the jets are poorly represented by a climate model (strong bias), a common changing impact of ENSO on EMedR in observations and model could be modulated by very different SST multidecadal patterns.

Resumen (Spanish)

Introducción

El clima de Europa y la región mediterránea ha estado tradicionalmente asociado con variabilidad interna de la atmósfera, y especialmente, con el modo Oscilación del Atlántico Norte (NAO[1]). No obstante, existen también contribuciones externas asociadas con la temperatura superficial del mar (SST[2]). En concreto, trabajos anteriores han encontrado una señal significativa de ENSO sobre el sector del Atlántico Norte y Europa (NAE[3]), si bien ésta no ha sido unanimemente aceptada (Brönnimann (2007)). Actualmente existen además indicios crecientes que proponen un comportamiento no estacionario de la relación troposférica ENSO-NAE, lo que podría contribuir a una mejora de la pobre capacidad actual de los sistemas de predicción estacional para Europa (Van Oldenborgh, 2005). En relación con lo anterior, en esta tesis se ha estudiado la teleconexión entre ENSO y el primer modo de variabilidad de la precipitación Europea y Mediterránea (de ahora en adelante EMedR[4]), así como su posible modulación asociada a variabilidad multidecadal. Todo ello ha sido analizado en profundidad para finales de invierno y principios de primavera, estación considerada como la más apropiada para el estudio de la influencia de ENSO en el sector NAE.

Objetivos

Los objetivos principales de esta tesis son:

1. Identificar el primer modo de variabilidad de la EMedR y su relación con ENSO en el período instrumental.

2. Analizar los mecanismos físicos que explican esta teleconexión y su evolución temporal.

[1] Del inglés North Atlantic Oscillation
[2] Del inglés Sea Surface Temperature
[3] Del inglés North Atlantic European
[4] Del inglés European and Mediterranean Rainfall

3. Estimar la contribución interna, asociada con el sistema acoplado océano-atmósfera, en la mencionada teleconexión.

4. Evaluar el impacto ENSO sobre la EMedR para distintos forzamientos ENSO y estados base de la SST.

Datos y Metodología

A lo largo de esta tesis se emplean datos de rejilla basados en observaciones superficiales, *re-análisis*, y simulaciones numéricas. Los primeros son: ERSSTv3b, HadISST, y precipitación de la Universidad de Delaware y del GPCC. Éstos se complementan con datos del 20CR re-análisis y con simulaciones largas de control en condiciones pre-industriales procedentes de modelos del CMIP5. Finalmente se llevan a cabo diferentes experimentos de sensibilidad con el modelo ACCESS (AGCM[5]).

Además, se han utilizado distintas herramientas matemáticas ampliamente empleadas en variabilidad climática: EOF, MCA, análisis cluster, mapas de regresión y compuestos, etc.

Resultados

Los resultados de esta tesis, compilados en 4 artículos científicos, se dividen en las partes siguientes:

1. **Existe, en el registro observacional, una teleconexión no estacionaria entre ENSO y el primer modo de variabilidad de la EMedR (López-Parages and Rodríguez-Fonseca, 2012).** Se llevan a cabo correlaciones, en ventanas móviles de 21 años, entre la componente principal de la primera EOF de la EMedR y el índice Niño3.4. En Octubre-Noviembre-Diciembre (OND) aparece una relación variable en fase con la Oscilación Decadal del Pacifico (PDO[6]), encontrando correlaciones estadísticamente significativas entre la componente principal de la lluvia y el índice Niño3.4 unícamente en fases extremas de la PDO. En Febrero-Marzo-Abril (FMA) se encuentra una relación no estacionaria evolucionando en fase con la Oscilación Multidecadal del Atlántico (AMO[7]). Esta evolución tipo AMO es

[5]Del inglés Atmospheric General Circulation Models
[6]Del inglés Pacific Decadal Oscillation
[7]Del inglés Atlantic Multidecadal Oscillation

consistente con resultados anteriores (Mariotti et al., 2002; Sutton and Hodson, 2003; Knippertz et al., 2003). Así, bajo fases de AMO negativas, lluvia anómala positiva sobre Europa central, y lluvia anómala negativa sobre Escandinavia y la región mediterránea, se relaciona con SST anómalas y positivas sobre el Pacífico tropical. Estos períodos se indican como *P*. Bajo fases de AMO positivas, la relación anterior es casi opuesta pero claramente más débil. Estos períodos se indican como *N*. Estos resultados apuntan a una teleconexión variable entre ENSO y el primer modo de la EMedR, sugiriendo, asimismo, un papel modulador de la variabilidad natural.

2. **ENSO-Primer modo de variabilidad de la EMedR: una teleconexión no estacionaria e interna al sistema océano-atmósfera (López-Parages et al. (2014), (López-Parages et al., 2015a).** La teleconexión antes mencionada es analizada en simulaciones largas de control en condiciones pre-industriales procedentes de 18 modelos diferentes del CMIP5, indentificando una relación variable y consistente con la observacional. Ésta responde a variaciones significativas de los *jet streams* a escalas multidecadales, lo que a su vez parece estar forzado por la SST subyacente. Dependiendo de la configuración del estado base de la SST, las ondas de Rossby relacionadas con ENSO son capaces de alcanzar o no el sector NAE. Sólo para décadas *P* se detecta la señal de ENSO en la EMedR. Estos resultados confirman como la no estacionariedad de la teleconexión puede estar modulada por variabilidad interna del sistema océano-atmósfera. Se plantea la siguiente hipótesis: *un mismo forzamiento Niño produce diferentes respuestas sobre el sector NAE dependiendo del estado base del océano.*

3. **ENSO-Primer modo de variabilidad de la EMedR: una teleconexión no estacionaria modulada por el estado base de la SST (López-Parages et al., 2015b).** Se han llevado a cabo, con el modelo ACCESS, un conjunto de experimentos en los que diversas señales idealizadas de SST de ENSO han sido superpuestas sobre diferentes estados base de SST. Los resultados obtenidos confirman como el impacto remoto de eventos ENSO, positivos y negativos, sobre el clima del NAE puede ser notablemente diferente dependiendo de la variabilidad de baja frecuencia de la SST. En particular, el estado base de la SST parece modular dos tipos de mecanismos asociados a ENSO: (1) la circulación directa de origen térmico (células de Walker y Hadley) que conecta las cuencas del Atlántico y Pacífico, y (2) la propagación de ondas de Rossby desde el Pacífico tropical hasta el Atlántico Norte. El primer mecanismo explica un impacto fortalecido de Niñas *de patrón central* sobre el sistema de altas presiones de Azores durante aquellas décadas en las que existe un estado base de SST *tipo P*. El segundo mecanismo explica un impacto reforzado de Niños *de patrón este* sobre la EMedR bajo el mismo estado base de SST. Estas características son consistentes con la señal variable de ENSO identificada en observaciones y modelos del CMIP5, y demues-

tran como la teleconexión estudiada puede estar modulada por variabilidad multidecadal de la SST.

Conclusiones

Las principales conclusiones de esta tesis son:

1. El primer modo de variabilidad de la EMedR a escalas interanuales, en OND y FMA, está relacionado con El Niño de un modo no estacionario en el registro observacional.

2. La teleconexión no estacionaria identificada en FMA puede ser reproducida por variabilidad interna del sistema acoplado océano-atmósfera.

3. La ausencia de estacionariedad en dicha teleconexión puede ser explicada por cambios multidecadales de los *jet streams* forzados por el océano.

4. Experimentos de sensibilidad realizados con el modelo ACCESS demuestran como el estado base de la SST puede modular la teleconexión anterior. Esta modulación ocurre de manera diferente según la fase, amplitud y patrón espacial de ENSO.

5. Los *jet streams* extratropicales desempeñan un papel crucial para teleconexiones trópico-extratrópico. De acuerdo con nuestro resultados, si un modelo no representa adecuadamente los jets (bias fuerte), un mismo impacto variable de ENSO sobre la EMedR en observaciones y modelo podría estar modulado por patrones multidecadales de SST muy diferentes.

1

Preface

Climate is an always evolving system which must be regarded as a living entity (Peixoto and Oort, 1992). It is composed by many subsystems, including the atmosphere, hydrosphere, cryosphere, and biosphere, having each of them its own characteristics and responses. These components of the climate are connected to each other and so, an integrated approach should be considered to investigate the global climate and its related processes and impacts all over the world. To this aim, physics laws, which are expressed in mathematical terms, are needed.

Climate changes at different times scales, from years to glacial periods, and the study of how it occurs along time is known as *Climate Variability*. To evaluate these changes climate researchers assume a quasi-constant state, which is referred to as *mean state* or *climatology*. The selection of a convenient climatology is a subjective decision, being dependent on the timescales that climate researchers are interested in (yearly, decadal, multidecadal, centennial, millennial...). The fluctuations around the mentioned climatology are known as *anomalies*, and its evolution along the time, with positives and negatives values, define an *anomalous time series*. Those spatial points with a similar anomalous time series are grouped in a set of spatial patterns or *climate variability modes*, which many times represent a set of recurring phenomena. Thus, the huge complexity of the climate system can be simplified in terms of its variability modes, contributing in that way to focus the studies on specific processes and dynamical mechanisms.

According to the IPCC report (Solomon, 2007) Climate variability may be due to natural internal processes within the climate system (*internal variability*), or to variations in natural or anthropogenic external forcing (*external variability*). Nevertheless, similar as for climatology definition, researchers refer to internal or external variability depending on the climate subsystem they are engaged in. Hence, atmosphere researchers and oceanographers consider the ocean and the atmosphere external forcings, respectively. And if the ocean and atmosphere are analysed as a whole, all the processes taking place in both of them contribute to the internal variability of the coupled system.

A striking and interesting characteristic of the climate system is that it harbours *teleconnection*, defined as linkages between weather and climate anomalies that occur over relatively large distances. Regarding the atmosphere, teleconnections are strongly influenced by transient behaviour of the planetary-scale waves, which are primarily forced by the continent-ocean heating contrasts. These atmospheric teleconnections can link regions thousands of kilometers away to each other. They are identified through statistical analysis (most of them based on correlations in space and time) and their associated underlying mechanisms are dynamically explained by changes in the rotational and/or the divergent flow, as it will be thoroughly analyzed in Chapter 4 of the present study.

This thesis is focused on the stationarity of the atmospheric teleconnection between the anomalous Euromediterranean rainfall and El Niño-Southern Oscillation (ENSO). This phenomenon is associated with changes in the sea surface temperatures (SSTs) over the tropical Pacific mainly acting at interannual (year to year) timescales. Hence, the Pacific ocean influence, which leads to adjustments of internal properties of the atmosphere, is considered here as an *external forcing* of the atmosphere. The aforementioned teleconnection poses different and exciting not completely understood issues. Firstly, as the North Atlantic European Climate (NAE) is strongly controlled by the large internal variability of the circulation over the North Atlantic (Quadrelli and Wallace, 2002), a significant impact of El Niño on European climate is still under debate. Secondly, the link between El Niño and the NAE climate seems to had not been stationary in time (Knippertz et al., 2003; Sutton and Hodson, 2003; Gouirand and Moron, 2003; Greatbatch et al., 2004), with changes at multidecadal timescales. Thus, a better understanding of the underlying dynamical mechanisms associated with this changing teleconnection could favor the improvement of the poor skill of current seasonal forecast systems over Europe (Van Oldenborgh and Burgers, 2005). In this way, the role that multidecadal ocean variability could play is a matter of fundamental importance. Furthermore, considering the *extremely likely* human influence in the observed climate change since mid-20th century (Solomon, 2007), to distinguish between natural and anthropogenic causes of the changing El Niño-NAE teleconnection is an additional challenge to be faced.

For all the above reasons, the present thesis pretends to shed some light on the non-stationary behavior of the already not-completely understood ENSO teleconnection with the NAE climate, with special attention to the impact on the European and Mediterranean rainfall.

2

State of the Art

The scientist is not a person who gives the right answers, he's one who asks the right questions.

Científica no es la persona que responde las preguntas acertadas, sino la que hace las preguntas acertadas.

Claude Lévi-Strauss,
Mythologiques

2.1 Some notions about Atmospheric General Circulation

Atmospheric General Circulation, which is primarily driven by the equator-pole net radiation difference, encompasses the complete statistical description of large scale atmospheric motions (AMS Glossary, 2015). Tropical and polar regions receive more and less incoming energy from the Sun than they emit back to the space, respectively (Figure 2.1a). The resultant energetic imbalanced is minimized by different processes (Figure 2.1b).

Through hydrostatic balance, it is possible to demonstrate that the warmth over the tropics leads to the expansion of tropical air columns. A meridional pressure gradient is then established with respect to the polar regions. According to this, George Hadley suggests, in 1735, one giant meridional cell in which air rises near the equator and, by conservation of mass, flows poleward aloft (Figure 2.2a). This simple circulation described by G. Hadley, which approximately agrees with observations over the tropics, does not agree with the circulation at extratropical latitudes, where most of the meridional flow takes the form of some highs and lows, with length scales of the order of 1000 km, usually denoted as large-scale *eddies*. These eddies are responsible for the existence of a secondary thermally indirect circulation in which the angular momentum is transfered poleward. The resultant divergence of eddy momentum fluxes in high latitudes at upper troposphere contributes to the formation of a new weak thermally direct polar circulation cell. Thus,

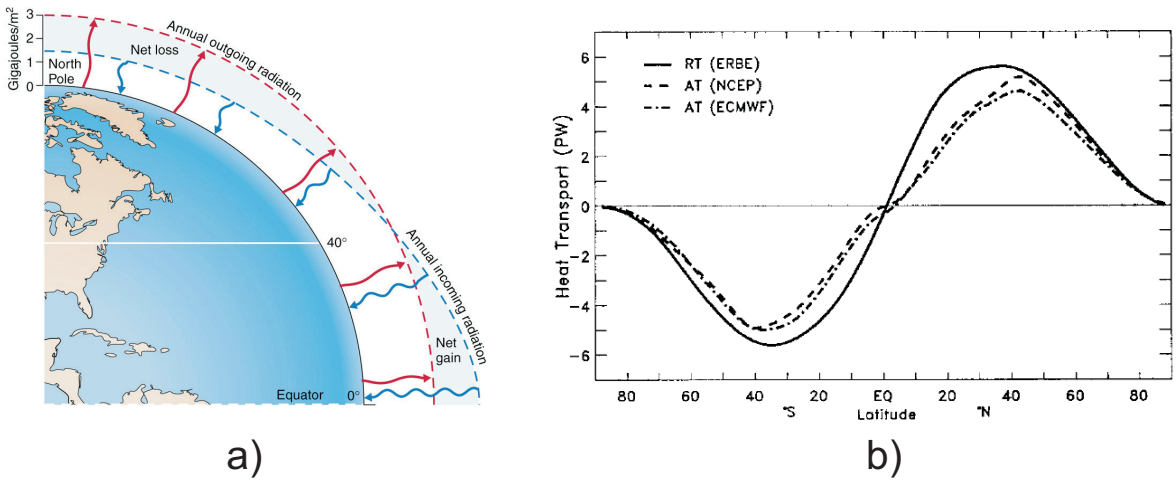

Figure 2.1: a) Schematic figure for the annual incoming (blue) and outcoming (red) radiation at different latitudes. From $http://www.geog.ucsb.edu/$ b) Total heat transport from different sources (TOA radiation RT, NCEP, and ECMWF). A more detailed explanation can be found in Trenberth and Caron (2001).

.

instead of the single-cell configuration proposed by G. Hadley, three annual-mean circulation cells appear in each hemisphere (Figure 2.2b): one in the tropical regions (the so-called *Hadley cell*), another in midlatitudes (the *Ferrel cell*), and finally a third one in the polar regions (the *Polar cell*). The surface signature of this atmospheric circulation is characterised by subtropical high and subpolar low pressure belts covering both hemispheres (Figure 2.3). Furthermore, as air conserve the angular momentum along its movement, the northern (southern) hemisphere flow is deflected to the east (west) due to the Earth's rotation (*Coriolis effect*) and hence, surface easterly winds or *trade winds* appear in the subtropics (latitudes lower 30°), as well as westerly winds or *westerlies* between 30° and 60°, and again easterly winds or *easterlies* in high latitudes (Figure 2.2b).

As a consequence of the aforementioned extratropical configuration, a strong meridional temperature gradient is found at midlatitudes, separating the warm tropical air from the cold polar air. Assuming at this point that the horizontal flow is geostrophic, and considering pressure coordinates (go to Peixoto and Oort (1992) for a more detailed description), the vertical shear of horizontal wind at pressure p can be expressed as:

$$\left(\frac{\partial u_g}{\partial p}, \frac{\partial v_g}{\partial p}\right) = \frac{R}{fp}\left(\left(\frac{\partial T}{\partial y}\right)_p, -\left(\frac{\partial T}{\partial x}\right)_p\right) \tag{2.1}$$

being f the Coriolis parameter, R the gas constant, and u_g and v_g the zonal and meridional geostrophic winds, respectively. Equation 2.1 is known as *thermal wind equation* in reference to the fictitious *thermal wind*, which actually represents the vertical shear of horizontal wind. Thus,

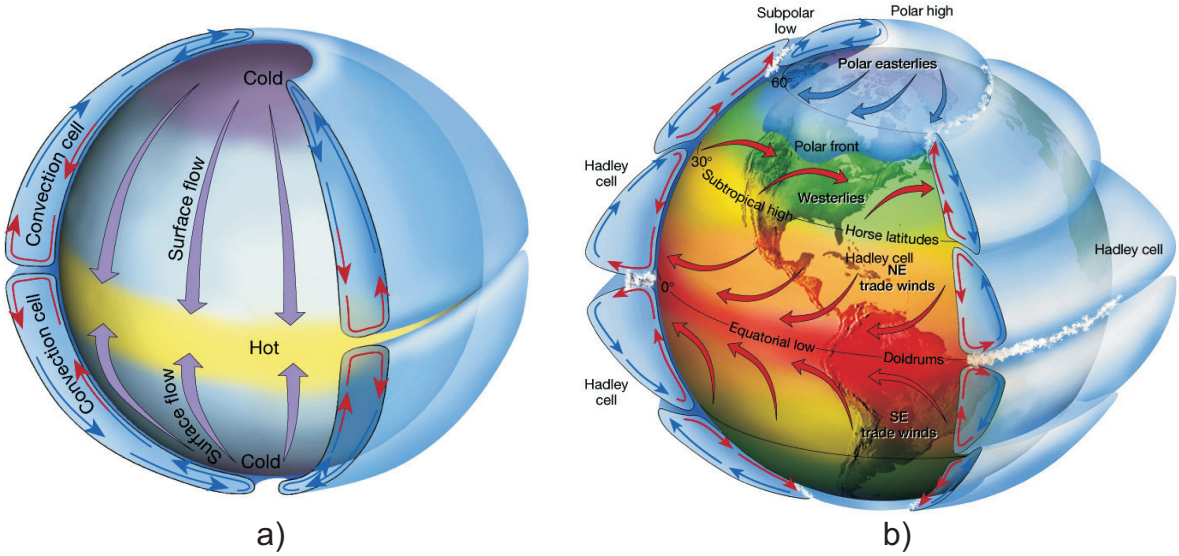

Figure 2.2: a) One-cell atmospheric model in a non-rotating Earth proposed by G. Hadley. b) three cell atmospheric model in a rotating earth. From Lutgens and Tarbuck (2001).

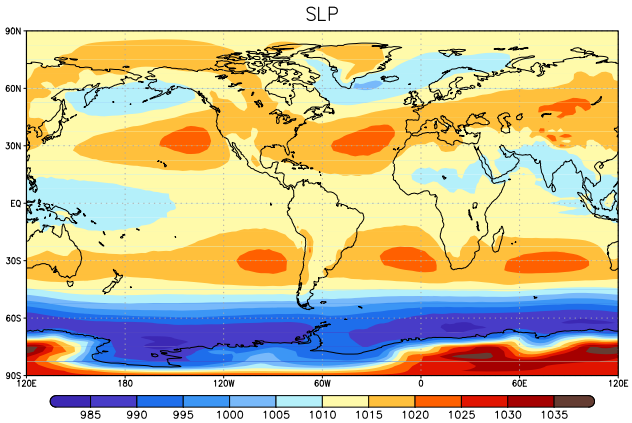

Figure 2.3: Annual Mean Sea Level Pressure (hPa), 1949-2014. From NCEP-NCAR reanalysis.

since temperature decreases poleward, $\frac{\partial T}{\partial y} < 0$ in the northern hemisphere and $\frac{\partial T}{\partial y} > 0$ in the southern hemisphere; hence $\frac{1}{f}\frac{\partial T}{\partial y} < 0$ in both. According to Equation 2.1, $\frac{u_g}{\partial p} < 0$ and hence, with increasing height (decreasing pressure) winds become increasingly eastward (westerly). As it was previously noted, the meridional temperature gradient is most pronounced in midlatitudes and hence, a maximum of westerlies is found there. In particular, the strongest winds occurs at upper troposphere (near 200 hPa) where the north-south temperature gradient is also maximum. As it will be repeatedly mentioned along this thesis, the resultant *extratropical jet stream* (Figure 2.4), which varies in position and intensity along the year (Figure 2.5; top), represents a key agent in the extratropical response to ENSO, being of special importance the relative position of the two main branches over mid-latitudes, which are the East Asian jet (EA-jet) and the North Atlantic jet (NA-jet) (Figure 2.5; bottom).

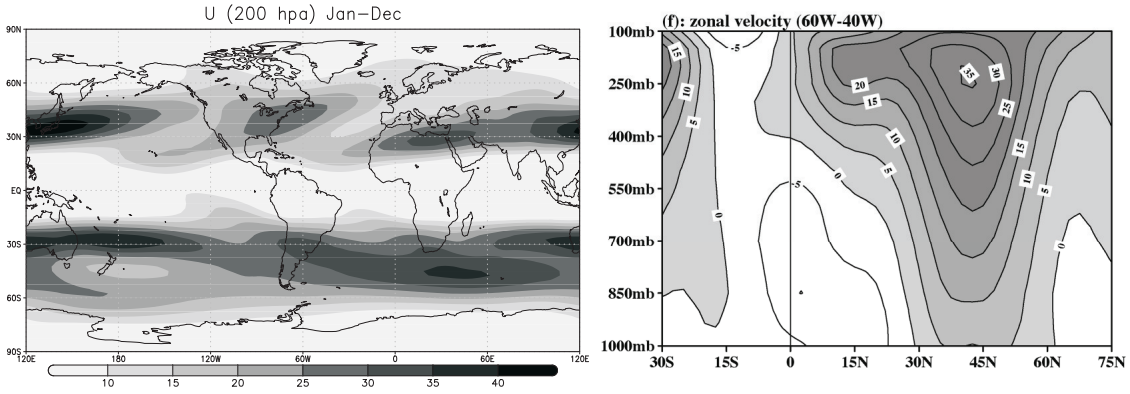

Figure 2.4: Left, averaged zonal mean flow at 200 hPa (January-December, 1949-2015). From NCEP-NCAR reanalysis. Right, zonal wind cross section (January) between 60°W and 40°W. Positive values are shaded. Please note that the strong eastward winds at upper troposphere are associated with the extratropical jet stream. From Wang (2002a). Units in $m \cdot s^{-1}$.

Zonal circulation cells are also identified in the tropics, where the strong convection induces changes in the horizontal convergence and divergence and, hence, vertical motions in the atmospheric column (see Section 4.1). The first zonal circulation system is described as a cell in which air rises over the warm western tropical Pacific ocean and sinks over the cold eastern tropical Pacific ocean (Bjerknes, 1969). It is called as *Walker Cell* as a tribute to the works done by Gilbert Walker during the 1920's (Walker, 1925a,b; Walker and Bliss, 1928). Nowadays, it is known how this Pacific Walker cell is part of a hemispheric band of Walker cells through which the tropical regions are connected to each other, changing along the year in relation to the latitudinal movements of the *Intertropical Convergence Zone (ITCZ)*.

2.1.1 Atmospheric circulation over the North Atlantic sector

The North Atlantic region is placed between the subtropical high and the subpolar low pressure belts of the Northern Hemisphere. The Azores high and the Greenland low pressure systems are part of theses belts and their relative strengthening along the year, which control the westerlies, influences the climate variability over Europe (Figure 2.6). These westerlies are enhanced in winter season when the jet stream, dominated by the so-called *eddy* activity, is also strong. This eddy activity occurs at high frequencies and it is caused by the intense gradients of temperature that take place along the eastern coast of North America (near Newfoundland region), inducing strong *eddy heat fluxes*. As a consequence, deep baroclinicity, which favours the cyclone formation, is found over this area. Once the cyclones are formed, they propagate along the extratropical jet stream, causing in that way the exchange of energy and momentum with the mean flow, which in turn influences the dynamical evolution of the own cyclogenetic activity and so, the downstream

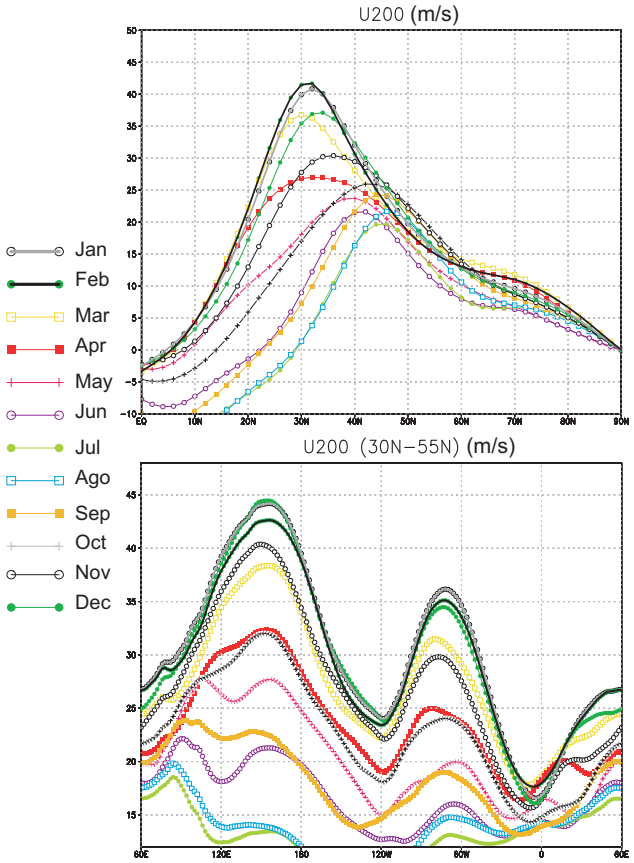

Figure 2.5: Left, meridional-vertical cross section of the zonal mean flow at 200 hPa in the northern hemisphere. Right, zonal-vertical cross section by averaging the zonal mean flow at the same level between $30^{o}N$ and $55^{o}N$. From 20CR database (1871-2010). The two maximum located, approximately, at 150E and 80W reflect the EA-jet and NA-jet respectively. Units in $m \cdot s^{-1}$.

propagation of storm tracks over the European Continent. Thus, a bidirectional influence between eddies and zonal mean flow occurs over the North Atlantic, being maximum in winter season, when the thermal contrasts along the eastern North American coast are also maximum (Hoskins and Valdes, 1990).

European climate variability can be also affected by changes in the easterly surface winds or *trades winds*, which flows towards the south-west over the Tropical North Atlantic (*TNA*). These northern hemisphere trades winds converge with the southern hemisphere ones at the *ITCZ*, which is closely but not exactly located over the geographical equator and moves to the north or to the south along the year. This seasonal evolution is also found for the Azores high pressure system and the so-called *subtropical jet stream* (Figure 2.7), being the latter located over North Africa in winter and over the Mediterranean area in summer. This jet stream, different from the previous mentioned extratropical jet stream, is thermally driven. The rising air over the ITCZ flows to higher latitudes due to the meridional gradient of temperature. Hence, along its displacement it is

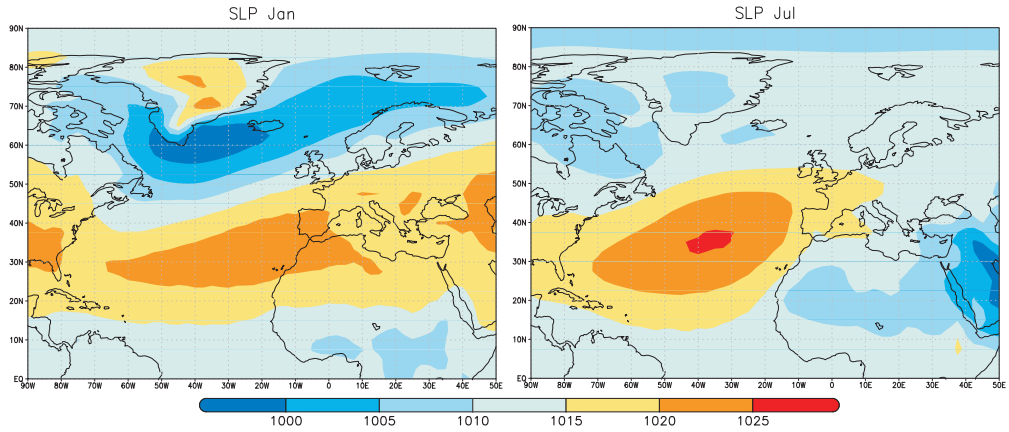

Figure 2.6: Mean Sea Level Pressure (hPa) in January (left) and July (right), 1949-2014. Please realize that a different feature of the Azores high and the Icelandic low pressure systems is found in winter and summer seasons. From NCEP-NCAR reanalysis.

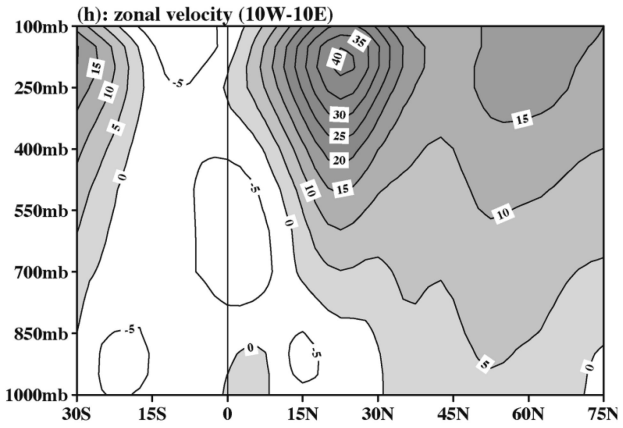

Figure 2.7: Zonal wind cross section (January) between 10°W and 10°E. Note that the strong eastward winds at upper troposphere are associated with the subtropical jet stream. From Wang (2002a). Units in $m \cdot s^{-1}$.

deflected to the east due to the *Coriolis effect*. This feature, which is specially marked over the TNA in winter (Mediterranean region in summer), generates strong easterlies at upper troposphere and so, the resultant subtropical jet stream. At mid latitudes, part of the previous mentioned northward meridional flow descends, causing in that way the Azores high pressure system. In the return pathway of this flow at surface levels towards the equator, the winds are again affected by the Coriolis effect, which in this case deflects the flow to the west. Thus, the already described trade winds appear, and the thermally driven circulation cell (the Hadley cell circulation) is closed.

Thus, the spatial configuration and intensity of the pressure systems over the North Atlantic can be influenced by different factors. Its variability, from internal or external sources, determines the anomalous storm track activity and the related surface impacts over Europe.

2.2 The Ocean: A climate subsystem coupled to the atmosphere

The ocean, as the atmosphere, plays an important role to redistribute polewards the excess of energy in low latitudes, thereby reducing the north-south gradient of temperature. As it can be seen from global distribution of SSTs (Figure 2.8a) the tropical oceans are noticeably warmer than the extratropical ones. This meridional distribution identified over the ocean surface is specially clear due to the tendency of the oceans to transfer more slowly the heat than other climate subsystems, like the atmosphere. It is said, therefore, that ocean has *thermal inertia*. In addition, by comparing the eastern and western sides of the different ocean basins, it is found that in the tropics the waters on the west tend to be warmer than over the east, whereas in high latitudes the opposite appears. This zonal asymmetry occurs as a result of the wind surface influence on the ocean. Over those tropical regions in which the surface winds are strong, the Coriolis effect together with the frictional coupling of the ocean and the winds cause a net movement of surface water at about 90^{o} to the right (left) of the wind direction in the Northern (Southern) Hemisphere. This feature is known as *Ekman Transport* and, as a consequence, surface water is replaced by cold water that well up from below (upwelling), which explains the cold waters identified in low latitudes to the east (Figure 2.8a). The zonal asymmetry over the mid latitudes, however, respond to the direct effect of ocean geostrophic currents. Over the North Atlantic, for instance, the ocean is anomalously warm in the east side due to the influence of both, the Gulf Stream and the Labrador currents (Figure 2.8b). Something similar occurs in other parts of the globe, where different oceanic surface currents systems or *Gyres*, closely related to the high and low pressure systems previously described in Section 2.1, redistribute the equator-pole energy imbalance.

Nevertheless, the meridional transport of energy occurs differently depending on the ocean basin (Figure 2.9a). Thus, whereas in the Pacific a heat poleward transport is found in the whole basin (northward in the northern hemisphere and southward in the southern hemisphere), over the Atlantic a northward transport is found in both, the southern and the northern hemisphere (Trenberth and Caron, 2001). This fact is influenced by the ocean circulation associated with the so-called *Atlantic Meridional Overturning Circulation (AMOC)*, which is the Atlantic section of the *Global Meridional Overturning Circulation (MOC*; see Figure 2.9b). Hence, the AMOC transports heat from the south and tropical Atlantic to the subpolar and polar North Atlantic, where this heat is released to the atmosphere with substantial impacts on climate over large regions. It is therefore clear that the study of the ocean circulation is not only important *per se*, but also crucial for understanding the atmospheric climate. Thus, the exchanges of energy between the ocean and the atmosphere subsystems through heat (sensible and latent) and momentum fluxes drive the regional oceanic and atmospheric circulations which, in turn, can modify the climate on remote

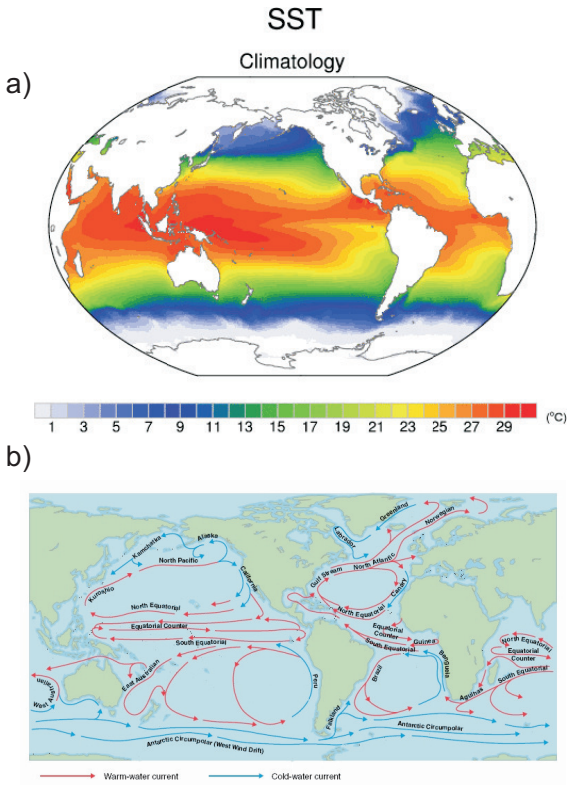

Figure 2.8: a) Long-term mean SST distribution (°C) from satellite passive microwave measurements, 1982-2008; from Deser et al. (2010) b) Global ocean currents from $https://cimss.ssec.wisc.edu/sage/oceanography/$.

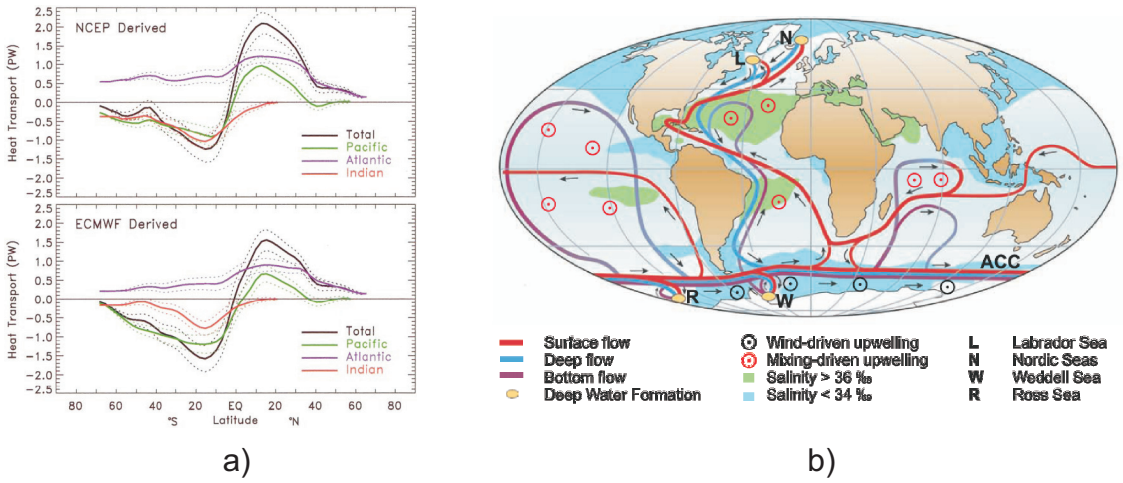

Figure 2.9: a) Zonal annual mean ocean heat transports based upon the surface fluxes for February 1985-April 1989 for the total, Atlantic, Indian, and Pacific basins for NCEP and ECMWF atmospheric fields; From (Trenberth and Caron, 2001). b) Simplified sketch of the global overturning circulation system. From Kuhlbrodt et al. (2007)

.

regions. In particular, along this thesis the SST field is insistently used in order to characterise the anomalous oceanic patterns influencing the atmosphere.

2.3 Climate Variability

Climate Variability refers to temporal variations of the climate system, typically longer than those associated with synoptic weather events (AMS Glossary, 2015), around a certain mean state. This thesis is focused on the non stationary impact of ENSO on the European and Mediterranean rainfall and, in particular, on the possible modulating role of the ocean mean state variability. Thus, we are interested in exploring the ocean decadal and multidecadal variability influence (considered here as low frequency variability) on a specific interannual atmospheric teleconnection (considered here as high frequency variability).

2.3.1 Interannual Variability

2.3.1.1 Variability of the North Atlantic European sector

Different structures are typically used in order to describe the recurrent atmospheric patterns occurring over the North Atlantic. Some examples are the well-known *East Atlantic (EA)*, *Scandinavian (SCA)*, and *East Atlantic/Western Russia (EA/WR)* patterns (Wallace and Gutzler, 1981; Barnston and Livezey, 1987). Nevertheless, the most prominent and recurrent pattern at different timescales over the North Atlantic European (NAE) sector is the *North Atlantic Oscillation (NAO;* Visbeck et al. (2003)). The NAO, which is most noticeable during the boreal cold season (November-April), refers to Sea Level Pressure (SLP) fluctuations between the Azores high and the Icelandic low pressure systems. As a consequence, a redistribution of atmospheric mass occurs between subpolar and subtropical latitudes, intensifying or reducing the SLP difference between Azores and Iceland centers, and defining the positive and negatives NAO phases, respectively (Figure 2.10). As the strength of the zonal flow is related to this meridional gradient of pressure, this SLP seesaw produces large changes in zonal mean flow and moisture transport over the North Atlantic, modifying the stormstracks travelling from North America to the European continent (Rogers, 1997) and hence, the precipitation regime (Rodwell et al., 1999; Hurrell et al., 2003). Under positive NAO phases, there are below normal values of SLP across the high latitudes of the North Atlantic and above normal values of SLP over the central North Atlantic. The opposite occurs under negative NAO phases. As a consequence, positives (negatives) NAO scores are related to higher (weaker) amount of precipitation over Europe north (south) of 45^{o}N and reduced precipitation to the south (north) (Hurrell, 1995). These impacts of NAO over Europe and the Mediterranean region have been thoroughly analysed (Van Loon and Rogers (1978); Wallace and Gutzler (1981); Pozo-Vázquez et al. (2000, 2001a); Sanchez-Gomez et al. (2001); Castro-Díez et al. (2002); Gámiz-Fortis et al. (2002); Rodríguez-Fonseca and Serrano (2002); Rodríguez-Fonseca and de Castro

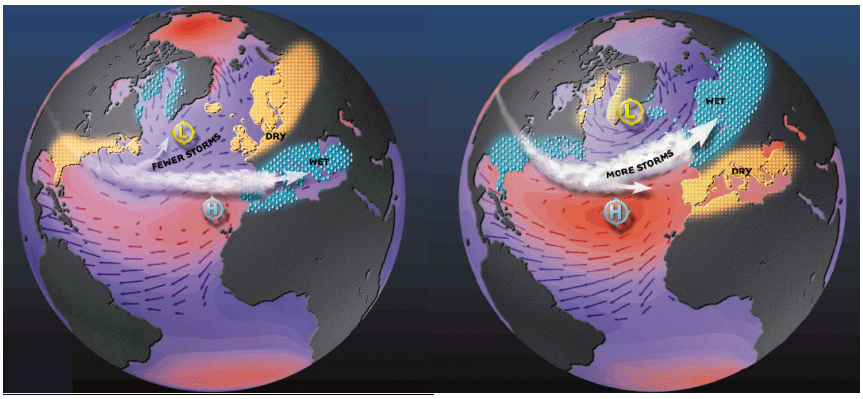

Figure 2.10: NAO conditions in negative (left) and positive (right) phases. From http://www.ldeo.columbia.edu/res/pi/NAO/ by Martin Visbeck

(2002); Trigo et al. (2004), among others).

A general overview of NAO characteristics and its associated impacts can be found in Hurrell et al. (2003) and Thompson et al. (2003), and, more recently, in Pinto and Raible (2012) and Hurrell and Deser (2015).

It is still a matter of debate in climate research community if the NAO is truly a unique mode of North Atlantic climate variability or if, on the contrary, it represents a regional expression of a large-scale oscillation of atmospheric mass between mid and high latitudes over the Northern Hemisphere, usually known as *Arctic Oscillation (AO)* or *Northern Annular Mode (NAM)* (Thompson and Wallace, 1998). The underlying physics of the AO/NAM is not completely understood, with some authors representing the AO as an oscillation between subpolar and subtropical latitudes in the North Atlantic and the North Pacific (Wallace and Thompson, 2002), and others considering the AO as a part of a stationary wave of wavenumber 5 embedded in the extratropical jet (Branstator, 2002; Watanabe, 2004). In addition, Quadrelli and Wallace (2002) suggest an El Niño Southern Oscillation (ENSO) impact on the AO/NAM mode, which is coherent with the results obtained by García-Serrano et al. (2011), who found how the AO/NAM could emerge as a combination of internal (NAO-related) and forced (ENSO-related) variabilities.

The trigger for NAE climate variability in general, and the driver for NAO variability mode in particular, are therefore unclear. Thus, while Stephenson et al. (2000) point to a pure stochastic process (unpredictable), other works address important external factors including (1) the Tropical Atlantic (Visbeck et al., 2003; Chen et al., 2015) and the tropical Pacific (Toniazzo and Scaife, 2006; Brönnimann, 2007) variability, (2) the western flow from the North Pacific (Honda and Nakamura, 2001; Pinto et al., 2011; Drouard et al., 2015), (3) the downward propagation of stratospheric anomalies (Baldwin and Dunkerton, 2001), and (4) the solar radiation variability (Shindell

et al., 2001). In either case, deviations of the climate over the NAE sector are still mainly associated with internal atmospheric variability. And this occurs although different studies have found a SST signature associated with the NAO, which can provide a certain skill for seasonal prediction several months in advance (Czaja and Frankignoul (1999); Rodwell and Folland (2002); Rodríguez-Fonseca et al. (2006), among others). Nevertheless, the skill of current seasonal forecast systems over Europe is limited (Van Oldenborgh and Burgers, 2005), and hence, a large effort should be made to improve it. Along this thesis the link between ENSO and the NAE climate is thoroughly analysed, which hopefully will contribute to this goal.

2.3.1.2 ENSO: A Remote External Forcing

El Niño and the Southern Oscillation (ENSO) is the globally dominant climate mode at interannual timescales. This phenomenon represents a free oscillation of the coupled ocean-atmosphere system over the tropical Pacific or the Indo-Pacific region (Philander et al., 1989; Allan et al., 1996; Harrison and Larkin, 1998; Diaz and Markgraf, 2000; Glantz, 2001; McPhaden et al., 2006), being El Niño and the Southern Oscillation its oceanic and atmospheric components respectively.

El Niño (La Niña) episodes are associated with a weakening (strengthening) of the climatological trade winds and, as a consequence, warm (cold) SST anomalies appearing along the coast of Ecuador and Peru. It was called in that way by the local fishermen, who realised how these anomalous warming (cooling) of the waters generally occurred around Christmas time. Nowadays, it is known that these anomalous SSTs extend to the center of the tropical Pacific (Figure 2.11a), being November to January the mature phase of El Niño (La Niña) events. An overview of SST seasonal cycle associated with ENSO can be found in Wang (2002b). The aforementioned changes in the equatorial SSTs are associated with large anomalies in atmospheric circulation. Specifically, strong variations in surface pressure over the eastern and western tropical Pacific are found during ENSO events, defining in that way the Southern Oscillation or atmospheric component of ENSO. As a consequence, large east-west shifts of mass over the tropical Pacific atmosphere take place. This coupled oscillation between the ocean and the atmosphere is explained by the *Bjerknes feedback mechanism* (1969). According to this theory, when the tropical Pacific is anomalously warm (as for El Niño episodes), the SST zonal gradient changes and the zonal atmospheric circulation is perturbed. Thus, trade winds are weakened, decreasing in that way the oceanic upwelling (and hence cooling) in the eastern Pacific and so, reinforcing the initial warm SST conditions. The opposite feedback mechanism occurs for La Niña episodes.

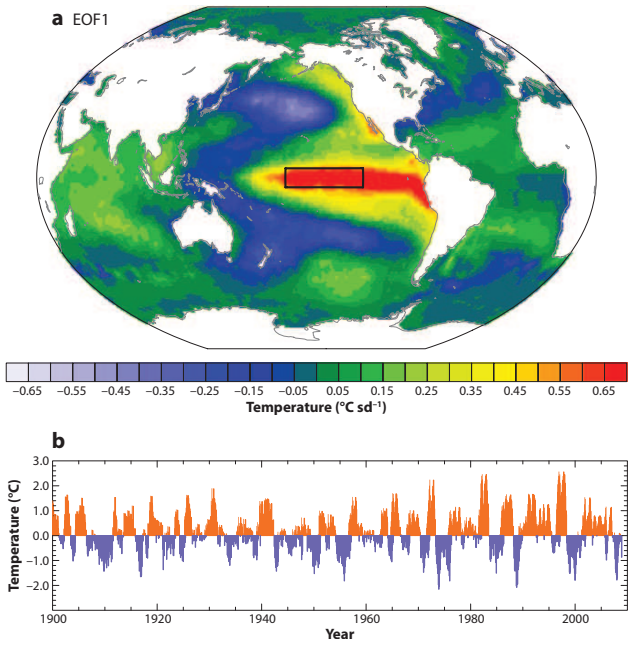

Figure 2.11: a) Leading empirical orthogonal function (EOF) of detrended monthly SST anomalies over the global oceans based on the HadISST dataset, 1900–2008. This mode, which accounts for 19% of the variance, depicts the ENSO phenomenon. b) Monthly SST anomaly time series in the Niño 3.4 region (5°N-5°S, 170°-120°W: outlined by the rectangle on the pattern). From Deser et al. (2010).

Thus, during El Niño episodes the atmospheric deep convection over the maritime continent is shifted to the central equatorial Pacific, which produces enhanced precipitation and midlevel heat release above. As a consequence, a pair of low level (upper level) cyclones (anticyclones) to the west of the anomalous warming together with a low pressure to the east, appears. This *Gill-Matsuno response* (see Chapter 4 for a more detailed description) produces changes in global circulation by the alteration of the Hadley and Walker cells (divergent flow) or the triggering of atmospheric Rossby waves (rotational flow), which can connect the Pacific basin to tropical and extratropical regions by *atmospheric bridges* (Lau and Nath, 1996; Klein et al., 1999; Alexander et al., 2002). Thus, ENSO phenomenon is able to modulate the global climate (Alexander et al., 2002; Slingo and Annamalai, 2000). Several studies based on rain-gauges records from land stations (e.g. Ropelewski and Halpert (1987, 1989); Kiladis and Diaz (1989)) or including satellite estimates and reanalysis model outputs (e.g. Xie and Arkin (1997); Dai et al. (1997)) have been documented about the global impacts of ENSO on rainfall. It has been found how the leading EOF of global precipitation is an ENSO-related pattern (Figure 2.12) and, as a consequence, ENSO is considered as the most important determinant of variability in global precipitation fields (Dai et al., 1997; Dai and Wigley, 2000). A detailed description of ENSO teleconnection with extratropical latitudes, and more specifically with the NAE sector, is shown in Section 2.4.

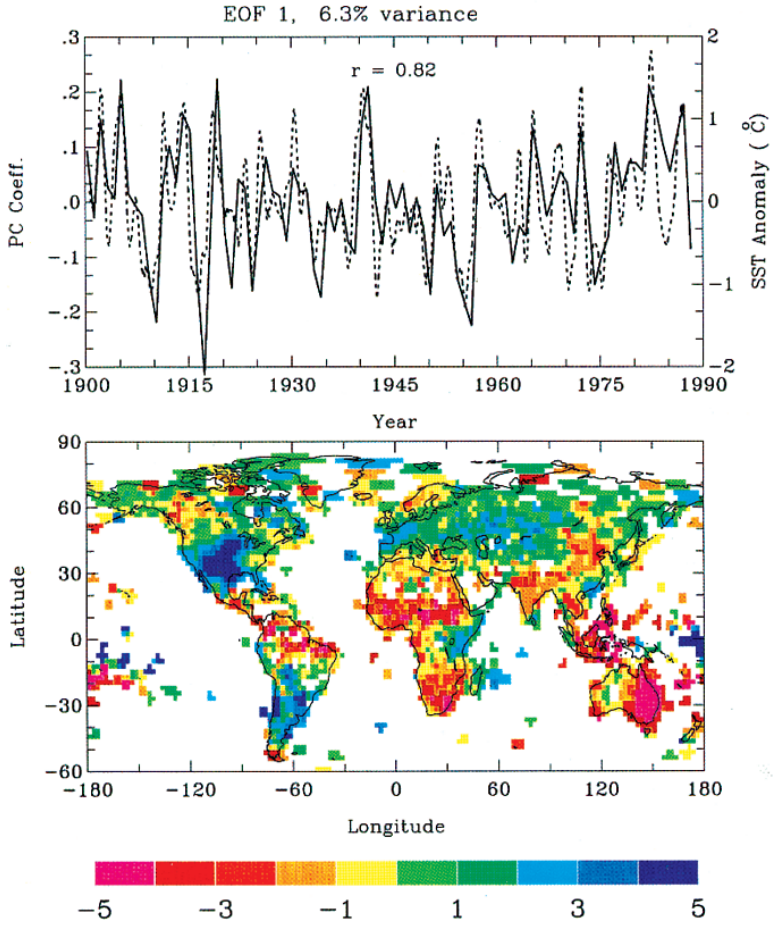

Figure 2.12: Temporal coefficients (top; solid line) and spatial pattern (bottom) of the first leading EOF of annual precipitation anomalies. Also shown (dashed line) is the bimonthly SST anomalies over the equatorial Pacific, which are associated with ENSO (Wright, 1984). Please note to the top that both timeseries are strongly correlated each other. From Dai et al. (1997).

Noticeable differences have been detected between El Niño and La Niña episodes in both, time evolution (Larkin and Harrison, 2002; Ohba et al., 2010; Okumura and Deser, 2010) and spatial signature. Related to the later are the two main SST patterns associated with ENSO, usually known as Eastern Pacific (*EP* or *canonical*) and Central Pacific (*CP*, *Modoki*, or *dateline*; see Trenberth and Stepaniak (2001); Kao and Yu (2009)). They are representative of the most intense El Niño and La Niña events respectively, and are partially explained by the non-linearities of the ENSO phenomenon (Dommenget et al., 2013). In particular, a series of publications have found a non-linear response of zonal winds in the central Pacific to SST anomalies (Kang and Kug, 2002; Philip and van Oldenborgh, 2009; Frauen and Dommenget, 2010). Regarding their impacts, discernible differences in relation to EP and CP events have been detected (Kug et al., 2009; Kao and Yu, 2009; Choi et al., 2011). Those associated with the NAE sector are also investigated along this thesis (López-Parages et al., 2015b).

Different ways of measuring the strength of ENSO are used (Trenberth, 1997). For El Niño (oceanic component), the most common practice is to average the SST over certain regions of the tropical Pacific, which are named as NIÑO1+2, NIÑO3, NINO4, and NIÑO3.4. The latter is calculated over the central Pacific (5ºS-5ºN,170ºW-120ºE; see rectangle in Figure 2.11a) and it is considered a convenient index to analyse El Niño time evolution (Sterl et al., 2007). These SST-based indices are statistically positive for El Niño phase and negative for La Niña phase. Other indices are also calculated to measure the Southern-Oscillation (atmospheric component of ENSO). The Southern Oscillation Index, defined as the standarised SLP difference between Tahiti (17ºS, 149ºW) and Darwin (12ºS, 130ºE), is frequently used. Contrary to the oceanic indices, positives values of SOI are related to La Niña episodes and negative values to El Niño ones.

ENSO events occur every few years, with periodicities that change from two to seven years (Philander et al., 1989), and a time length around a year or occasionally more (Allan and D'Arrigo, 1999). As it is previously noted, it is considered the globally dominant mode at interannual timescales. Nevertheless, ENSO varies from interannual to multiannual, or even interdecadal timescales, being the latter usually referred to as *ENSO-like* variability or Inter-decadal Pacific Oscillation (IPO). This low frequency variability of ENSO, which is not completely understood by the scientific community, is analysed in more detail in the next subsection.

2.3.2 Decadal and Multidecadal Ocean Variability

Along this thesis, it is exposed how the SST mean state, which is assumed here as a synonym of SST background state or SST climatology, can be of great importance for the ENSO-NAE teleconnection. In particular, it is analysed the influence of oceanic low frequency variability modes, such as the *Atlantic Multidecadal Oscillation* (Kerr, 2000), or the *Pacific Decadal Oscillation* (Mantua et al., 1997), in the aforementioned link. It is worth clarifying that, as this study is focused on interannual timescales, decadal and multidecadal SST variability is considered here as variability of the SST mean state.

2.3.2.1 Atlantic Multidecadal Oscillation

Atlantic Multidecadal Oscillation (AMO) is a natural SST variability mode occurring in the Atlantic basin, being identified as a coherent large-scale pattern with a time period of about 50-70 years (Kerr, 2000; Enfield et al., 2001; Knight et al., 2005). Its positive (negative) phase is characterised by warmer (cooler) than average SSTs over the North Atlantic Ocean (Figure 2.13; top). Positive AMO phases have been detected in late 19th century, the middle decades of the 20th

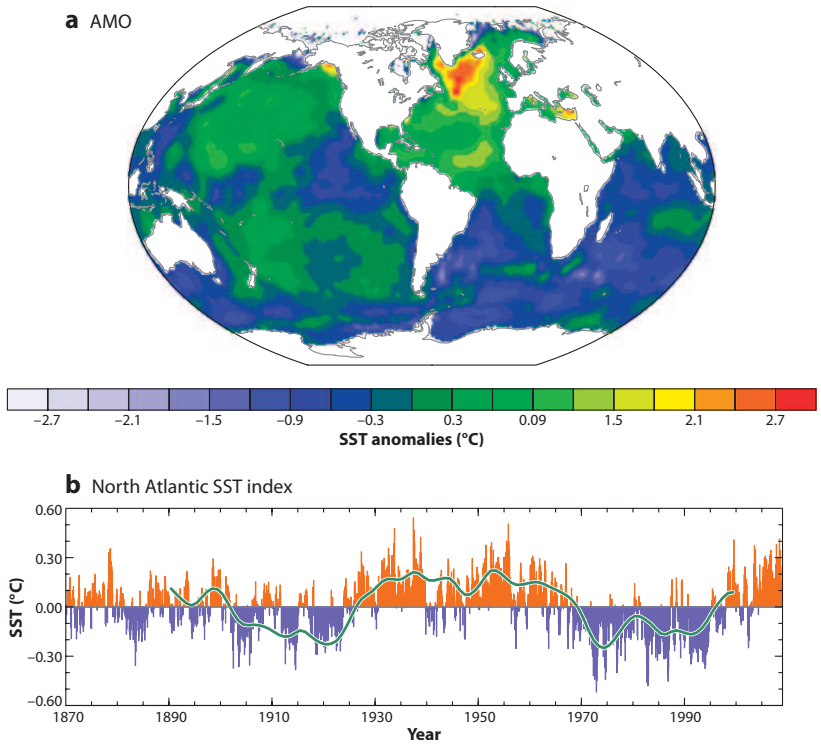

Figure 2.13: (a) Regression pattern of monthly SST anomalies (after removing the global mean SST anomaly) on a North Atlantic SST Index, based on the HadISST data set during 1870–2008. (b) The North Atlantic SST Index, defined as the average monthly SST anomaly over the North Atlantic (0^o-70^oN) minus the global mean monthly SST anomaly (red and blue bars). The green line depicts an estimate of the natural (e.g., not due to forcing external to the ocean-atmosphere system) component of the 10-year low-pass-filtered North Atlantic SST index. From Deser et al. (2010).

century, and the beginning of the present century; whilst negative AMO phases are found in the beginning of the 20th century and during the 1970's and 1980's (Figure 2.13; bottom).

Although the origin of AMO is not yet fully understood (Dima and Lohmann, 2007; Gulev et al., 2013), AMO-like oscillations have been found in long time series records (Delworth and Mann, 2000; Gray et al., 2004; Chylek et al., 2010, 2012) and in long control simulations of some climate models (Mahajan et al., 2011; Delworth and Zeng, 2012; Wei and Lohmann, 2012; Yang et al., 2013; Zhang et al., 2013), both pointing out to a connection with the AMOC (Latif et al., 2004; Knight et al., 2005; Medhaug and Furevik, 2011; Zhang et al., 2013). However, an alternative theory relating SST variability to fluctuations in atmospheric concentrations of anthoropogenic and natural aerosols have been also proposed in the last years (Evan et al., 2009; Booth et al., 2012). AMO seems to be associated with changes all over the world, and it is considered as a dominant factor of oceanic influence on current global warming (Chylek et al., 2014). Over the NAE sector, AMO is associated with multidecadal changes in hurricane activity over the Atlantic (Zhang and Delworth, 2006; Trenberth and Shea, 2006; Knight et al., 2006), and with summertime climate

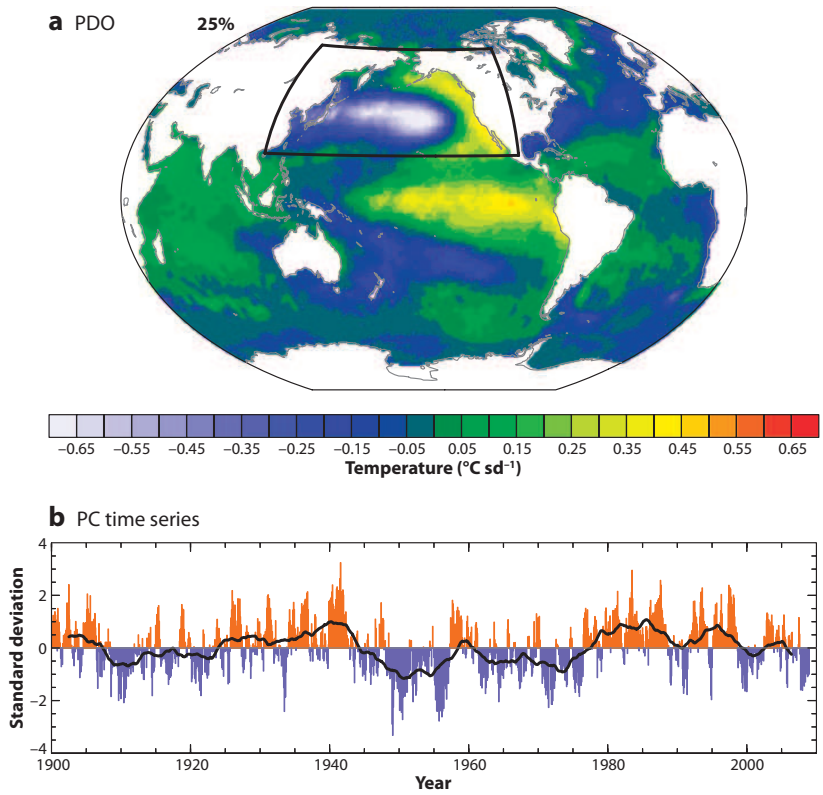

Figure 2.14: (a) The leading empirical orthogonal function (EOF) of monthly SST anomalies over the North Pacific (after removing the global mean SST anomaly) based on the HadISST data set during 1900–2008. Although the EOF calculation was restricted to the North Pacific (region outlined by the black rectangle), the pattern is displayed globally by regressing the monthly SST anomalies at each location on the principal component (PC) time series. (b) Associated PC time series showing the unsmoothed record (red and blue bars) and the 5-year running mean record (black line). From Deser et al. (2010).

of North America and western Europe (Sutton and Hodson, 2005). A link with the occurrence of wintertime Euro-Atlantic blocking has been also suggested by Häkkinen et al. (2011), which could be related to the decadal variations in northern extratropical jet variability recently found by Woollings et al. (2014).

2.3.2.2 *Pacific Decadal Oscillation*

Pacific decadal and interdecadal variability has been defined in different ways by different authors and using different indices over different parts of the Pacific Ocean. According to this, the *Interdecadal Pacific Oscillation (IPO* or *ENSO-like decadal variability*) is the main basin-wide mode of SST variability in the whole Pacific basin at decadal timescales (Zhang et al., 1997); whilst the *Pacific Decadal Oscillation (PDO*, Figure 2.14) is the leading EOF mode of SST over the North Pacific (Mantua et al., 1997). This decadal variability of Pacific SSTs was discovered in relation to

cyclical variations in salmon and other fisheries in the mid 1990s (Hare and Francis, 1995; Zhang et al., 1997; Mantua et al., 1997). The physical underlying mechanism is still unclear (Mantua and Hare, 2002) but it is considered by several authors as an internal mode involving tropical and mid-latitudes air-sea processes of the coupled ocean-atmosphere system (Desser et al., 2004; Meehl and Hu, 2006; Meehl et al., 2009). The PDO is dominated by decadal periods of about 30 years, and its positive (negative) phase is associated with a warming (cooling) in the tropics and a cooling (warming) in the North Pacific Sector. It is over this area were the most notable impacts of PDO have been found (Mantua et al., 1997; Minobe, 1997), occurring through changes in the location and intensity of the Aleutian low.

There have been found positive PDO phases from about 1915 to 1945, negative from about 1945 to 1976, positive again from 1977 to 1999, and finally a new negative phase from 1999 to the present. In particular, the change of PDO phase in 1977 has been related to the widely analysed *1976/1977 Climate Transition or Climate Shift* (Nitta and Yamada, 1989; Trenberth, 1990; Miller et al., 1994; Graham, 1994), which exerted a modulating effect on ENSO variability and related teleconnections (Gershunov and Barnett, 1998).

2.4 ENSO-NAE teleconnection

A significant influence of El Niño-Southern Oscillation over the NAE is not completely accepted by climate researchers, being much less understood than that over the tropics (Harrison and Larkin, 1998; Alexander et al., 2002; Diaz and Markgraf, 2000; Wang and Picaut, 2004; Wang, 2004; McPhaden et al., 2006) and the North Pacific - American Continent (Trenberth et al., 1998) due to the large internal variability of the circulation over the North Atlantic (Quadrelli and Wallace, 2002). Related to this, European climate variability has been mainly linked to internal processes (Van Loon and Rogers, 1978; Wallace and Gutzler, 1981) and SST signatures (Czaja and Frankignoul, 1999; Drévillon et al., 2001; Rodwell and Folland, 2002; Rodríguez-Fonseca and de Castro, 2002; Rodríguez-Fonseca et al., 2006) associated with the NAO.

Nevertheless, several studies have found a consistent and statistically significant ENSO signal on the NAE climate (Fraedrich and Müller, 1992; Moron and Plaut, 2003), specially in late winter and early spring seasons, when El Niño (La Niña) tends to be accompanied by a negative (positive) NAO-like pattern (Figure 2.15). This fact does not mean that ENSO effect should be simply described in terms of NAO even though its surface signature may be reminiscent of the NAO pattern (García-Serrano et al., 2011). Indeed, the two leading modes of anomalous streamfunction at upper troposphere over the NAE found by these authors are associated with ENSO and

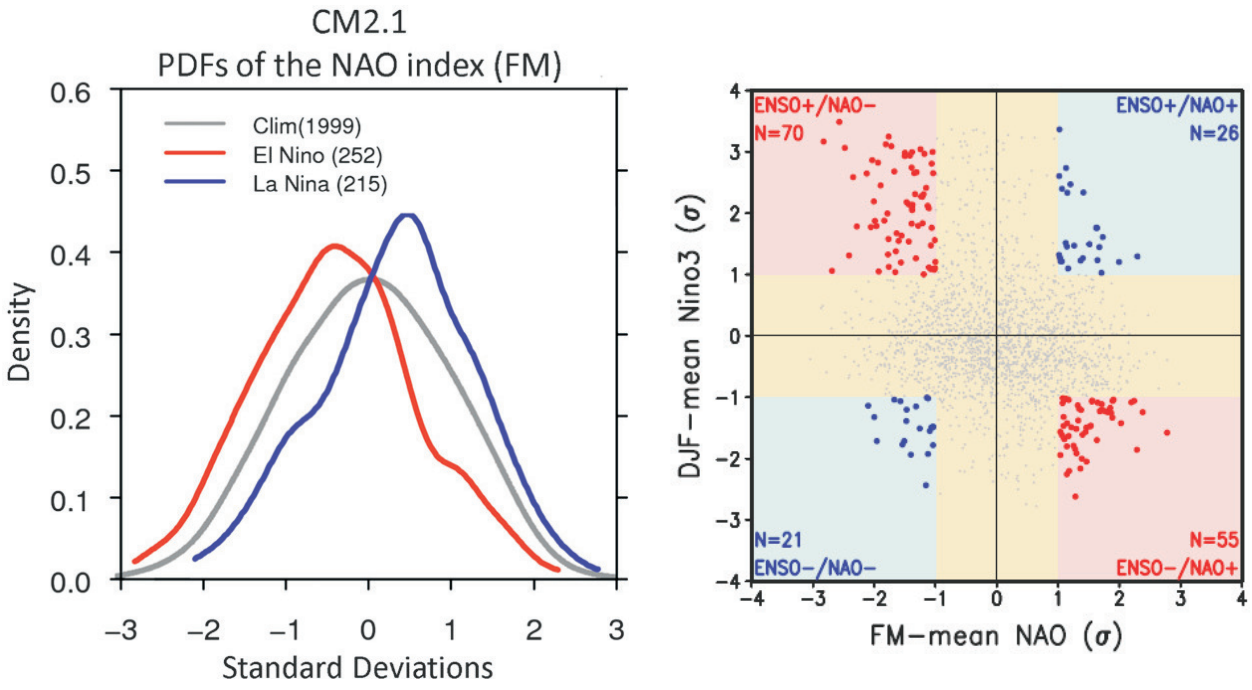

Figure 2.15: Left, PDFs of the normalised FM-mean NAO indices for El Niño (red), La Niña (blue) and all winters (grey) in the CM2.1 simulation. Right, scatterplot of normalised DJF-mean Niño3 index vs normalised FM-mean NAO index for the 2000 years CM2.1 dataset. Taken from Li and Lau (2012).

the internal NAO, representing two well differentiated teleconnection dynamics (Figure 2.16), a distinction that has been supported by several works (Van Oldenborgh et al., 2000; Rodwell and Folland, 2002; Wang, 2002a; Deweaver and Nigam, 2002).

ENSO influence on the NAE climate via the troposphere is mainly explained by (1) changes in the thermally driven direct circulation in relation to variations in the anomalous convection, and (2) changes in the rotational flow by the modification of the planetary vorticity and hence, the triggering of extratropical Rossby waves.

Regarding the former, moisture-laden air converges onto the warmest regions of the Earth's surface, where the air rises and condenses, causing widespread cloudiness and heavy precipitation. Elsewhere, subsidence of air from the upper troposphere occurs, preventing the clouds growing and so, a substantial rainfall. As it is described in Section 4.1, these thermally driven circulations occurs in zonal and meridional directions through changes in the Walker and Hadley cells respectively. Therefore, when an ENSO episode occurs, the normal conditions of this direct circulation are perturbed by the Southern Oscillation (or atmospheric component of ENSO). As a consequence, six anomalous centers of action of velocity potential can be identified (see Figure 2.17): three over the equator (western Pacific, eastern Pacific, and Atlantic) and three over mid latitude regions (west

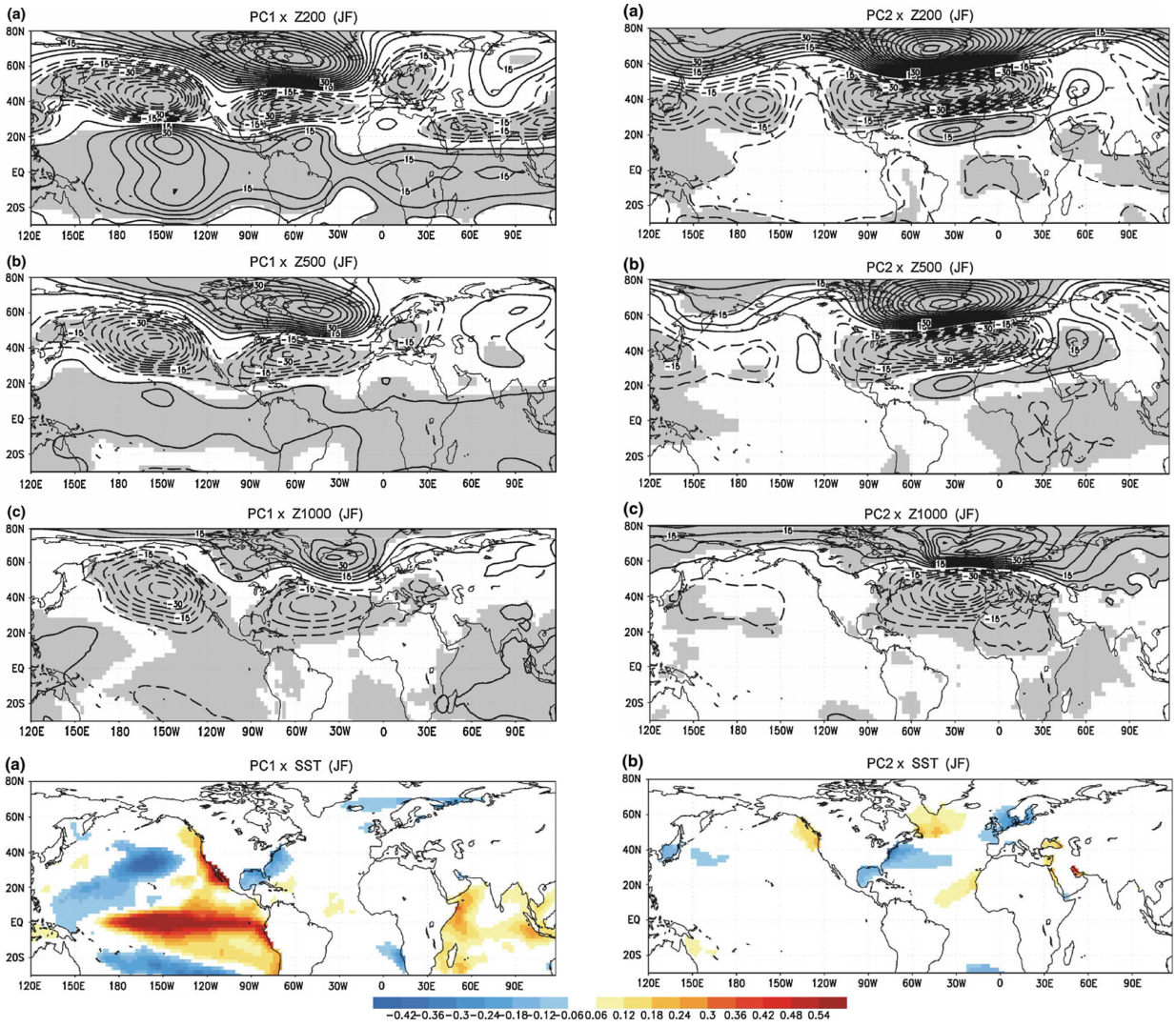

Figure 2.16: Regression maps of geopotential height (ERA40) at 200 hPa (Z200; top), 500 hPa (Z500; second row), 1000 hPa (Z1000; third row), and SST (bottom; ERSST), onto the leading (left) and second (right) PC obtained from an EOF analysis of the 200hPa anomalous winter streamfunction over the NAE region (5ºS-80ºN/90ºW-40ºE). Magnitudes correspond to one std dev of the time series. Modified from García-Serrano et al. (2011).

Pacific, near Caribbean Sea, and Europe). These centers along the globe represent a weakening (for El Niño events; strengthening for La Niña events) of the previous mentioned Pacific and Atlantic Walker circulations, and its related anomalous Hadley cells at subtropical latitudes (Wang, 2002a; Wang and Picaut, 2004), respectively. According to this, it is well established that El Niño (La Niña) affects the tropical Atlantic and weakens (reinforces) the Atlantic Hadley circulation (Ruiz-Barradas et al., 2003; Wang and Picaut, 2004). As a consequence, the Azores high and the related westerlies are affected, and the climate variability over the NAE changes. This impact seems to depend on SSTs over the TNA, as it has been proposed by several authors (Mathieu et al., 2004;

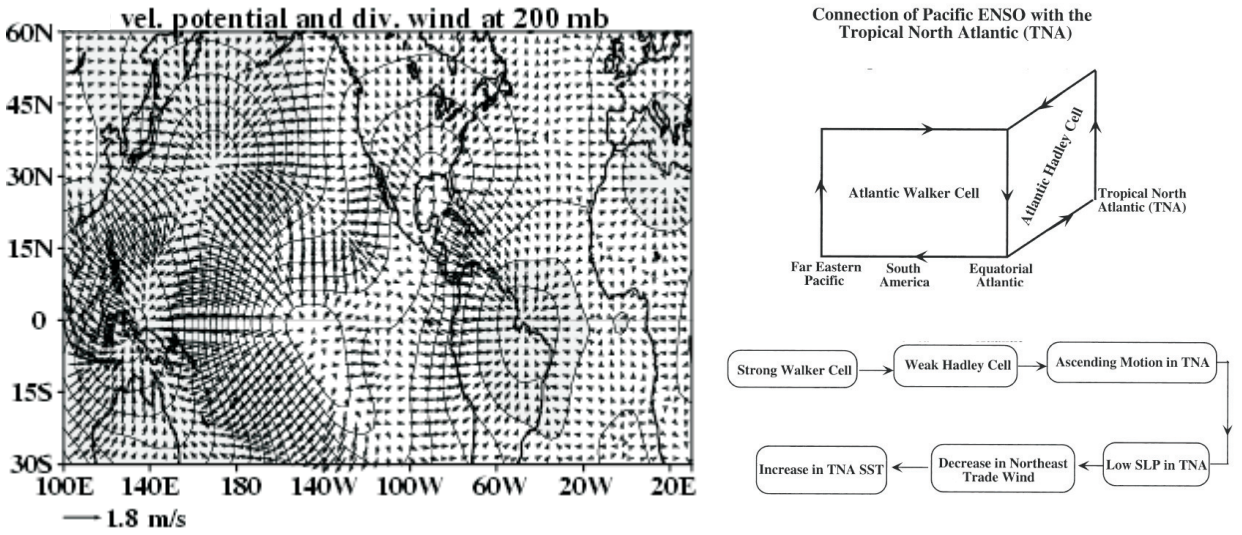

Figure 2.17: Left, 200 mb velocity potential and divergent wind response during the mature phase of El Niño (November to January). Right, schematic diagram showing how the Pacific El Niño affects the TNA. From Wang (2002a).

Pozo-Vázquez et al., 2001a; Gouirand and Moron, 2003; Sutton and Hodson, 2003). Related to this, two recent studies by Sung et al. (2013) and Ham et al. (2014), based on observations and Global Circulation Models (GCM), suggest that SST conditions in late winter over the TNA control the NAO-like reponse associated with ENSO. Thus, for El Niño events the warm TNA SSTs intensify the negative NAO-like response and viceversa. A similar modulation is found for La Niña teleconnection, for which a positive NAO-like pattern seems to be stronger under cold TNA SST conditions. These features do not occur, however, if El Niño (La Niña) does not continue throughout January-February-March, as in this case, the atmospheric bridge connecting Pacific and Atlantic basins is not persistent enough to induce changes over the TNA (Sung et al., 2013). A nonlinear response of ENSO over the NAE in relation to that on the Northern Hemisphere circulation has been also found (Wu and Hsieh, 2004; Pozo-Vázquez et al., 2005a).

Regarding the rotational flow, the most accepted dynamical mechanism which explains the ENSO-North Atlantic tropospheric teleconnection implies the disturbance of the Aleutian low through changes on the Pacific Hadley circulation in early and mid winter, and then the downstream propagation of Rossby wavetrains across North America from January (Honda et al., 2001; Moron and Gouirand, 2003). It is from this month when the canonical Tropical Northern Hemisphere pattern (TNH), which is organised in three centers of actions along the North Pacific-American sector (Mo and Livezey, 1986; Barnston and Livezey, 1987; Livezey and Mo, 1987; Trenberth et al., 1998), is completely established (Bladé et al., 2008), together with a split of the Rossby wavetrain

impacting over Eurasia (Karoly et al., 1989). Hence, the resultant rotational atmospheric response to ENSO forcing is formed by a TNH-like pattern and the above-mentioned split of the wavetrain, revealing a quasi barotropic structure, and representing the leading rotational mode of upper level streamfunction in the NAE (García-Serrano et al., 2011). Several authors suggest that synoptic eddies play an important role in maintaining or amplifying this stationary wave disturbance over the North Atlantic associated with ENSO (Merkel and Latif, 2002; Pohlmann and Latif, 2005). Therefore, slight changes in the stationary planetary waves could induce strong variations in baroclinicity over Newfoundland and the surrounding areas, influencing in that way the growth conditions of tropospheric eddies and so, the storm track activity over the whole North Atlantic (Fraedrich and Müller, 1992; Cassou and Terray, 2001b; Raible et al., 2004). Thus, an effective and persistent ENSO teleconnection with the NAE, being considered as a downstream effect, may comprise interactions between different scales of flow (Martineu et al., 1999; Alpert et al., 2006). According to this, Cassou and Terray (2001a,b) suggest that the transient eddy feedback on the mean flow might promote an asymmetric response over the NAE between El Niño and La Niña episodes.

It is worth noting how the aforementioned TNH pattern, which appears due to the tropical forcing associated with ENSO, sometimes resembles an eastward shifted version of the *Pacific North American teleconnection pattern* (PNA). The latter is, however, considered as a natural internal mode of the atmosphere (Barnston and Livezey, 1987), but seems to be also partially forced, as approximately 51% of the PNA occurrences coincide with ENSO (Bonsal and Shabbar, 2011). Considering therefore that PNA is related to both, intrinsic and forced variability, along this thesis it is more frequently used the TNH as the pattern characterizing the Northern Hemisphere response associated with ENSO. In either case, it is convenient to observe how the interevent variability of ENSO is large, and so, the use of these canonical patterns must be used for guidance only.

A global teleconnection pathway from the Pacific region to Europe via the stratosphere has also been showed (Ineson and Scaife, 2009). This stratospheric mechanism, which likely plays an important role in improving seasonal forecast over the NAE sector (Butler et al., 2014), implies the upward propagation of planetary waves from the troposphere to the stratosphere in winter, a weakening of the stratospheric polar vortex (Manzini et al., 2006; Garfinkel and Hartmann, 2008), and a more frequent occurrence of the so-called *sudden stratospheric warmings (SSWs)*. It is worth mentioning how the latter are preceded by blocking events, which in turn are modulated by ENSO. Furthermore, as it has been recently found, the SSWs episodes are crucial for CP El Niño events, whose polar stratospheric response can be the opposite depending on whether the CP El Niño occurs in winters with or without SSWs (Iza and Calvo, 2015). Finally, the anomalous stratospheric perturbations are downward propagated to the troposphere in late winter (Ineson and

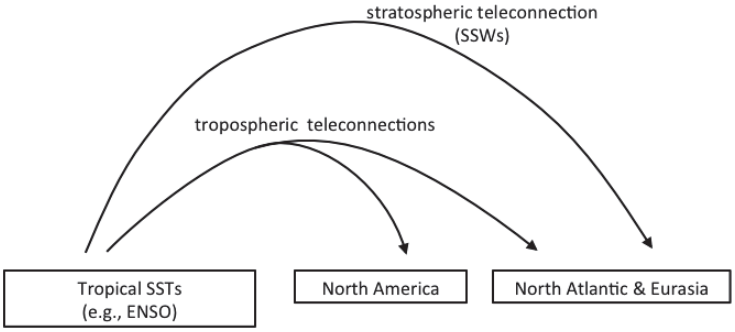

Figure 2.18: Schematic of possible pathways by which ENSO can influence the northern extratropics. From Butler et al. (2014).

Scaife, 2009; Cagnazzo and Manzini, 2009; Bell et al., 2009), the characteristic season for which the ENSO-NAE link via the troposphere is also stronger. This possible simultaneity makes difficult to distinguish the tropospheric and stratospheric signal over the North Atlantic (Figure 2.18). It is also interesting to note that extratropical stratospheric response of ENSO seems to interact in a non-linear way with other sources of variability such as the *quasi-biennal oscillation (QBO)* and the 11 year solar cycle, which makes difficult the isolation of each individual contribution (Calvo and Marsh, 2011). Thus, more research is still needed in this area.

The above described characteristics of climate variability over the North Atlantic highlights the complexity of finding a robust signal detection of ENSO, which is related to the poor skill of current seasonal forecast systems over Europe (Van Oldenborgh and Burgers, 2005). However, the available literature point to a robust ENSO response (Brönnimann, 2007), seasonal dependent (Moron and Gouirand, 2003; Mariotti et al., 2002), and possibly nonlinear (Wu and Hsieh, 2004; Pozo-Vázquez et al., 2005a). Moreover, the relation between ENSO and the NAE seems to had not been stationary in time (Knippertz et al., 2003; Sutton and Hodson, 2003; Gouirand and Moron, 2003; Greatbatch et al., 2004). Hence, the seasonal predictability of European climate through ENSO might be variable and much greater than expected, at least, for specific time periods. Thus, the need for stronger effort to characterise, quantify, and understand this possible non-stationary link between ENSO and the NAE at interannual timescales is needed. This issue, which is introduced with more details in the next subsection, is the main objective of the present thesis.

2.4.1 Non-stationary behaviour

The changing signal identified over the North Atlantic during ENSO years could be attributed to the chaotic behavior of the atmosphere system (internal variability), or to a cause and effect relationship associated with an external forcing. In the latter case, two plausible reasons arise: (1)

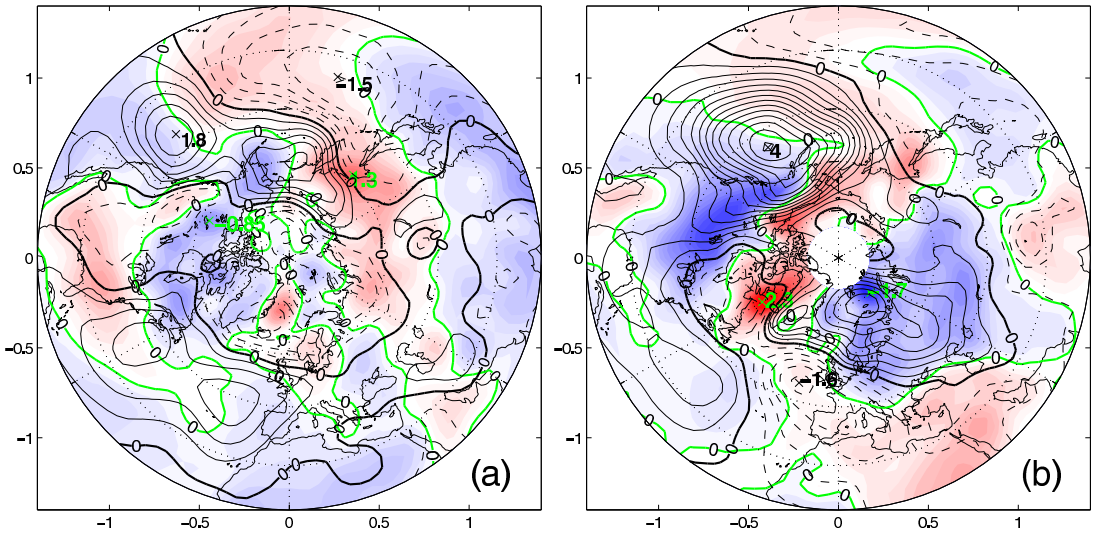

Figure 2.19: Linear regression of NCEP-NCAR SLP (contours) and 1000mb temperature (color shading) against the SOI index during 1958-1977 (left) and 1978-1997 (right). From Greatbatch et al. (2004).

a changing ENSO forcing and (2) a changing propagation mechanism of ENSO signal from the Pacific towards the North Atlantic.

Regarding the non-stationary ENSO forcing associated with SSTs, Greatbatch et al. (2004) suggest that the ENSO-related signal emerging from the tropics was 2 or 3 times stronger in amplitude in 1978-1997 time period than before (1958-1977), which might lead to different impacts in Europe (Figure 2.19). This fact could be explained by the changes along the 20th century in the strength of ENSO (Sutton and Hodson, 2003; Torrence and Webster, 1998) and by the existence of different ENSO modes before and after the 1970s *Climate Shift* (An et al., 2006). According to the latter, Larkin and Harrison (2005) find a different signal of ENSO over Europe depending on the location of the stronger SST anomalies (in the eastern or in the central tropical Pacific). Related to this, EP and CP ENSO events have in recent years caught quite some attention, specially due to the possibility that they could be excited by changes in the background state (Fedorov and Philander, 2000; Wang and An, 2002; An et al., 2006; Yeh et al., 2009; Choi et al., 2011; Chung and Li, 2013), being the aforementioned 1970s *Climate Shift* one of these changes.

It is also interesting that these distinguishable El Niño events, which are controlled by distinct dynamics (Ashok et al., 2007), seem to impact differently at extratropical latitudes, being however the available papers not coherent among them. Thus, while Hegyi and Deng (2011) find that CP warm events leads to an anomalous ridge (opposite to canonical warm events) over the North Pacific, Graf and Zanchettin (2012) find that they lead to an anomalous trough in the same area

(even stronger than canonical warm events). As a consequence, the former authors associate CP warm events with the positive phase of the AO, while the latter authors associate it with a negative NAO. In addition, the role of the background state in favouring the occurrence of EP and CP ENSO events, and their related non-stationary impacts on extratropical regions such as the NAE, is still far to be completely understood. It is also appropriated to note how remote impacts associated with tropical convection are sensitive to absolute rather than anomalous values of SST and so, spatial displacements of those areas where deep convection take place could depend on, not only the anomalous ENSO signal, but also the underlying SST background state.

Regarding the non-stationary propagation of ENSO signature, Sutton and Hodson (2003) provide strong evidences about that the influence of the oceans on interannual variability in the North Atlantic has been important from 1871 to 1999 except for central decades of the 20th century, attributing this changing influence to, not only the varying ENSO variability (Torrence and Webster, 1998), but also the multidecadal variation in Atlantic Ocean SSTs (Kerr, 2000). Although they consider these two causes as independent among them, the possibility that they may be related in some way is also noted. A similar idea is proposed by Dong and Sutton (2002), who suggest that slow variations in the Atlantic thermohaline circulation could modulate ENSO. Finally, Kang et al. (2014) recently demonstrate that there is an AMO influence on the basic state in the tropical Pacific and, as a consequence, on ENSO. A remaining question is if the low frequency ocean variability of the Atlantic (or other ocean basins) could also modulate the propagation of the ENSO signal and not only the ENSO phenomenon itself.

As described in Section 4.2.1, propagation of extratropical Rossby waves strongly depend on the intensity and spatial configuration of the zonal mean flow. Thus, in those regions where jet-streams are weak the perturbations are meridionally propagated describing an arching pattern; whilst in those regions where jet-streams are intense the planetary waves are efficiently trapped in the zonal flow describing a global hemispheric pattern (Hoskins and Karoly, 1981; Branstator, 1983, 2002; Hoskins and Ambrizzi, 1993; Ambrizzi et al., 1995). Considering that extratropical jetstreams are partially caused by the meridional gradient of temperature in the Earth's atmosphere (see Equation 2.1), a change in their spatial configuration and so, an alteration in tropical-extratropical teleconnections through Rossby waves, is expected if the underlying surface temperatures vary along the time. According to this, the changing ENSO signal over NAE sector identified in previous studies could be partially explained by variations in the preferential pathways of Rossby wavetrains from the tropical Pacific to the North Atlantic, which in turn could be modulated by low frequency changes in the underlying SSTs.

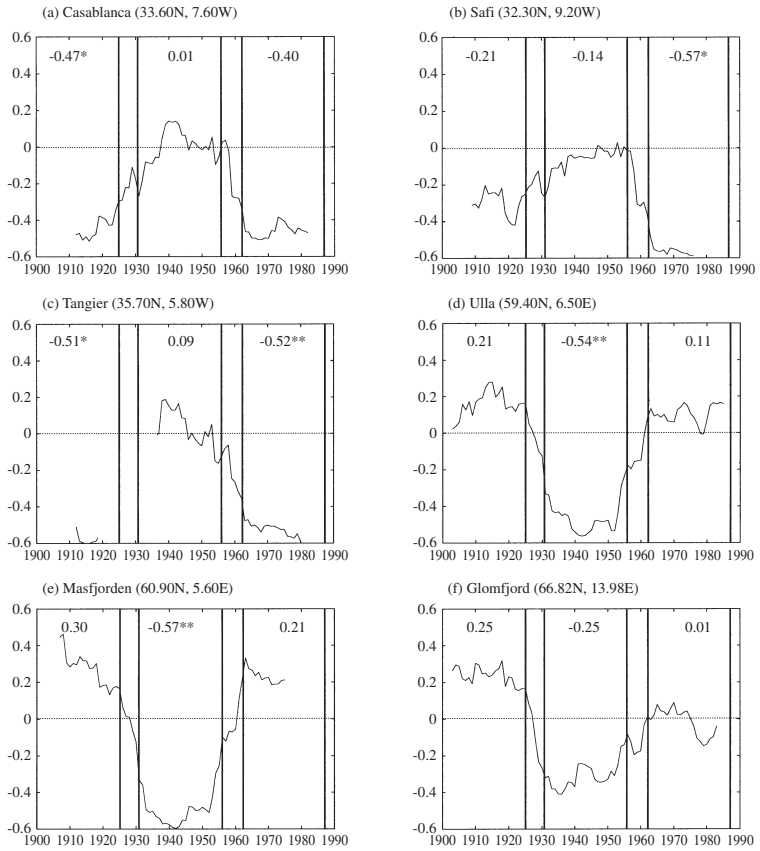

Figure 2.20: The 25 year running correlations between winter (DJF) NIÑO3 index and spring (MAM) precipitation for several Moroccan and Norwegian stations for the period from 1900 to 1990. The correlation value is assigned to the middles of the 25 year windows. Only periods for which at least 15 years of data are available were plotted. Vertical black lines indicate the limits of the investigation periods chosen. The correlation value for each period is given in the respective figure. Asterisks indicate significance at the 95% (*) and 99% levels (**). From Knippertz et al. (2003).

As it was disclosed before, many studies point to a non-stationary link between ENSO and the NAE sector. Regarding a changing impact in precipitation, Knippertz et al. (2003) distinguish three periods representing different characteristics with regard to the relation of ENSO with European-North African rainfall and the NAO: 1900-1925 and 1962-1987 which display similar signatures, and an anomalous period from 1931 to 1956 (Figure 2.20). This changing link basically agrees with Mariotti et al. (2002), who found a variable impact of ENSO over western Mediterranean rainfall. However, the possible modulating factor of these non-stationary features is still unknown. Zanchettin et al. (2008) attribute a changing ENSO-related response in European wintertime rainfall, specially in central Europe, to multidecadal phases of the PDO/IPO. Nevertheless, they also suggest the need to reduce the degrees of freedom of this type of problems involving distinct dynamics occurring at different timescales. To that end they propose, for instance, to isolate the timescales we are interested in by a filtering procedure, or to focus the analysis just on a few

empirical orthogonal functions. However, it cannot be ruled out that these variable features could reflect stochastic fluctuations rather than long-term physical changes in the climate system, as it is noted by Knippertz et al. (2003). Furthermore, several studies speculate that these non-stationary behaviours, specially those identified before an after the 1970s *Climate Shift* might be an artefact due to the low observational coverage prior the 1970's, and specifically, the lack of satellite data. This implies that many of the studies carried out along the last 20 years are based on reanalysis covering both, the pre-satellite and post-satellite periods, which could introduces spurious non-stationary features.

Related to this Van Oldenborgh and Burgers (2005) find little evidence for a changing behaviour of ENSO teleconnections with global precipitation during the instrumental period, but with the possible exception of Europe. However, other studies based on Global Circulation Climate Models (GCM) point to a true non-stationary link. Raible et al. (2001) observe two decadal regimes for NAO-variability in ECHAM4 model simulations, being only one of them linked to ENSO. They attribute this fact to a non-stationary mode with a PNA pattern and connections with the tropics and the North Atlantic. A variable link between PNA and NAO in both, observations and multicentury coupled GCM simulations, is found by Pinto et al. (2011). Considering that PNA is closely related to ENSO variability, this fact also addresses to a non-stationary link between ENSO and the NAE sector.

As it has been exposed along this section, a large amount of works point to non-stationary signatures of ENSO on extratropical latitudes. However, a physical explanation for the possible underlying mechanisms has been little analysed in the available literature. In particular, the role that ocean mean state could play as modulator of ENSO teleconnection with extratropical climates has been disregarded along the last decades. As a consequence, nowadays, the assumption of stationary predictor-predictand relationships is still usually considered, which could be crucial for those regions where the skill of seasonal forecast systems is poor, as is the case of Europe and the Mediterranean region.

3

Objectives

In view of the state of the art described in the previous chapter, the general objective of the present thesis is to shed light on a possible non-stationary behaviour of the ENSO teleconnection with the NAE climate, with special attention to the impact on European and Mediterranean rainfall (denoted in this thesis as EMedR) in late winter and early spring.

This general objective is divided into the following specific goals:

1. **To detect the leading EMedR variability mode and its relation to ENSO in the observational record.**
   - *Is this relationship stationary in time?*

2. **To analyse the physical mechanisms associated with the teleconnection between ENSO and the leading EMedR mode and its evolution in time.**
   - *Which dynamical mechanisms could explain a changing teleconnection?*
   - *Could these non-stationary features be attributed to a modulation associated with variations in the ocean background state?*

3. **To evaluate the internal contribution, associated with the coupled ocean-atmosphere climate system, to the stationarity of the teleconnection between ENSO and the leading EMedR mode.**
   - *Is the observational ENSO-related impact on the leading EMedR mode reproduced in absence of external forcings?*
   - *Is the teleconnection between ENSO and the leading EMedR mode non-stationary under these circunstances?*

- *Which is the modulating factor and associated mechanisms?*

4. **To assess the ENSO-related impact over Europe and the Mediterranean region for distinct ENSO forcings and SST mean states.**

   - *Which differences in the atmospheric response are identified between El Niño and La Niña episodes?*
   - *Which differences in the atmospheric response are identified between Central Pacific and Eastern Pacific events?*
   - *Which differences in the atmospheric response are identified between normal and strong ENSO events?*
   - *How sensitive are all these ENSO-related responses to the underlying SST background state?*

4

Basic Concepts of Atmospheric Teleconnections

I want to know (...) I want to know where the wind comes from

Quiero saber (...) Quiero saber de donde viene el viento

Dalton Trumbo,
Spartacus

As it has been previously noted the concept of *atmospheric teleconnection* is related to linkages over great distances of seemingly disconnected weather anomalies. These teleconnections are interesting on its own, but those associated with SST processes are of special importance. The reason lies in the tendency of the oceans to transfer more slowly the heat with its surroundings than others climate subsystems, like the atmosphere. This *thermal inertia* of the oceans provides a forecast tool that could be used by decision-makers to mitigate the impacts, or even to take advantage of teleconnected climate events. This predictive capability on seasonal, annual, or even decadal timescales, is considered as an important matter for the climate research community.

The region where a teleconnection is triggered is known as *forcing area*, and in case of an ocean-related teleconnection, it is usually associated with zones of strong ocean-atmosphere interactions. In these regions, intense vertical movements of the air take place, causing changes at the upper troposphere. As a result, relative pressure differences between surface and upper levels produce a *baroclinic structure* of the atmospheric column. As a consequence, different interactions occur in zonal and meridional directions due to changes in the divergent (or irrotational) and the non-divergent (or rotational) flow, which induce variations on distant regions. Thus, an atmospheric teleconnection is established.

In the next subsections the theoretical framework supporting the tropical-extratropical teleconnetions mechanims (such as that related to ENSO-NAE link), is thoroughly described in terms of divergent and rotational flow. This separation of the rotational and the divergent parts of the

total horizontal wind $\vec{V}$ is afforded by the two-dimensional Helmholtz theorem (Mancuso, 1967; Krishnamurti, 1971; Krishnamurti et al., 1973; Stephens and Johnson, 1978; Sardeshmukh and Hoskins, 1985, 1987):

$$\vec{V} = \vec{V_\psi} + \vec{V_\chi} \tag{4.1}$$

$$\vec{V} = \vec{k} \times \bigtriangledown\psi + \bigtriangledown\chi \tag{4.2}$$

being ψ the streamfunction, χ the velocity potential, $\vec{k}$ the local unit normal vector, and $\bigtriangledown$ the horizontal gradient operator.

4.1 Divergent circulation

Velocity potential, χ, is a scalar potential related to non-rotational fields, which in turn are associated with atmospheric vertical motions. This magnitude can be expressed by the continuity equation in the isobaric system (Holton, 1992) as:

$$\bigtriangledown \cdot \vec{V_\chi} + \frac{\partial\omega}{\partial p} = 0 \tag{4.3}$$

$$\omega(p) = \int_p^{p_s} (\bigtriangledown \cdot \vec{V_\chi}) dp \tag{4.4}$$

where ω is the vertical velocity in isobaric coordinates, p the pressure at a specific level in the atmosphere, and p_s the pressure at surface.

According to this, in the tropics, where atmospheric and oceanic heating associated with convection induces changes in the horizontal convergence and divergence, vertical movements in the atmospheric column are driven (Equation 4.4.). A so-called *deep-convection* situation is found if these vertical motions take air parcels from lower troposphere up to levels above 500hPa, which generally requires SSTs exceeding a threshold of 26º-28º (Graham and Barnett, 1987). Under these circumstances, low level convergence and upper level divergence occurs and, as a consequence, a direct circulation is found in zonal and meridional directions. Thus, anomalous Walker and Hadley Circulation Cells are established, respectively (see Section 2.1).

Considering the Equation 4.4, the atmospheric teleconnection mechanisms associated with these thermally driven circulation cells, usually known as "atmospheric bridges", are best characterized in terms of the divergent component of the flow (Figure 4.2). Thus, along this thesis, those part of the ENSO-NAE link associated with changes in Walker and Hadley circulations are described through variations in the velocity potential field, χ (see Section 5.1.3).

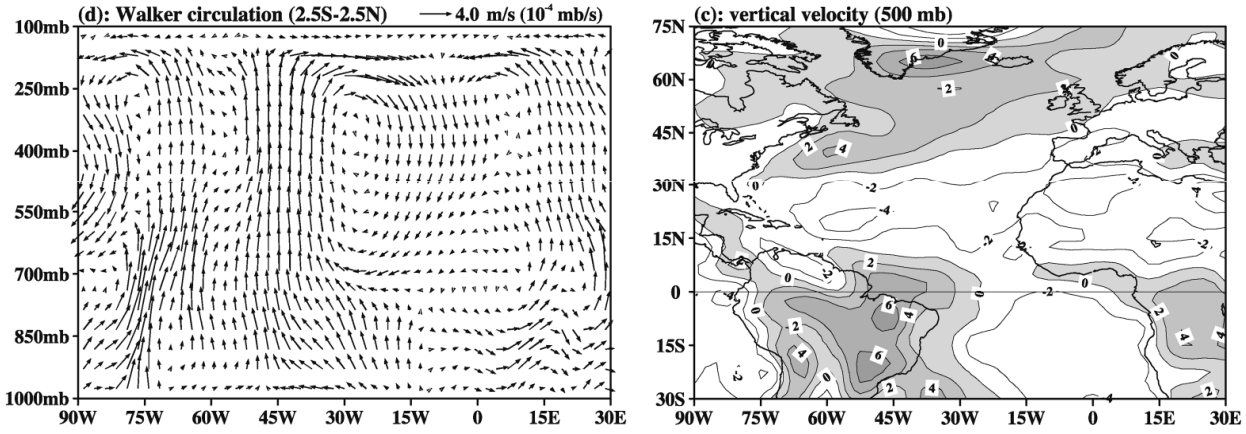

Figure 4.1: The boreal winter (January) climatologies of tropospheric circulation patterns. Left, zonal-vertical circulation cross section by averaging divergent wind and vertical velocity between 2.5°S and 2.5°N (left). Right, 500-mb vertical velocity ($10^{-4}mbs^{-1}$). Modified from Wang (2002a).

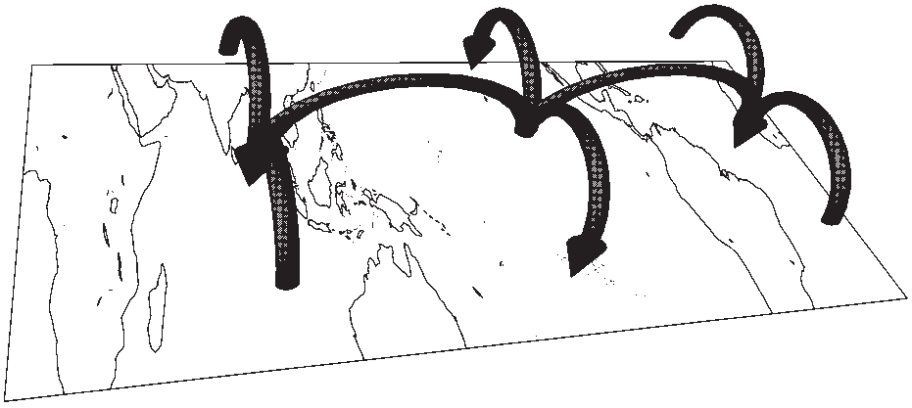

Figure 4.2: Schematic diagram indicating some of the tropical changes in large-scale vertical motion that accompany El Niño events. From Klein et al. (1999).

4.2 Rotational Circulation

The definition of a purely non-divergent flow implies that $\bigtriangledown \cdot V_\psi = 0$. According to this, and neglecting the vertical advection and twisting terms, *Vorticity Equation* can be written (Holton, 1992) as:

$$\frac{d(\zeta + f)}{dt} + (\zeta + f) \bigtriangledown \cdot \vec{V_\chi} = 0 \tag{4.5}$$

where ζ represents the vertical component of the vorticity with respect to the Earth (the relative vorticity), and f represents the planetary vorticity (Coriolis parameter). The sum of both, $\zeta + f$ is known as absolute vorticity.

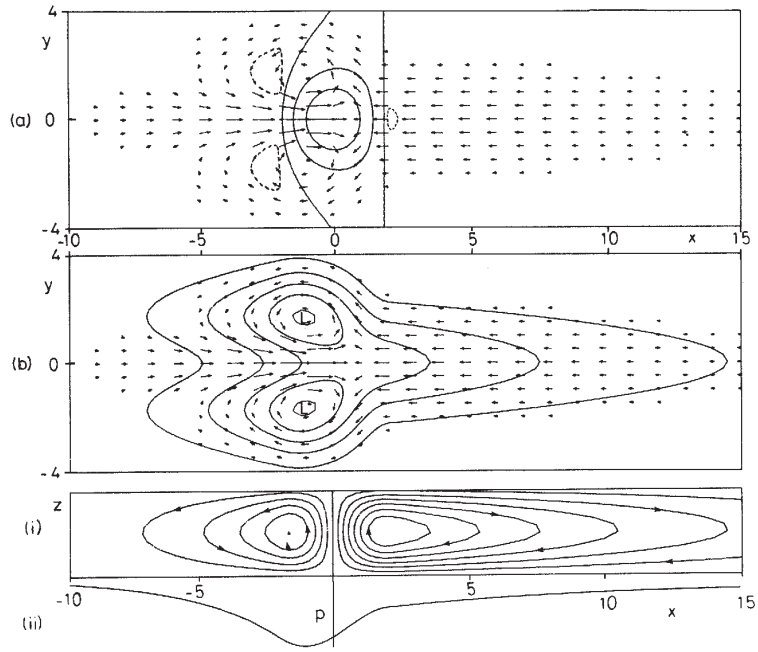

Figure 4.3: Atmospheric response to an anomalous equatorial heating. From top to bottom: (1) surface winds (vectors) and vertical velocity (contours), (2) surface winds (vectors) and SLP (contours), and (3) circulation along the equator. From Gill (1980).

When $\vec{V}$ is decomposed into the rotational and the divergent part (see Equation 4.1), Vorticity Equation can be stated as:

$$\frac{\partial \zeta}{\partial t} + \vec{V_\psi} \cdot \bigtriangledown(\zeta + f) = -(\zeta + f) \bigtriangledown \cdot \vec{V_\chi} - \vec{V_\chi} \cdot \bigtriangledown(\zeta + f) \tag{4.6}$$

where terms on the left describe the propagation of planterary waves, or *Rossby Waves*, and terms on the right represent the so-called Rossby waves sources (Sardeshmukh and Hoskins, 1988; Qin and Robinson, 1993).

In tropical latitudes, Rossby waves sources can be associated with upper-level divergence induced by equatorial SST anomalies. The atmospheric response to this equatorial heating (Figure 4.3) is well captured by baroclinic models (Davey and Gill, 1987) and is characterised by a pair of low (upper) level cyclones (anticyclones) located poleward and to the west of the heat source, and low pressure that extends well to the east of the anomalous heating (Matsuno, 1966; Gill, 1980). This equatorial signal is associated with a *kelvin wave* travelling to the east, while the off equatorial signature reflects the first centre of action of a extratropical Rossby wave moving to the west. This response has a baroclinic structure. The resultant response at extratropical latitudes is, however, barotropic. It is analysed in detail in the next subsection.

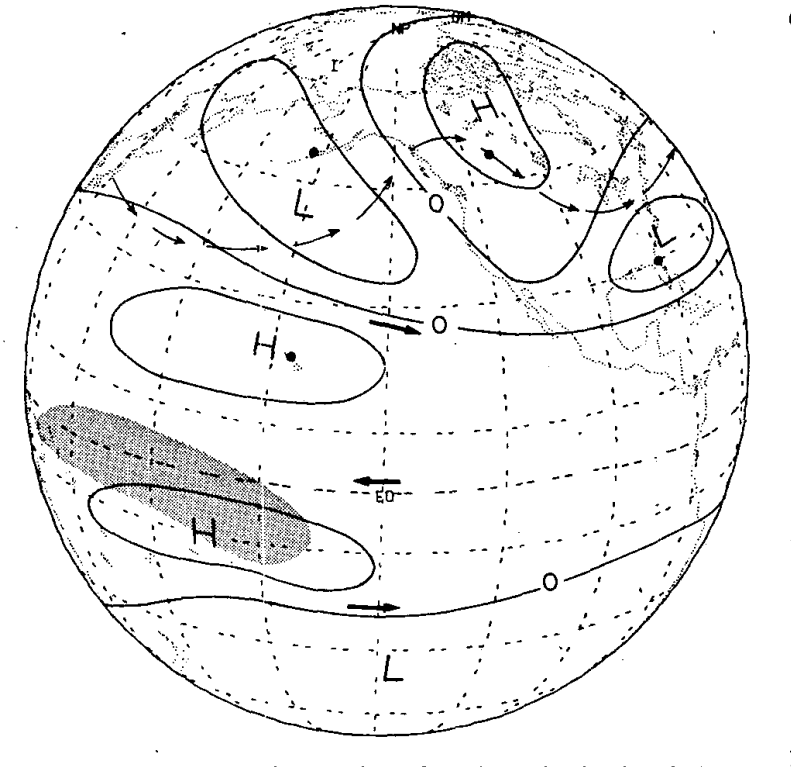

Figure 4.4: Schematic illustration of the hypothesised global pattern of middle and upper tropospheric geopotential height anomalies (solid lines) during a Northern Hemisphere winter which falls within an episode of warm SSTs in the equatorial Pacific. From Horel and Wallace (1981).

4.2.1 Extratropical Wave Propagation

In extratropical regions, the previous described Gill-Matsuno model completely fails (Lee et al., 2009), and the rotational flow is properly represented by a barotropic non-divergent model in which the horizontal divergence $\bigtriangledown \cdot V_\chi \approx 0$ and so, according to Equation 4.4, vertical movements are negligible ($\omega \approx 0$; Hoskins and Karoly, 1981; Branstator, 1983; Hoskins and Ambrizzi, 1993). Under these circumstances, Equation 4.5 (and Equation 4.6) can be simplified as:

$$\frac{d(\zeta + f)}{dt} = 0 \tag{4.7}$$

Thus, extratropical Rossby Waves are considered as alternating high and low pressure systems in which the absolute vorticity $\zeta + f$ is conserved (Figure 4.4). They are, in stationary conditions, of order of the distance between the large scale semi-permanent troughs and ridges in the middle troposphere (AMS Glossary, 2015).

Recasting the vorticity in terms of streamfunction ($\zeta = \bigtriangledown\psi^2$), and considering a basic flow with zonal wind only dependent on latitude, and no meridional wind:

$$\frac{d \bigtriangledown \psi^2}{dt} + (\beta - \frac{\partial^2 U}{\partial y^2})\frac{\partial \psi}{\partial x} = 0 \tag{4.8}$$

where β represents the change of planetary vorticity with latitude ($\frac{\partial f}{\partial y}$) and U the mean zonal flow. Now, introducing a two dimensional wave-like form for streamfunction ($\psi = e^{i(kx+ly-wt)}$), results in the following dispersion relationship:

$$\omega = kU - k\frac{\beta}{k^2 + l^2} + k\frac{\frac{\partial^2 U}{\partial y^2}}{k^2 + l^2} \tag{4.9}$$

for which the total wavenumber K_s, for stationary Rossby waves ($\omega = 0$), is:

$${K_s}^2 = k^2 + l^2 = \frac{\beta - \frac{\partial^2 U}{\partial y^2}}{U} \tag{4.10}$$

being k and l the zonal and meridional wave numbers, respectively.

According to this, the angle α made by the Rossby wavetrain with the x axis (west-east direction) is given by:

$$cos\alpha = \frac{k}{K_s} = k\sqrt{\frac{U}{\beta - \frac{\partial^2 U}{\partial y^2}}} \tag{4.11}$$

Therefore, according to the linear barotropic equation analysed here, extratropical Rossby waves propagation highly depends on the intensity and spatial configuration of the surrounding zonal mean flow U and, as a consequence, of the extratropical jet streams. As it is shown in Branstator (2002), for those regions in which the jet is weak the disturbances tend to be arch shaped, having a prominent meridional structure but much more limited zonal extend (bottom in Figure 4.5). In these cases, Rossby waves associated with tropical adiabatic heating are efficiently propagated towards high latitudes, being refracted towards lower latitudes in the point where $K_s = k$ ($cos\alpha = 1$). On the contrary, for those regions with strong zonal mean flow, Rossby waves are organized in chains that stretch out in the zonal direction (top in Figure 4.5). This *waveguide effect* of the zonal mean flow at upper troposphere, which has been thoroughly analysed by several authors (Hoskins and Karoly, 1981; Branstator, 1983; Hsu and Lin, 1992; Hoskins and Ambrizzi, 1993; Ambrizzi et al., 1995; Ding and Wang, 2005), plays an important role for tropical-extratropical teleconnections. Hoskins and Ambrizzi (1993) show how Rossby ray paths are refracted in a manner similar to that described by Snell's law in Optics. According to

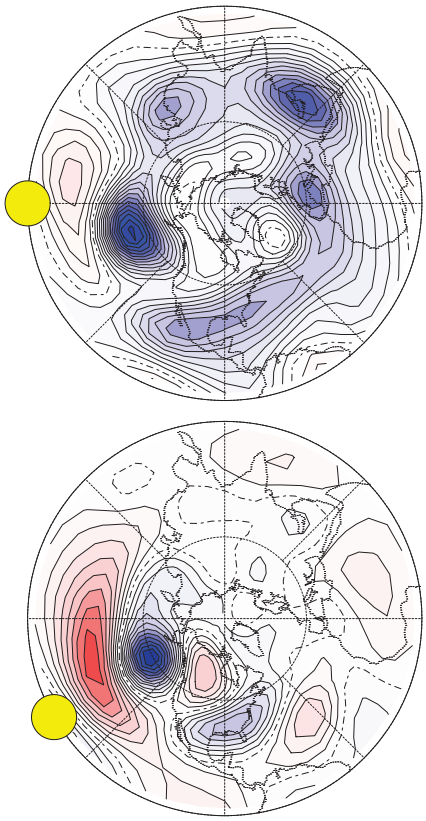

Figure 4.5: Anomalous 300hPa streamfunction response of the AGCM NSIPP1 to equatorial heating at (top) 180W and (bottom) 150W. See Branstator (2004) for details.

this, the radius of curvature of the Rossby waves pathway is given by the simple expression:

$$r = \frac{{K_s}^2}{k\frac{dKs}{dy}} \tag{4.12}$$

Thus, as they demonstrate in the mentioned paper, Rossby rays are always refracted towards latitudes with larger values of K_s (Figure 4.6a), being the curvature clockwise if K_s increases towards the equator and anticlockwise if it increases towards the pole. Hence, K_s behaves like a refractive index for stationary Rossby waves. As it is previously noted, if a Rossby wave reaches a certain latitude Y_{TL} at which $K_s = k$ ($l = 0$), it is reflected (Figure 4.6b). In addition, following the notation of Figure 4.6b, given a local maximum in K_s, a planetary wave whose total wavenumber is between $K_s = K1$ and $K_s = K2$, is trapped. This maximum in K_s provides, therefore, a Rossby waveguide. And the higher this local maximum, the higher is the rank of allowed values of wavenumber. Furthermore, according to Equation 4.11, if the spatial configuration of the mean flow is such that K_s is high, $cos\alpha \approx 0$ and $\alpha \approx \frac{\pi}{2}$, and hence, meridional propagation of Rossby waves is favoured. This reasoning is used along this thesis to address whether the Rossby waves associated with ENSO are guided or not by the zonal mean flow at upper levels in a pathway towards

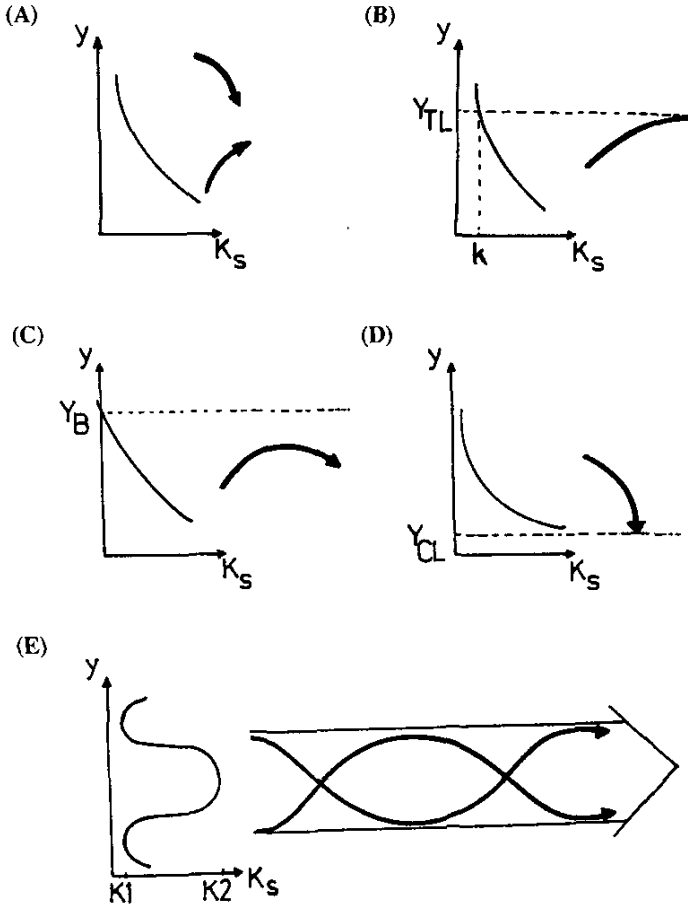

Figure 4.6: Schematic Ks profiles and ray path refraction. In each panel, Ks is shown as a function of y and schematic ray path shown by heavy lines with arrowheads. a) simple refraction; b) reflection from a turning latitude Y_{TL} at which $Ks = k$; c) reflection of all wavenumbers before Y_B at which ($\beta - \frac{\partial f}{\partial y} = 0$); d) refraction into a critical latitude Y_{CL} at which $U = 0$; e) waveguide effect of a Ks maximum. From Hoskins and Ambrizzi (1993).

the NAE sector. It is necessary to note, however, how this discussion in terms of a refractive index, based on linear theory, is clearly inadequate in the so-called *critical line*, which is reached when the wave phase speed matches the zonal wind speed and K_s becomes infinite. The reason is that in the vicinity of this area the nonlinear effects become important (Warn and Warn, 1978; Brunet and Haynes, 1996; Abatzoglou and Magnusdottir, 2006). Hence, the results obtained around this critical line, which for stationary waves corresponds to the region where the westerly zonal wind changes to easterlies (Lin et al., 2007), should be interpreted with caution.

5

Data and Methodology

To observe is to look at what is different among things which are similar.
To understand is to look at what is common among things which are different,
or in a compact way, to look for the minimum expression of the maximum sharing.
All human knowledge is an oscillation between observation and understanding.

Observar es mirar qué hay de diferente entre cosas que se parecen.
Comprender es mirar qué hay de común entre cosas diferentes,
o de manera compacta, buscar la mínima expresión de lo máximo compartido.
Todo conocimiento humano es una oscilación entre observación y comprensión.

Jorge Wagensberg Lubinski,
IV seminario de Creatividad e Inclusión social

In this section, the data used along this thesis, which are basically compounded by observations, reanalysis, and simulated data from General Circulation Models, are described. Also, the different techniques and methods applied to extract the information from climate variability, and to evaluate the statistical significance of the results, are shown.

5.1 Data Description

Along the different studies that compose this thesis, the following types of data are analysed:

1. Data from Observations and Reanalyses.

2. Data from ocean-atmosphere coupled models.

3. Data from sensitivity experiments performed with an atmospheric general circulation model.

5.1.1 Observational Data and Reanalyses

Along this thesis gridded data based on surface observations and reanalysed data are combined. The former are based on measurements made from ships, buoys (both moored and drifting), and real stations, representing, in principle, the real data. Complex regressions and interpolation methods are used to generate values on a regular grid from the irregular station network, which facilitate their use for climate research studies. However, these observational data at a global scale are often inadequate due to the sparse coverage in space and time, and the lack of precision and accuracy because of deficient instrumentation or maintenance. On the other hand reanalyses, for which variable in time observations networks are integrated in a climate forecast model, provide gridded datasets of many atmospherics and oceanic variables with a temporal resolution of a few hours. These homogeneous reanalysed products have also problems, as the assimilation schemes and resolution of different models, and the choice of observations, can produce some large differences among the distinct reanalyses databases. Particularly deficient are these data in those regions where no observations are available, as they are determined only by the forecast model. Thus, considering that real data is *somewhere* between model outputs and observational measurements, a combination of both, is often convenient.

Two main variables are used along this thesis to characterise the ENSO impact on Europe and the Mediterranean: Sea Surface Temperature (SST) and precipitation. To avoid possible spurious non-stationary features from non-homogeneous satellite data (see Section 2.4.1), SST and precipitation databases based on: (1) gridded data based on surface observations, or (2) non satellite-based re-analysed products, are considered.

Regarding SST, monthly mean values from the *Extended Resconstructed Sea Surface Temperature* (ERSSTv3b; Smith et al. (2008)) and the *Hadley Centre Sea Ice and Sea Surface Temperature* (HadISST; Rayner et al. (2003)) are used. The former data are based on historical observations from the International Comprehensive Ocean-Atmosphere Data Set (ICOADS), which is probably the most complete and heterogeneous collection of surface marine data in existence. The resultant ERSSTv3b database, for which statistical methods that allow stable reconstruction using sparse data are applied, covers almost the whole globe (88^{o}S-88^{o}N), with a spatial resolution of 2^o longitude x 2^o latitude, from 1854 to the present. In contrast to previous ERSST versions, ERSSTv3b does not include satellite data, which prevent small residual biases. HadISST is obtained by interpolation of observed data from Met Office Marine Data Bank (MDB), including also observations from ICOADS where there were no MDB data. Sea ice data are taken from digitised charts and microwave retrievals, among others. HadISST is also a very useful globally-complete database in atmospheric research, being provided on a 1^o longitude x 1^o latitude grid, and covering

Table 5.1: Description of the observational and reanalyses data used in this thesis

Variable	Acronym	Data set	Resolution	Time coverage	Reference
Sea Surface Temperature	SST	*ERSSTv3b*	2º x 2º	1854 onwards	Smith et al. (2008)
		HadISST	1º x 1º	1870 onwards	Rayner et al. (2003)
Precipitation	PCP	*Delaware*	0.5º x 0.5º	1900-2008	Matsuura and Willmott (2009)
		GPCC	0.5º x 0.5º	1901-2007	Schneider et al. (2008)
Sea Level Pressure	SLP	*20CR*	2º x 2º	1871-2010	Compo et al. (2011)
		*NCAR**	5º x 5º	1899-2009	Trenberth and Paolino (1980)
Zonal and Meridional flow	U,V	*20CR*	2º x 2º	1871-2010	Compo et al. (2011)

* Only available for the domain 12.5ºN-90ºN.

a time period from 1870 to the present.

Regarding precipitation, the data used along this thesis are the rainfall data Version 3.02 from the *University of Delaware* (Delaware; Matsuura and Willmott (2009)) and the Full Data Reanalysis Product Version 4 from the *Global Precipitation Climatology Centre* (GPCC; Schneider et al. (2008)), being both of them based on quality-controlled *in situ* data from thousands of stations world-wide. Delaware data, which spans 1900-2008 time period, is compiled from several updates sources including the Global Historical Climatology Network (CHCN2), the GC-Net data (Steffen et al., 1996), the National Center for Atmospheric Research (NCAR) daily India data, and the South American monthly precipitation station records (Webber and Willmott, 1998), among others. Full Data Reanalysis Product V4 (1901-2007) is based on all GPCC stations. Both databases, Delaware and GPCC, are land-only monthly means interpolated in a 0.5º x 0.5º regular grid, which make easy their use for many climate variability studies.

To address the dynamical mechanisms explaining the impact of ENSO over Europe and the Mediterranean, additional variables besides SST and rainfall, are also needed. The 5º longitude x 5º latitude resolution SLP dataset from NCAR (Trenberth and Paolino, 1980), which begins in 1899 and covers the northern hemisphere from 12.5ºN to the North Pole, is used in this thesis. Furthermore, atmospheric fields from the *20th century reanalysis V2* (20CR; Compo et al. (2011))

provided by the NOAA/OAR/ESRL PSD (http://www.esrl.noaa.gov/psd/), are also widely used. In particular, Sea Level Pressure (SLP) and horizontal wind (U and V components) are taken from 20CR. This comprehensive global atmospheric circulation dataset, which is released in a 2º longitude x 2º latitude global grid, spans the whole 20th century, assimilating only surface pressure reports and using observed monthly sea surface temperature and sea ice distributions as boundary condition. It is, therefore, a very useful tool for analysing large climatic anomalous series in model validations and diagnostic studies.

5.1.2 Simulated data

Climate models could be defined as a mathematical representation of the processes that take place in the climate system. They are based on well established physical and chemical principles, being the equations derived from them so complex that they must be solved numerically. In general, the equations are those for momentum, continuity, the equation of state, the thermodynamic energy equation, and water vapor continuity, although simplified sets of governing equations may also be used (AMS Glossary, 2015). Climate models provide a discrete solution in space and time. Depending on the spatial resolution of the numerical grid the time step, which is the interval between one set of solutions and the next, varies: the finer the resolution the shorter the interval between each computation. There is no perfect model for all purposes and so, depending on the objective we were interested in, one type of models or others could be selected. Thus, considering the finite computational capacity, to select the processes that must be explicitly included in the model compared to those that can be neglected or represented simplified, is an important skill for modellers. Even for models with the highest resolutions, simplifications are needed. Furthermore, many processes are still not sufficiently well known to include their detailed behaviour in models. As a consequence, to account for these processes not included explicitly in the model, *parameterizations* are designed, being based on empirical evidence and/or theoretical arguments.

According to the previous paragraph, a way of differentiating between models is related to the complexity of the processes they include. A global description of the climate system is provided by the *General Circulation Models* (GCMs), which simulate explicitly, with as much fidelity as possible, the various processes occurring in the atmosphere, ocean, cryosphere and land surface (Peixoto and Oort, 1992). In climate studies focused on tropospheric teleconnections and involving timescales from interannual to multidecadal, GCMs are classically divided into *Atmospheric General Circulation Models* (AGCMs), *Ocean General Circulation Models* (OGCMs), and *Coupled General Circulation Models* (CGCMs), depending on the physics they explicitly represent. As it has been previously noted climate models also require some inputs derived from observations

or other model studies, which depend on the type of model considered. Hence, for a model that represents explicitly the physics of the atmosphere, the ocean and the sea ice information in the form of *boundary conditions* should be provided. On the contrary, for an ocean model, the ocean dynamics is explicitly included and the atmosphere information is provided. Along this thesis an AGCM, and a set of CGCMs, are used to analyse the ENSO teleconnection with the European and Mediterranean rainfall. They are thoroughly exposed in the next subsections.

5.1.2.1 *pi-Control simulations from CMIP5 Models*

The Coupled Model Intercomparison Project (CMIP) organised by the Working Group on Coupled Modelling (WGCM) and involved in the World Climate Research Programme's (WCRP), was created in 1995 to provide a set of climate simulations, from different ocean-atmosphere-cryosphere-land GCMs, in which some boundary conditions are standardised among the distinct models. In this way research community can study the resultant outputs in a systematic way, which favor a better understanding of the past, present, and future climate changes arising from either natural, unforced variability or in response to changes in radiative forcing, in a multi-model context. From 1995 to the present time, different phases are developed: CMIP1, CMIP2, CMIP3, and the current CMIP5. The CMIP5 protocol (Hibbard et al., 2007; Meehl et al., 2007), which was endorsed by the 12th Session of the WGCM, include two types of climate experiments: (1) long-term integrations (century time scale) started from preindustrial conditions (pre-1850), and (2) decadal prediction experiments (Meehl et al., 2009) initialised with observed ocean and sea ice conditions. In this thesis, control simulations of the long-term integrations (hereinafter *piControl*) in which the pre-1850 conditions are kept constant (quasi equilibrium), are analysed for 18 different CGCM models (Table 5.2). This set of *piControl* simulations is a very convenient tool for assessing the processes associated with internal coupled variability. For this reason, it is used in order to better understand if the non-stationary ENSO-NAE teleconnection can be explained by internal variability of the coupled ocean-atmosphere system (Chapter 6; see López-Parages et al. (2015a)). For complete details about CMIP5 experimental phase please refer to Taylor et al. (2012). It is worthwhile to note that a new CMIP6 phase is already designed in the WGCM 18th Session. Hopefully, it will be available in the next future.

Table 5.2: Description of CMIP5 models. From left to right: Number of model, Acronym of the model, pi-Control simulation length, original horizontal resolution, atmospheric vertical layers, and references.

Nº Model	Acronym*	pi-Control length	Resolution (Lon x Lat)	Atmospheric vertical layers	Reference
1	*BCC-CSM1.1*	500	2.8°	26	Xiao-Ge et al. (2013)
2	*CanESM2*	996	2.8°	40	Chylek et al. (2011)
3	*CCSM4*	501	1.3° x 0.9°	27	Gent et al. (2011)
4	*CNRM-CM5*	850	1.4°	31	Voldoire et al. (2013)
5	*CSIRO-Mk3.6.0*	500	1.9°	18	Rotstayn et al. (2010)
6	*GISS-E2-R*	550	2.5° x 2.0°	40	Schmidt et al. (2014)
7	*GISS-E2-H*	540	2.5° x 2.0°	40	Schmidt et al. (2014)
8	*FGOALS-g2*	700	2.8°	26	Bao et al. (2013)
9	*HadGEM2-CC*	240	1.9° x 1.3°	60	Martin et al. (2011)
10	*HadGEM2-ES*	575	1.9° x 1.3°	38	Martin et al. (2011)
11	*INM-CM4*	500	2.0° x 1.5°	21	Volodin et al. (2010)
12	*MIROC5*	670	1.4°	40	Watanabe et al. (2010)
13	*MIROC-ESM-CHEM*	255	2.8°	80	Watanabe et al. (2011)
14	*MPI-ESM-LR*	1000	1.9°	47	Giorgetta et al. (2013)
15	*MRI-CGCM3*	500	1.1°	48	Yukimoto (2011)
16	*NorESM1-M*	501	1.9°	26	Bentsen et al. (2013)
17	*IPSL-CM5A-LR*	1000	3.8° x 1.9°	39	Dufresne et al. (2013)
18	*MIROC4h*	240	0.6°	56	Sakamoto et al. (2012)

* From top to bottom, in order of appeareance, the institutions involved are: Beijing Climate Center, China Meteorological Administration; Canadian Centre for Climate Modelling and Analysis; National Center for Atmospheric Research; Centre National de Recherches Meteorologiques / Centre Europeen de Recherche et Formation Avancees en Calcul Scientifique; Commonwealth Scientific and Industrial Research Organisation in collaboration with the Queensland Climate Change Centre of Excellence; NASA Goddard Institute for Space Studies; LASG, Institute of Atmospheric Physics, Chinese Academy of Sciences, and CESS, Tsinghua University; Met Office Hadley Centre; Institute for Numerical Mathematics;Atmosphere and Ocean Research Institute (The University of Tokyo), National Institute for Environmental Studies, and Japan Agency for Marine-Earth Science and Technology; Japan Agency for Marine-Earth Science and Technology, Atmosphere and Ocean Research Institute (The University of Tokyo), and National Institute for Environmental Studies; Max Planck Institute for Meteorology (MPI-M); Meteorological Research Institute; Norwegian Climate Centre; Institut Pierre-Simon Laplace.

5.1.2.2 Sensitivity Experiments

Modeling studies in which the response of a climate model to some known or hypothetical change in a forcing is analysed, are called as *Climate sensitivity experiments*. In this thesis an AGCM is used in order to analyse the atmospheric response to specific anomalous SST patterns, being these *prescribed SSTs* therefore the boundary conditions of our experiments. An inherent limitation of these sensitivity experiments is the assumption of an infinitive calorific capacity of the ocean thermal source, that is, the prescribed SST pattern. Another non-realistic feature is the absence of air-sea fluxes impeding the exchange of energy between the ocean and the atmosphere. Nevertheless, in spite of these limitations the sensitivity experiments with AGCMs trough prescribed SST patterns are currently considered as a very helpful tool for identifying cause and effect relationships in the climate system.

Although the knowledge of a specific SST forcing of the climate system introduces a potential source of predictive skill, it is usually accepted that the atmosphere behaves as a chaotic system (Lorenz, 1963; Lorenz and Hilborn, 1995; Palmer, 1993), and so, deterministic predictability is limited. Related to this, multiple integrations, or *ensemble simulations* (McGuffie and Henderson-Sellers, 2005), with a single model using identical radiative forcing scenarios but starting from different initial atmospheric conditions, are performed by climate variability groups. These distinct initial conditions can be used to quantify the random component of interannual variability, whereas the relative similarity between the different *members* of the ensemble is used to quantify the potentially predictable component of variance (Rowell, 1998). The former (internal variability) is represented by the variance; the latter (forced variability) by the ensemble mean. Hence, as more members are considered the correlation between the ensemble mean and the observations increases (Mehta et al., 2000), being therefore the *ideal ensemble* that one with infinitive realizations.

The sensitivity experiments to be discussed along this thesis are all performed with a low resolution version (3.75° x 2.5° lon-lat resolution and 38 levels in the vertical) of the atmospheric component of the Australian Community Climate and Earth System Simulator (ACCESS) model. This model is made up of the Met Office (UKMO) Unified Model AGCM with Hadley Centre Global Environment Model version 2 (HadGEM2) physics (Davies et al., 2005; Martin et al., 2010; Martin et al., 2011). Please refer to Bi et al. (2013) for a more detailed description.

In this thesis ACCESS is partially coupled, in some specific regions, to a simple slab ocean model (Washington and Meehl, 1984; Dommenget and Latif, 2002; Murphy et al., 2004; Dommenget, 2010). Hence, the SSTs of these regions are able to respond to the different spatial patterns of observational SSTs with which the model is forced. A flux correction, however, is required to force the model SSTs to closely follow a reference SST climatology (1950-2010). This

model is used along this thesis in order to evaluate the ENSO-NAE teleconnection under different ocean mean states. To this aim, 50 ensemble members are generated by superimposing different idealised ENSO SST patterns (Dommenget et al., 2013) over distinct SST background conditions (see López-Parages et al. (2015b)).

5.1.3 Rotational and Divergent components of the flow

As it is noted in Section 4, the rotational and divergent parts of the total horizontal wind $\vec{V}$ can be expressed in terms of the streamfunction ψ and the velocity potential χ, respectively. Nevertheless, these variables are not always provided in the observational datasets or model outputs and so, they must be often indirectly calculated. This is the case of this thesis, in which ψ and χ are obtained by solving their respective Poisson equations:

$$\bigtriangledown^2\psi = \zeta \tag{5.1}$$

$$\bigtriangledown^2\chi = D \tag{5.2}$$

being ζ and D the vorticity and divergence of the horizontal flow, respectively. To solve Equation 5.1 and Equation 5.2, a Extension Library for the Open Grid Analysis and Display System (OpenGrADS; http://opengrads.org/doc/udxt/fish/), which only require a global and uniform velocity field $\vec{V}$, is used. The same library is applied in López-Parages et al. (2014) to calculate the so-called *divergent wind*. Details on the algorithms included in the aforementioned library are thoroughly exposed in Swarztrauber and Sweet (1975).

Another variable calculated in this thesis is the *wave activity flux (WAF)*, which is a vector approximately parallel to the local group velocity of Rossby waves. This magnitude can be very useful in snapshot analyses for either migratory and stationary disturbances propagating through a zonally varying basic flow (see Takaya and Nakamura (2001) for further details). In this thesis (López-Parages et al., 2015b) it is computed directly from the zonally asymmetric part of the anomalous streamfunction regression maps (assuming stationary Rossby waves and neglecting vertical movements).

5.2 Methodology

5.2.1 Data Pre-Processing

5.2.1.1 Calculation of Anomalies

As it was introduced in Chapter 2, climate variability studies are often carried out in terms of the fluctuations of a specific climate variable around its mean state, or climatology. For each time step, the climate anomaly is calculated by substracting the mean value from the value at that time:

$$Y'(t) = Y(t) - \overline{Y} \tag{5.3}$$

where $Y(t)$ and $Y'(t)$ represent the absolute and anomalous values at time t, and $\overline{Y}$ represents the mean value. Along this thesis, monthly and seasonal anomalies are calculated according to the expression 5.3, removing in that way the annual cycle (Xoplaki et al., 2003). In particular, as our research is mainly focused on the teleconnection between ENSO and the leading EMedR mode in late winter and early spring, most of the anomalous values calculated in this thesis correspond to FMA-mean anomalies. In some cases, it has been also useful to express the anomalies divided by its standard deviation, defining therefore the so-called *standardised anomalies*. They generally provide more information about the magnitude of the anomalies because influences of dispersion are removed. Specifically, when rainfall is studied in large spatial domains it can present important differences in mean and variance among the different grid points. Furthermore, it does not usually follow a normal distribution. In that cases, its analysis in terms of standardised anomalies is, therefore, very useful.

5.2.1.2 Filtering techniques in time domain

The variability of a physical field is caused by diverse processes happening at different times scales (Von Storch and Zwiers, 2001). Hence, depending on the purpose of the analysis we were interested in, some frequencies could be of greater interest than others and so, it might be useful to reduce the amplitude of variations at other frequencies by statistically filtering them out before analysing the time series. Along this thesis, which is focused on interannual timescales, two different *high-pass filters* have been applied in order to amplify the high-frequency variability (year-to-year) in the time domain.

Fast Fourier Transform filter

This filter is based on a *discrete Fourier transform*, which converts a finite list of equally spaced samples from its original time domain to the frequency domain, in which the isolation of certain bands frequencies of special interest, is made easier. However, the computational time required to calculate these discrete Fourier transforms is usually exorbitant and so, their applications are limited. To solve this problem, some algorithms have been developed. The *fast Fourier transform algorithm* (FFT; Duhamel and Vetterli (1990); Frigo and Johnson (1998)), which is widely used in scientific analysis, has been used in this thesis to isolate the shorter variations (interannual) from those of lower frequencies (decadal and multidecadal). The functions applied in this thesis to implement the transform (Equation 5.4) and inverse transform (Equation 5.5) pair for vectors y and Y of length N can be stated as:

$$Y_k = \sum_{j=1}^{N} y_j {\omega_N}^{(j-1)(k-1)} \tag{5.4}$$

$$y_j = \frac{1}{N} \sum_{k=1}^{N} Y_k {\omega_N}^{-(j-1)(k-1)} \tag{5.5}$$

where $\omega_N = e^{(-2\pi i)/N}$ is one of N roots of unity.

Interannual filter

A second filter used along this thesis is applied by taking the difference between the absolute values of two consecutive years (Equation 5.6).

$$\triangle y = y_t - y_{t+1} \tag{5.6}$$

This procedure, which highly attenuates the amplitudes of low-frequency signals, is widely-used for detrending time series (Bjerknes, 1969; Box and Jenkins, 1976). In this thesis this method is applied, as the FFT, in order to easily distinguish the mechanisms associated with interannual variability. For a further detailed description of this inter-annual filter please refer to Stephenson et al. (2000).

Moving average filter

A third type of filter, usually known as *moving average* or *running mean*, has been also used. However, in this case it is applied in order to highlight decadal and multidecadal cycles, being therefore

considered as a *low-pass filter*. Mathematically, the running mean is a convolution which operates by averaging a number of points from the input signal according to the following expression:

$$y_i = \frac{1}{M} \sum_{j=0}^{M-1} x_{i+j} \tag{5.7}$$

where x is the input signal, y the output signal, and M the number of points in the average. Although the moving mean is a modest *low-pass filter*, it is an exceptionally good *smoothing filter* in which the sharpest step responses are kept (Smith, 1997). Thus, this easy procedure has been used along thesis to detect strong decadal or multidecadal evolution in long time series. Related to this, *running correlations* or *sliding window correlations* have been widely applied along this thesis to assess if correlations between two variables vary in time. The correlation is computed in a window of the first m values, then the window is moved by one position, and the correlation is recalculated. The procedure is repeated until the correlations are obtained for the whole data series.

5.2.2 Discriminant Analysis Techniques

As it has been already mentioned along this thesis, the huge complexity of the climate system makes difficult focusing on specific climatic processes and dynamical mechanisms. To this aim, some statistical discriminant techniques have been developed for helping the researcher to isolate certain directions in which the climate variability is organised. The resultant outputs are usually known as *climate variability modes*. Related to this, two indispensable tools are the so-called *Empirical Orthogonal Functions* (EOF) and *Maximum Covariance Analysis* (MCA). Both are described in detail in the next subsections.

5.2.2.1 Empirical Orthogonal Functions

The *Empirical Orthogonal Functions* (EOF), or *Principal Component Analysis* (PCA), was described by Pearson (1901) and Hotelling (1935), and it was introduced into meteorology by Lorenz (1956) afterwards. This technique is applied in order to determine the directions in which the maximum variability of an anomalous field, mathematically described in a two dimensional space-time matrix, is organised. Let us consider an anomalous field $\overrightarrow{Y'}(t)$ expressed as a set of row vectors $\overrightarrow{Y'}$ (with j elements corresponding to the spatial points) for each time step t. The covariance matrix C is given by:

$$C = \frac{1}{N} \sum_{t} \overrightarrow{Y'}(t) \overrightarrow{Y'}(t)^T \tag{5.8}$$

where $\overrightarrow{Y'}(t)^T$ denotes the transposed matrix of $\overrightarrow{Y'}(t)$. This covariance matrix C, which has j x j dimensions, can be transformed in order to follow the next characteristic equation:

$$|C - \lambda I| = 0 \tag{5.9}$$

The solutions of the Equation 5.9 are, by definition, the eigenvalues λ of the matrix C:

$$C\overrightarrow{e_m} = \lambda_m \overrightarrow{e}_m \tag{5.10}$$

where $\overrightarrow{e}_m$, which is the eigenvector associated with the eigenvalue λ_m, satisfies orthonormality:

$$\begin{cases} \overrightarrow{e_m} \cdot \overrightarrow{e_m}^T = 1 \\ \overrightarrow{e_m} \cdot \overrightarrow{e_n}^T = 0 \quad \text{if } m \neq n \end{cases} \tag{5.11}$$

$$\lambda_m > 0 \tag{5.12}$$

Furthermore, being E the matrix containing the eigenvector $\overrightarrow{e}_m$, it satisfies the next relationship:

$$E^{-1}CE = \Lambda \tag{5.13}$$

where Λ is a positive defined matrix in which all λ_m values are arranged in the main diagonal and 0 values appear in the rest.

In Climate Variability studies the eigenvector $\overrightarrow{e}_m$ represents a spatial distribution usually known as *Empirical Orthogonal Function* (EOF), and its time evolution $\alpha_m(t)$, or *Principal Component* (PC), can be obtained by simply projecting the transposed anomalous field $Y'(t)^T$ onto the transposed $\overrightarrow{e}_m^T$ (Equation 5.14).

$$\alpha_m(t) = \overrightarrow{Y'}(t)^T \cdot \overrightarrow{e_m^T} \tag{5.14}$$

In some cases $\alpha_m(t)$ can be standardised and projected again onto the anomalous field $Y'(t)^T$, so that the units of the resultant $\overrightarrow{e}_m$ are the same as those from the field per standard deviation of $\alpha_m(t)$ (see Section 5.2.4). Finally, $Y'(t)$ could be simply reconstructed as a lineal combination of the M eigenvectors $\overrightarrow{e}_m$ (Equation 5.15).

$$\overrightarrow{Y'}(t) \approx \left(\sum_{m=1}^{M} \alpha_m(t) \cdot \overrightarrow{e_m} \right)^T \tag{5.15}$$

These EOFs ($\overrightarrow{e}_m$) are specified such that the mean squared error (Equation 5.16) is minimal (Von Storch and Zwiers, 2001).

$$mse = \sum_t \left(\overrightarrow{Y'}(t) - \left(\sum_{m=1}^{M} \alpha_m(t) \cdot \overrightarrow{e_m} \right)^T \right)^2 \tag{5.16}$$

It is usually convenient to label the eigenvectors $\overrightarrow{e}_m$ so that the eigenvalues λ_m are in descending order (λ_1>λ_2>λ_3>λ_4>...>λ_M), representing its sum the total variance of the field $\overrightarrow{Y}'(t)$. Hence, this total variance is broken up into M components, being the fraction of variance ($fvar$) associated with each specific mode $\overrightarrow{e}_m$ given by the following percentage:

$$fvar = \left(\lambda_m \Big/ \sum_{m=1}^{M} \lambda_m \right) \cdot 100 \tag{5.17}$$

Thus, EOF analysis is nowadays a useful tool in climate variability, as it captures the time evolution $\alpha_m(t)$ of recurrent spatial patterns $\overrightarrow{e_m}$, representing certain variance λ_m, of the anomalous field $\overrightarrow{Y}'(t)$ (Figure 5.1). However, as the EOFs are constrained by the orthogonality condition (Equation 5.11) and the real-world processes do no need to have orthogonal patterns, the physical interpretation of EOFs should be done with caution. In general, as less variance explains a specific mode, as much more complicated is its physical interpretation. Hence, the optimal election of a number of reliable modes is often difficult. Related to this, North et al. (1982) proposed a criterion by which two consecutive modes can be or not considered as independent (orthogonal) among them. This approximation for the typical error of the estimated EOFs, which has been used along this thesis, considers a mode as independent if the distance between its corresponding eigenvalue with the nearby one is clearly greater than the so-called sampling error (Equation 5.18, being N the number of data).

$$\lambda_m - \lambda_{m+1} > \lambda_m \cdot \sqrt{2/N} \tag{5.18}$$

As it has been previously showed, EOF analysis is very successful in comprising the complicated variability of an original data set into the fewest possible number of modes while retaining most of the total variance. However, while it can represent standing oscillations in time (those that are in phase or out of phase along a data array), it cannot represents, in its simple configuration, features that have variable phase relationships such as propagating waves. Related to this, an extension of the traditional EOF technique has been also developed in order to detect propagating phenomena in multivariate data sets. It is usually denoted as *Extended EOFs* (Weare and Nasstrom, 1982) and its mathematical procedure is essentially the same as for ordinary EOFs, lying the main difference in the preprocessing of the data. Specifically, while in ordinary EOFs the covariance

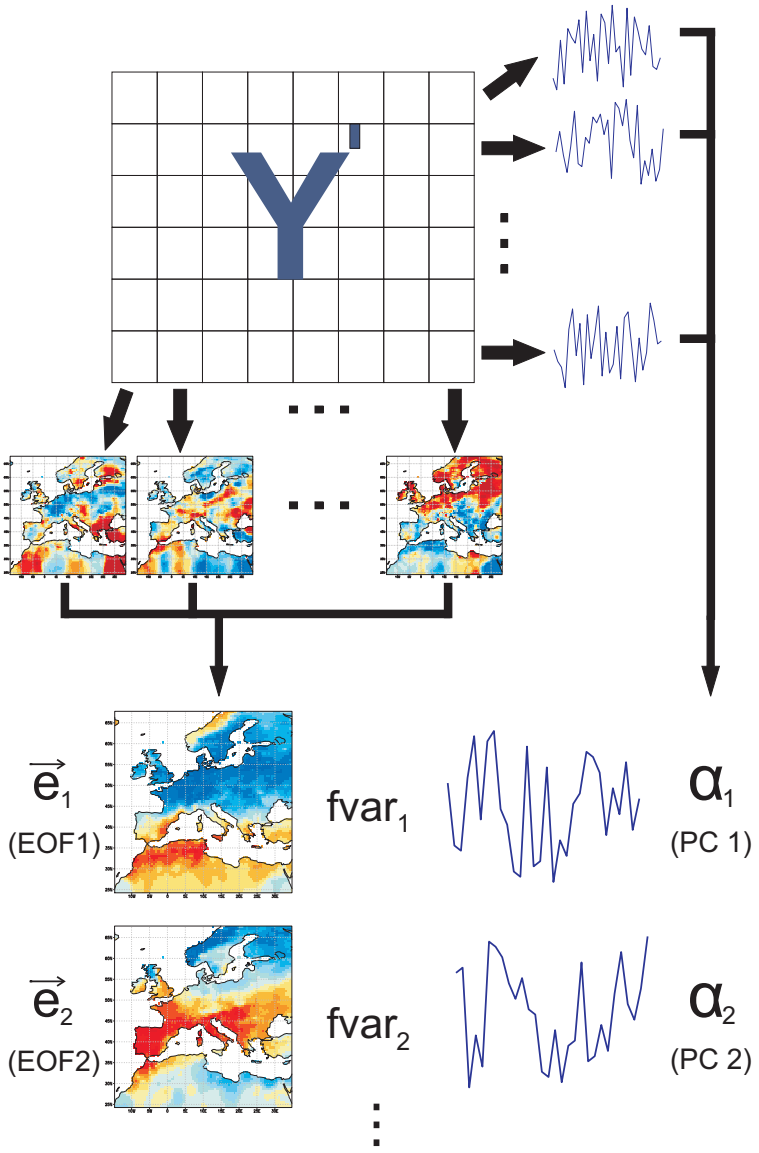

Figure 5.1: Simplified sketch of the EOF analysis. Inspired from Rodríguez-Fonseca (2001).

matrix C contains a certain field of anomalous values measured at different spatial points at a given time ($\overrightarrow{Y}'(t)$), in extended EOFs, C contains the anomalous values of the field at different locations and distinct times $\overrightarrow{Y}'(t1, t2, t3...)$. In this way, the spatial or temporal auto-covariability of the field Y for a number of locations and for different time lags, can be investigated. For a more detailed description of Extended EOFs please refer to Venegas (2001).

An Extended-EOF analysis has been applied at the end of the present thesis (Chapter 7) in order to investigate the teleconnection between El Niño and the EMedR at distinct months along the year.

5.2.2.2 Maximum Covariance Analysis

An analogous technique to the EOF, but searching for pairs of directions that represent the strongest joint patterns of variations, is the *Maximum Covariance Analysis* (MCA). Thus, while EOF is designed in order to detect the main modes of variability of a single variable (Equation 5.3), the MCA (Bretherton et al., 1992) is provided to isolate coupled modes of variability between time series of two distinct variables, which define the usually known as *predictant field* $\overrightarrow{Y'}(t)$ and *predictor field* $\overrightarrow{Z'}(t)$.

MCA is based on the *Singular Value Decomposition* (SVD) mathematical method, which is applied in order to look for linear combinations of the anomalous fields $Y'(t)$ and $Z'(t)$ (Equation 5.19) such that the covariability between the resultant time series (U, V) is maximised (Equation 5.20). As SVD is applied to the covariance matrix C (Equation 5.21), the procedure is usually called as MCA.

$$\begin{cases} Y'(t) & = Y(t) - \overline{Y} \\ Z'(t) & = Z(t) - \overline{Z} \end{cases} \tag{5.19}$$

$$\begin{cases} U = R^T Y'(t) \\ V = Q^T Z'(t) \end{cases} \tag{5.20}$$

$$C = \frac{1}{N} \sum_t \overrightarrow{Y'}(t) \overrightarrow{Z'}(t)^T \tag{5.21}$$

Note that matrix C is a non-diagonalizable matrix due to its non-squared configuration. Nevertheless, considering R and Q as orthogonal matrices, it is possible to find a diagonal and positive defined matrix Λ which satisfies the following relationship:

$$\begin{cases} CC^T & = R\Lambda Q^T Q \Lambda^T R^T = R\Lambda^2 R^T \\ C^T C & = Q^T \Lambda^T R R^T \Lambda Q = Q^T {\Lambda^T}^2 Q \end{cases} \tag{5.22}$$

Thus, the column vectors in R (including the same number of elements of $\overrightarrow{Y'}(t)$) are the eigenvectors of CC^T, and the column vectors of Q (including the same number of elements of $\overrightarrow{Z'}(t)$) are the eigenvectors of $C^T C$. And the M elements in the diagonal of Λ represent the squared values of the eigenvalues associated with the covariance matrix C. According to this, the so-called *squared covariance fraction* (scf) is obtained as:

$$scf_m = {\lambda^2}_m \Big/ \sum_{m=1}^{M} {\lambda^2}_m \tag{5.23}$$

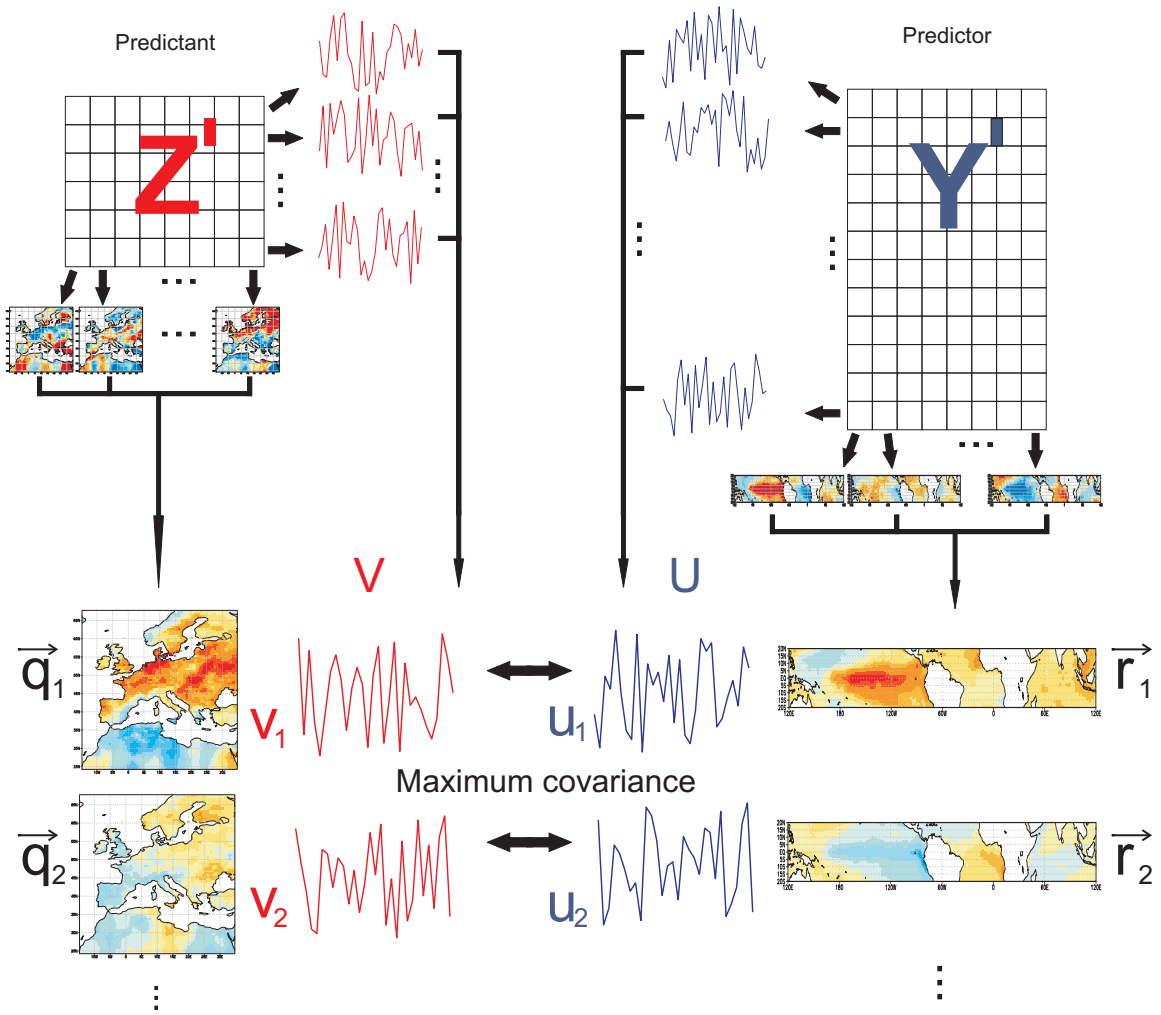

Figure 5.2: Simplified sketch of the MCA analysis. Inspired from Rodríguez-Fonseca (2001).

In this way, similar to EOF analysis, the anomalous fields $Y'(t)$ and $Z'(t)$ can be expressed as a linear combination of the M eigenvectors $\overrightarrow{r_m}$ and $\overrightarrow{q_m}$, respectively (Equation 5.24).

$$\begin{cases} \overrightarrow{Y'}(t) & = \left(\sum_{m=1}^{M} u_m(t) \cdot \overrightarrow{r_m}\right)^T \\ \overrightarrow{Z'}(t) & = \left(\sum_{m=1}^{M} v_m(t) \cdot \overrightarrow{q_m}\right)^T \end{cases} \tag{5.24}$$

where $u_m(t)$ and $v_m(t)$ represent the time series associated with the spatial patterns $\overrightarrow{r}_m$ and $\overrightarrow{q}_m$ for each m mode. These time series, which are equivalent to the PC in EOF analysis (please compare Equation 5.14 and Equation 5.25), are known as *expansion coefficients* (EC).

$$\begin{cases} u_m(t) & = \overrightarrow{Y'}(t)^T \cdot r_m^T \\ v_m(t) & = \overrightarrow{Z'}(t)^T \cdot q_m^T \end{cases} \tag{5.25}$$

5.2.3 Cluster Analysis

Cluster analysis deals with separating data into groups, or clusters, whose identities are not known in advance (Wilks, 2011). The main idea ot this technique is that cluster should be composed of points separated by small distances, relative to the distances between clusters. To this aim, different clustering algorithms exist. In particular, in this thesis a *k-means partitional scheme* from the numerical computing environment *MATLAB* has been used. It is an iterative and data-partitioning algorithm that assigns n observations to exactly one of k clusters defined by centroids (Lloyd, 1982). It is developed in order to minimize the average squared distance between points in the same cluster (Arthur and Vassilvitskii, 2007).

The algorithm proceeds as follows:

1. Randomly choose an observation, from de data set x (with n observations), as the initial centroid (c_1).
2. Compute distances from each observation x_n to c_1 ($d(x_n, c_1)$)
3. Select the next centroid c_2 from x with probability:
$$\frac{d^2(x_n, c_1)}{\sum_{j=1}^{n} d^2(x_j, c_1)}$$
4. To choose centroid j:
   - Compute the distances from each observation to each centroid, and assign each observation to its closest centroid.
   - Select each subsequent centroid with a probability proportional to the distance from itself to the closest center that you already chose:
$$\frac{d^2(x_n, c_1)}{\sum_{[h;x_h \epsilon C_p]} d^2(x_h, c_p)}$$
   where C_p is the set of all observations closest to the centroid c_p and x_h belongs C_p.
5. Repeat step 4 until the k centroids are chosen

Clustering analysis has been widely used in climate variability studies, and very often in relation to rainfall (Michelangeli et al. (1995); Corte-Real et al. (1998); Cassou et al. (2004); Santos et al. (2005); Moron et al. (2008); Polo et al. (2011); Durán et al. (2015), among others). In this thesis, it is applied in order to find those centroids characterizing the distinct manners by which ENSO and the leading EMedR mode are linked in CMIP5 models (see López-Parages et al. (2015a)).

5.2.4 Representation of the Results

Most of the results obtained along this thesis are spatial structures, or maps, associated with specific variations in time (principal components, expansion coefficients, time indices etc). They are:

- *Regression maps*, which are constructed by projecting an anomalous field of a certain variable onto the values of a specific time series, being the latter usually standardised. In these cases the regression map represents the spatial structure of the field associated with the time series, and its values are expressed in units of the specific variable per standard deviation of the aforementioned time series. This is a particularly useful approach, since one standard deviation corresponds to a typical fluctuation in the time series.

- *Correlation maps*, which are obtained by correlating the time series to the time series of the anomalous field at each grid point (Bretherton et al., 1992).

- *Correlation maps*, which are obtained by correlating a particular time series (index, PC, expansion coefficient from MCA, etc) to the time series of the anomalous field at each grid point (Bretherton et al., 1992).

- *Composites maps*, which are calculated by averaging selected values of the anomalous climatic field, being chosen according to a certain threshold of a standardised time series (usually considered as one standard deviation).

The representation of results from MCA have some interesting and distinctive features. As it was exposed in Section 5.2.2.2, MCA results are expressed in terms of coupled modes of covariability between two different fields, comprising each of these modes two spatial patterns and two time series (usually denoted as EC). According to this, the maps of a specific variable can be calculated in relation to its respective timeseries, or in relation to the other, defining in that way the so-called *homogeneous maps* and *heterogeneous maps*. They are usually plotted for the predictant and predictor fields respectively.

As it is expected, all the aforementioned results have to be properly evaluated in terms of each statistical confidence. To this aim, different statistical significance analysis have been developed. They are thoroughly exposed in the next subsection.

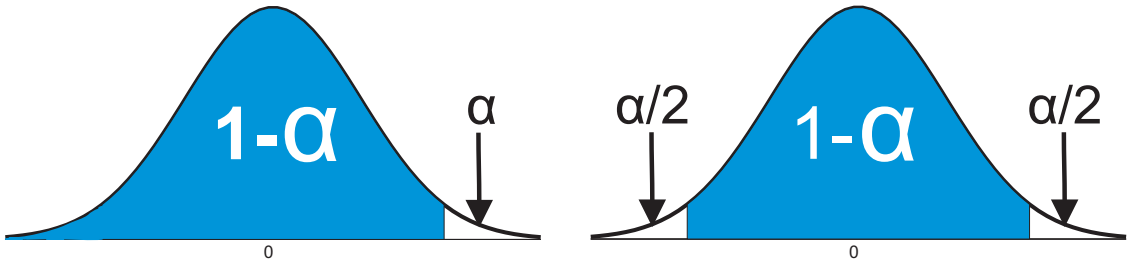

Figure 5.3: Probability Density Function of a one-tailed (left) and a two-tailed (right) test.

5.2.5 Statistical Significance Analysis

Statistical tests are designed in order to determine whether a given set of data (from observations or model outputs) contains useful information consistent with a concept that was formulated *a priori*. This concept is usually known as *null hypothesis* (Ho), and it can be rejected (if sufficient evidence is found that it is false) or to not rejected (if sufficient evidence can not be found that it is false). The probability α of rejecting Ho, being true, is called the *significance level*, and the so-called *confidence level* is obtained as $1 - \alpha$ (Figure 5.3). Both of them are usually expressed in percentage ($\%$). To evaluate these parameters some statistical tests, whose associated distribution are considered known if Ho is true, are used. They are divided in *parametric tests* and *non parametric tests*, requiring the former the assumption of a certain probability distribution. The latter methods are advantageous when it is no possible to make specific distributional assumptions.

5.2.5.1 Non-parametrics Test

The non-parametric approach applied in this thesis is based on the construction of artificial data sets from a given collection of real data by resampling the observations in a manner consistent with Ho. In general, these tests have two main advantages: (1) as the procedures consist entirely of operations on the data themselves, no assumptions regarding an underlying parametric distribution for the data are necessary, and (2) any statistic that may be suggested as important by the physical nature of the problem forms the basis of the test itself (Wilks, 2011). In particular, the non-parametric Monte-Carlo and Wilcoxon-Mann-Whitney tests, have been used. Both of them are permutation tests depending on the so-called principle of *exchangeability*, which implies that, under Ho, the labels identifying particular data values as belonging to one sample or another are arbitrary, and so, they are exchangeable.

Monte-Carlo Test

The basic idea of Monte-Carlo tests is to build up a collection of artificial data batches of the same size as the actual data. Then, the test statistic of interest for each artificial batch is computed, constituting therefore an estimated null distribution against which to compare the test statistic computed from the original data.

A typical Monte Carlo test involves the following:

- Randomly generates a large number n of data sets from the actual data
- Compute the numerical values of the test statistic r for each n data set: $r_1, r_2, r_3...r_n$
- If n is large enough, $r_1, r_2, r_3...r_n$ can be considered a good approximation to the true sampling properties of r. Under these circumstances the real parameter R can be considered as statisticaly significant, with a confidence level of $100(1-\alpha)$, if the absolute value of r is located before the $n(1-\alpha)$-teeth in the *Probality Density Function* (PDF; Figure 5.3).

This approach have been widely applied in this thesis by simulating large number of data for which the associated time series have been randomly constructed.

Wilcoxon-Mann-Whitney Test

The Wilcoxon-Mann-Whitney rank-sum test was devised in the 1940s by Wilcoxon, and by Mann and Whitney. The null hypothesis is that two data samples S1 and S2, with n_1 and n_2 observations, have the same distribution and so, the same mean ($\mu_1 = \mu_2$). If Ho is true, μ_1 and μ_2 are independent of the ordering of n_1 and n_2. The Wilcoxon-Mann-Whitney test exploits this fact by examining the positions of the observations of S1 or S2 when the combined sample of both is sorted in increasing order. Hence, the concept of *rank* is introduced as the ith smallest observation in S1 (or S2) in the joint sample. If the sum of ranks held by the members of S1 and S2 (R_1 and R_2) is significantly different from a random sum of ranks, S1 and S2 come from the same distribution (Wilks, 2011).

Thus, a test statistic U, which is a function not of the data values themselves, but of their ranks within the joint sample, can be defined as:

$$\begin{cases} U_1 &= R_1 - \dfrac{n_1(n_1+1)}{2} \\ U_2 &= R_2 - \dfrac{n_2(n_2+1)}{2} \end{cases} \tag{5.26}$$

where R_1 and R_2 are the sum of ranks held by the members of S1 and S2, respectively.

For large values of n_1 and n_2 (both larger than about 10), the Ho distribution of U is approximately Gaussian (Equation 5.27).

$$z = \frac{U - \mu_u}{\sigma_u} \tag{5.27}$$

Under these circumstances the mean μ_u and the standard deviation σ_u are given by:

$$\begin{cases} \mu_u &= \dfrac{n_1 n_2}{2} \\ \sigma_u &= \left(\dfrac{n_1 n_2 (n_1 + n_2 + 1)}{12} \right)^{1/2} \end{cases} \tag{5.28}$$

Along this thesis, the Wilcoxon-Mann-Whitney has been used to evaluated the statistical significance of changes in the mean state associated with the ENSO-NAE teleconnection.

5.3 Synapses of the research

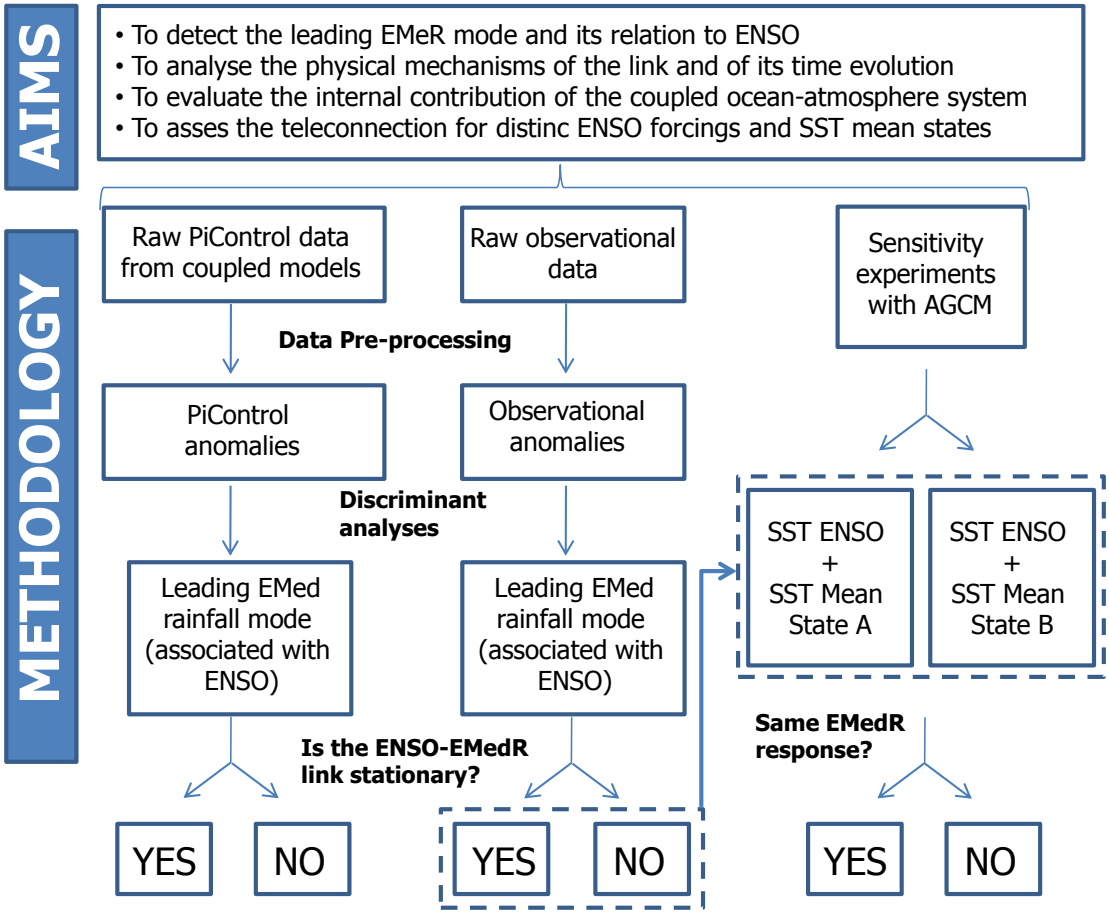

Figure 5.4: Simplified synapses of the main objectives, data, and methodology considered in this thesis

6

Results

It is really quite impossible to say anything with absolute precision,
unless that thing is so abstracted from the real world
as to not represent any real thing

Es casi imposible decir algo con absoluta precisión,
a menos que sea tan abstracto que no represente
nada en el mundo real

Richard Phillips Feynman,
New Textbooks for the 'New' Mathematics. Engineering and Science 28, no.6

6.1 ENSO - Leading EMedR mode: a changing teleconnection

In this part of the results section a non-stationary teleconnection between ENSO and the leading EMedR, at interannual timescales, is found in fall-early winter and in late winter-early spring from 1900 onwards.

These results are presented in the following publication:

6.1.1 López-Parages, J. and Rodríguez-Fonseca, B.: Multidecadal modulation of El Niño influence on the Euro-Mediterranean rainfall, Geophys. Res. Lett., 39, L02704, doi:10.1029 2011GL050049, 2012.

6.1.1 López-Parages, J. and Rodríguez-Fonseca, B. (2012)

Multidecadal modulation of El Niño influence on the Euro-Mediterranean rainfall

Jorge López-Parages[1] and Belén Rodríguez-Fonseca[1]

Received 20 October 2011; revised 6 December 2011; accepted 8 December 2011; published 20 January 2012.

[1] El Niño influence on the Euro-Mediterranean Rainfall (EMedR) has changed along the 20th century, and the reasons for this lack of stationarity, which represents an important issue in the climate change context, are still unclear. Here, the causes of this changing relationship are studied at interannual timescales. To this aim the EMedR is analyzed using observations from 1900 to 2008. Results confirm the lack of stationarity, showing how the teleconnections with El Niño appear modulated by multidecadal oscillations of the anomalous Sea Surface Temperature (SST) over the Atlantic and Pacific basins. The study presents statistically significant evidences about how the Atlantic Multidecadal Oscillation (AMO) seems to modulate El Niño teleconnection for late winter-spring, while modulation in fall could be controlled by the Pacific Decadal Oscillation (PDO). The results of this study have important implications in seasonal and decadal predictability, but they also represent a step forward in the understanding of the role of changes in the ocean mean state on the interannual teleconnections.
Citation: López-Parages, J., and B. Rodríguez-Fonseca (2012), Multidecadal modulation of El Niño influence on the Euro-Mediterranean rainfall, *Geophys. Res. Lett.*, *39*, L02704, doi:10.1029/2011GL050049.

1. Introduction

[2] El Niño-Southern Oscillation (ENSO) is the globally dominant climate mode at interannual timescales. Its influence over the Pacific and the tropics has been thoroughly analyzed [*Harrison and Larkin*, 1998; *Alexander et al.*, 2002; *Diaz and Markgraf*, 2000; *Wang*, 2004; *Wang and Picaut*, 2004; *McPhaden et al.*, 2006]. Nevertheless, over the North Atlantic sector, most of the studies point out to the North Atlantic Oscillation (NAO) as the leading pattern controlling its atmospheric variability. The NAO exerts its influence through Sea Level Pressure (SLP) fluctuations between the subpolar and the subtropical North Atlantic basin, modifying the stormtracks that reach the Euro-Mediterranean region [*Rogers*, 1997], and hence, the precipitation [*Rodwell et al.*, 1999; *Hurrell et al.*, 2003]. An interesting point is that, at interannual timescales, the regional atmospheric spatial pattern at surface levels over the Euro-Atlantic region associated with the Pacific El Niño presents a similar structure to the one associated with the NAO [*Brönnimann*, 2007; *García-Serrano et al.*, 2011]. In this way, although most of the NAO signal has an internal origin, external contributions associated with Sea Surface Temperature (SST) changes in the Pacific can have a determinant impact on the centers of action of the NAO. There are two possible ways to explain El Niño influence on the North Atlantic sector: by Rossby waves propagation due to changes in anomalous upper level convergence and divergence, or through the Walker and Hadley circulations [*Wang, C.*, 2002; *Brönnimann*, 2007]. A global teleconnection pathway from the Pacific region to Europe via the stratosphere has also been showed [*Ineson and Scaife*, 2009]. However, these signals are less well understood than those influencing on the Pacific due to the highly variable extratropical circulation of the Atlantic basin [*Trenberth et al.*, 1998; *Quadrelli and Wallace*, 2002].

[3] Previous studies have found nonstationary features in the impact of ENSO and NAO over Europe along the 20th century. These studies include interdecadal shifts in the location of NAO centers [*Vicente-Serrano and López-Moreno*, 2008], different impacts of ENSO before and after the 1970s [*Greatbatch et al.*, 2004], multidecadal variations in the relationship between ENSO and the western Mediterranean rainfall [*Mariotti et al.*, 2002], or a changing ENSO impact depending on the NAO and multidecadal oscillations of the SST over the Pacific [*Zanchettin et al.*, 2008]. However, none of these studies has restricted the analysis to the internannual signal, distinguishing in this way the multidecadal modulation of the interannual variability from the purely multidecadal variability not removed in the analysis.

[4] The present study focuses, for the first time, on the role that natural multidecadal modes, such as Atlantic Multidecadal Oscillation (AMO) [*Enfield et al.*, 2001] or Pacific Decadal Oscillation (PDO) [*Mantua et al.*, 1997] play in the modulation of the El Niño influence on the leading interannual mode of the EMedR. Two remaining issues, which are still under debate, are analyzed in this paper: 1) the El Niño impact over the Euro-Mediterranean climate variability at interannual timescales; 2) the stationarity of this El Niño impact and related sources.

[5] The paper is divided as follows. Section 2 presents the data used and the methodology followed. In section 3 the results are showed. Finally, in section 4, a brief summary and discussion are presented, attempting to give some physical hypothesis supporting the non stationary relationships identified.

2. Data and Methods

[6] This work is performed analyzing gridded data and climate indices along the 20th century, all provided by observational databases and avoiding the use of reanalysis products due to errors and limitations inherent in the reanalyzed climate dataset.

[1]Departamento de Física de la Tierra, Astronomía y Astrofísica I, Instituto de Geociencias, UCM-CSIC, Universidad Complutense de Madrid, Madrid, Spain.

0094-8276/12/2011GL050049

[7] The variables analyzed are precipitation, Sea Level Pressure (SLP) and Sea Surface Temperature (SST). Regarding rainfall, University of Delaware rainfall data (K. Matsuura and C. J. Willmott, Terrestrial precipitation: 1900–2008 gridded monthly time series, version 2.01, 2009, available at http://climate.geog.udel.edu/~climate/html_pages/Global2_Ts_2009/README.global_p_ts_2009.html) from 1900 to 2008, and GPCC data [*Schneider et al.*, 2008] from 1901 to 2007, are used. Both databases are land-only and cover a global gridded domain with a 0.5 × 0.5 lat-long resolution. SLP comes from NCAR [*Trenberth and Paolino*, 1980], from 1899 to 2008 (0.5 × 0.5 lat-long resolution), while SST comes from two different datasets: ERSSTv3 [*Smith et al.*, 2008] from 1854 to present (2° × 2° lat long), and HadISST1 [*Rayner et al.*, 2003] from 1870 to present (1° × 1° lat long).

[8] Regarding the climate indices, Niño3.4, Atlantic Multidecadal Oscillation (AMO) and Pacific Decadal Oscillation (PDO) are used in this study. Niño 3.4 index has been calculated with the SST databases mentioned above, computing the SST anomaly in the Equatorial Pacific region [5°S -5°N, 170°W-120°W]. Also with these SST datasets, AMO index is obtained as the ten-year running mean of detrended Atlantic SST anomalies north of the equator [*Enfield et al.*, 2001]; and PDO index is defined as the leading principal component of November to March detrended SST anomalies for the Pacific north of 20N latitude [*Mantua et al.*, 1997].

[9] In a preliminary study, the rainfall variability of the 12 possible 3-months seasons of the year, from JFM to DJF, is analyzed. The analysis is focused on the interannual seasonal precipitation over the Euro-Mediterranean region (iEMedR, [24°N-68°N, 15°W-35°E]), retaining the high frequency variability by computing the difference between the rainfall scores of one year and the next [*Stephenson et al.*, 2000]. This interannual filtering has been also applied for the SST and SLP (iSST and iSLP respectively). In a second step, the spatially coherent patterns that maximize the variance (thereafter called as "modes") of the iEMedR are determined in a linear way by applying a Principal Component Analysis (PCA/EOF [*Von Storch and Zwiers*, 2001]), as is suggested by *Zanchettin et al.* [2008]. Although they point to a switching behavior of ENSO effects driven by the Pacific Decadal Oscillation (PDO), they propose to focus on a few leading empirical orthogonal functions to reduce the degrees of freedom. Here, regression maps are computed projecting the iEMedR, iSST, and iSLP, onto the leading Principal Components (PC1s), and highlighting those gridpoints with significant correlation scores between the anomalous timeseries and the PC1s. Looking for the stationarity of El Niño impact, sliding windows correlation analysis between the PC1 and the Niño3.4 index is applied. Finally, periods with or without significant correlations are analyzed separately. Along the whole study, 95% confidence level of significance, which is determined by a non parametric Monte Carlo test with 400 permutations, is chosen.

3. Results

[10] We start by examining how the variability of the iEMedR has been organized during the whole 20th century. EOF analysis of this field is applied for all the possible 3-months seasons of the year, obtaining a similar spatial pattern for all of them. The leading mode is clearly separated (following *North et al.* [1982]) from the second one, for late winter-spring and fall months (Figures S1 and S2 in the auxiliary material).[1] For this reason, as representative of these two seasons, the analysis is focused in February-March-April (FMA) and October-November-December (OND). In particular, for FMA, the associated spatial pattern (Figure 1a) presents significant scores in central Europe, including the British Islands, opposite in sign to those over the Mediterranean region and northwestern Africa. In OND (Figure 1d), the leading mode is broadly similar to that obtained for FMA, although the Northern Scandinavia center gets significant and the Mediterranean center gets weaker. The regression of the anomalous iSST onto the PC1 (Figure 1c) presents, for FMA, a significant structure over the tropical Pacific in an El Niño type configuration, with the maximum anomalies over the Niño3.4 region. Over the North Pacific, an extratropical horseshoe pattern appears. Despite the similarities in the leading iEMedR mode for FMA and OND, the projection of the anomalous iSST onto the OND PC1 does not show any significant pattern over the tropical Pacific, although the map reveals an El Niño signal (Figure 1f). In both seasons the PC1s present a lack of stationarity in their variability, as it can be seen in the statistically significant changes in its variance along the 20th century (Figures 1b and 1e). In this way, and taking into account El Niño signal in the iSST regression maps, decadal changes in the PC1s amplitude could be related to changes in its relationship with the tropical Pacific, indicating a non stationary relationship with El Niño, in agreement with previous studies [*Mariotti et al.*, 2002; *Knippertz et al.*, 2003; *Greatbatch et al.*, 2004]. To assess the stationarity of this El Niño-iEMedR relationship, 21-year window moving correlations between PC1s and Niño3.4 index are computed for the whole 20th century (Figure 2), obtaining how the evolution of these correlations exhibits a clear multidecadal periodicity. Different windows are tested (Figure S3) and the results remain the same. On the one hand, for FMA, significant correlations appear in the beginning of the 20th century and after the 1960s, but not in the 1940s and 1950s. A highlighting result is the fact that these correlations evolve in

[1] Auxiliary materials are available in the HTML. doi:10.1029/2011GL050049.

Figure 1. FMA and OND leading modes of iEMedR. FMA mode: (a) Leading empirical orthogonal function (EOF1; contours, ci = 0,1 mm per std in the PC) of the FMA anomalous rainfall (Delaware) over the EM region (24.25– 67.75°N/ 14.75°W-34.75°E). (b) Associated standardized principal component (PC1, referenced on the right axis) and its variance (black line, referenced on the left axis). (c) Regression map of anomalous iSST (ERSST) onto the PC1 (contours, ci = 0,05° per std in the PC) . Bottom Panel, OND mode: (d, e, and f) the same as Figures 1a, 1b, and 1c but for OND. In all the maps, shading represents statistical significant areas, according to a Monte Carlo correlation test at 95% confidence level. Blue bands in Figures 1b and 1e represent significant changes in the PC1 variance using the same test and threshold as in the maps.

phase with a low frequency SST pattern that agrees with the Atlantic Multidecadal Oscillation (AMO index, gray line in Figure 2 (bottom); see also regression map in Figure S4 in the auxiliary material). Another important result is how in OND the correlations evolve in phase with the Pacific Decadal Oscillation (PDO index as a gray line in Figure 2 (top) and regression map in Figure S4 in the auxiliary material), except for the last positive phase of PDO after

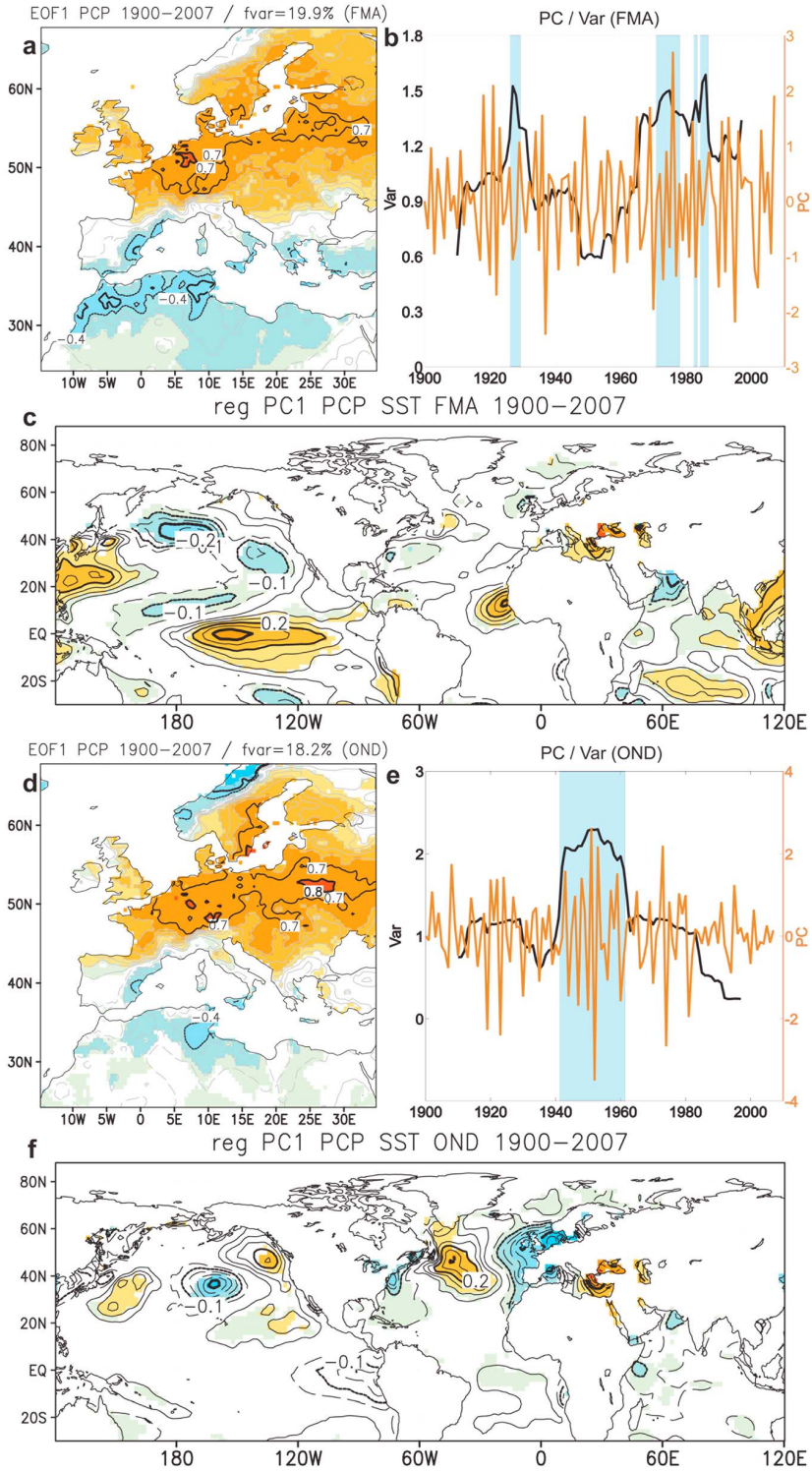

Figure 1

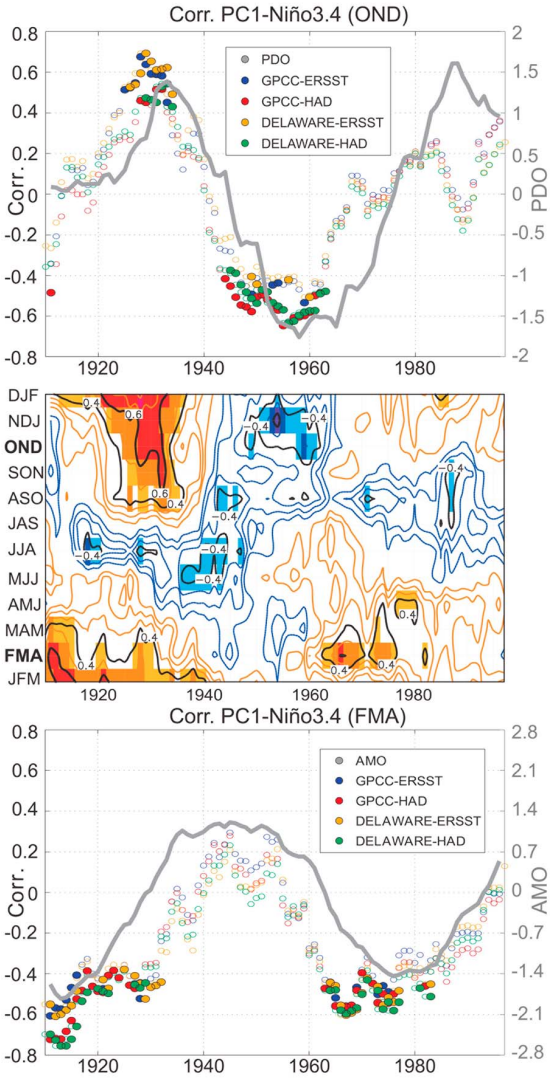

Figure 2. Correlations with Niño3.4 index. (top) Results for OND: 21 year moving window correlations (left axis) between the leading iEMedR PC1 and Niño3.4 index in OND for different PCP and SST datasets according to the legend. In grey line, the standardized PDO index based on *Mantua et al.* [1997] definition is plotted, referenced on the right axis. (middle) Results for all the year: 21 year moving window correlations between the leading iEMedR PC1 (Delaware) and Niño3.4 index (ERSST) for each of the 3 months seasons of the year. (bottom) Results for FMA: the same as the Figure 2 (top) but for FMA. In grey line, the standardized AMO based on *Enfield et al.* [2001]. The sign of the correlation has been changed to better show how the evolution of the correlations is in phase with the AMO. Fill dots and shaded areas represent periods with a 95% significant correlation according to a Monte-Carlo correlation test.

the 1970s, when the correlations do not reach the significant level. In the case of FMA, correlations with the Niño3.4 index appear significant only for negative phases of the AMO, but not for positive ones. In OND, the correlations are significant in both, negative and positives phases of PDO (except after the 1970's). It is important to mention that this multidecadal modulation of El Niño influence on the leading iEMedR mode in FMA and OND by both, AMO and PDO, occurs broadly for all the late winter-spring months and for all the fall months respectively (Figure 2 (middle) and Figure S5 in the auxiliary material). The next question is to try to formulate a hypothesis about the mechanism by which the link between El Niño and iEMedR changes at multidecadal timescales for each of the considered

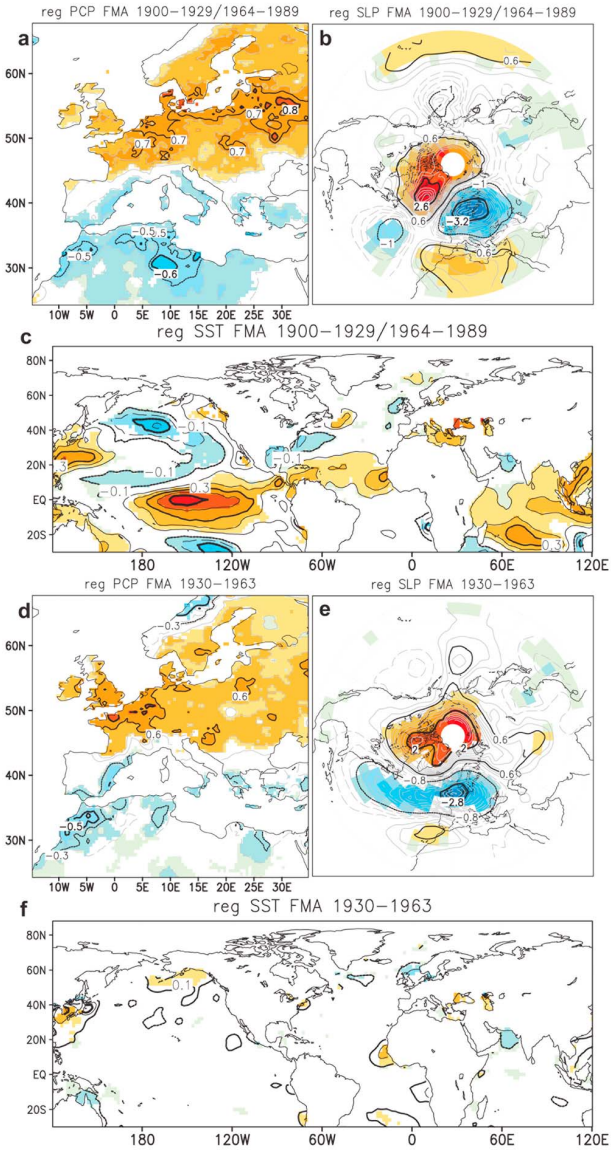

Figure 3. FMA Regression maps, for selected periods of the AMO, calculated between the PC1 and: (a) PCP (Delaware; contours, ci = 0,2 mm per std in the PC), (b) SLP (contours, ci = 0,2 hPa per std in the PC) , (c) SST (ERSST; contours, ci= 0,1° per std in the PC) for the period 1900-1929/1964-1989. (d, e, and f) The same as Figures 3a, 3b, and 3c but for the period 1930–1963. In all the maps, magnitudes correspond to one std dev of the PC. Statistical significant areas, according to a Monte-Carlo correlation test at 95% confidence level, are shaded.

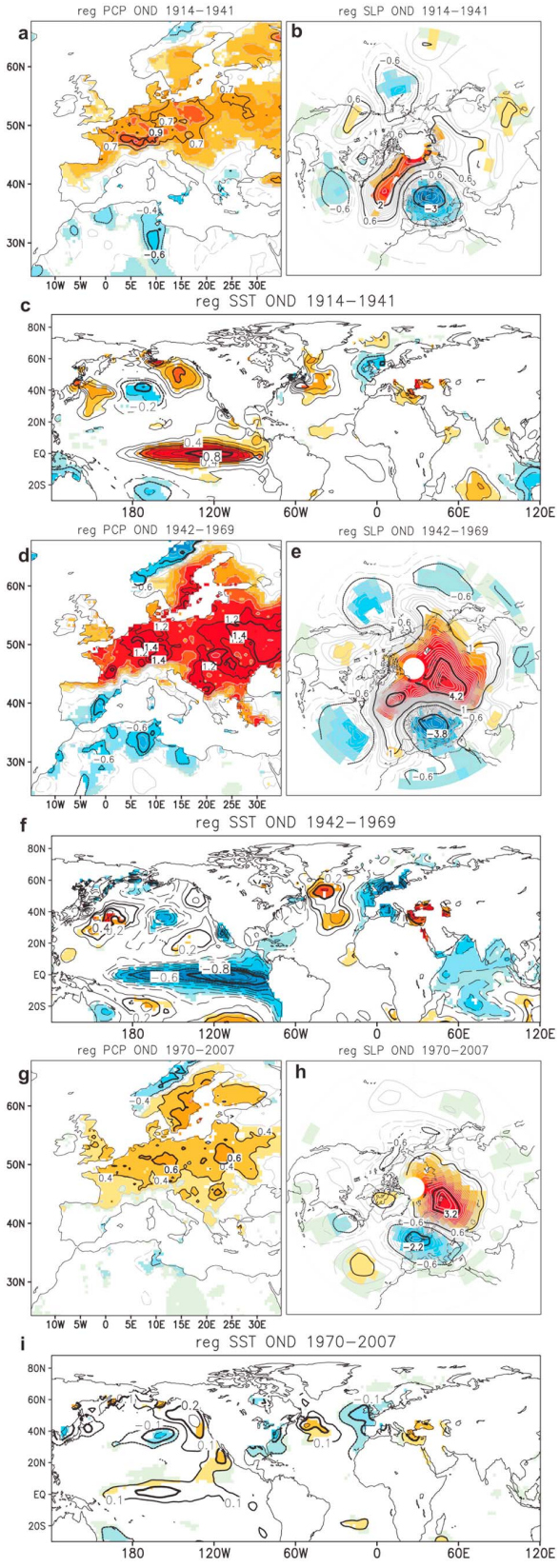

seasons. To this aim, periods with or without significant correlations with the Niño3.4 index are analyzed separately, including in the analysis SLP data, which is the only available atmospheric variable with observations for the whole 20th century. For those years within an AMO negative phase (Figures 3a–3c), the iSST regression map projects an El Niño pattern over the Pacific, while over the Atlantic basin, the significant areas resemble the SST signal of the meridional gradient mode proposed by *Wang, C.* [2002]. The iSLP pattern presents a quadrupolar structure in the North Atlantic with a strong center over the Iberian Peninsula and Northern Africa. Over the Pacific, a positive significant center appears in the tropical region, reflecting the typical Southern Oscillation (SO) pattern. Nevertheless, for those years within positive AMO phase (Figures 3d–3f), when the El Niño-iEMedR relationship disappears, no El Niño signal is found in the ocean, the precipitation pattern weakens, and the iSLP pattern is confined to the Atlantic-European region resembling a NAO structure, mainly related to internally driven changes in the zonal flow.

[11] Similar analysis for the leading mode of OND shows the same precipitation pattern opposite correlated with El Niño phenomenon (Figures 4a–4f) depending on the PDO phase. In this way, the rainfall pattern obtained before the 1940s (positive phase of the PDO) in relation to a warm SST tongue in the tropical Pacific, appears after the 1940s (negative phase of PDO) in relation to a cold SST tongue; and the opposite. The iSST anomalies and the iSLP spatial patterns are broadly similar over the extratropics, except for the western Pacific and Asia iSLP signal, which could be associated with different atmospheric sources for this tropical-extratropical connection. After the 1970s (Figures 4g–4i), when another positive phase of PDO occurs, no significant El Niño signal appears and the precipitation pattern decreases with respect to the one identified in the positive phase of PDO before the 1940s.

4. Summary and Discussion

[12] This paper deals with the non stationary relationship between El Niño and iEMedR along the 20th century, focusing the analysis in "late winter-spring" and in fall seasons. The leading mode of the interannual rainfall presents a tripolar spatial structure with increased precipitation over central Europe, and the opposite over Northern Scandinavia and the Mediterranean. This mode is significantly related to El Niño in a nonstationary way, presenting a multidecadal modulation. Hence, the spatial projection of the anomalous iSLP onto this leading mode depends also on the decades considered and, for those decades in which the leading PC does not correlate with El Niño, the iSLP patterns presents a zonally symmetric structure, suggesting a configuration associated with internally driven changes in the zonal flow. On the opposite side, for those decades in which the leading PC correlates with El Niño, the iSLP pattern suggests the presence of a tropical forcing. This result agrees with *Ting et al.* [1996], who showed that the extratropical climate

Figure 4. Regression maps in OND for selected periods. As Figure 3 but for particular periods of the PDO: (a, b, and c) correspond to the period 1915–1942, (d, e, and f) for the period 1943–1970 and (g, h, and i) for the period 1971–2008.

anomalies over the northern hemisphere could be understood as a linear combination of teleconnections associated with changes in the zonal mean flow and the ENSO states. This study also agrees with the fact that changes in the location of the anomalous tropical heat source would be producing differences in the extratropical teleconnection [*Ting and Sardeshmukh*, 1993].

[13] Multidecadal changes in the ENSO-EMedR relationship have also been found for these seasons by other authors [*Mariotti et al.*, 2002, *Knippertz et al.*, 2003, *Greatbatch et al.*, 2004], but none of them point to a specific multidecadal pattern as modulator of ENSO teleconnections. Using different methodologies and periods than the above mentioned authors, the present study adds a relevant result to the state of the art, which is the fact that the correlation between the leading interannual rainfall mode and El Niño appears modulated in phase with multidecadal variability patterns, such as AMO and PDO. In late-winter and spring, significant correlations with El Niño appear during negative phases of the AMO, being stronger over central Europe and the Mediterranean, whilst for positive phases of the AMO, the rainfall pattern is weaker. On the basis of this result, a possible mechanism to explain the role of AMO modulating the El Niño-iEMedR relationship in FMA, can be found from the study of *Wang, C.* [2002] due to the similarities in the SST patterns. Although the location of the centers of action could be different, the iSLP configuration identified here over the Pacific (Figure 3) is coherent with the Walker-Hadley mechanism [*Wang, C.*, 2002; *Cassou and Terray*, 2001] as the one linking the SSTs anomalies in the Atlantic and Pacific basins. Therefore, this Walker-Hadley mechanism could be enhanced during negative phases of AMO, getting significant the El Niño-iEMedR teleconnection. For positive phases of AMO, this mechanism is not effective and, thus, internal variability appears as the dominant mechanism. Our results also agree with *Sutton and Hodson* [2003], who suggested that the influence of the ocean on the interannual variability of the North Atlantic climate may have two causes: first, variations in the strength of ENSO, and second, SST changes in the Atlantic Ocean. In fall, the factor modulating the El Niño-iEMedR relationship points to decadal variability of the SST over the Pacific, appearing significant correlations for both, negative and positives phases of the PDO index. It is interesting how, in this case, the same rainfall structure is significantly correlated or anticorrelated with El Niño depending on the phase of the PDO. This change in the El Niño-iEMedR teleconnection could be associated with the reported decadal changes in El Niño behavior due to variations in the background state of the Pacific ocean [*Wang*, 1995; *Wang and An*, 2002], which in turn changes at multidecadal timescales in phase with the PDO. This result agrees with *Zanchettin et al*. [2008], who proposed that the low-frequency modulation of ENSO impacts on European wintertime rainfall (defined from October to March) is associated with multidecadal phases of the PDO via changes in the dynamical behavior of ENSO. The link between extra-tropical atmospheric circulation and central type El Niño events [*Di Lorenzo et al.*, 2010] may provide one additional hypothesis explaining the apparent multidecadal modulation of El Nino influences on iEMedR by the PDO. It is worth mentioning also that the different phases of the PDO are characterised by different frequencies of ENSO events [*Kiem et al.*, 2003; *Verdon and Franks*, 2006], a feature that could be further analyzed. Finally, considering that the global warming observed since 1970's are reproduced when models include anthropogenic effect [*Intergovernmental Panel on Climate Change*, 2007], human influence should be further study as a possible cause of the lack of significant El Niño impact on the fall iEMedR after this decade.

[14] This study is supported by observational analysis of both, ocean and atmospheric data, and it points to the fact of considering the changes in the mean state as a modulator factor of ENSO teleconnections, a result that has important implications in seasonal and decadal predictability. Although decadal fluctuations could be generated by physically varying teleconnections or by chance [*van Oldenborgh and Burgers*, 2005], the analysis performed in the present study for specific phases of both, AMO and PDO, points to a physically coherent modulation of the El Niño-iEMedR relationship by changes in the ocean background state. Nevertheless, further analysis discerning the nonlinear responses, and sensitivity experiments with General Circulation Models (GCMs), are necessary to investigate the underlying dynamics and to test the hypothesis inferred here from the observations.

[15] **Acknowledgments.** The study has been partially supported by the National Spanish Projects: TRACS (CGL2009-10285), MOVAC (200800050084028), and (CGL2011-13564). Many thanks to the University of Delaware, GPCC, NCAR, NOAA, and the UK Met Office for the provided data, which have made possible this study. We would also like to thank Elsa Mohino, Teresa Losada and Javier García-Serrano for their useful comments. JLP is granted by the MICINN of the Spanish Government.

[16] The Editor thanks the two anonymous reviewers for their assistance in evaluating this paper.

References

Alexander, M. A., et al. (2002), The atmospheric bridge: Influence of ENSO teleconnections on air-sea interaction over the global oceans, *J. Clim.*, *15*, 2205–2231, doi:10.1175/1520-0442(2002)015<2205:TABTIO>2.0.CO;2.

Brönnimann, S. (2007), Impact of El Niño–Southern Oscillation on European climate, *Rev. Geophys.*, *45*, RG3003, doi:10.1029/2006RG000199.

Cassou, C., and L. Terray (2001), Oceanic forcing of the wintertime low-frequency atmospheric variability in the North Atlantic European sector: A study with the ARPEGE model, *J. Clim.*, *14*, 4266–4291, doi:10.1175/1520-0442(2001)014<4266:OFOTWL>2.0.CO;2.

Diaz, H., and V. Markgraf (Eds.) (2000), *El Niño and the Southern Oscillation: Multiscale Variability and Global and Regional Impacts*, Cambridge Univ. Press, New York, doi:10.1017/CBO9780511573125.

Di Lorenzo, E., et al. (2010), Central Pacific El Niño and decadal climate change in the North Pacific, *Nat. Geosci.*, *3*, 762–795, doi:10.1038/ngeo984.

Enfield, D. B., A. M. Mestas-Nuñez, and P. J. Trimble (2001), The Atlantic multidecadal oscillation and its relation to rainfall and river flows in the continental U.S., *Geophys. Res. Lett.*, *28*, 2077–2080, doi:10.1029/2000GL012745.

García-Serrano, J., B. Rodriguez-Fonseca, I. Bladé, P. Zurita-Gotor, and A. de la Cámara (2011), Rotational atmospheric circulation during North Atlantic-European winter: The influence of ENSO, *Clim. Dyn.*, *37*, 1727–1743, doi:10.1007/s00382-010-0968-y.

Greatbatch, R. J., J. Lu, and K. A. Peterson (2004), Nonstationary impact of ENSO on Euro-Atlantic winter climate, *Geophys. Res. Lett.*, *31*, L02208, doi:10.1029/2003GL018542.

Harrison, D. E., and N. K. Larkin (1998), El Niño-Southern Oscillation sea surface temperature and wind anomalies, *Rev. Geophys.*, *36*, 353–399, doi:10.1029/98RG00715.

Hurrell, J. W., Y. Kushnir, G. Ottersen, and M. Visbeck (2003), An overview of the North Atlantic Oscillation, in *The North Atlantic Oscillation: Climatic Significance and Environmental Impact*, *Geophys. Monogr. Ser.*, vol. 134, edited by J. W. Hurrell et al., pp. 1–35, AGU, Washington, D. C., doi:10.1029/134GM01.

Ineson, S., and A. A. Scaife (2009), The role of the stratosphere in the European climate response to El Niño, *Nat. Geosci.*, *2*, 32–36, doi:10.1038/ngeo381.

Intergovernmental Panel on Climate Change (2007), *Climate Change 2007: The Physical Science Basis. Contribution of Working Group I to the Fourth Assessment Report of the Intergovernmental Panel on Climate Change*, edited by S. Solomon et al., Cambridge Univ. Press, Cambridge, U. K.

Kiem, A. S., S. W. Franks, and G. Kuczera (2003), Multi-decadal variability of flood risk, *Geophys. Res. Lett.*, *30*(2), 1035, doi:10.1029/2002GL015992.

Knippertz, P., U. Ulbrich, F. Marques, and J. Corte-Real (2003), Decadal changes in the link between El Niño and springtime North Atlantic Oscillation and European-North African rainfall, *Int. J. Climatol.*, *23*, 1293–1311, doi:10.1002/joc.944.

Mantua, N. J., S. R. Hare, Y. Zhang, J. M. Wallace, and R. C. Francis (1997), A Pacific interdecadal climate oscillation with impacts on salmon production, *Bull. Am. Meteorol. Soc.*, *78*, 1069–1079, doi:10.1175/1520-0477(1997)078<1069:APICOW>2.0.CO;2.

Mariotti, A., N. Zeng, and K.-M. Lau (2002), Euro-Mediterranean rainfall and ENSO: A seasonally varying relationship, *Geophys. Res. Lett.*, *29*(12), 1621, doi:10.1029/2001GL014248.

McPhaden, M. J., S. E. Zebiak, and M. H. Glantz (2006), ENSO as an integrating concept in Earth science, *Science*, *314*, 1740–1745, doi:10.1126/science.1132588.

North, G. R., T. L. Bell, R. F. Cahalan, and F. J. Moeng (1982), Sampling errors in the estimation of empirical orthogonal functions, *Mon. Weather Rev.*, *110*, 699–706, doi:10.1175/1520-0493(1982)110<0699:SEITEO>2.0.CO;2.

Quadrelli, R., and J. M. Wallace (2002), Dependence of the structure of the Northern Hemisphere annular mode on the polarity of ENSO, *Geophys. Res. Lett.*, *29*(23), 2132, doi:10.1029/2002GL015807.

Rayner, N. A., D. E. Parker, E. B. Horton, C. K. Folland, L. V. Alexander, D. P. Rowell, E. C. Kent, and A. Kaplan (2003), Global analyses of sea surface temperature, sea ice, and night marine air temperature since the late nineteenth century, *J. Geophys. Res.*, *108*(D14), 4407, doi:10.1029/2002JD002670.

Rodwell, M. J., D. P. Rowell, and C. K. Folland (1999), Oceanic forcing of the wintertime North Atlantic Oscillation and European climate, *Nature*, *398*, 320–323, doi:10.1038/18648.

Rogers, J. C. (1997), North Atlantic storm track variability and its association to the North Atlantic Oscillation and climate variability of northern Europe, *J. Clim.*, *10*, 1635–1647, doi:10.1175/1520-0442(1997)010<1635:NASTVA>2.0.CO;2.

Schneider, U., et al. (2008), *Global Precipitation Analysis Products of the GPCC*, Global Precip. Climatol. Cent., Offenbach, Geramny.

Smith, T. M., R. W. Reynolds, T. C. Peterson, and J. Lawrimore (2008), Improvements to NOAA's historical merged land-ocean surface temperature analysis (1880–2006), *J. Clim.*, *21*, 2283–2296, doi:10.1175/2007JCLI2100.1.

Stephenson, D. B., V. Pavan, and R. Bojariu (2000), Is the North Atlantic Oscillation a random walk?, *Int. J. Climatol.*, *20*, 1–18, doi:10.1002/(SICI)1097-0088(200001)20:1<1::AID-JOC456>3.0.CO;2-P.

Sutton, R. T., and D. L. R. Hodson (2003), Influence of the ocean North Atlantic climate variability 1871–1999, *J. Clim.*, *16*, 3296–3313, doi:10.1175/1520-0442(2003)016<3296:IOTOON>2.0.CO;2.

Ting, M.-F., and P. D. Sardeshmukh (1993), Factors determining the extratropical response to equatorial heating anomalies, *J. Atmos. Sci.*, *50*, 907–918, doi:10.1175/1520-0469(1993)050<0907:FDTERT>2.0.CO;2.

Ting, M., M. P. Hoerling, T. Xu, and A. Kumar (1996), Northern Hemisphere teleconnection patterns during extreme phases of the zonal-mean circulation, *J. Clim.*, *9*, 2614–2633, doi:10.1175/1520-0442(1996)009<2614:NHTPDE>2.0.CO;2.

Trenberth, K. E., and D. A. Paolino (1980), The Northern Hemisphere sea-level pressure data set: Trends, errors, and discontinuities, *Mon. Weather Rev.*, *108*, 855–872, doi:10.1175/1520-0493(1980)108<0855:TNHSLP>2.0.CO;2.

Trenberth, K. E., G. W. Branstator, D. Karoly, A. Kumar, N.-C. Lau, and C. Ropelewski (1998), Progress during TOGA in understanding and modeling global teleconnections associated with tropical sea surface temperatures, *J. Geophys. Res.*, *103*(C7), 14,291–14,324, doi:10.1029/97JC01444.

van Oldenborgh, G. J., and G. Burgers (2005), Searching for decadal variations in ENSO precipitation teleconnections, *Geophys. Res. Lett.*, *32*, L15701, doi:10.1029/2005GL023110.

Verdon, D. C., and S. W. Franks (2006), Long-term behaviour of ENSO: Interactions with the PDO over the past 400 years inferred from paleoclimate records, *Geophys. Res. Lett.*, *33*, L06712, doi:10.1029/2005GL025052.

Vicente-Serrano, S. M., and J. I. López-Moreno (2008), Nonstationary influence of the North Atlantic Oscillation on European precipitation, *J. Geophys. Res.*, *113*, D20120, doi:10.1029/2008JD010382.

Von Storch, H., and F. Zwiers (2001), *Statistical Analysis in Climate Research*, Cambridge Univ. Press, Cambridge, U. K.

Wang, B. (1995), Interdecadal changes in El Niño onset in the last four decades, *J. Clim.*, *8*, 267–285, doi:10.1175/1520-0442(1995)008<0267:ICIENO>2.0.CO;2.

Wang, B., and S. I. An (2002), A mechanism for decadal changes of ENSO behavior: roles of background wind changes, *Clim. Dyn.*, *18*, 475–486, doi:10.1007/s00382-001-0189-5.

Wang, C. (2002), Atlantic climate variability and its associated atmospheric circulation cells, *J. Clim.*, *15*, 1516–1536.

Wang, C. (2004), ENSO, Atlantic climate variability and the Walker and Hadley circulations, in *The Hadley Circulation: Present, Past and Future*, *Adv. Global Change Res*, vol. 21, edited by H. F. Diaz and R. S. Bradley, pp. 173–202, Kluwer Acad., Dordrecht, Netherlands, doi:10.1007/978-1-4020-2944-8_6.

Wang, C., and J. Picaut (2004), Understanding ENSO physics: A review, in *Earth's Climate: The Ocean–atmosphere Interaction*, *Geophys. Monogr. Ser.*, vol. 147, edited by C. Wang et al., pp. 21–48, AGU, Washingtion, D. C., doi:10.1029/147GM02.

Zanchettin, D., S. W. Franks, P. Traverso, and M. Tomasino (2008), On ENSO impacts on European wintertime rainfalls and their modulation by the NAO and the Pacific multi-decadal variability described through the PDO index, *Int. J. Climatol.*, *28*, 995–1006, doi:10.1002/joc.1601.

J. López-Parages and B. Rodríguez-Fonseca, Departamento de Física de la Tierra, Astronomía y Astrofísica I, Instituto de Geociencias, UCM-CSIC, Universidad Complutense de Madrid, Pza. de las Ciencias, E-28040 Madrid, Spain. (parages@fis.ucm.es)

Supplementary Material

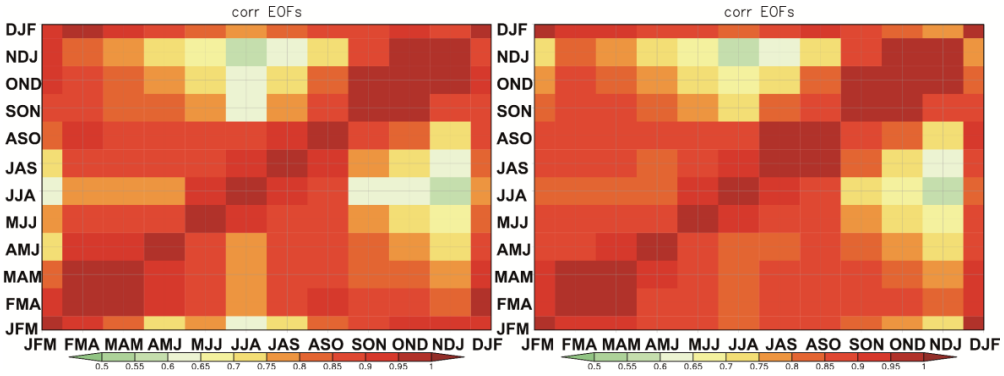

Figure S1: EOFs correlations. Spatial correlations between seasonal leading iEMedR EOFs along the year. All the correlations are shaded, representing 99% significant correlations according to a Monte-Carlo test. Left, results using rainfall data from Delaware database. Right, from GPCC database.

As can be seen in the figure S1, high significant correlations are obtained between the leading EOFs from each of the 3 months seasons analyzed, particularly between FMA-MAM and SON-OND-NDJ.

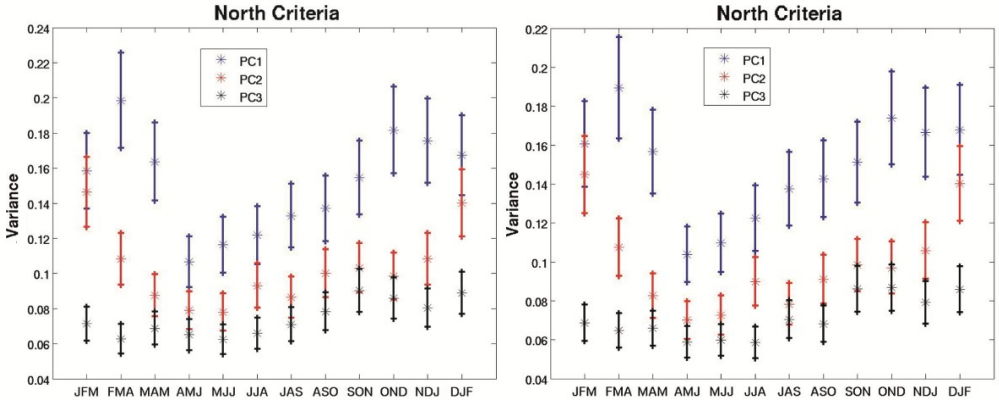

Figure S2: Variance explained for each PC. Variance explained by the leading (blue), second (red), and third (black) iEMedR variability modes for each 3 months season. Left, results obtained using Delaware data. Right, using GPCC database. The error bars represent the sampling errors based on the North Criteria [North et al. 1982].

As it is shown in the figure S2, the leading and second modes are separated for each 3 months season, except for JFM and DJF. However, the major differences between them appear in late winter-spring and in fall months.

Considering the previous figures, the similarities between the PCA results obtained using data from Delaware and GPCC are clear.

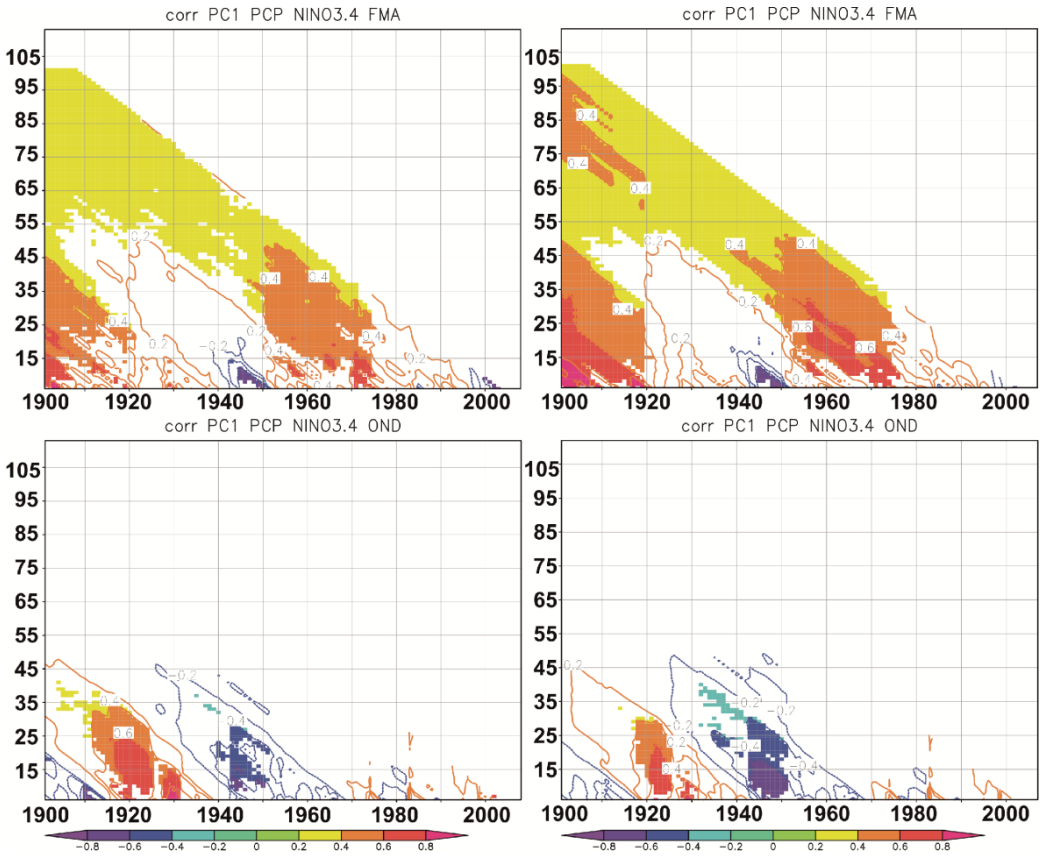

<u>Figure S3:</u> Correlations with El Niño3.4 index using different windows length. Sliding windows correlations between leading PC (Delaware) and Niño 3.4 index. On top the results for FMA. On bottom for OND. Left, Niño 3.4 index based on ERSST database. Right, based on Had database. The length of the moving windows varies according to the left axis.

From figure S3 we deduce that the results obtained in figure 2 are not sensitive to the length of the sliding window.

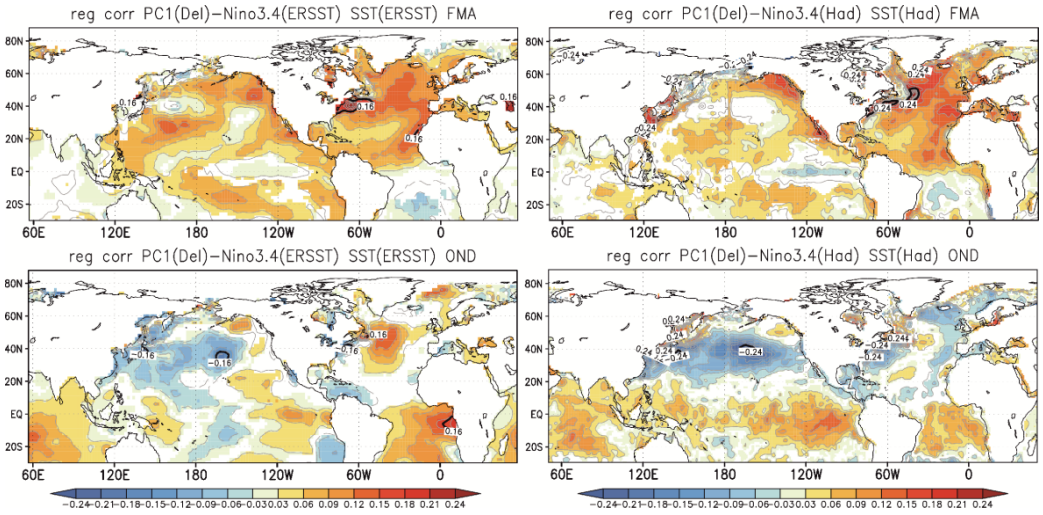

<u>Figure S4:</u> Regression maps of the annual SST. Regression map of the anomalous 21 years running mean SST onto the 21 year sliding windows correlation series between PC1 and Niño 3.4 index. From top to bottom the results for FMA and OND. Left, Niño 3.4 index is obtained using ERSST database (timeseries formed by yellow dots in figure 2). Right, the same but for Had database (timeseries formed by green dots in figure 2). For OND the regression map is calculated using timeseries until 1960. Units are in º per correlation unit.

It is possible to identify, for FMA, an interhemispheric SST dipole in the Atlantic basin. This pattern is similar to the canonical AMO one (warm phase). The results are broadly the same for ERSST and Had database.

For OND, it can be seen a SST pattern over the North Pacific basin which resembles the PDO one (warm phase). When ERSST database is used, it is possible to identify cold SST anomalies in the interior of the North Pacific basin and warm anomalies over the

North American coast. The latter does not appear so clearly when Had SST database is used. Furthermore, other differences between ERSST and Had databases over the tropical Pacific and the Atlantic basin are found.

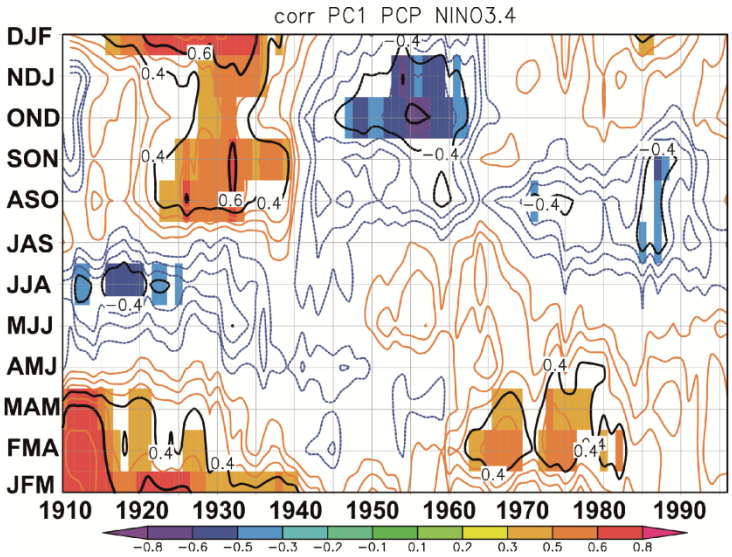

<u>Figure S5:</u> Correlations between the leading iRMedR PC and El Niño3.4 index for all the seasons. 21 year moving window correlations between the leading iEMedR PC (Delaware) and Niño3.4 index (Had) for each of the 3 months season of the year. Only the areas with 95% significant correlations (under a Monte Carlo significant test) are shaded.

The figure S5 shows the different iEMedR-Nino3.4 relationships along the year. For late winter-spring months, significant correlations appear in the beginning of the 20th century and after the 1960's, but not in the 1940's and 1950's. For fall-early winter months, significant correlations are identified in both, negative and positives phases of PDO (except after the 1970's). This figure is similar to figure 3, which was obtained using SST from ERSST database.

6.2 ENSO - Leading EMedR mode: a teleconnection modulated by internal variability

In this part of the results section, the role that internal variability of the ocean-atmosphere coupled system plays on the non-stationary teleconnection between ENSO and the leading EMedR mode is explored.

These results are presented in the following publications:

6.2.1 López-Parages, J., Rodríguez-Fonseca, B., and Terray, L.: A mechanism for the multidecadal modulation of ENSO teleconnection with Europe, Clim. Dyn., 45, 867–880, doi:10.1007/s00382-014-2319-x, 2014.

6.2.2 López-Parages, J., Rodríguez-Fonseca, B., Mohino, E., and Losada, T. : Multidecadal modulation of ENSO teleconnection with Europe in CMIP5 models, J. Climate, *under review (JCLI-S-15-00678)*, 2015.

6.2.1 López-Parages, J. et al. 2014

A mechanism for the multidecadal modulation of ENSO teleconnection with Europe

Jorge López-Parages · Belén Rodríguez-Fonseca · Laurent Terray

Received: 7 April 2014 / Accepted: 2 September 2014

Abstract El Niño phenomenon is the main oceanic driver of the interannual atmospheric variability and a determinant source of predictability in the tropics and extratropics. Several studies have found a consistent and statistically significant impact of El Niño over the North Atlantic European Sector, which could lead to an improvement of the skill of current seasonal forecast systems over Europe. Nevertheless, this signal seems to be non-stationary in time and it could be modulated by the ocean at very low frequencies. Hence, the seasonal climate predictability based on El Niño could be variable and only effective for specific time periods. This study considers the multidecadal changes in the ocean mean state as a possible modulator of ENSO-European rainfall teleconnection at interannual timescales. A long control simulation of the CNRM-CM5 model is used to substantiate this hypothesis and to assess if it can be relevant to explain the non-stationary behavior seen in the twentieth century. The model reproduces the leading rainfall mode over the Euro-Mediterranean region, and its non stationary link with El Niño. This teleconnection has been identified in coincidence with changes of the zonal mean flow at upper levels, which influence the propagation of the waves from the tropics to extratropics through the atmosphere and, hence, to explain the changing impact over Europe. However, the non-stationary impact observed along the twentieth century could also be related to the observed changes in the interannual oceanic forcing signal itself. The results obtained suggest, for both hypotheses, an important role of the natural internal variability of the ocean at multidecadal timescales.

Keywords Atmospheric teleconnection · ENSO · European rainfall · Multidecadal modulation

Electronic supplementary material The online version of this article (doi:10.1007/s00382-014-2319-x) contains supplementary material, which is available to authorized users.

J. López-Parages (✉) · B. Rodríguez-Fonseca
Departamento de Física de la Tierra, Astronomía y Astrofísica I (Geofísica y Meteorología). Instituto de Geociencias UCM-CSIC, Facultad de C.C. Físicas, Universidad Complutense de Madrid (UCM), Pza de las Ciencias, 28040 Madrid, Spain
e-mail: parages@fis.ucm.es

L. Terray
Climate Modelling and Global Change Team, CERFACS/CNRS, 42 Avenue 14 Gaspard Coriolis, 31057 Toulouse, France

1 Introduction

The climate variability over the North Atlantic European Sector (NAES) is mainly linked to the North Atlantic Oscillation (NAO; Van Loon and Rogers 1978; Wallace and Gutzler 1981), which is characterized by a Sea Level Pressure (SLP) seesaw between the Azores high and the Icelandic low (Walker 1924). This fluctuation between subpolar and subtropical North Atlantic latitudes influences the stormtracks, and hence, the associated precipitation regime (Rodwell et al. 1999; Hurrell et al. 2003). Although the NAO is mainly associated with internal atmospheric variability, it is also influenced by changes in Sea Surface Temperature (SST), which could lead to predictability at seasonal to interannual time scales (Czaja and Frankignoul 1999; Hurrell et al. 2003). Several studies have found a consistent and statistically significant ENSO signal on the European climate (Fraedrich and Müller 1992; Moron and Plaut 2003). Interestingly, its low-level atmospheric pattern is similar to the one associated with the internal NAO (García-Serrano et al. 2010). In general, El Niño tends to be associated with a negative phase of the NAO (Brönnimann

Published online: 26 October 2014

2007). This raises the issue of a robust detection of the atmospheric response to ENSO as the forced response projects onto the leading mode of internal variability. Furthermore, an additional factor is that the influence of the NAO (Hilmer and Jung 2000; Lu and Greatbatch 2002; Vicente-Serrano and López-Moreno 2008) and ENSO (López-Parages and Rodríguez-Fonseca 2012; Greatbatch et al. 2004; Mariotti et al. 2002; Zanchettin et al. 2008) over the North Atlantic European climate, has not been stationary along the twentieth century. Hence, the seasonal climate predictability could be variable and only effective for specific time periods, contributing in that way to the poor skill of current seasonal forecast systems over Europe (Van Oldenborgh and Burgers 2005).

A recent study of López-Parages and Rodríguez-Fonseca (2012, hereafter LPRF12) indicates, using observational data of rainfall, SLP and SST along the twentieth century, that the leading mode of interannual rainfall in the European region is significantly correlated with El Niño during some particular decades whilst, in others, there is no link with any large scale oceanic pattern. The spatial structure of the associated SLP field was similar to the traditional NAO. However, to better determine the dynamical link, the study of upper atmospheric levels is crucial, as was demonstrated by García-Serrano et al. (2010). ENSO influence over NAES can take place through different mechanisms which could include the alteration of the thermally driven overturning atmospheric circulation (Wang 2002, 2004; Wang and Enfield 2003; Ruiz-Barradas et al. 2003), downstream propagation of Rossby waves, including or not the stratosphere (Hastenrath 2003; Cassou and Terray 2001; Honda et al. 2001; Castanheira and Graf 2003; Ineson and Scaife 2008), or combinations of these mechanisms. The former occurs by the alteration of the Walker and Hadley circulations in relation to changes in the convection. The latter is explained through changes in the vorticity due to the meridional displacement of the flow at upper levels as a result of the divergence associated with the convection in the tropics. This vorticity disturbance triggers Rossby waves propagating over the extratropics and altering the atmospheric circulation over remote regions. In this way, a non-stationary impact of ENSO over Europe should be related to a non-stationary behavior of one (or both) of the previous mechanism. Recent studies have also found noticeable differences in the impacts of the two major ENSO patterns, Eastern and Central Pacific events (Kug et al. 2009; Kao and Yu 2009; Choi et al. 2011), the former being representative of the most intense El Niño events and the latter linked with the most intense La Niña ones (Dommenget et al. 2012). In this study non-Linear impacts of ENSO are not analyzed, each kind of episodes could be related to different non-stationary features of the abovementioned mechanisms (An and Wang 1999; Fedorov 2000; An 2009; Choi et al. 2011; Yeh et al. 2011). A possible hypothesis that could explain the changing impact of ENSO over the NAES is associated with a modulation of the teleconnection by which the forcing signal is transmitted to the target area depending on the background state. Hence, an interesting issue to be explored here is the influence of oceanic low frequency variability modes, such as Atlantic Multidecadal Oscillation (AMO, Enfield et al. 2001), or Pacific Decadal Oscillation (PDO, Mantua et al. 1997), in the modulation of the atmospheric teleconnection mechanisms at interannual timescales. In this sense, LPRF12 found how the correlation between the leading rainfall mode in Europe and the anomalies over the Niño3.4 region evolves at multidecadal timescales in phase with AMO, and PDO, depending on the season considered. Building on these previous studies, the main questions we wish to address in the present work are as follows: (1) is there any SST multidecadal pattern, internal to the ocean, that could be able to modulate the ENSO teleconnection with Europe? (2) How does this SST pattern modulate the teleconnections? (3) What are the associated dynamical mechanisms? (4) Is there any preferred phase of these multidecadal SST modulating patterns for which the ENSO-Europe teleconnection is more efficient?

Therefore, the present study is mainly related to the non-stationary influence of ENSO over the NAES and how the internal variability of the slowly variant background state of the ocean can modulate this teleconnection.

The available literature suggests January to March as an appropriate season to study the ENSO influence over Europe (Brönnimann 2007), being convenient to separate the weak ENSO-related circulation over the North Atlantic in early winter with the much stronger one during mid-late winter (Toniazzo and Scaife 2006; Gouirand et al. 2007). Even in the North Pacific, the canonical Tropical Northern Hemisphere pattern (TNH, Mo and Livezey 1986; Barnston and Livezey 1987; Livezey and Mo 1987; Trenberth et al. 1998) related to ENSO is not completely established until January (Bladé et al. 2008). For these reasons this work is focused on the non-stationary ENSO-European rainfall teleconnection in late winter early spring, selecting the season February–March–April, according to LPRF12. A complete analysis cannot be carried out using only observations due to the shortness of the record and limited sampling of multidecadal SST modes. It is thus of interest to use a model approach where the non-stationary behavior could be assessed on multi-centennial simulations. To this aim, a long coupled simulation with constant pre-industrial forcing has been analyzed to complement the observational analysis. If the changes identified in the ENSO-European rainfall relationship along the twentieth century could be reproduced only considering the internal variability of the climate system, it would suggest that the responsible

mechanism of the non-stationary behavior is not necessarily related to anthropogenic changes.

The paper is organized as follows. We begin by presenting the data and methods used (Sect. 2). In Sect. 3 the covariability of European rainfall and tropical SSTs is analyzed for observations. The same analysis is applied to a long control simulation of the CMIP5-CM5 coupled model in Sect. 4. In Sect. 5, observed and modeled composites maps of different fields are compared to each other. Then, in Sect. 6, some plausible hypotheses of the non-stationary features identified are presented and finally, in Sect. 7, a brief summary is presented.

2 Data and methods

This work is focused on the interannual precipitation over the Euro-Mediterranean region (iEMedR; 24°N–68°N, 15°W–35°E), in late winter-early spring (February–March–April, FMA).

Two different observational databases have been used: University of Delaware rainfall data (Matsuura and Willmott 2009, version 2.01, http://climate.geog.udel.edu/climate/html_pages/), and Global Precipitation Climatology Centre data (GPCC; Schneider et al. 2008). Both data are monthly climatology of precipitation spanning the whole twentieth century and the beginning of the twenty-first century. They are land-only in coverage and are based on interpolated data from stations. Regarding the SST data, ERSSTv3 (Smith et al. 2008) from 1854 to present (2° × 2° lat long), and HadISST1 (Rayner et al. 2003) from 1870 to present (1° × 1° lat long) have been used. To pose a possible dynamical mechanisms and be able to compare it with the model outputs, atmospheric fields from the twentieth century Reanalysis V2 data provided by the NOAA/OAR/ESRL PSD (Boulder, Colorado, USA; http://www.esrl.noaa.gov/psd/), have also been used.

The climate model data are provided by a long control coupled simulation (hereinafter PICTRL) of the CNRM-CM5 model (cf. Voldoire et al. 2013). This model includes the ARPEGE-Climat (v5.2) atmospheric model (1.4° × 1.4°, 31 vertical levels, being 26 of them in the troposphere), the NEMO (v3.2) ocean model (ORCA1°, 42 vertical levels), the ISBA land surface scheme and the GELATO (v5) sea ice model coupled through the OASIS (v3) system. The PICTRL analyzed here is an 800 year long simulation where all external forcings (solar, volcanic and anthropogenic Greenhouse Gases and aerosols) are kept constant at their observed values of 1850.

Regarding the methodology, a Maximum Covariance Analysis (MCA, or Singular Value Decomposition; Bretherton et al. 1992) has been applied to identify the modes that explain the maximum covariance between the anomalous Euro-Mediterranean rainfall and tropical SST (20°N–20°S). Each mode comprises two spatial structures (singular vectors), two time series (expansion coefficients; U and V for the predictor and predicted field respectively), and the covariance fraction, which is a measure of the percentage of covariability explained by each mode. The most common procedure when analyzing MCA results is to plot the projection of the predictor field (tropical SSTs here), and the field to predict (Euro-Mediterranean rainfall), on the standardized U, obtaining in that way the homogeneous and heterogeneous maps respectively. Along this study some composite maps also based on U have been obtained, being 1 standard deviation of U the threshold selected in PICTRL, and 0.75 standard deviation in observations. This difference in the threshold is considered to balance the number of cases selected in both, model and observations. These composites have been calculated to analyze the changes in the spatial patterns depending on the time period, and also to infer possible related dynamical mechanisms.

To retain only the interannual variability for all the fields analyzed here, periods longer than 7 years have been subtracted by applying a temporal filter based on a Discrete Fourier Transform. Looking for the stationarity of El Niño impact, different sliding window correlation analysis have been applied along the study, using 21 year as the reference window, for comparison with previous studies.

The correlation statistical significance has been determined by a non parametric approach using a Monte-Carlo test with 400 permutations. The spatial patterns significance has been also determined by non parametric approaches such as, Monte-Carlo test, or Wilcoxon-Mann–Whitney test (Wilks 2005).

3 Rainfall-SST covariability: observational results

As it was shown in LPRF12, the teleconnection between El Niño and the European rainfall leading mode of variability in late winter-early spring seems to be non-stationary on time, changing along the twentieth century in phase with the Atlantic Multidecadal Oscillation (AMO). The leading EOF is shown in Fig. 1a, which is consistent with the ENSO signal over the European rainfall (Fraedrich and Müller 1992; Moron and Plaut 2003; Pozo-Vazquez et al. 2005). In order to delve into the existence of this impact and to discard it as a statistical artifice, a time index based on this leading EOF has been used. This index has been calculated as the difference of area-average rainfall over Western Europe and Western Mediterranean region. These areas are two centers of actions of the leading EOF (black boxes in Fig. 1a), and they do not coincide with those in the second and third modes of variability (see Figure A1 of supplementary material). Time correlation between

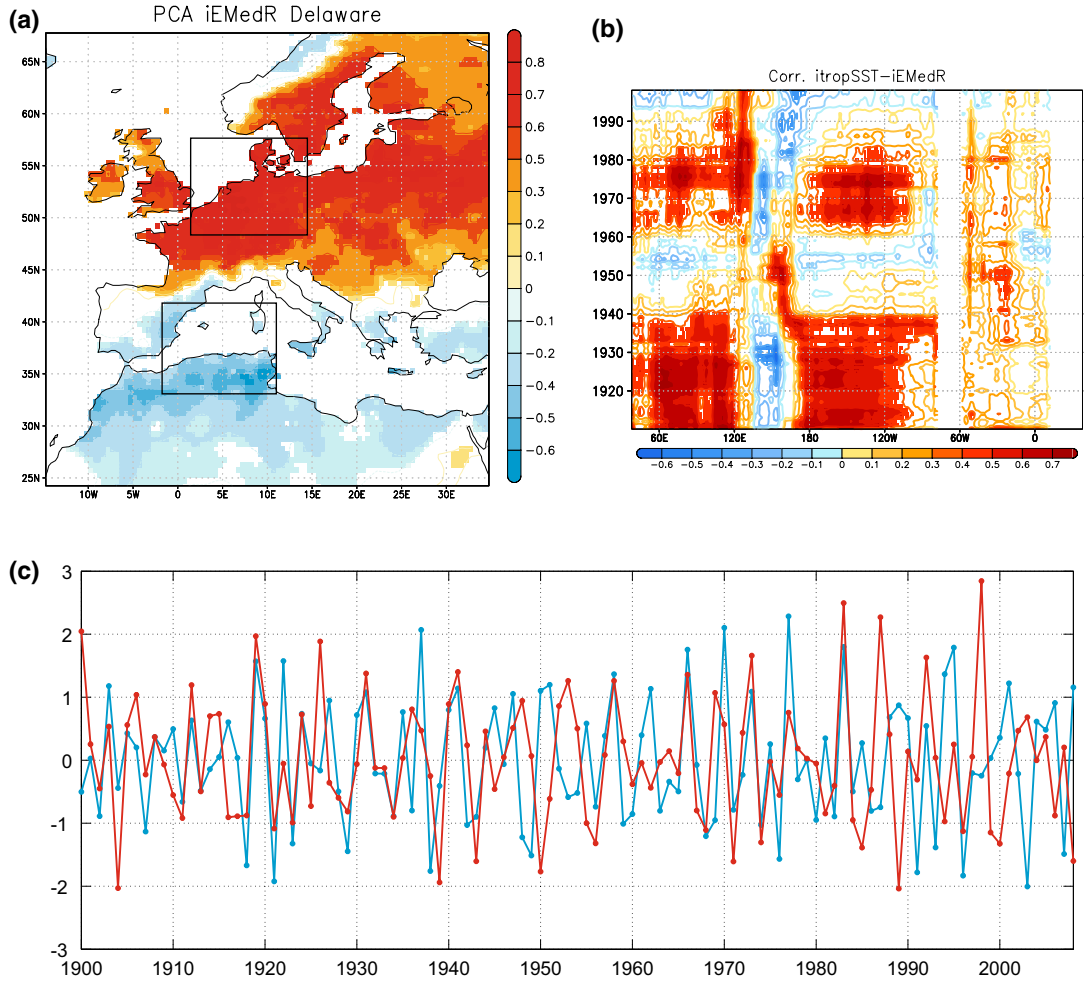

Fig. 1 **a** Leading rainfall empirical orthogonal function over the Euro-Mediterranean region (EOF1, standardized rainfall per standard deviation in the associated PC1). **b** 21-Years sliding windows correlation between the PC1 and tropical SSTs (5°S–5°N). **c** Standardized PC1 (*blue*) and Niño34 (*red*) Indices. *Black boxes* in (**a**) indicate the regions used to calculate the rainfall index mentioned in the manuscript (Western Europe minus Western Mediterranean). Statistical significant areas, according to a Monte-Carlo test at the 95 % level, are *shaded*

the leading PC and the above-mentioned index is 0.83, which supports the absence of a mathematical artifact in the calculation of the leading EOF. The link with the equatorial SSTs is, moreover, non-stationary on time (Fig. 1b). Thus, strong correlations with the whole Indo-Pacific equatorial basin are positive from 1900s to 1940s and from 1960s to 1980s. However, for the years in between and, in the beginning of the twenty-first century, the correlations are weaker and of opposite sign. For the whole twentieth century, the SST pattern coincides in sign in the Pacific and Indian oceans, while being opposite over the Maritime Continent. Although the magnitude of the correlation scores slightly differs between HadISST and ERSST (not shown), in both cases the maximum values are located over the Niño3.4 region, as in LPRF12. In agreement with Fig. 1b, the Euro-Mediterranean rainfall PC1 and the Niño3.4 index (Fig. 1c) broadly correlate from 1900 to 1940 (0.47), and from 1965 to 1984 (0.42) approximately, while they are mainly anticorrelated from 1944 to 1964 (−0.23), and from 2003 to 2008 (−0.73).

The previous results reinforce those of LPRF12 and show how, although the dipolar rainfall pattern identified as EOF1 is present along the whole observational period, it might be enhanced and potentially predictable when its relation with tropical SSTs is stronger. It also shows that this link mainly takes place in the twentieth century during negative phases of AMO. As it was indicated in Sect. 2, MCA is a discriminant analysis tool which is very useful for finding coupled patterns in climate data and, thus, for

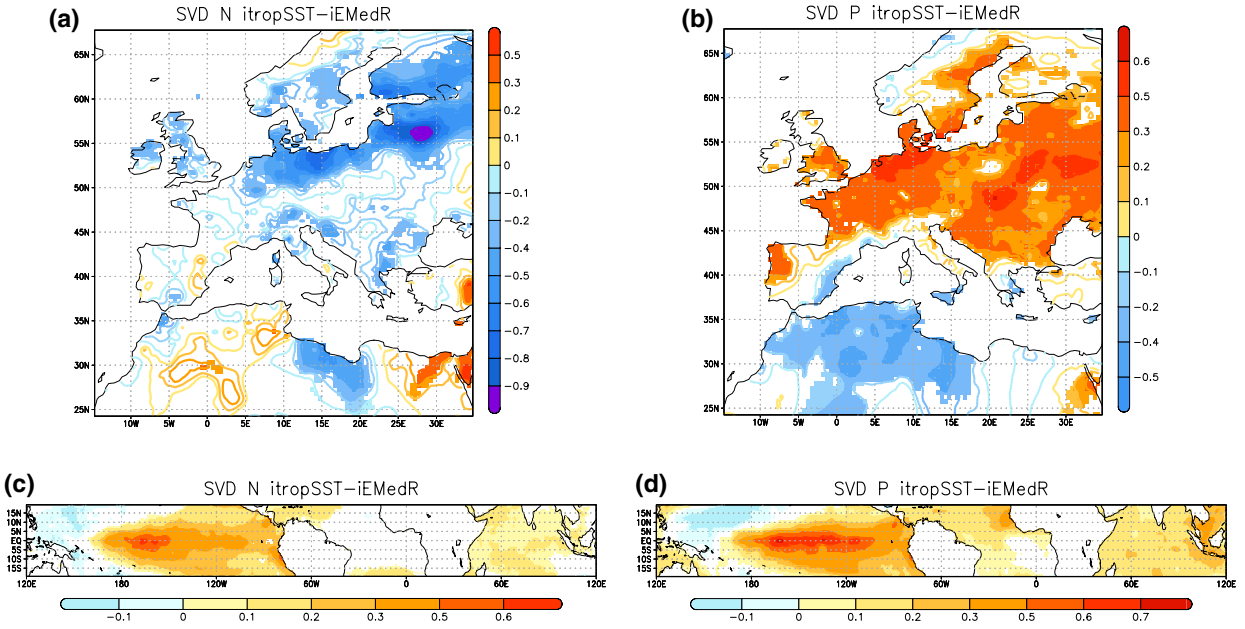

Fig. 2 Homogeneus (*bottom*) and heterogeneous (*up*) regressions maps of respectively SST (° per std. deviation in U) and rainfall (standardized rainfall per standard deviation in U) onto the MCA SST expansion coefficient (U) obtained for N and P periods. On the *left* (**a**, **c**) the leading covariability mode for observed N periods (1944–1964 and 2003–2008) and, on the *right* (**b**, **d**), the same for observed P periods (1900–1940 and 1965–1984)

determining the most frequent predictors for a variable to predict. With the purpose of confirming the changing coupling between rainfall and SST, two different MCA analyses linking the Euro-Mediterranean rainfall and the tropical SST have been performed selecting two different samples according to the changing relationship previously identified. The first sample covers the periods 1944–1964, and 2003–2008, which correspond to the years with negative correlations between rainfall and Niño3.4 (Fig. 1c). The second sample (1900–1940 and 1965–1984) corresponds to the periods with positive correlations between the same indices. Hereinafter these periods will be referred as N (Negative correlations) and P (Positive correlations) periods respectively.

The leading mode of covariability for the P period (Fig. 2b, d), which explains 31.1 % (28.3 % for ERSST) of the total covariance, resembles the link identified in LPRF12 (see Fig. 1 of LPRF12). The spatial correlation between the rainfall anomalous pattern obtained in LPRF12 and that obtained here from the MCA_P is 0.88 (0.85 for ERSST). On the other hand, for N periods (Fig. 2a, c), the leading mode, which in this case explains 23.3 % (21.6 % for ERSST) of the total covariance, shows a similar SST pattern than in P periods, but in relation to a completely different rainfall pattern. The spatial correlation between the rainfall pattern from LPRF12 and that obtained here from the MCA_N is −0.61 (−0.59 for ERSST). These rainfall maps obtained for each MCA broadly coincide with the simple regression of rainfall anomalies on the Nino3.4 index (see Figure A2 of supplementary material) for the selected periods. Although the tropical SSTs for both MCAs are similar, it is worth to highlight the enhanced signal identified in P over the Tropical North Atlantic (TNA) and the Maritime continent regions. This issue will be discussed in Sect. 5.

As the observed changing link between rainfall and tropical Pacific SSTs appears in phase with the AMO, and this oceanic mode is internal to the ocean, a long coupled control simulation has been used to test if this non-stationary relationship could be reproduced by the model multidecadal internal variability without any changes in external forcing.

4 Model performance

It is first necessary to assess the ability of the model to reproduce the leading mode of observed interannual rainfall variability. The observed and simulated modes present a similar spatial pattern (Fig. 3a), with significant scores in central Europe, including the British Islands, and the surrounding areas of the Baltic Sea. These anomalies are opposite in sign to those over the Mediterranean region, the northwestern Africa, and the north of Scandinavia. This leading rainfall

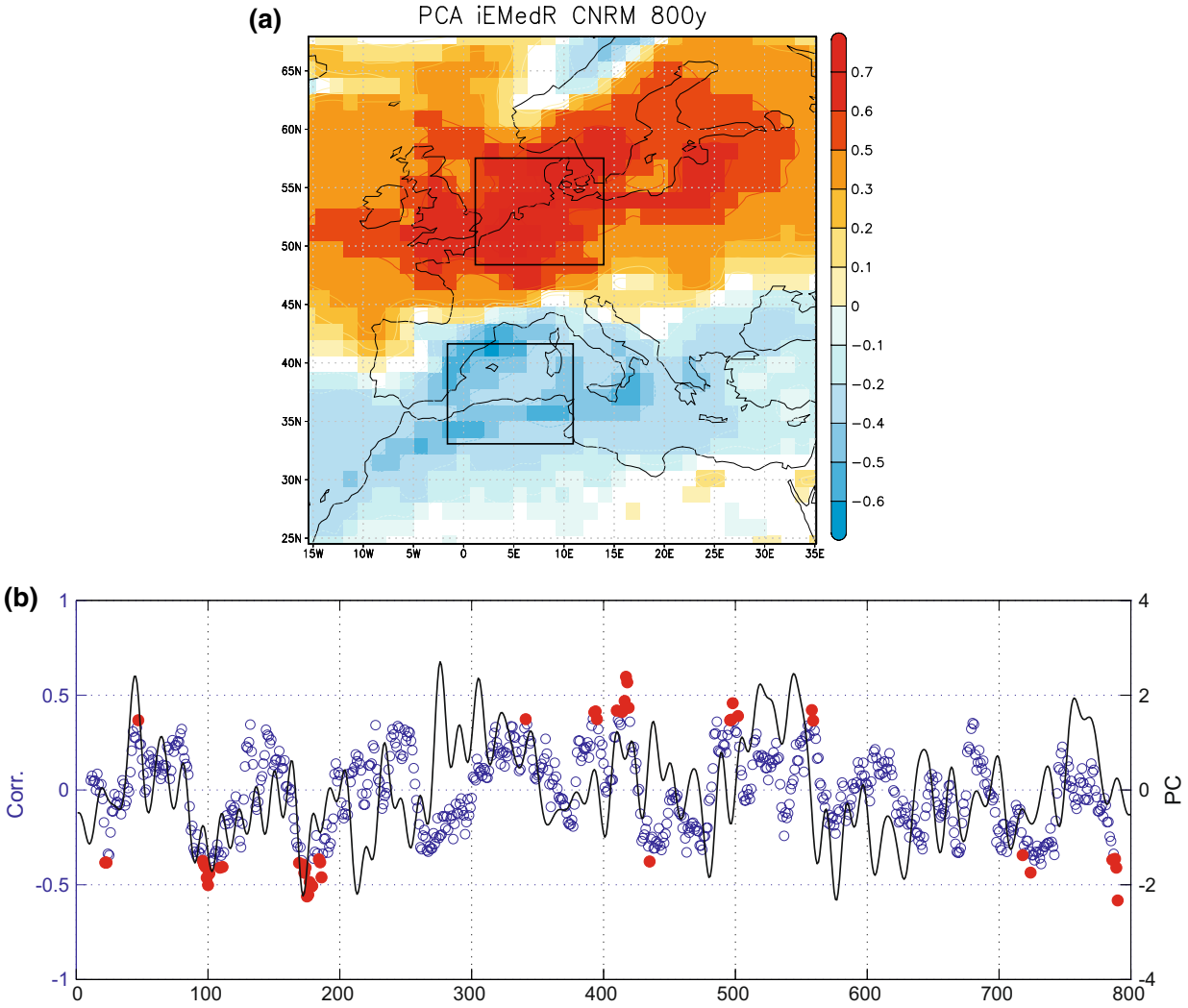

Fig. 3 **a** Leading empirical orthogonal function in PICTRL over the Euro-Mediterranean region (EOF1, standardized rainfall per standard deviation in the associated PC1). **b** 21-Years sliding windows correlation between the interannual rainfall PC1 and the Niño3.4 index (*dots*), and PC1 of an EOF analysis of the low frequency SSTs (*black line*, for which only higher periods than 13 years have been considered). *Fill dots* and *shaded areas* represent 95 % significance according to a Monte-Carlo test

mode can be described through the same simple index previously used in observations (see black boxes in Fig. 1a). In this case PC1 is correlated at 0.89 with the defined index. Slight differences with observational EOF1 are found in the intensity and location of the centers of action, and in the decrease of the explained variance by the leading mode (19.2 % in observations and 14.4 % in PICTRL). This fact is probably explained by the large difference in the number of years analyzed in observations (109 years) and PICTRL (800 years). In spite of this decrease in the explained variance, the leading mode of PICTRL is well separated to the second one according to the criteria of North et al. (1982). Looking for the stationarity of the rainfall mode, 21-yr window sliding correlations have been calculated here (Fig. 3b) between the rainfall leading PC and the Niño3.4 index, indicating a quasi-cyclic behavior in the relationship and, as a consequence, periods with positive, negative, or even no correlation. This time evolution is highly similar to the leading PC of the low frequency SST variability of the model (Fig. 3b). PICTRL, which is a long control simulation, is a useful tool to assess the time evolution identified in the moving correlations (see also Figure A3) and its possible connection with multidecadal modes such as AMO, as was proposed in LPRF12.

As in the observations, two different, and opposite, relationships emerge between rainfall and El Niño along the PICTRL, suggesting the existence of different underlying dynamics that alternate at multidecadal timescales. To further analyze this issue, periods with negative (N, 169 years)

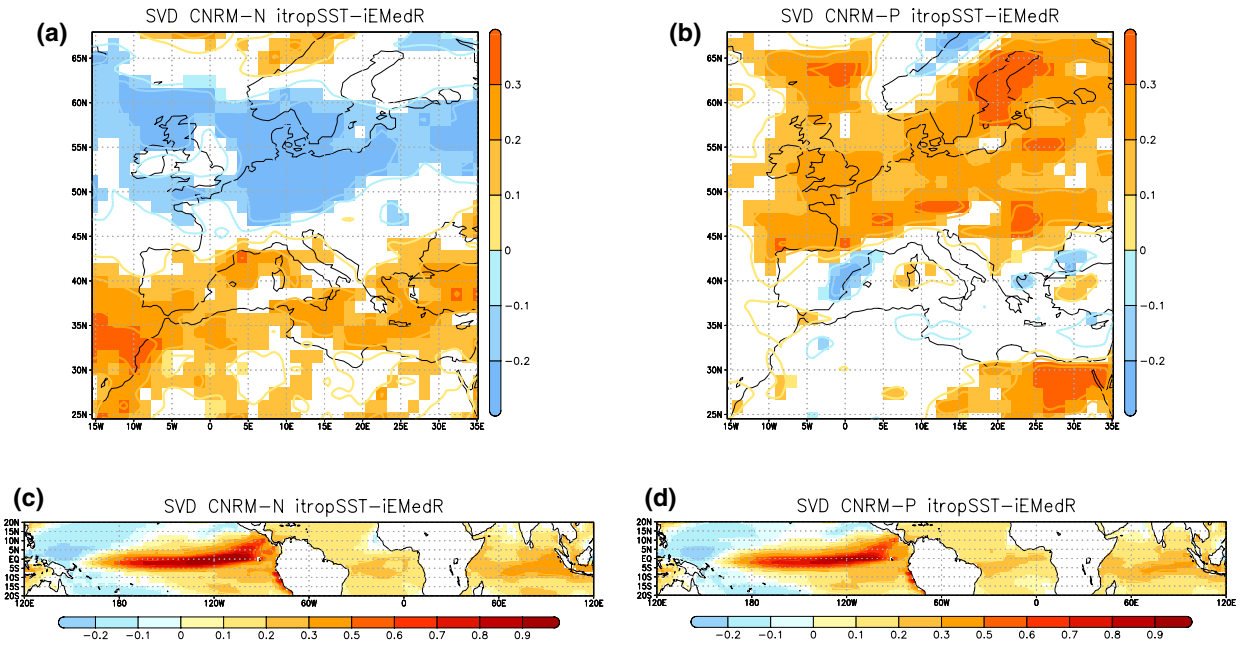

Fig. 4 Same as Fig. 2 but for the long control run in the model CNRM-CM5 (PICTRL)

and positive (P, 137 years) significant correlations have been analyzed separately.

MCA analysis between model anomalous rainfall and tropical SSTs has been performed for P and N. The leading modes of covariability account for 20.0 % and 21.9 % of the total variance, respectively. The resultant oceanic patterns (Fig. 4c, d) resemble the ones obtained in observations (Fig. 2c, d). However, unlike it happens in observations, the model ENSO signal is almost the same in P and N, putting forward how in PICTRL, the interannual SST forcing seems to be stationary. Nevertheless, its impact on rainfall is opposite in P and N periods over central Europe and the Mediterranean region. The spatial correlation between the rainfall patterns obtained for each period and the EOF1 for the whole PICTRL (Fig. 3a) are −0.90 and 0.71 for N and P respectively, reinforcing the idea of a changing impact over the Euro-Mediterranean area for the same tropical forcing.

In the next section the atmospheric variables related to the leading modes of covariability obtained for N and P periods are analyzed in order to infer different hypothesis for the dynamical mechanisms involved in the teleconnection.

5 Dynamical mechanisms in the teleconnection

Several composites maps have been calculated for each time period and for different variables involved in the above mentioned mechanisms. The expansion coefficient of tropical SSTs (hereinafter U) from each MCA has been used to perform "high minus low" composites maps as the difference between events for which U is greater than (high events), or lower than (low events) an imposed threshold (see Sect. 2).

The observational results are represented in Fig. 5 for N and P periods. In both cases, a warming (cooling) in El Niño and a extratropical horseshoe pattern over the North Pacific (Fig. 5a, b) appears in relation to an anomalous upper level divergence (convergence) over the central equatorial basin (Fig. 5c, d) and a weakening (strengthening) of the subtropical Pacific anticyclone. However, the tropical divergence together with its rotational response is clearly enhanced in P periods (Fig. 5c, d), as a consequence of the stronger El Niño amplitude in decades in which the north Atlantic is cooler than the south Atlantic, as it happens in P periods (Dong et al. 2006; Zhang et al. 2011). In agreement with Wang (2002), El Niño signal over the Pacific appears together with a heating in the Tropical North Atlantic (TNA), in association with a weakening of the Azores high (Fig. 5f). The connection takes place through changes in the Walker and Hadley circulations, as it can be seen by the Atlantic anomalous upper level convergence over South America and divergence over the TNA region (Fig. 5d). As the TNA region highly influences the ENSO-related atmospheric response over the NAE sector (Mathieu et al. 2004), its stronger signal for selected P periods, a time period with a stronger relation of El Niño with the rest of the tropical basins (Losada et al. 2010, 2012), could explain the non stationary impact of El Niño over the European climate.

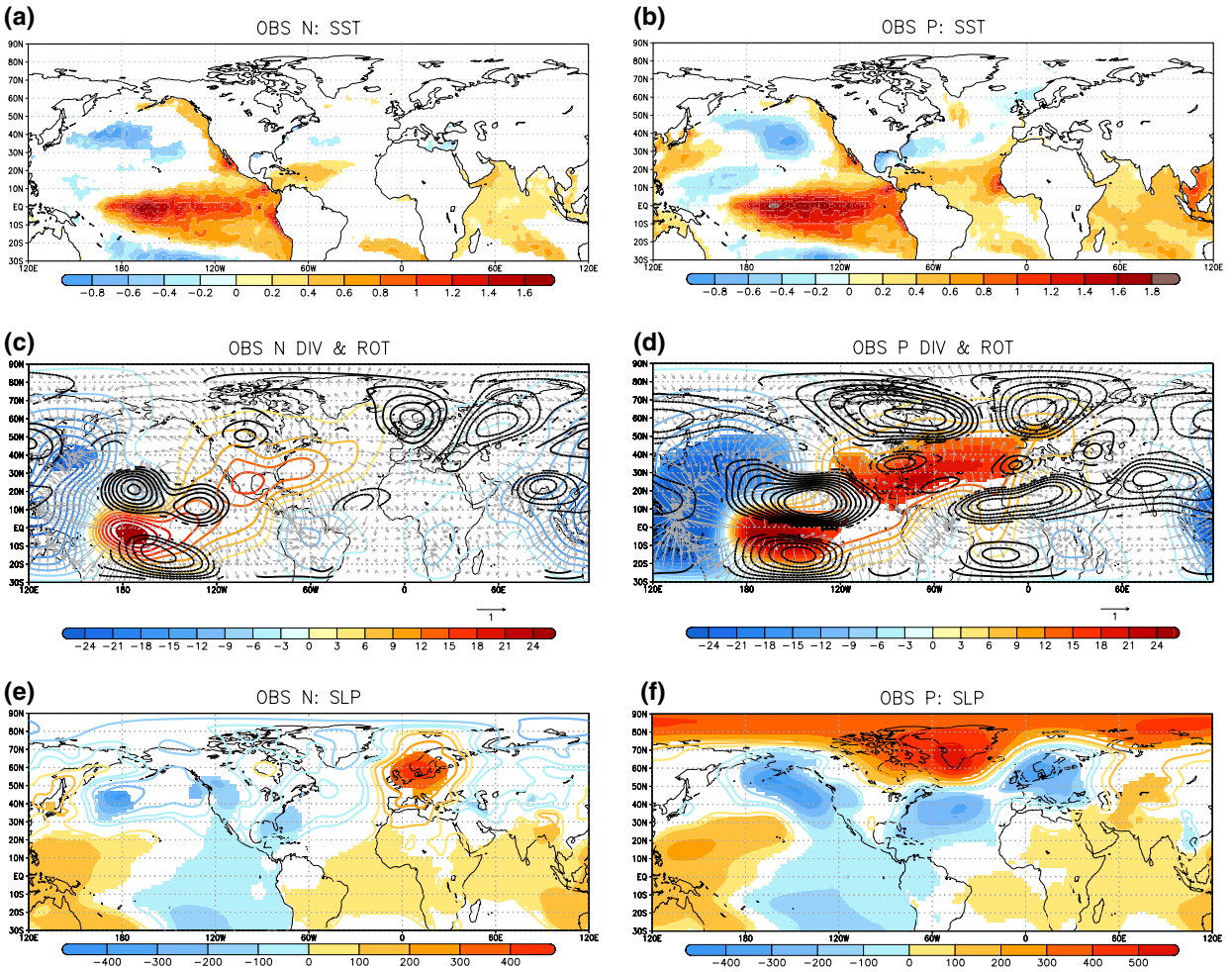

Fig. 5 High (higher that 0.75) minus low (lower that −0.75) composites maps, in N and P periods, based on the first SST MCA standardized expansion coefficient U for **a**, **b** HadISST (°); **c**, **d** potential velocity (in colour, 10^5 m^2 s^{-2}), streamfunction (*black contours*, $ci = 10^6$ m s^{-2}), and divergent wind (*arrows*, m s^{-1}) at 200 hPa, and **e**, **f** sea level pressure (Pa). Statistical significant areas, according to a Monte-Carlo test at the 95 % level, are *shaded*. In **c** and **d** only the 95 % significant streamfunction is contoured (being *solid lines* positive values and *dashed lines* negative ones)

This feature could, however, be also associated with the multidecadal variability of the Atlantic Warm Pool that is known to vary in phase with the AMO (Wang et al. 2008b). In general, the significant differences identified over the extratropical Atlantic and Pacific suggest a changing influence of the atmosphere on the underlying ocean (Fig. 5a, b). Regarding the tropical Indo-Pacific basin, warmer SSTs are observed in P from the Maritime continent to the Japan Islands. Thus, Rossby Wave Sources over these regions might be intensified in response to the warmer ocean. Moreover, in P as well, a stronger longitudinal gradient seems to take place over the west equatorial Pacific, in agreement with Meng et al. (2012), who have related it to a weakening of the Walker Circulation in association with a warmer Indian ocean. As a consequence of the changes in the tropical upper level divergence, an anomalous rotational circulation appears to balance the variation in the planetary vorticity to preserve the potential vorticity. For both, N and P periods, two twin anticyclones straddling the equator over the tropical Pacific reflect the typical Gill-type atmospheric response to equatorial anomalous heating (Gill 1980). However, only for P periods, the wavetrain propagating from the tropical Pacific resembles the well known TNH pattern. Moreover, a strong negative center of action also appears in P over Scandinavia. The whole quadrupolar atmospheric pattern over the North Atlantic-European sector has a quasi-barotropic structure (Fig. 5d, f) except for the Iberian Peninsula center that is not significant at surface levels. This configuration is coherent with the leading mode of upper level streamfunction in mid-winter obtained

by García-Serrano et al. (2010), and related to El Niño extratropical rotational atmospheric response. Complementary to that study, in which the stationary behavior is not discussed, this spatial structure (see Figs. 1, 3 of that paper) is found here just for selected P periods. The centre of action located over Scandinavia in P might be due to a split of the ENSO wavetrain originated in the tropical Pacific, as was suggested by García-Serrano et al. (2010) for January–February. The appearance of this pattern over the North Atlantic (Fig. 5d, f), and the role of low frequency changes in the ocean on its nonstationary behavior, will be further analyzed below.

For N decades, however, in agreement with a weaker heating at surface and a weaker divergent flow at upper levels, the TNH pattern weakens and the resultant configuration over North-Atlantic Europe (Fig. 5c) is different. At surface (Fig. 5e), the strong center of action located over the North Sea resembles an atmospheric blocking pattern. Thus, it seems that these blocking structures could be favored in N periods, in agreement with recent results putting forward an enhancement of the frequency of blocking events under positive phases of the AMO (Häkkinen et al. 2001).

Model results are represented in Fig. 6 for N and P periods. Contrary to the observations, the SST patterns and the associated perturbation of the divergent flow are highly similar to each other (Fig. 6a, b). The stronger influence in P of the atmosphere on the extratropical Atlantic and Pacific basins is, however, well reproduced by the model. The significant divergence signal over the North Atlantic, which is found in PICTRL for both N and P, resembles the response found just for P in observations. The significant upper level convergence over the equatorial Atlantic for PICTRL (Fig. 6c, d) appears in relation to an underlying warming (Fig. 6a, b), indicating the dominant influence of the remote warming in comparison with the local warming (which would induce divergence at upper levels). A significant velocity potential signal is also identified in PICTRL over the Indian Ocean, being slightly stronger for P periods. A striking feature is that these similar divergent responses for P and N are related to different rotational responses over the NAES (Fig. 6c, d). Over this region, the wave pattern at upper levels seems to significantly reach the European continent in P, the response being broadly the same as the one identified in observations at surface (Figs. 5f, 6f) and upper levels (Figs. 5d, 6d). Conversely, in N, the North Atlantic region is less perturbed by the TNH pattern and a dipolar configuration emerges at surface (Fig. 6e), resembling an internally driven NAO configuration and not the blocking pattern that appears in the observations (Fig. 5e).

Previous works have documented changes in the location of the actions centers of the NAO along the twentieth century (Hilmer and Jung 2000; Lu and Greatbatch 2002; Vicente-Serrano and López-Moreno 2008). Thus, our results could suggest an additional non-stationary external forcing over the NAES that could contribute to the documented changes in the observed NAO structure.

In agreement with the above mentioned results, it seems that the model is able to reproduce the observed impact of ENSO over the Northern Hemisphere and the Euro-Mediterranean region, at least, for selected periods (P). However, although the mechanism could be related to the Walker-Hadley atmospheric bridge and the TNH pattern, a different extratropical response occurs in relation to almost the same tropical heating in PICTRL for N periods (see Figure A4 of supplementary material). At this point a question emerges: if the forcing from the tropical Pacific SSTs is considered stationary in PICTRL, why the impact over the European rainfall is so different? A plausible explanation is that the zonal mean flow at upper levels, which influences the propagation of Rossby waves (Hoskins and Ambrizzi 1993), changes due to variations of the low-frequency oceanic forcing. This issue is analyzed in the next section.

6 Contribution of mean state changes to the interannual teleconnection

As it has been previously shown, tropical heating associated with El Niño is similar in N and P periods for PICTRL, so the distinct signals identified for each kind of period could reasonably be attributed to variations in the mean state. The characteristics of a control simulation make easier the inference of the role of low frequency SST internal variability because external forcings are constant and thus not considered. According to the results obtained in PICTRL, the changes in El Niño teleconnection observed over the North Atlantic and the Euro-Mediterranean region could be explained through changes in the internal mean state (not forced by the GW).

The rotational flow at upper levels previously plotted in Figs. 5d and 6c, d is presented in Fig. 7 in a north polar stereographic projection, identifying a similar configuration for those periods with a significant divergence flow signal associated with ENSO (P and N in PICTRL and P in observations). Nevertheless, the TNH pattern over the NAE sector is clearly weaken in PICTRL for N periods (Fig. 7a), while in P (Fig. 7b), the configuration over the North Atlantic is significantly stronger and highly similar with the observations (Fig. 7c). According to the basic Rossby Wave Theory proposed by Hoskins and Ambrizzi (1993), the planetary waves are always refracted towards latitudes with higher Rossby wavenumbers (Ks). As a consequence, positive anomalies of Ks indicate regions with a reinforced waveguide. Thus, the northward displacement of the Indo-Pacific jet in P (Fig. 8a), and its related Rossby waveguide

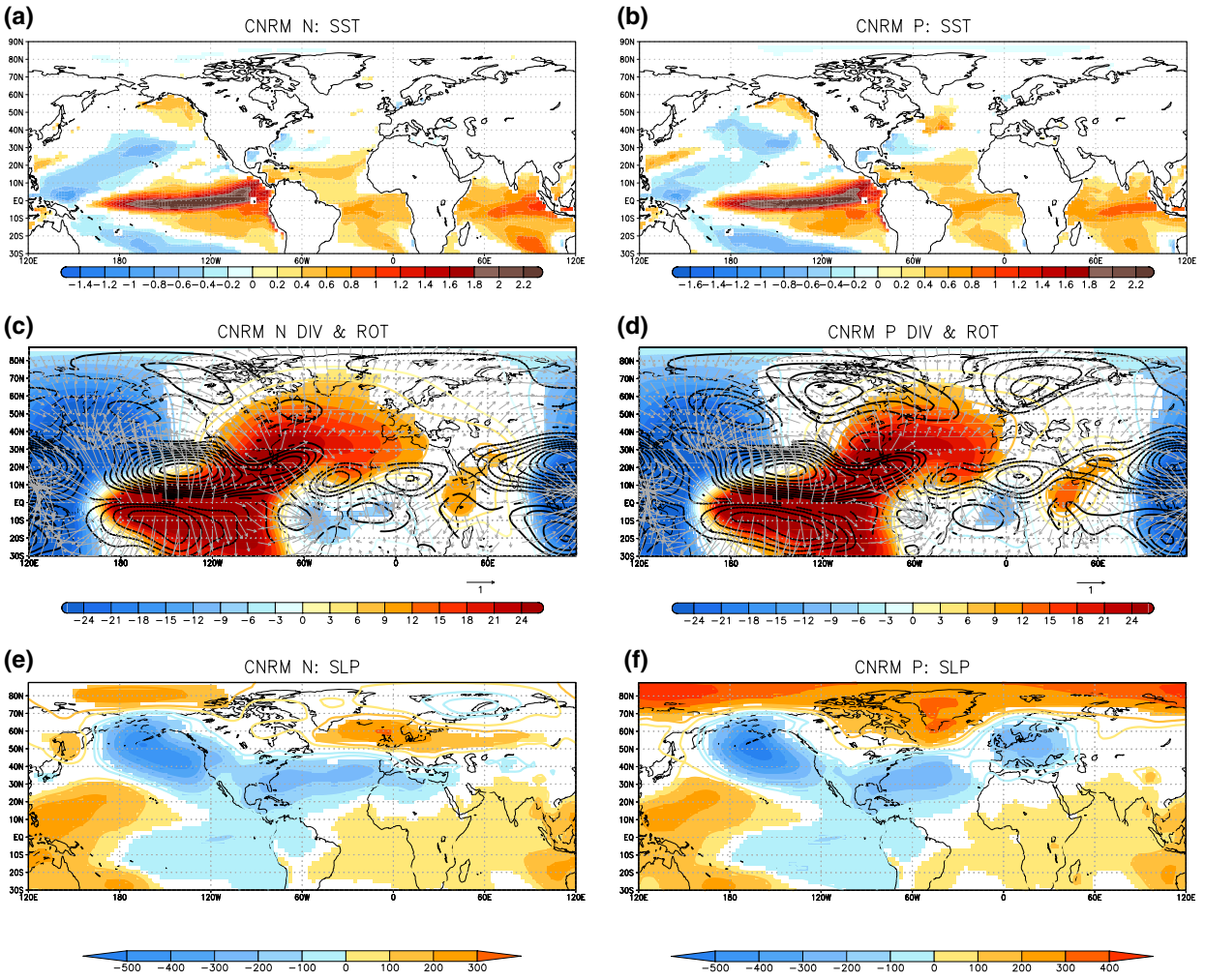

Fig. 6 Same as Fig. 5 but for the long control run in the model CNRM-CM5 (PICTRL). Here, higher values than 1 (U > 1 standard deviation) and lower values than −1 (U < −1 SD) have been considered for the composites maps

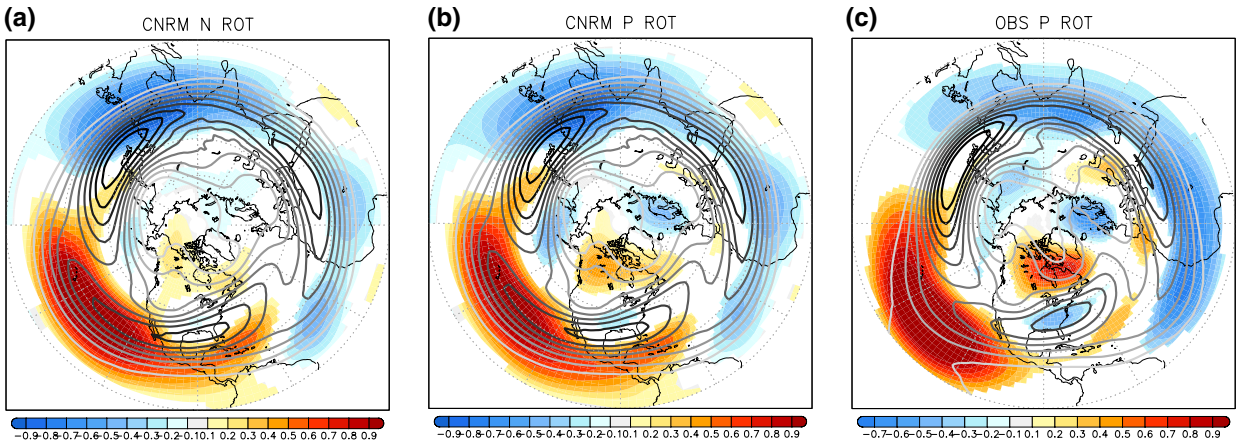

Fig. 7 Same composites maps of streamfunction (*shaded*; 10^7 m s^{-2}) as in **a** Fig. 6c, **b** Fig. 6d, and **c** Fig. 5d. In contours the zonal mean flow at 200 hPa (contours, ci = 5 m s^{-2}), being the maximum and minimum value represented 10 and 50 m s^{-2} in each case

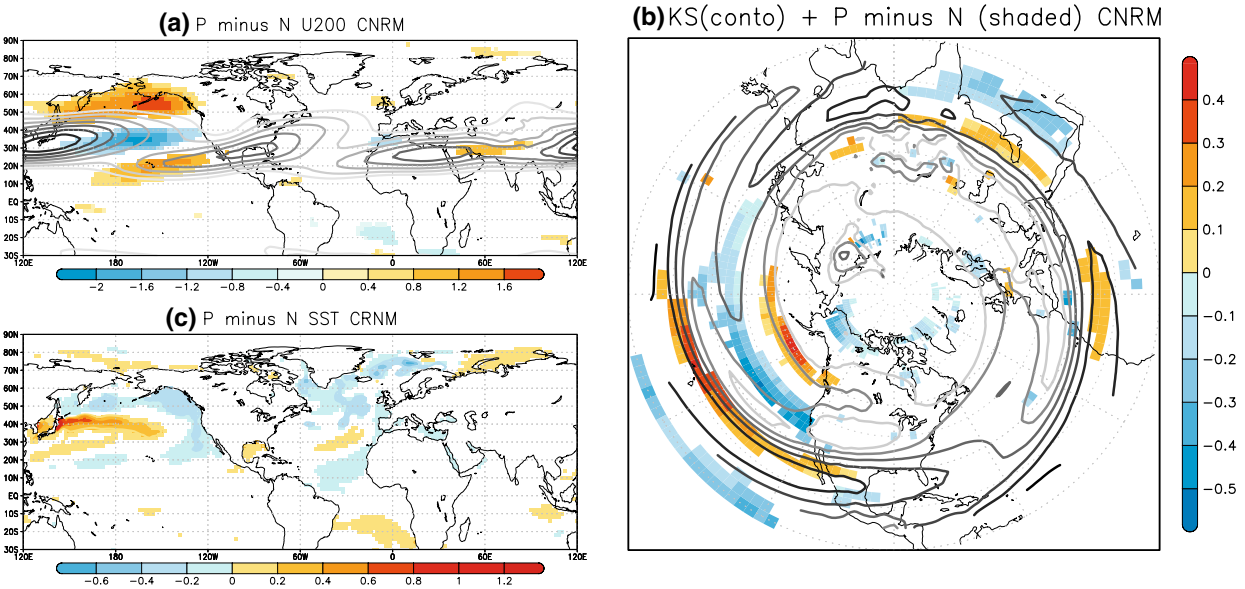

Fig. 8 High (P periods) minus low (N periods) significant composites maps in PICTRL for **a** zonal mean flow at 200 hPa (m s^{-1}), **b** mean Rossby wavenumber at 200 hPa (Ks) and **c** SST (°). The climatological zonal mean flow (**a**) and the climatological mean Rossby wavenumber (**b**) at 200 hPa are also shown in contours levels, being the maximum and minimum value represented 20 and 50 m s^{-1} (ci = 5 m s^{-1}) in the former case, and 3 and 8 (ci = 1) in the latter case. Only the 90 % statistical significant areas, according to the Wilcoxon-Mann–Whitney test, are plotted

(Fig. 8b), over the North Pacific, can explain the enhanced propagation of the disturbances to higher latitudes for P periods in the model. Hence, a stronger ENSO-related rotational atmospheric pattern over the NAES (García-Serrano et al. 2010) is identified (Fig. 7b). This difference could explain the non-stationary impact on rainfall between P and N periods in the model. The rotational flow configuration shown in Fig. 7 is also coherent with a remote displacement of the disturbances along the northern hemisphere due to the above-mentioned waveguide effect of the zonal mean flow (Hoskins and Karoly 1981; Branstator 1992, Hsu and Lin 1992; Hoskins and Ambrizzi 1993; Ambrizzi et al. 1995; Branstator 2002). Thus, it seems that a more efficient waveguide effect and so, a stronger hemispheric response, could also contribute in P to the above mentioned ENSO-related rotational impact over the North Atlantic.

These changes in the zonal mean flow are related to the underlying ocean multidecadal variability (Fig. 8c), which signal appears significant over the North Pacific and Atlantic basins, resembling typical multidecadal variability patterns associated with the well known PDO (Mantua et al. 1997) and AMO modes (Knight et al. 2005). As the jet streams are partially caused by the meridional temperature gradient in the earth's atmosphere, a significant change in their location could be expected if the underlying ocean temperature varies along the time. Thus, the non-stationary impact over the NAE sector identified in PICTRL could ultimately be explained by changes in the zonal mean flow forced by the slowly variant component of the ocean.

The observational results point to the same impact over the NAES for P periods, in agreement with López-Parages and Rodríguez-Fonseca (2012). Some slight differences appear, however, in the location of the extratropical centers of action in PICTRL (Fig. 7b) and observations (Fig. 7c), with a westward displacement in the former case. This fact could be explained by both, the more westerly location of the forcing region (see Figs. 5, 6), and the less elongated Indo-Pacific jet (Fig. 7b, c), in the model.

7 Summary

In this paper the link between the leading mode of interannual anomalous rainfall in the Euro Mediterranean region and El Niño found in López-Parages and Rodríguez-Fonseca (2012) has been further investigated using a long control simulation of the CNRM-CM5 model. The aim of the study is to find if the observed multidecadal modulations of ENSO teleconnections with Europe can be reproduced by the internal low frequency variability of the coupled system without invoking any role for anthropogenic forcing. The study is focused on the late-winter early spring, which is a characteristic season in which ENSO exerts an influence over North Atlantic and Europe (Brönnimann 2007; Zhang

et al. 2011). The working hypothesis is that ENSO teleconnections are not stationary and the multidecadal natural variability of the ocean acts as a modulator, in agreement with the results of López-Parages and Rodríguez-Fonseca (2012).

In this way, the correlation between the observed Euro-Mediterranean rainfall and ENSO is stronger in some decades (P) than in others (N). For P, broadly in coincidence with twentieth century negative phases of AMO, an increase of rainfall over central Europe and a decrease over the Mediterranean area occurs jointly with a warming over the tropical Pacific and Indian basins, and a cooling over the Maritime continent. As the correlations obtained evolve in phase with the AMO, which is a natural internal variability mode of the ocean, a long coupled control simulation has been considered as a useful dataset to analyze the internal effect in the observed modulation.

In particular, the CNRM-CM5 model long control simulation has been used. This model reproduces the observed leading rainfall mode and its non-stationary link with El Niño, confirming in this way that the natural variability has an effect in modulating the impacts of El Niño in the extratropical North Atlantic region.

In the above-mentioned P periods two dynamical mechanisms are contributing to the ENSO teleconnection. Thus, alteration of the thermally driven direct circulation (Wang 2002), and the ENSO related rotational North Atlantic mode (Garcia-Serrano et al. 2010), significantly affect the surface European rainfall in both, model and observations. The resultant configuration over the NAE sector has been previously associated with a non-stationary forcing from the tropics (Greatbatch et al. 2004), but also with a teleconnection pathway via the stratosphere (Ineson and Scaife 2008). In the latter work it is argued that the response over the NAES in late winter is explained by the occurrence of sudden stratospheric warming's, and so, a good representation of the stratosphere become crucial. Here, the same impact has been reproduced by a model which do not fully represent stratospheres processes ("low-top model"). Then, although the stratosphere could play also an important role, the teleconnection could be reproduced through tropospheric mechanism if the non-stationary features are considered. Nevertheless, this does not exclude a possible significant role for the stratosphere that could be analyzed in a similar setup with high-top models.

The ENSO related rotational flow impact is modulated, in PICTRL, by changes in the zonal mean flow at upper levels forced by the ocean. Hence, the surface signal over the NAES changes as well, resembling in N periods a negative phase of the NAO. The observed N periods, coinciding with positive phases of the AMO, are characterized by a weakening of the ENSO signal. As a consequence, the previously commented mechanisms are also weakened and, an atmospheric blocking pattern appears in relation to an El Niño signal over the tropical Pacific. This link between ENSO and the enhanced frequency of blocking events under positive phase of AMO (Häkkinen et al. 2001) should be further investigated in the future.

Although this study is focused on late winter and early spring, non stationarities modulated at multidecadal timescales takes place from autumn to spring (see Fig. 2 of LPRF12). Thus, similar changes in the zonal mean flow forced by the ocean could also explain the changing impact identified in these seasons. This seasonal time difference in the nonstationary ENSO-NAES teleconnection is a task to be further researched in future works.

Our results thus point to an important role (although not unique) of the multidecadal changes in the zonal flow forced by natural internal oceanic variability, in the modulation of El Niño effect on the European rainfall. As a fraction of the oceanic variability is linked to the Atlantic Meridional Overturning Circulation that is projected to weaken in the twenty-first century, it is possible that the interaction between El Niño and Europe change again in the next decades. Another explanation to the nonstationary impact of the same ENSO signal over the NAES could be related to a changing SSTs background state of the tropical Pacific, which in turn could be also forced by the Atlantic Ocean (Sutton and Hodson 2007). To get further insight into these issues, and to investigate nonlinear responses, sensitivity experiments with General Circulation Models (GCMs) should be also done in the future.

Acknowledgments We are indebted to CERFACS for providing the CNRM-CM5 control simulation, which has made possible this study. We thank to the University of Delaware, GPCC, NOAA, and the UK Met-Office for the provided data. The study has been partially supported by the National Spanish Projects: TRACS (CGL2009-10285) and MULCLIVAR (CGL2012-38923-C02-01). JLP also thanks the FPI grant BES-2010-042234 of the Ministerio de Economía y Competitividad of Spanish Goverment. We would like to thank the anonymous reviewers for their helpful comments, which greatly helped to improve the manuscript.

References

Ambrizzi T, Hoskins BJ, Hsu HH (1995) Rossby wave propagation and teleconnection patterns in the austral winter. J Atmos Sci 52:3661–3672

An SI (2009) A review of interdecadal changes in the nonlinearity of the El Niño-Southern Oscillation. Theoret Appl Climatol 97(1–2):29–40. doi:10.1007/s00704-008-0071-z

An SI, Wang B (1999) Interdecadal change of the structure of the ENSO mode and its impact on the ENSO frequency. J Clim 13:2044–2056

Barnston AG, Livezey RE (1987) Classification, seasonality, and persistence of low-frequency atmospheric circulation patterns. Monsoon Weather Rev 115:1083–1126

Bladé I, Newman M, Alexander M, Scott J (2008) The late fall extratropical response to ENSO: sensitivity to coupling and convection in the tropical west Pacific. J Clim 21:6101–6118

Branstator G (1992) The maintenance of low-frequency atmospheric anomalies. J Atmos Sci 49:1924–1946

Branstator G (2002) Circumglobal Teleconnections, the Jet Stream Waveguide, and the North Atlantic Oscillation. J Clim 15(14):1893–1910. doi:10.1175/1520-0442(2002)015<1893:CTTJSW>2.0.CO;2

Bretherton CS, Smith C, Wallace JM (1992) An intercomparison of methods for finding coupled patterns in climate data. J Clim 5(6):541–560. doi:10.1175/1520-0442(1992)005<0541:AIOMFF>2.0.CO;2

Brönnimann, S (2007) Impact of El Niño–Southern Oscillation on European climate. Rev Geophys 45:RG3003, doi:10.1029/2006RG000199

Cassou C, Terray L (2001) Oceanic forcing of the winter-time low-frequency atmospheric variability in the North Atlantic European sector: a study with the ARPEGE model. J Clim 14:4266–4291

Castanheira JM, Graf HF (2003) North Pacific-North Atlantic relationships under stratospheric control? J Geophys Res 108(D1):4036. doi:10.1029/2002JD002754

Choi J, Kug SAJ, Nin E (2011) The role of mean state on changes in El Nino's flavor. 1205–1215. doi:10.1007/s00382-010-0912-1

Czaja A, Frankignoul C (1999) Influence of the North Atlantic SST on the atmospheric circulation. Geophys Res Lett 26(19):2969–2972. doi:10.1029/1999GL900613

Dommenget D, Bayr T, Frauen C (2012) Analysis of the non-linearity in the pattern and time evolution of El Niño southern oscillation. Clim Dyn 40(11–12):2825–2847. doi:10.1007/s00382-012-1475-0

Dong B, Sutton RT, Sutton AA (2006) Multidecadal modulation of El Niño-Southern Oscillation (ENSO) variance by Atlantic Ocean sea surface temperatures. Geophys Res Lett 33:L08705. doi:10.1029/2006GL025766

Enfield DB, Mestas Nuñez AM, Trimble PJ (2001) The Atlantic multidecadal oscillation and its relation to rainfall and river flows in the continental US. Geophys Res Lett 28(10):2077. doi:10.1029/2000GL012745

Fedorov AV (2000) Is El Nino changing? Science 288(5473):1997–2002. doi:10.1126/science.288.5473.1997

Fraedrich K, Müller K (1992) Climate anomalies in Europe associated with ENSO extremes. Int J Climatol 12:25–31. doi:10.1002/joc.3370120104

García-Serrano J, Rodríguez-Fonseca B, Bladé I, Zurita-Gotor P, Cámara A (2010) Rotational atmospheric circulation during North Atlantic-European winter: the influence of ENSO. Clim Dyn 37(9–10):1727–1743. doi:10.1007/s00382-010-0968-y

Gill AE (1980) Some simple solutions for heat-induced tropical circulations. Q J R Meteorol Soc 106:447–462

Gouirand I, Moron V, Zorita E (2007) Teleconnections between ENSO and North Atlantic in an ECHO-G simulation of the 1000–1990 period. Geophys Res Lett 34(6). doi: 10.1029/2006GL028852

Greatbatch RJ, Lu J, Peterson KA (2004) Nonstationary impact of ENSO on Euro-Atlantic winter climate. Geophys Res Lett 31:L02208. doi:10.1029/2003GL018542

Häkkinen S, Rhines PB, Worthen DL (2001) Atmospheric blocking and Atlantic multidecadal ocean variability. Science 334(6056):655–659. doi:10.1126/science.1205683

Hastenrath S (2003) Upper-air circulation of the Southern Oscillation from the NCEP-NCAR reanalysis. Meteorol Atmos Phys 83:51–65

Hilmer M, Jung T (2000) Evidence for a recent change in the link between theNorth Atlantic Oscillation and Arctic Sea ice export. Geophys Res Lett 27(7):989–992. doi:10.1029/1999GL010944

Honda M, Nakamura H, Ukita J, Kousaka I, Takeuchi K (2001) Interannual seesaw between the Aleutian and Icelandic lows, part I: seasonal dependence and life cycle. J. Climate. 14:1029–1041

Hoskins BJ, Ambrizzi T (1993) Rossby wave propagation on a realistic longitudinally varying flow. Atmos. Sci. 50:1661–1671

Hoskins BJ, Karoly K (1981) The steady response of a spherical atmosphere to thermal and orographic forcing. J Atmos Sci 38:1179–1196

Hsu HH, Lin SH (1992) Global teleconnections in the 250-mb streamfunction field during the northern hemisphere winter. Monsoon Weather Rev 120:1169–1190

Hurrell JW, Kushnir Y, Ottersen G, Visbeck M (2003) An overview of the North Atlantic Oscillation, in the North Atlantic Oscillation: climatic significance and environmental impact

Ineson S, Scaife AA (2008) The role of the stratosphere in the European climate response to El Niño. Nat Geosci 2(1):32–36. doi:10.1038/ngeo381

Kao HY, Yu JY (2009) Contrasting Eastern-Pacific and Central-Pacific types of ENSO. J Clim 22(3):615–632. doi:10.1175/2008JCLI2309.1

Knight JR, Allan RJ, Folland CK, Vellinga M, Mann ME (2005) A signature of persistent natural thermohaline circulation cycles in observed climate. Geophys Res Lett 32. doi:10.1029/2005GL024233

Kug JS, Jin FF, An SI (2009) Two types of El Niño events: cold tongue El Niño and warm pool El Niño. J Clim 22(6):1499–1515. doi:10.1175/2008JCLI2624.1

Livezey RE, Mo KC (1987) Tropical-extratropical teleconnections during the Northern Hemisphere winter. Part II: relationships between monthly mean Northern Hemisphere circulation patterns and proxies for tropical convection. Monsoon Weather Rev 115:3115–3132

López-Parages J, Rodríguez-Fonseca B (2012) Multidecadal modulation of El Niño influence on the Euro-Mediterranean rainfall. Geophys Res Lett 39(2). doi:10.1029/2011GL050049

Losada T, Rodríguez-Fonseca B, Polo I, Janicot S, Gervois S, Chauvin F, Ruti P (2010) Tropical response to the Atlantic Equatorial mode: AGCM multimodel approach. Clim Dyn 5:45–52

Losada T, Rodríguez-Fonseca B, Mohino E, Bader J, Janicot S, Mechoso CR (2012) Tropical SST and Sahel rainfall: a non-stationary relationship. Geophys Res Lett 39:L12705. doi:10.1029/2012GL052423

Lu J, Greatbatch RJ (2002) The changing relationship between the NAO and northern hemisphere climate variability. Geophys Res Lett 29(7):1–4. doi:10.1029/2001GL014052

Mantua NJ, Hare SR, Zhang Y, Wallace JM, Francis RC (1997) A Pacific interdecadal climate oscillation with impacts on salmon production. Bull Am Meteor Soc 78:1069–1079

Mariotti A, Zeng N, Lau KM (2002) Euro-Mediterranean rainfall and ENSO: a seasonally varying relationship. Geophys Res Lett 29(12):1621. doi:10.1029/2001GL014248

Mathieu PP, Sutton RT, Dong B, Collins M (2004) Predictability of winter climate over the North Atlantic European region during ENSO events. J Clim 17(1996):1953–1974. doi:10.1175/1520-0442(2004)017<1953:POWCOT>2.0.CO;2

Matsuura K,Willmott CJ, Terrestrial Precipitation (2009) 1900-2008 Gridded Monthly Time Series version 2.01, http://climate.geog.udel.edu/climate/html_pages/

Meng Q, Latif M, Park W, Keenlyside NS, Semenov VA, Martin T (2012) Twentieth century Walker Circulation change: data analysis and model experiments. Clim Dyn 38:1757–1773. doi:10.1007/s00382-011-1047-8

Mo KC, Livezey RE (1986) Tropical-extratropical geopotential height teleconnections during the Northern Hemisphere winter. Monsoon Weather Rev 114:2488–2515

Moron M, Plaut G (2003) The impact of El Niño Southern Oscillation upon weather regimes over Europe and the North Atlantic boreal winter. Int J Climatol 23:363–379. doi:10.1002/joc.890

North GR, Bell TL, Cahalan RF, Moeng FJ (1982) Sampling errors in the estimation of empirical orthogonal functions. Monsoon Weather Rev 110:699–706. doi:10.1175/1520-0493(1982)110<0699:SEITEO>2.0.CO;2

Pozo-Vazquez D, Gomiz-Fortis SR, Tovar-Pescador J, Esteban-Parra MJ, Castro-Diez Y (2005) El Niño-southern oscillation events and associated European winter precipitation anomalies. Int J Climatol 25(1):17–31. doi:10.1002/joc.1097

Rayner NA, Parker DE, Horton EB, Folland CK, Alexander LV, Rowell DP, Kent EC, Kaplan A (2003) Global analyses of sea surface temperature, sea ice, and night marine air temperature since the late nineteenth century. J Geophys Res 108(D14):4407. doi:10.1029/2002JD002670

Rodwell MJ, Rowell DP, Folland CK (1999) Oceanic forcing of the wintertime North Atlantic oscillation and climate variability of northern Europe. Nature 10:1635–1647

Ruiz-Barradas A, Carton JA, Nigam S (2003) Role of the atmosphere in climate variability of the tropical Atlantic. J Clim 16:2052–2065

Schneider U et al (2008) Global precipitation analysis products of the GPCC. Global Precipitation Climatology Centre, Offenbach

Smith TM, Reynolds RW, Peterson TC, Lawrimore J (2008) Improvements to NOAA's historical merged land-ocean surface temperature analysis (1880–2006). J Clim 21:2283–2296. doi:10.1175/2007JCLI2100.1

Sutton RT, Hodson DLR (2007) Climate response to basin-scale warming and cooling of the North Atlantic Ocean. J Clim 20:891–907. doi:10.1175/JCLI4038.1

Toniazzo T, Scaife A (2006) The influence of ENSO on winter North Atlantic climate. Geophys Res Lett 33(24). doi:10.1029/2006GL027881

Trenberth KE, Branstator GW, Karoly D, Kumar A, Lau NC, Ropelewski C (1998) Progress during TOGA in understanding and modeling global teleconnections associated with tropical sea surface temperatures. J Geophys Res 103(C7):14291–14324. doi:10.1029/97JC01444

Van Loon H, Rogers J (1978) The seesaw in winter temperatures between Greenland and Northern Europe. Part I: general description. Monsoon Weather Rev 106:296–310

Van Oldenborgh GJ, Burgers G (2005) Searching for decadal variations in ENSO precipitation teleconnections. Geophys Res Lett 32:L15701. doi:10.1029/2005GL023110

Vicente-Serrano SM, López-Moreno JI (2008) Nonstationary influence of the North Atlantic Oscillation on European precipitation. J Geophys Res 113(D20):D20120. doi:10.1029/2008JD010382

Voldoire A, Sanchez-Gomez E, Salas y Mélia D, Decharme B, Cassou C, Sénési S, Valcke S et al (2013) The CNRM-CM5.1 global climate model: description and basic evaluation. Clim Dyn 40(9–10):2091–2121. doi:10.1007/s00382-011-1259-y

Walker GT (1924) Correlation in seasonal variations of weather, IX A further study of world weather. Mem India Meteorol Dep 24(9):275–333

Wallace JM, Gutzler DS (1981) Teleconnections in the geopotential height field during the northern hemisphere winter. Monsoon Weather Rev 109:784–812. doi:10.1175/1520-0493(1981)109

Wang C (2002) Atlantic climate variability and its associated atmospheric circulation cells. J Clim 15(13):1516–1536. doi:10.1175/1520442(2002)015<1516:ACVAIA>2.0.CO;2

Wang C (2004) ENSO, climate variability and the Walker and Hadley circulations. In: Diaz HF, Bradley RS (eds) The Hadley circulation: present, past and future. Advances in global change research, vol 21. Springer, New York, pp 173–202

Wang C, Enfield DB (2003) A further study of the tropical western hemisphere warm pool. J Clim 16:1476–1493. doi:10.1175/1520-0442-16.10.1476

Wang C, Lee SK, Enfield DB (2008) Atlantic warm pool acting as a link between Atlantic multidecadal oscillation and Atlantic tropical cyclone activity. Geochem Geophys Geosyst 9:Q05V03. doi:10.1029/2007GC001809

Wilks DS (2005) Statistical methods in the atmospherics sciences. Academic Press. ISBN:13: 978-0-12-75196

Yeh SW, Kirtman BP, Kug JS, Park W, Latif M (2011) Natural variability of the central Pacific El Niño event on multi-centennial timescales. Geophys Res Lett 38(2). doi:10.1029/2010GL045886

Zanchettin D, Franks SW, Traverso P, Tomasino M (2008) On ENSO impacts on European wintertime rainfalls and their modulation by the NAO and the Pacific multi-decadal variability described through the PDO index. Int J Climat 28:995–1006. doi:10.1002/joc

Zhang L, Wang C, Wu L (2011) Low-frequency modulation of the Atlantic warm pool by the Atlantic multidecadal oscillation. Clim Dyn 39(7–8):1661–1671. doi:10.1007/s00382-011-1257-0

Supplementary Material

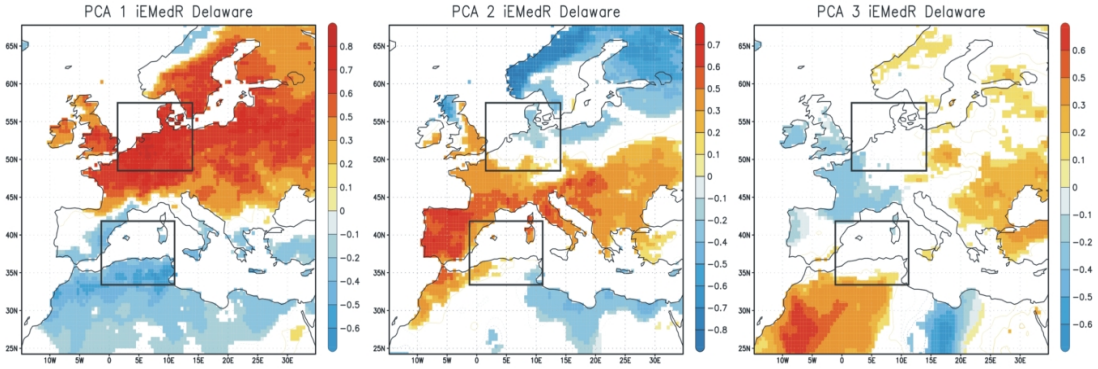

a) b) c)

Figure A1: a) Leading (19.2% of the total variance), b) second (11.9%) and c) third (5.9%) rainfall empirical orthogonal function over the Euro-Mediterranean region (standardized rainfall per standard deviation in the associated PC). Black boxes indicate the regions used to calculate the rainfall index (Western Europe minus Western Mediterranean). Statistical significant areas, according to a Monte-Carlo test at the 95% level, are shaded.

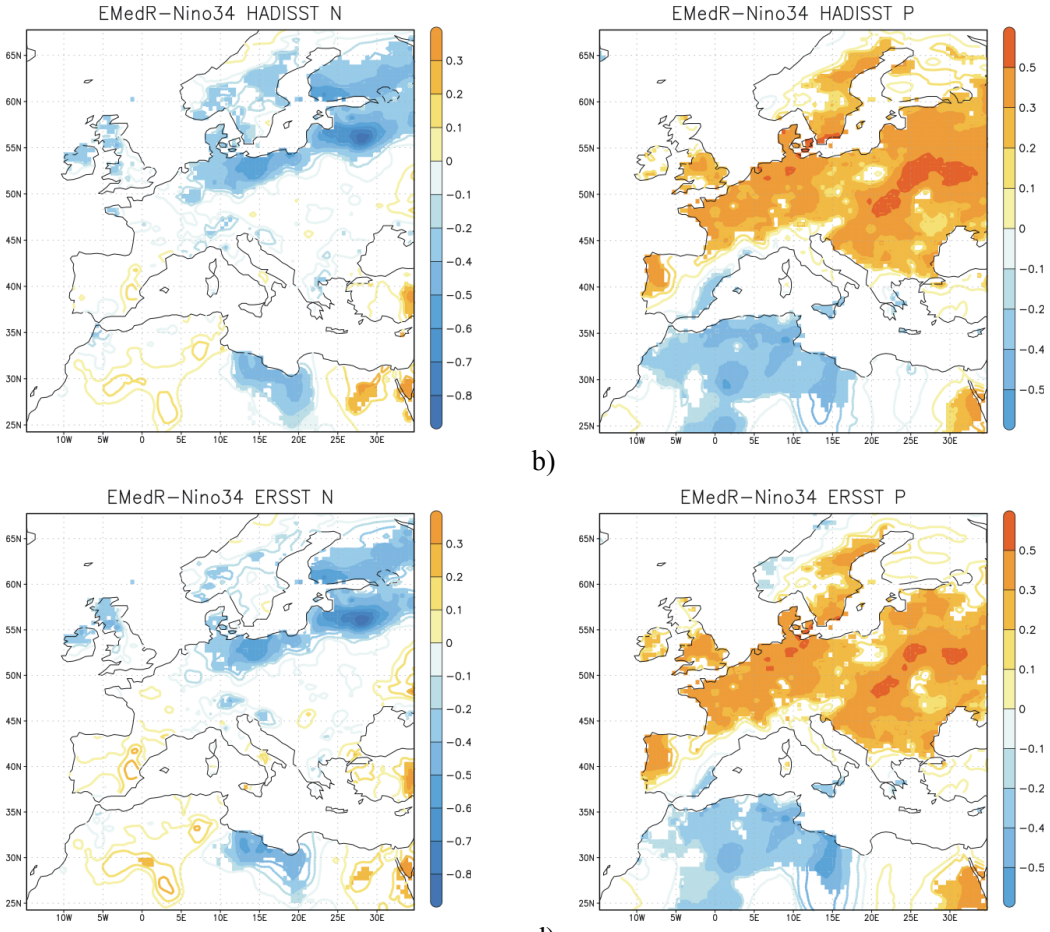

a) b) c) d)

Figure A2: Regressions maps of rainfall (standardized rainfall per standard deviation in Nino34 index) onto the Niño 34 index calculated for N and P periods. On the left the patterns for observed N periods (1944-1964 & 2003-2008), and on the right the same for observed P periods (1900-1940 & 1965-1984). Niño34 index has been obtained for both, HadISST (top) and ERSST (bottom) databases. Statistical significant areas, according to a Monte-Carlo test at the 95% level, are shaded.

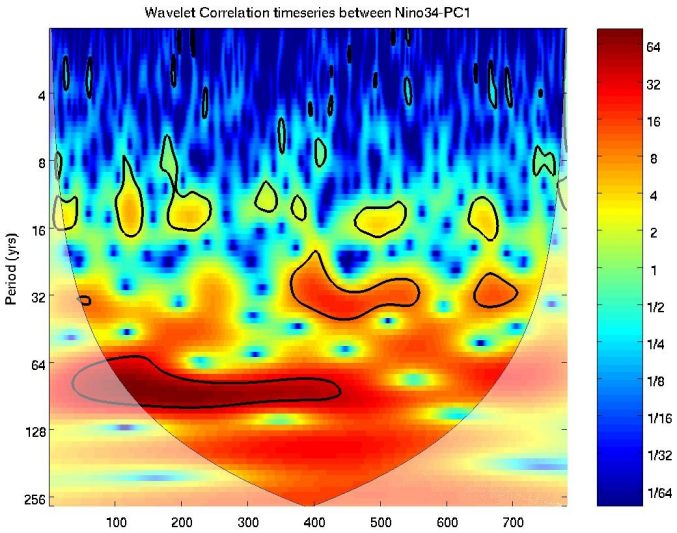

Figure A3: Wavelet analysis of the 21 sliding windows correlation curve between iEMedR PC1 and iNino34 index (see figure 3b).

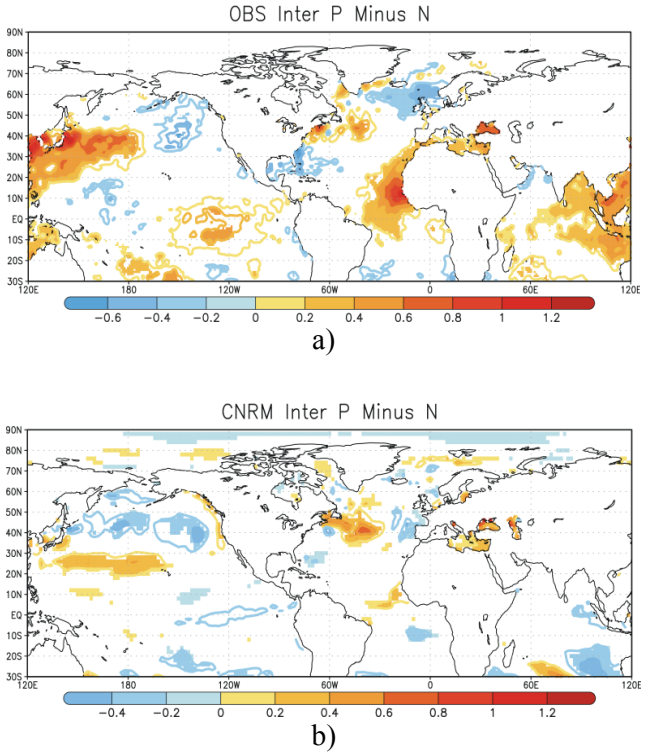

Figure. A4. Difference (P minus N) between SST composites maps in a) Figure 5 and b) Figure 6. Statistical significant areas, according to a Monte-Carlo test at the 95% level, are shaded.

6.2.2 López-Parages, J. et al. 2015a

Multidecadal modulation of ENSO teleconnection with Europe in CMIP5 models

JORGE LÓPEZ PARAGES*, BELÉN RODRÍGUEZ-FONSECA, ELSA MOHINO AND TERESA LOSADA

Departamento de Física de la Tierra, Astronomía y Astrofísica I (Geofísica y Meteorología). Instituto de Geociencias UCM-CSIC, Madrid, Spain.

ABSTRACT

Many studies point to a robust ENSO signature on the North Atlantic European (NAE) sector associated with a downstream effect of Rossby wavetrains. Some of these works also address a non-stationary behaviour of the aforementioned link, but only few have explored the possible modulating factors. In this study the internal causes within the ocean-atmosphere coupled system influencing the ENSO teleconnection with the EuroMediterranean rainfall, have been analysed. To this aim, unforced long-term preindustrial control simulations from 18 different CMIP5 models have been used. A non-stationary impact of ENSO on EuroMediterranean rainfall, being spatially consistent with the observational one, is found. This variable feature is explained by a changing ENSO-related Rossby wave propagation from the tropical Pacific to the NAE sector, which, in turn, is modulated by multidecadal variability of the climatological jet streams associated with the underlying Sea Surface Temperature (SST). Our results point, therefore, to a modulation of the ENSO-EuroMediterranean rainfall teleconnection by the internal (and multidecadal) variability of the ocean-atmosphere coupled system.

1. Introduction

El Niño-Southern Oscillation (ENSO) response at extratropical latitudes has been mainly related to the poleward and eastward propagation of Rossby wavetrains triggered from the Pacific basin (Hoskins and Karoly 1981; Mo and Livezey 1986; Sardeshmukh and Hoskins 1988). As a consequence, the strongest signature on remote regions, which is considered as a downstream effect (Honda et al. 2001; Moron and Gouirand 2003), has usually been found several months after the mature phase of the ENSO event. This is the case of the North Atlantic European Sector (NAE), for which the main ENSO response has been detected in late winter and early spring (see Figure 3 from Brönnimann (2007)). The resultant pattern resembles the North Atlantic Oscillation (NAO) surface signal, reveals a quasi barotropic structure, and represents the leading rotational mode of upper level streamfunction in the NAE region (García-Serrano et al. 2011). Its surface impact is, however, far to be completely accepted, which is probably partially explained by the large internal variability of the circulation at mid-latitudes (Quadrelli and Wallace 2002). As a consequence, ENSO influence on European climate sector is not clear and diverging views arise, with some authors pointing to a robust signal (Fraedrich and Müller (1992); Moron and Plaut (2003); Moron and Gouirand (2003)) and others with a sceptic view on it (e.g. Ropelewski and Halpert (1987)). Related to this, López-Parages and Rodríguez-Fonseca (2012) have recently found a significant impact of ENSO on EuroMediterranean rainfall for certain decades along the 20th century. A variable feature of rainfall have been also detected in the nearby Arabian Peninsula (Almazroui et al. 2012) in relation to a changing link with ENSO at multidecadal timescales (Kang et al. 2015). These results have contributed to the growing evidence advocating for a non-stationary behaviour of the tropospheric ENSO-NAE link on time scales ranging from decadal to multidecadal (Sutton and Hodson 2003; Gouirand and Moron 2003; Greatbatch et al. 2004). Hence, the poor seasonal predictability of EuroMediterranean climate (Van Oldenborgh and Burgers 2005) might be variable and at least, for specific time periods, much greater than expected.

The aforementioned changing link between ENSO and the EuroMediterranean rainfall has been found in phase with the Atlantic Multidecadal Oscillation (AMO, Mariotti et al. (2002); Knippertz et al. (2003); López-Parages and Rodríguez-Fonseca (2012)) suggesting, therefore, an effective modulating role of the AMO. However, the underlying mechanisms explaining the influence of AMO, or

*Corresponding author address: Departamento de Física de la Tierra, Astronomía y Astrofísica I (Geofísica y Meteorología). Instituto de Geociencias UCM-CSIC, Facultad de C.C. Físicas , Universidad Complutense de Madrid (UCM), Pza de las Ciencias, 28040, Spain
E-mail: jlopezpa@ucm.es

maybe other multidecadal variability modes, in the modulation of ENSO response over Europe, is still unresolved.

It is necessary to note that the search for observational evidences of this possible multidecadal modulation presents serious difficulties. Firstly, El Niño (and La Niña) forcing has changed in intensity (Torrence and Webster 1998; Sutton and Hodson 2003; Greatbatch et al. 2004) and spatial patterns (An et al. 2006) in the past. Hence, to associate a changing remote impact of ENSO with an effective modulation in the propagation of the response towards distant regions, rather than with a direct effect of the non-stationary forcing itself, is highly complicated. Secondly, the observations are limited and present in-homogeneities in both space and time, which can introduce spurious non-stationary features. Related to this, Van Oldenborgh and Burgers (2005) found little evidence for a changing behavior of ENSO teleconnections with global precipitation during the instrumental period, but with the possible exception of Europe. Nevertheless, even though the uncertainties associated with observational data could be considered acceptable, the short data record raises questions about the confidence that one can have in results pointing to an atmospheric teleconnection changing at multidecadal timescales. As a consequence, long-term simulations from Coupled Global Circulation Models (CGCMs) emerge as a very convenient tool for testing responses associated with internal variability of the ocean-atmosphere coupled system. In this way, López-Parages et al. (2015) analyse the ENSO-EuroMediterranean rainfall link in a long control simulation of the CNRM-CM5 coupled model, finding periods with positive and negative significant correlations between El Niño3.4 index and the rainfall variability in central Europe, in accordance with the observed changing link detected along the 20th century (Figure 1). Hereinafter this differentiated links are referred as P (Positive correlation) and N (Negative correlation), respectively. The same authors propose multidecadal changes in the upper mean flow associated with internal alterations in the ocean-atmosphere coupled system as the main modulating driver. According to the linear barotropic theory, propagation of extratropical Rossby waves highly depends on the intensity and spatial configuration of the zonal mean flow and hence, on the extratropical jet-streams. Related to this, in those regions where jets are weak the perturbations are meridionally propagated describing an arching pattern; whilst in those regions where jet-streams are intense the planetary waves are efficiently trapped in the zonal flow describing a global hemispheric pattern (Hoskins and Karoly 1981; Branstator 1983, 2002; Hoskins and Ambrizzi 1993; Ambrizzi et al. 1995). Considering that extratropical jets are partially driven by the meridional atmospheric temperature gradients, a change in their spatial configuration is expected if the underlying surface temperature varies along time. As a consequence, a change in tropical-extratropical teleconnections associated with Rossby waves is also expected.

For all the above reasons, the purpose of the present study is to make a step forward in the study of internal causes explaining the changes in preferred pathways of Rossby wavetrains from the tropical Pacific to the NAE in relation to multidecadal changes in the SST. To this aim, long control simulations with preindustrial forcings from the Coupled Model Intercomparion Project Phase 5 (heinafter piControl-CMIP5, (Taylor et al. 2012)) have been used to better characterize the internal ENSO-NAE teleconnection. In particular, the study addresses the following questions: 1) Is the observed non-stationary impact of ENSO over European rainfall reproduced by piControl-CMIP5 simulations? 2) How is the internal underlying dynamical mechanism? 3) Can it be explained by changes in the high levels mean flow associated with well-known SST multidecadal variability modes?

The paper is organized as follows. Section 2 describes data and methods used in this study. Section 3 presents the different results obtained from distinct procedures and the relationship among them. And finally, Section 4 gives a summary and discussion.

2. Data and Methods

a. Data

As it has been previously noted, the present study is focused on unforced long-term preindustrial control simulations (piControl). In particular, the piControl output from 18 different CMIP5 models (see Table 1) have been analysed, being previously interpolated onto a common regular 2.8 x 2.8 global grid.

b. Methods

1) INDEPENDENT EOFS

In order to determine the directions in which the maximum variability of the anomalous rainfall is organized in the models, Empirical Orthogonal Functions (EOFs) of the monthly EuroMediterranean precipitation is computed for each piControl simulation. According to previous studies (López-Parages and Rodríguez-Fonseca 2012; López-Parages et al. 2015), the observational leading Principal Component (hereinafter PC) of European interannual rainfall in late winter-early spring (February-March-April) projects on a spatial pattern with 3 centers of action over the Mediterranean region, Scandinavia, and Central Europe (Figure 1a from López-Parages et al. (2015); the same configuration is identified here in Figure 1). This PC is related to El Niño3.4 index in particular decades, a feature that can be checked by correlating both time series in sliding windows spanning 20 years. In the present study the same procedure is done by calculating *independent EOFs*, for each model, as follows: 1) the PC that

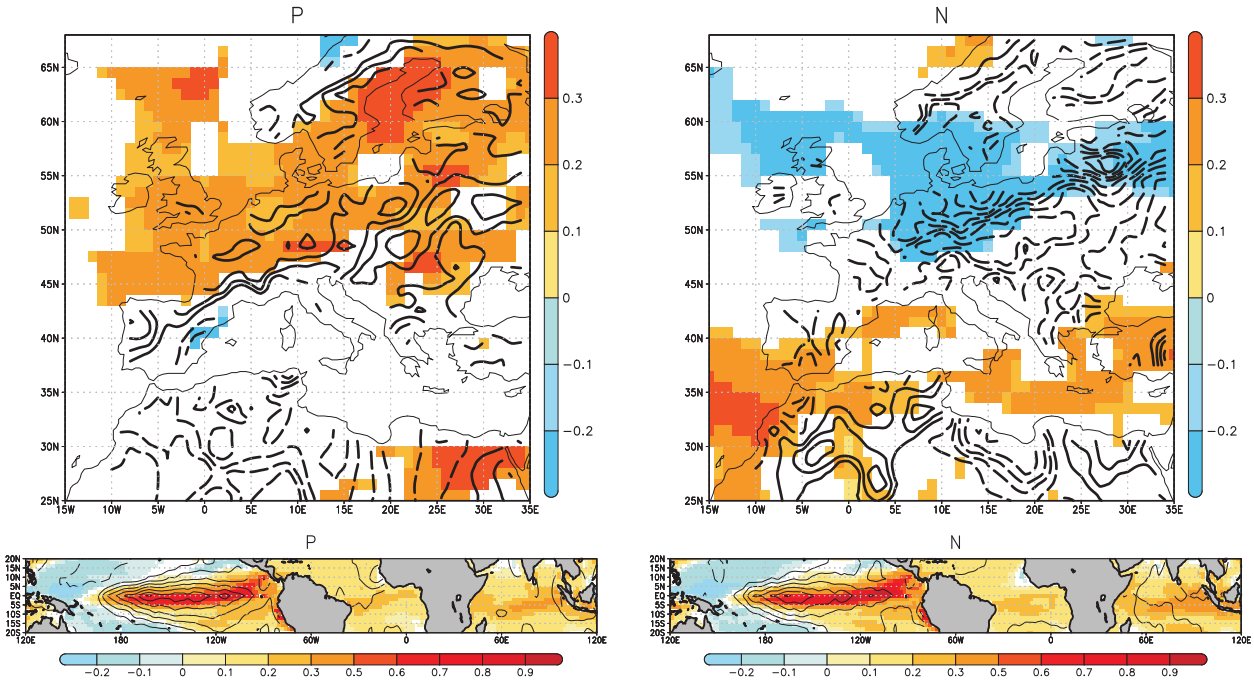

FIG. 1. Homogeneous (bottom) and heterogeneous (top) regression maps from a Maximum Covariance Analysis carried out in P (right) and N (left) periods for observations (contoured, being solid lines positive values and dashed lines negative ones), and CNRM-CM5 model (shaded the significant areas according a Monte-Carlo test at the 95% level). P and N represent 95% significant correlations (according a Monte-Carlo test) between the EuroMediterranean rainfall PC and El Niño34 index. Units are standardized rainfall per standard deviation in SST expansion coefficient, and K per standard deviation in SST expansion coefficient. Modified from López-Parages et al. (2015).

TABLE 1. **Description of CMIP5 models.** From left to right: Number of model, Name of model, pi-Control simulation length, original horizontal resolution, atmospheric vertical layers, and references.

N	Name	piControl length	Resolution (Lon x Lat)	Atm. vertical layers	References
1	BCC-CSM1.1	500	2.8°	26	Xiao-Ge et al. (2013)
2	CanESM2	996	2.8°	40	Chylek et al. (2011)
3	CCSM4	501	1.3° x 0.9°	27	Gent et al. (2011)
4	CNMR-CM5	850	1.4°	31	Voldoire et al. (2013)
5	CSIRO-Mk3-6-0	500	1.9°	18	Rotstayn et al. (2010)
6	GISS-E2-R	550	2.5° x 2.0°	40	Schmidt et al. (2014)
7	GISS-E2-H	540	2.5° x 2.0°	40	Schmidt et al. (2014)
8	FGOALS-g2	700	2.8°	26	Bao et al. (2013)
9	HadGEM2-CC	240	1.9° x 1.3°	60	Martin et al. (2011)
10	HadGEM2-ES	575	1.9° x 1.3°	38	Martin et al. (2011)
11	INM-CM4	500	2.0° x 1.5°	21	Volodin et al. (2010)
12	MIROC5	670	1.4°	40	Watanabe et al. (2010)
13	MIROC-ESM-CHEM	255	2.8°	80	Watanabe et al. (2011)
14	MPI-ESM-LR	1000	1.9°	47	Giorgetta et al. (2013)
15	MRI-CGCM3	500	1.1°	48	Yukimoto (2011)
16	NorESM1-M	501	2.5° x 1.9°	26	Bentsen et al. (2013)
17	IPSL-CM5A-LR	1000	3.8° x 1.9°	39	Dufresne et al. (2013)
18	MIROC4h	100	0.6°	56	Sakamoto et al. (2012)

project onto a spatial rainfall pattern closer to the observed leading EOF is selected for each of the models; 2) time periods for which there is a statistically significant correlation (positive or negative) between the PC and El Niño3.4 index in each model are selected; 3) the leading PC is projected for those particular periods and for each model; and 4) the results are analyzed together as a whole by computing the ensemble mean of the obtained regression maps.

2) EL NIÑO-RAINFALL EOF

A new approach has been proposed in this study in order to characterize the most frequent ways in which El Niño can influence on European rainfall. The method is also based on EOF analysis but, in this case, the EOF is applied to a matrix M that compiles a group of correlation maps calculated between the rainfall and El Niño3.4 index in 20 year sliding windows. Hence, all models and all 20-year correlation maps are included in M, for which the covariance matrix C has been maximized. The correlation matrix M at each year i and spatial point j, and its related covariance matrix C, are given by:

$$M_{i,j} = corr_j(Pr(i:i+19,j), N34(i:i+19)) \quad (1)$$

$$C = M \cdot M^T \quad (2)$$

where M^T denote the transposed matrix M. This new method has two main advantages. On the one hand, as the EOF is based on the El Niño-rainfall correlation matrix M, the resultant modes represent recurrent spatial patterns that relate El Niño and rainfall and not only a variability mode of rainfall (which could or not be related to ENSO). The associated PCs can therefore be directly interpreted as the time evolution of these specific links, that is, the low frequency variability of El Niño-rainfall link. On the other hand, as M is constructed by combination of all CMIP5 models, the resultant EOFs represent the common variability pattern. With this methodology, the length of data sample representing a specific dynamical mechanism, which is highly constrained in observational studies, is maximized. As will be demonstrated along this study, the use of this new method makes possible a better interpretation of the results obtained from the independent EOFs of the anomalous rainfall only, and can help understand the reliability of coupled models in capturing teleconnections. To this aim, the significant correlations obtained from the *independent EOFs* will be separated into two different clusters and represented in a new mathematical base defined from the *El Niño-rainfall EOF*. For this purpose the centroids associated with each cluster, which are based on pairwise Euclidean distances between points, are calculated by a *k-means clustering* method (Lloyd 1982).

3) DATA FILTERING AND STATISTICAL ANALYSIS

As in López-Parages et al. (2015), in order to focus the analysis on the non-stationary ENSO-NAE teleconnection at interannual times scales, a 7-year high-pass filter based on a Discrete Fourier Transform is applied to all the fields. Statistical significance has been determined by a non parametric approach using a Monte Carlo test with 400 resamplings.

3. Results

a. EuroMediterranean rainfall modes in CMIP5 models

The leading EOF of interannual rainfall obtained in observations, which has been found highly associated with ENSO (Figure 1a from López-Parages et al. (2015)), appears, in most of the CMIP5 models, as the second EOF (Table 2). These rainfall variability modes explain, on average, around a 15% of the total variance, being *CSIRO-Mk3* and *GISS-E2-R* the extreme cases with 10.8% and 19.1% respectively. Except *inmcm4* all the mentioned modes are considered robust according the criteria of North et al. (1982), reinforcing therefore their physical interpretations.

TABLE 2. From left to right: Number of model, Principal Component associated with that EuroMediterranean rainfall mode which is spatially closest to the leading observational one, spatial correlation between the selected EOF and the leading observational EOF, Variance explained by the corresponding mode.

N	PC	Corr. EOF1$_{obs}$	Exp. Var
1	PC2	0.86	17.3
2	PC2	0.92	11.5
3	PC2	0.92	13.2
4	PC1	0.92	14.6
5	PC2	0.84	10.8
6	PC1	0.93	19.1
7	PC1	0.94	17.5
8	PC2	0.58	10.9
9	PC2	0.84	14.4
10	PC2	0.85	16.1
11	PC2	0.95	16.8*
12	PC2	0.92	13.1
13	PC2	0.90	14.4
14	PC2	0.92	15.3
15	PC2	0.88	13.2
16	PC2	0.92	13.5
17	PC2	0.84	15.8
18	PC2	0.72	13.4

* Non independent mode according the criteria of North et al. (1982).

Two independent samples are then constructed by selecting, for each model, those periods in which the PCs associated with the aforementioned rainfall modes are significantly correlated with El Niño3.4 index. As it was indicated in the previous section, the ensemble mean of regression maps calculated by the projection of these PCs onto EuroMediterranean rainfall and global SST in both, P and N, is obtained (Figures 2a,b,c,d). As in observations (contoured in Figure 1), in P periods, positive (negative) anomalies are identified, in relation to El Niño (La Niña), over Central Europe, British Islands, and north-west part of the Iberian Peninsula, together with negative (positive)

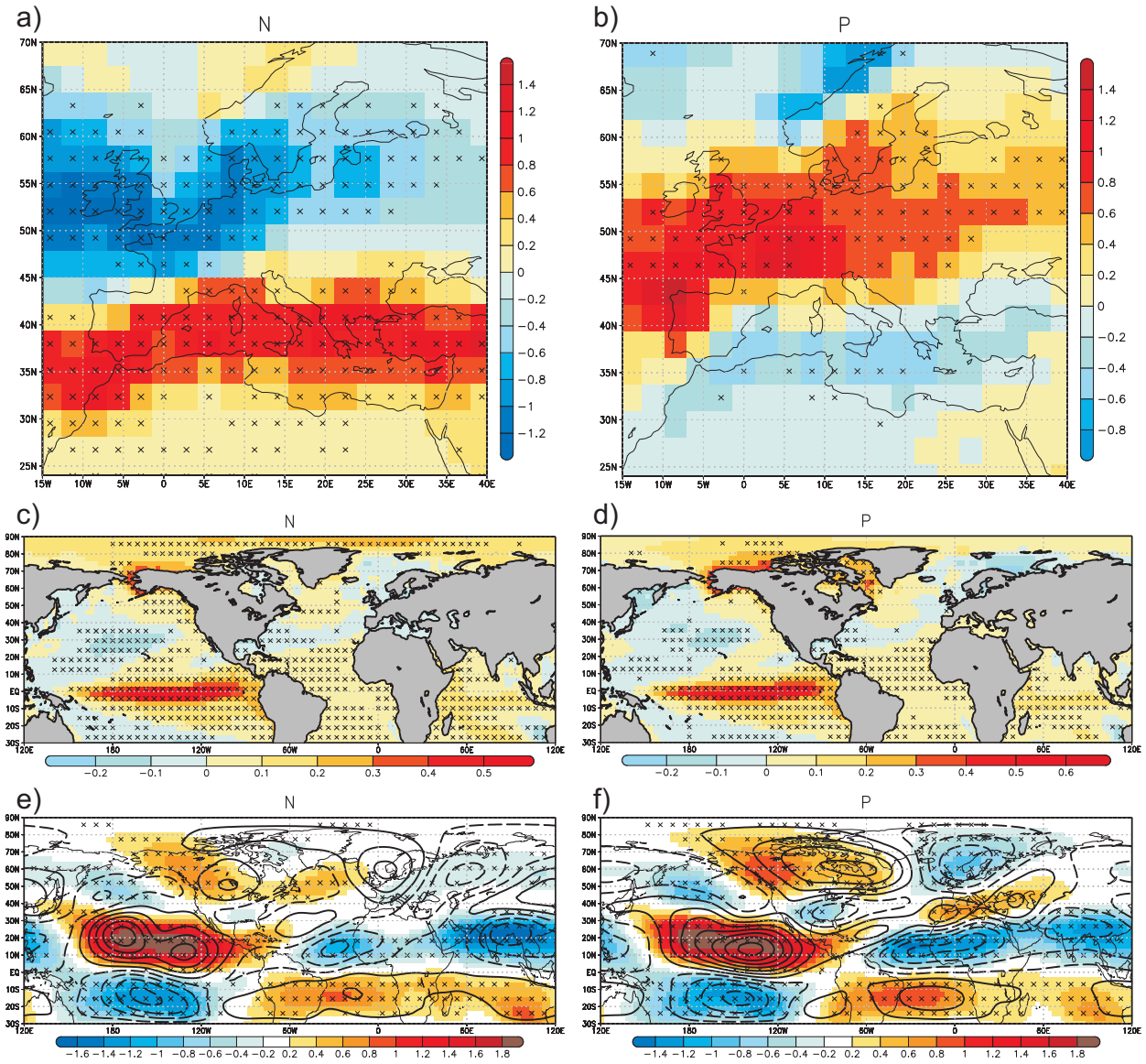

FIG. 2. **Interannual patterns.** Shaded the regression of a,b) Rainfall ($10^6 Kgm^{-2}s^{-1}$), c,d) SST (K), and e,f) streamfunction at 200hPa (psi200), onto the EuroMediterranean rainfall PC and averaged over the 18 CMIP5 models in those periods in which the correlation between the PC and the El Niño3.4 index is positive (P; right) or negative (N; left) at 95% significant level (according to a Monte-Carlo test). In e) and f) the high minus low composite maps (being solid lines positive values and dashed lines negative ones) characterizing the changing ENSO-EuroMediterranean rainfall link along the 20th century (taken from Figure 5 of López-Parages et al. (2015)) have been also added. The PC is selected, for each CMIP5 model, as the PC related to the spatially closest EOF with the observational EOF associated with ENSO (Figure 1 from López-Parages et al. (2015)). The black marks indicate the points where the regression coefficient sign coincides in at least 14 of the 18 models analyzed.

anomalies in the Mediterranean region and northern Scandinavia. In N, on the contrary, the sign obtained at the aforementioned regions is broadly the opposite. The ensemble mean of the rotational flow in terms of the streamfunction at 200hPa has been also plotted for P and N samples (shaded in Figures 2e,f), finding a noticeably reduced impact over the extratropical Northern Hemisphere in N. A weakened wave activity is also identified in the observed record when analysing the periods with a non-significant ENSO-EuroMediterranean rainfall teleconnection (contoured in Figure 2e). In contrast, those observational periods with a significant connection (which are the observed analogues to the simulated P periods), show not only a stronger Northern wave activity but also a striking similarity to the simulated P wave response at high levels (Figure 2f). In particular, the rotational response in P reflects a clear TNH pattern over the North Pacific American sector together with a negative center located

downstream over the northern Europe, resembling the documented leading rotational mode of upper level streamfunction in the NAE sector (García-Serrano et al. 2011). According to the sign of the anomalies identified for the different models, these spatial patterns can be considered as robust. A significant feature is that these noticeably different impacts of El Niño on the upper troposphere at extratropical latitudes and on the EuroMediterranean rainfall, are related to almost the same SST El Niño spatial pattern (Figures 2c,d). This changing signature of ENSO over the NAE sector obtained in piControl CMIP5 models is consistent with observations (contoured in Figures 1a,b, and Figures 2e,f) and hence, reinforces the hypothesis of a changing teleconnection associated with internal variability of the coupled ocean-atmosphere system. To understand how the internal variability can modulate this ENSO-European rainfall link is the main objective for the rest of this paper.

b. ENSO-EuroMediterranean rainfall link in a new base

As it was explained in subsection INDEPENDENT EOFs, Figures 2a,b are constructed by averaging, for selected periods (P and N), the EOFs from CMIP5 models that are the spatially closest to the leading observational EuroMediterranean rainfall EOF. However, although the selected modes can be similar among the different models, they are obtained by independent EOF analysis. Hence, as climate variability can be organized in different patterns for each model, these selected EOFs may represent distinct underlying dynamics. To shed further light on this issue, a new and common EOF for all CMIP5 models, which is based on a matrix that compiles a group of correlation maps calculated between rainfall and Niño3.4 index in 20 years moving windows, is calculated (see section 2 for a more detailed description). Hereinafter this new EOF will be referred to as *multidecadal niño correlation EOF* or simply *mnc-EOF* in contrast to the ones previously described in subsection 3a. In this way, mnc-EOF patterns represent the common impact of ENSO on EuroMediterranean rainfall in CMIP5 models, and the related *mnc-PCs* symbolise its evolution at multidecadal timescales. The leading mnc-EOF is characterized by negatives correlations over northern Europe and positive ones over the northern side of the Mediterranean region; whilst the second mnc-EOF is associated with positive correlations in northern Scandinavia and the southern part of the Mediterranean Sea, and negative correlations in the west side of Central Europe (Figure 3a,b). Note that the maximum (minimum) correlations identified in mnc-EOF1 and mnc-EOF2 are, approximately, 0.2 (-0.2) per standard deviation in mnc-PC1 and mnc-PC2. This represents, for instance, correlations around 0.4 (-0.4) for principal components values around 2.

These patterns, which reflect changing links between European rainfall and ENSO, could be forced by changes in the SST background state, as it was proposed in previous studies (López-Parages and Rodríguez-Fonseca 2012; López-Parages et al. 2015). Regarding this issue, the projection of SSTs (averaged on 20 years sliding windows) onto the leading mnc-PC is related to a warming of the western Pacific at tropical latitudes, the equatorial and northern subtropical Atlantic, and the southern Indian Ocean (Figure 3c). The projection onto the second mode (Figure 3d) resembles a positive IPO phase from observations and pi-Control simulations of CMIP5 models (Mantua et al. 1997; Villamayor and Mohino 2015), except for the negative anomalies identified over the eastern tropical Pacific. Over the North Atlantic, a horseshoe pattern is also discerned, with positive anomalies from the Labrador Sea to the east side of the Tropical North Atlantic, and negative anomalies over the Caribbean Sea and the Gulf Stream region. This pattern resembles changes in the regions of the subtropical gyres that are known to take place at multidecadal timescales (Latif and Barnett 1996; Tourre et al. 2001; Reverdin 2010). At this point it seems to be clear that these SST patterns play a noticeable role as modulator of the ENSO-EuroMediterranean rainfall teleconnection identified in subsection 3a. Nevertheless, in a particular period these two mnc-EOFs can coexist in different manners. Thus, it is important to determine the preferential values of mnc-PC1 and mnc-PC2 for which significant correlations between the leading observed rainfall pattern and El Niño (P and N) are favored. A first comparison of the corresponding time series suggests that positive interannual correlations are related to negative values of mnc-PC1 and mnc-PC1, and vice-versa (Figure 3; bottom). In order to further investigate this issue, the statistically significant correlations P and N are represented in a new base established by mnc-PC1 and mnc-PC2. Under this new base, the significant P and N correlations arrange in two different clusters (Figure 4). Note that these two clusters behave in an approximately linear way under the new base, finding most of P (N) windows under negative (positive) values of mnc-PC1 and mnc-PC2, consistently with the hypothesis deduced from (Figure 3). In the following analysis we have chosen to characterised each cluster by its corresponding centroid obtained from a k-means procedure (see subsection 2).

c. Modulating factors

As it was previously noted in section 1, López-Parages et al. (2015) hypothesize that the changing teleconnection between ENSO and the Euro-mediterranean rainfall is associated with multidecadal variations in the upper mean flow in phase with internal multidecadal changes in the underlying SSTs. In this work, and applying a cluster analysis, this hypothesis is evaluated in 18 CMIP5 models. The spatial patterns of the multidecadal anomalous SST and

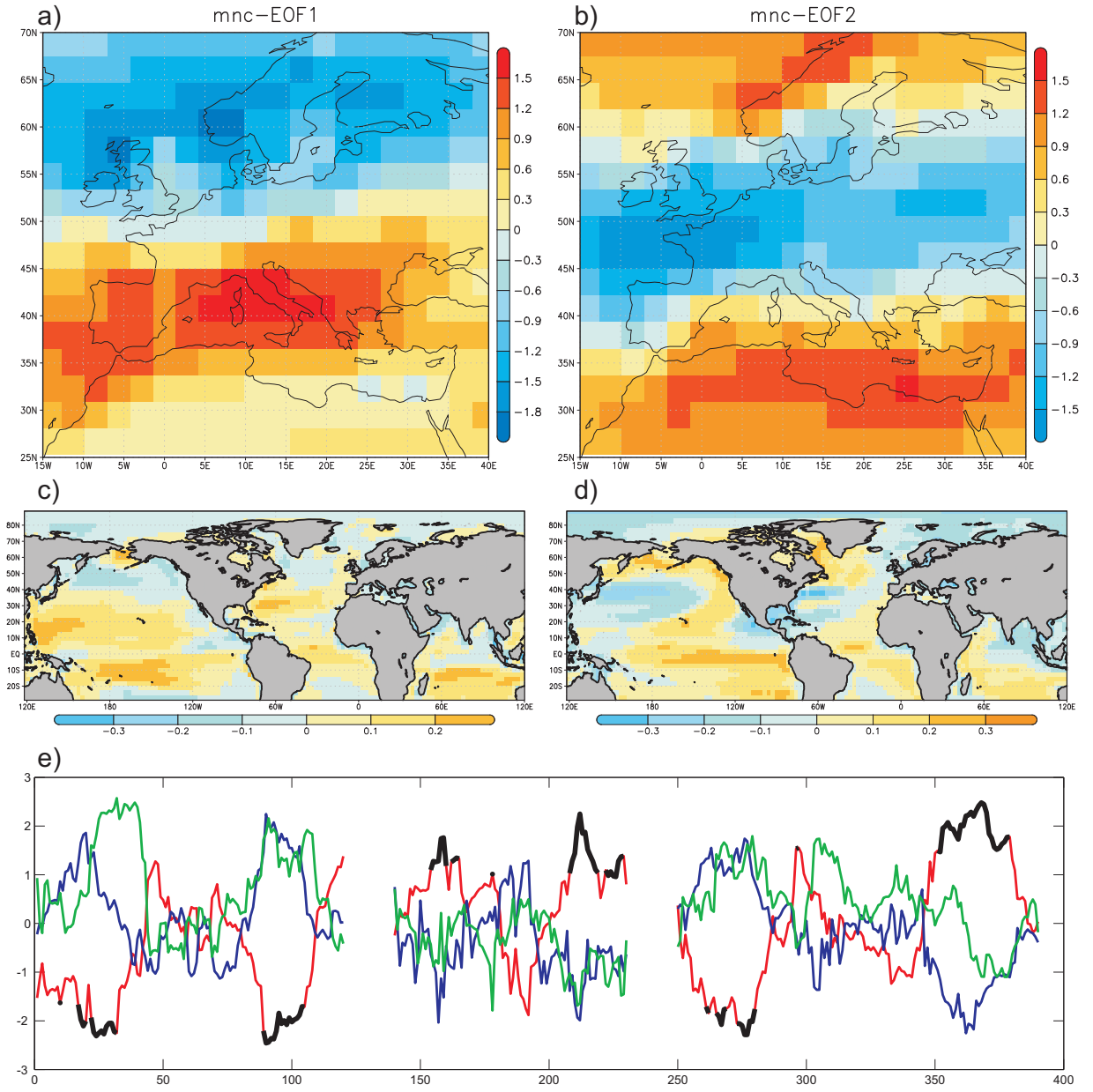

FIG. 3. **New base from El Niño-rainfall EOF**. Top: mnc-EOF1 (20.2% variance explained) and mnc-EOF2 (14.4% variance explained) of the ensemble multidecadal correlation matrix between rainfall and ENSO (for each spatial point, the sliding 20 years windows correlation between rainfall and Niño3.4 index, is included). Units are 10·(correlation per standard deviation in mnc-PC1 and mnc-PC2), respectively. Center) regression map of SST onto mnc-PC1 and mnc-PC2 (K per standard deviation in mnc-PC1 and mnc-PC2). Bottom) some selected periods (specifically for CNRM-CM5, HadGEM2-ES, and MIROC-ESM-CHEM models) of mnc-PC1 (blue), mnc-PC2 (green), and the 20 years moving windows correlation between the interannual-PC (EuroMediterranean rainfall) and El Niño3.4 index (red; in black those 95% significant correlations according to a Monte-Carlo test), are shown in order to illustrate the relationship among them.

upper level zonal wind (hereinafter U200) for the aforementioned clusters -associated with P and N periods- are calculated by multiplying the coordinates of the centroid k (α_k, γ_k) in the mnc-PC1 and mnc-PC2 base, by the corresponding projection of each PC onto the pertinent low-frequency filtered (by averaging on 20 year sliding windows) variables (see Eq. 3, Eq. 4, and Figure 5).

$$R_{k,U200} = \left(\frac{\alpha_k \cdot mncPC1 \cdot U200 + \gamma_k \cdot mncPC2 \cdot U200}{W} \right) \quad (3)$$

$$R_{k,SST} = \left(\frac{\alpha_k \cdot mncPC1 \cdot SST + \gamma_k \cdot mncPC2 \cdot SST}{W} \right) \quad (4)$$

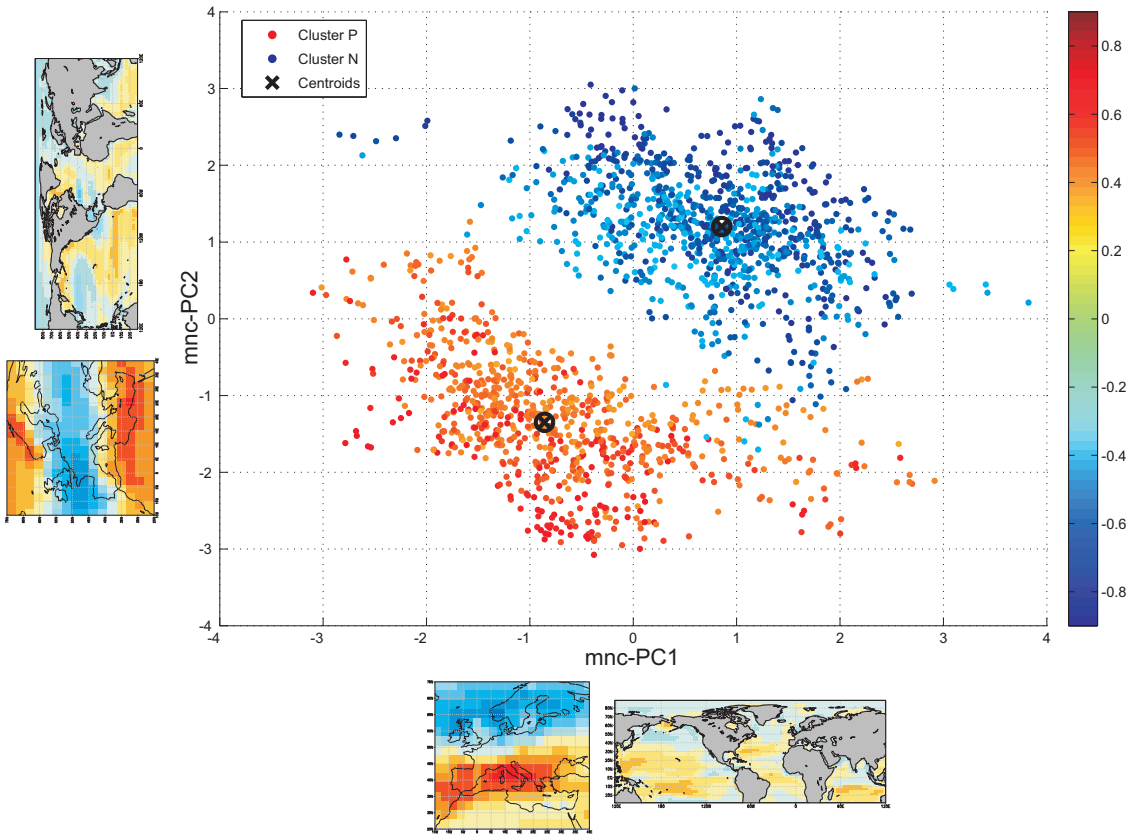

FIG. 4. Scatterplot of the 20 years moving windows significant correlations (according to a Monte-Carlo test at 95% significant level) between interannual-PC (EuroMediterranean rainfall) and El Niño3.4 index (positive correlations in red and negative correlations in blue), in relation to mnc-PC1 and mnc-PC2 values. Centroids are denoted with a black mark. For reference, rainfall and SST spatial patterns associated with mnc-PC1 and mnc-PC2 (from Figure 3) are included in the axis.

where W indicates the number of 20 years sliding windows considered. Figure 5 shows, therefore, the weighted projections of mnc-PC1 and mnc-PC2 onto SST and U200 according the coordinates of the corresponding centroid which characterise each cluster. In this way, the common variability among the different models is maximized.

TABLE 3. Coordinates of each centroid shown in Figure 4

	Centroid P	Centroid N
α	-0.9	0.9
γ	-1.4	1.2

Note that in Figure 5 we are showing the anomalous climatological state on which an El Niño or an La Niña influences the EuroMediterranean rainfall in the so-called P (Figures 4b,d) and N (Figures 4a,c) periods. The first characteristic to highlight from Figure 5 is the similar, but opposite, patterns found in P and N, which is explained by the linear disposition of the clusters in the new base (see mnc-PC1 versus mnc-PC2 in Figure 4; note also the similar α and γ coefficients obtained for both centroids in Table 3). Regarding the SST, an anomalous spatial pattern resembling a negative (positive) IPO appears highlighted in P (N) over the Pacific basin, identifying its characteristic horseshoe signal at mid-latitudes. This spatial pattern resembles a negative (positive) mnc-EOF2 over the North Pacific (see Figure 3d, and Figures 5c,d), but with an enhanced meridional SST gradient around 30^o, which is also influenced by the strong cooling (warming) of the tropical Pacific associated with a negative (positive) mnc-EOF1 (see Figure 3c, and Figure 5c,d). Over the Caribbean Sea and over the coast of California positive (negative) SST anomalies are found in P (N). In the former case this feature reflects the mnc-EOF2 signature; whilst in the latter case it reflects the influence of both, mnc-EOF1 and mnc-EOF2. Regarding the upper level mean flow, a weakened (strengthen) jet is found in P (N) over the North Pacific and the Central American Continent (Figures 5a,b). Con-

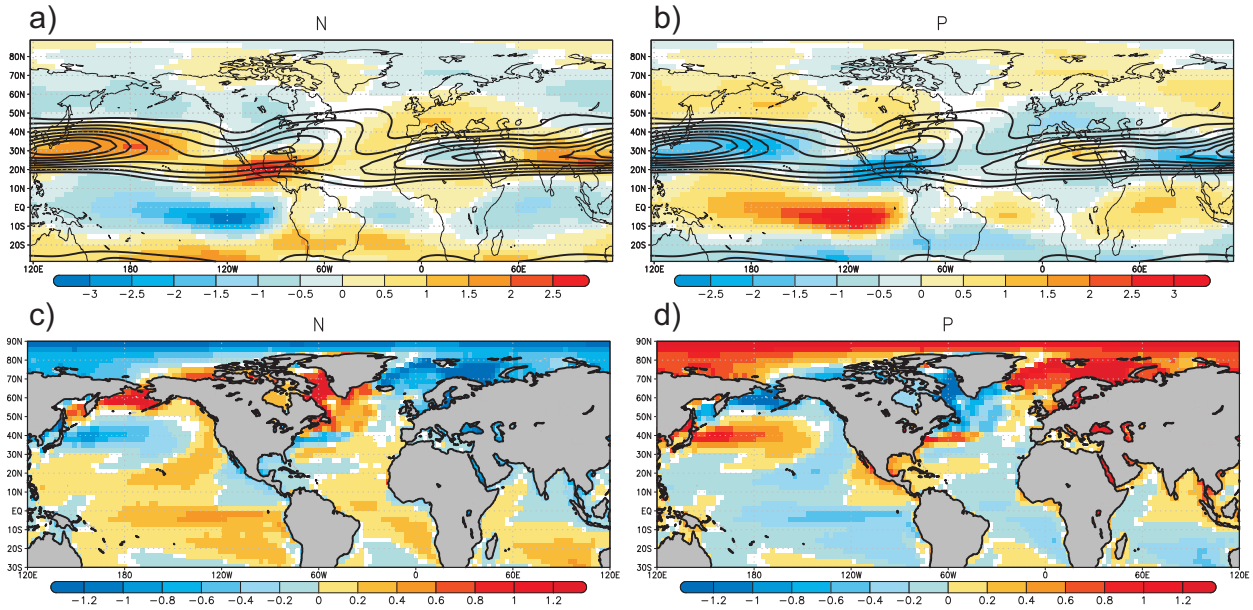

FIG. 5. **Multidecadal patterns.** SST (K; bottom) and U200 (ms^{-1}; top) weighted-regression maps (see equations 3 and 4) onto mnc-PC1 and mnc-PC2, for P (right) and N (left) periods. Only the 95% significant areas according to a Monte-Carlo test are shaded. For U200 (bottom), climatological values are also plotted in contours.

sidering that jet-streams are partially caused by the meridional temperature gradient, a significant change in jets is expected if air temperature gradients are altered. Related to this, the aforementioned weakening (enhancement) of the jet-streams in P (N) is coherent with the anomalous underlying SST pattern, which appears in a way that diminishes (amplifies) the climatological SST meridional gradient over these areas (see Figure A1 of supplementary material for details).

Up to now we have analysed in this subsection the anomalous climatological state obtained for P and N (Figure 5). Interannual phenomena like El Niño can take place superimposed on such climatologies. As it was shown in subsection 3a, in those cases the extratropical impacts appears noticeably different over the NAE sector (Figure 2). A remaining and unanswered question is to what extent the low frequency variability of the climatological SSTs is the responsible for the changes in the jet-streams which, in turn, would produce the distinct wave activity in P and N. To provide an answer to it we have calculated the Rossby wave number Ks, whose relative maximum values can be used as a sign of Stationary Rossby waveguides (Hoskins and Ambrizzi 1993). According to Hoskins and Ambrizzi (1993) Ks can be expressed as:

$$K_s = \left(\frac{\beta - \frac{\partial^2 U}{\partial y^2}}{U} \right)^{1/2} \tag{5}$$

where β represents the change of planetary vorticity with latitude ($\frac{\partial f}{\partial y}$) and U the zonal mean flow.

In Figure 6 the rotational response represented in Figure 2e,f in relation to CMIP5 models is showed again (shaded in Figure 2e,f but contoured in Figure 6) together with the corresponding climatological Ks values (shaded in Figure 6; top and center). Although the TNH pattern is reproduced in both, P and N samples, a remarkable enhancement of the downstream impact over the North Atlantic appears for the former case (Figure 6; top). This feature is explained by the reinforced waveguides over the North Pacific and the North American Continent in P (shaded red in Figure 6; bottom), which favour the Rossby wave propagation associated with ENSO from the tropical Pacific towards the NAE (contoured in Figure 6; bottom).

According to the definition of Ks (Eq. 5), in those areas surrounding the extratropical westerly jets ($U > 0$), Ks is defined only if the numerator of equation 5 is positive. Moreover, its magnitude, which is modulated by the intensity of U, depends on the second order derivative of the zonal flow, that is, on its concavity. According to this, jet-streams enhance its efficiency to propagate stationary Rossby waves in those areas where they are changed in a way that $\frac{\partial^2 U}{\partial y^2} < 0$.

By carefully looking at the P-N differences in the first and second order derivatives of the climatological U200 over the North Pacific and the North American Continent (shaded and contoured, respectively, in Fig. A2 of supplementary material), one can relate the enhanced Rossby waveguides in P with respect to N (Figure 6; bottom) to the weakened climatological U200 found, approximately, 10^o-20^ofurther south (Figures 5a,b). In turn, these min-

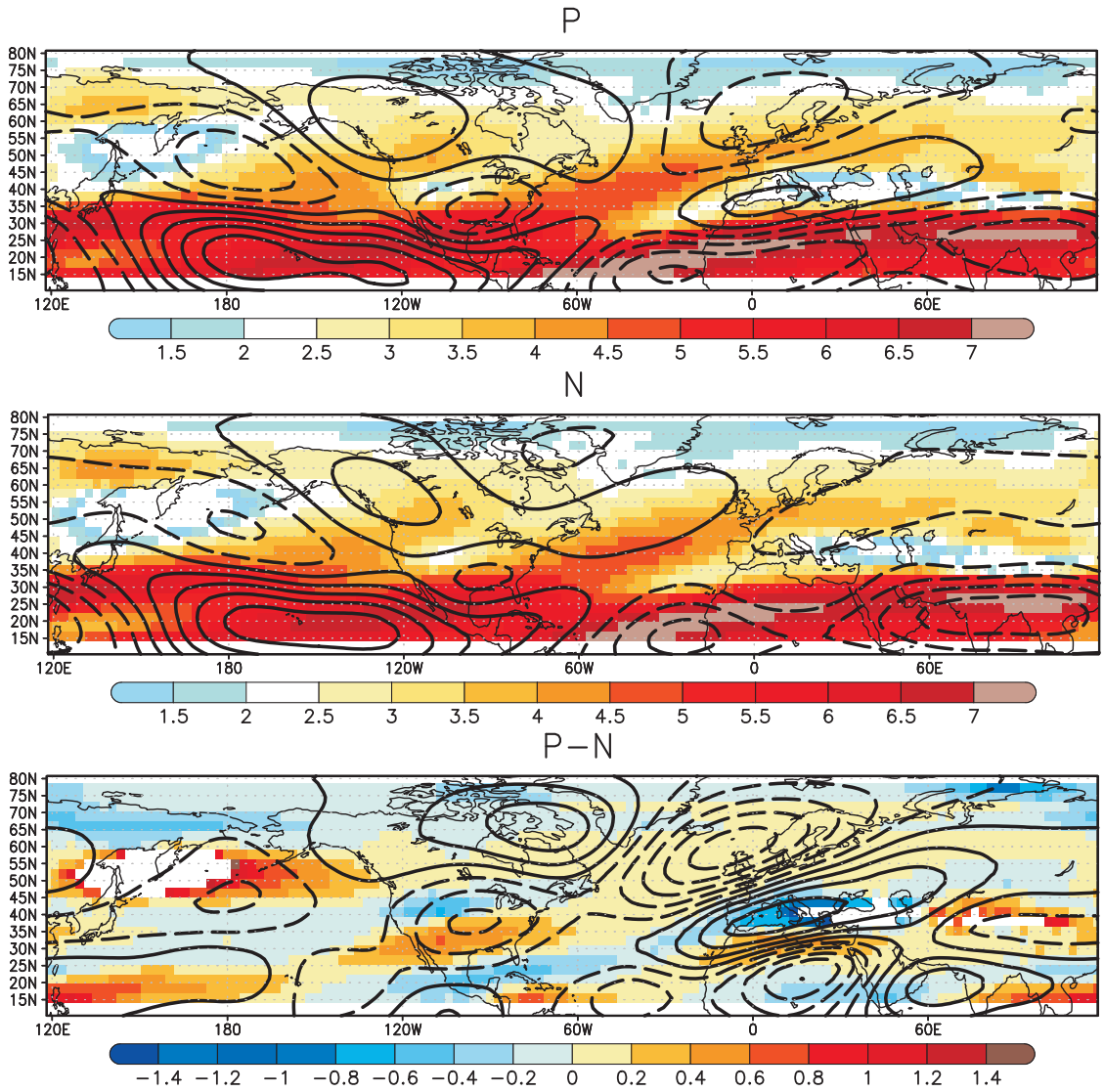

FIG. 6. **Changing interannual teleconnection.** Mean Stationary Rossby wavenumber KS at 200hPa (shaded) together with the streamfunction at 200hPa (contoured) averaged over the 18 CMIP5 models in those periods in which the correlation between the interannual PC of EuroMediterranean rainfall and El Niño3.4 index is positive (P periods; top) or negative (N periods; middle) at 95% significant level (according to a Monte-Carlo test). At the bottom the difference P-N. In P and N ci= $4 \cdot 10^5 ms^{-2}$, being the minimum contours represented $2 \cdot 10^5 ms^{-2}$ and $-2 \cdot 10^5 ms^{-2}$ for positive and negative streamfunction values, respectively. For P-N difference, ci= $2 \cdot 10^5 ms^{-2}$, being $10^5 ms^{-2}$ and $-10^5 ms^{-2}$ the minimum contours plotted for positive and negative values.

ima (maxima) of climatological U200 in P (N) over the North Pacific were previously related to the anomalous climatological SST meridional gradient. Thus, according to our results, the non-stationary teleconnection between ENSO and the EuroMediterranean rainfall identified in CMIP5 models (Figure 2) can be explained by the change in Rossby wave propagation from the tropical Pacific to the NAE sector (Figure 6), which in turn is produced by the low frequency variability of the jet-streams associated with the underlying SST (Figure 5 and Figures A1 and A2 of supplementary material).

4. Summary and Final Discussion

The internal contribution of the ocean-atmosphere coupled system to the non-stationary teleconnection, identified in previous observational works, between El Niño and the leading EuroMediterranean anomalous rainfall mode in late winter-early spring (López-Parages and Rodríguez-Fonseca 2012; López-Parages et al. 2015), has been thoroughly examined in this study. For this purpose, long-term preindustrial control simulations (piControl) from 18 dif-

ferent models involved in the Coupled Model Intercomparison Project Phase 5 (CMIP5), have been used.

For each model, the EuroMediterranean rainfall variability mode which is the closest to the leading observational one has been selected (the so-called CMIP5 *independent EOFs*). Then, those 20 years periods for which a significant correlation between the corresponding PC and El Niño34 index is found, are grouped and analysed as a whole by computing ensemble means of regression maps for different variables. The resultant patterns reflect a changing impact of ENSO on the EuroMediterranean rainfall in a way consistent with the spatial structures related to the non-stationary observational link (Mariotti et al. 2002; Knippertz et al. 2003; Sutton and Hodson 2003; Gouirand and Moron 2003; Greatbatch et al. 2004). This feature is characterized in both, observations and CMIP5 models, by a noticeably distinct downstream impact of ENSO-related Rossby waves over the NAE sector amongst different periods.

In order to find the optimum background state that modulates the ENSO teleconnection with the EuroMediterranean rainfall, the aforementioned changing link has been explored by an alternative approach. This new methodology looks for the time evolution of the teleconnection by calculating the principal directions in which the 20 year correlation map between ENSO and the EuroMediterranean rainfall evolve (see subsection 2). This new procedure, which highlights the common variability among the different CMIP5 models, makes possible the characterization of the ENSO teleconnection with the EuroMediterranean rainfall under a new base. To this aim, the significant correlations between the PCs from the independent EOFs and El Niño34 index are divided into two different clusters in the new mathematical base. Subsequently, as SST and zonal mean flow at the upper troposphere have been both addressed as modulators of the ENSO-EuroMediterranean rainfall teleconnection at interannual timescales (López-Parages et al. 2015), the spatial patterns of these fields which are associated with the mean state of each of the aforementioned clusters, have been obtained.

According to our results, those periods for which a strong (weak) ENSO-related wave activity is identified over the NAE, are characterised by a weakened (strengthened) jet stream over the North Pacific and the Central American Continent, which favour (undermine) the propagation of Rossby waves from the tropical Pacific to extratropical latitudes and their downstream impact over the EuroMediterranean region. It has been concluded that these changes in the upper tropospheric mean flow are associated with multidecadal variability of the underlying SST, which alters the meridional temperature gradient of the Earth's atmosphere and hence, the normal configuration of jet streams. This study demonstrates, therefore, that the non stationary behaviour of the ENSO-EuroMediterranean rainfall teleconnection found in observations can be reproduced by internal variability of the coupled ocean-atmosphere system.

Acknowledgments. This study was supported by the European project PREFACE (ref.603521), and the Spanish projects TRACS (CGL2009-10285) and MULCLIVAR (CGL2012-38923-C02-01). In particular, JLP thanks the FPI grant (BES-2010-042234) associated with the TRACS project.

References

Almazroui, M., M. N. Islam, P. D. Jones, H. Athar, and M. A. Rahman, 2012: Recent climate change in the Arabian Peninsula: Seasonal rainfall and temperature climatology of Saudi Arabia for 1979-2009. *Atmospheric Research*, **111**, 29–45, doi:10.1016/j.atmosres.2012.02.013.

Ambrizzi, T., B. J. Hoskins, and H.-H. Hsu, 1995: Rossby Wave Propagation and Teleconnection Patterns in the Austral Winter. *Journal of Atmospheric Sciences*, **52**, 3661–3672, doi:10.1175/1520-0469(1995)052⟨3661:RWPATP⟩2.0.CO;2.

An, S.-I., Z. Ye, and W. W. Hsieh, 2006: Changes in the leading ENSO modes associated with the late 1970s climate shift: Role of surface zonal current. *GRL*, **33**, L14609, doi:10.1029/2006GL026604.

Bao, Q., and Coauthors, 2013: The flexible global ocean-atmosphere-land system model, spectral version 2: FGOALS-s2. *Advances in Atmospheric Sciences*, **30**, 561–576.

Bentsen, M., and Coauthors, 2013: The Norwegian earth system model, NorESM1-MPart 1: description and basic evaluation of the physical climate. *Geosci. Model Dev*, **6 (3)**, 687–720.

Branstator, G., 1983: Horizontal Energy propagation in a Barotropic Atmosphere with Meridional and Zonal Structure. *Journal of Atmospheric Sciences*, **40**, 1689–1708, doi:10.1175/1520-0469(1983)040⟨1689:HEPIAB⟩2.0.CO;2.

Branstator, G., 2002: Circumglobal Teleconnections, the Jet Stream Waveguide, and the North Atlantic Oscillation. *Journal of Climate*, **15**, 1893–1910, doi:10.1175/1520-0442(2002)015⟨1893:CTTJSW⟩2.0.CO;2.

Brönnimann, S., 2007: Impact of El Niño-Southern Oscillation on European climate. *Reviews of Geophysics*, **45**, RG3003, doi:10.1029/2006RG000199.

Chylek, P., J. Li, M. Dubey, M. Wang, and G. Lesins, 2011: Observed and model simulated 20th century Arctic temperature variability: Canadian earth system model CanESM2. *Atmospheric Chemistry and Physics Discussions*, **11 (8)**, 22 893–22 907.

Dufresne, J.-L., and Coauthors, 2013: Climate change projections using the IPSL-CM5 Earth System Model: from CMIP3 to CMIP5. *Climate Dynamics*, **40**, 2123–2165, doi:10.1007/s00382-012-1636-1.

Fraedrich, K., and K. Müller, 1992: Climate anomalies in Europe associated with ENSO extremes. *International Journal of Climatology*, **12**, 25–31, doi:10.1002/joc.3370120104.

García-Serrano, J., B. Rodríguez-Fonseca, I. Bladé, P. Zurita-Gotor, and A. de La Cámara, 2011: Rotational atmospheric circulation during North Atlantic-European winter: the influence of ENSO. *Climate Dynamics*, **37**, 1727–1743, doi:10.1007/s00382-010-0968-y.

Gent, P. R., and Coauthors, 2011: The community climate system model version 4. *Journal of Climate*, **24 (19)**, 4973–4991.

Giorgetta, M. A., and Coauthors, 2013: Climate and carbon cycle changes from 1850 to 2100 in MPI-ESM simulations for the Coupled Model Intercomparison Project phase 5. *Journal of Advances in Modeling Earth Systems*, **5**, 572–597, doi:10.1002/jame.20038.

Gouirand, I., and V. Moron, 2003: Variability of the impact of El Niño-Southern Oscillation on sea-level pressure anomalies over the North Atlantic in January to March(1874-1996). *International Journal of Climatology*, **23**, 1549–1566, doi:10.1002/joc.963.

Greatbatch, R. J., J. Lu, and K. A. Peterson, 2004: Nonstationary impact of ENSO on Euro-Atlantic winter climate. *GRL*, **31**, L02208, doi:10.1029/2003GL018542.

Honda, M., H. Nakamura, J. Ukita, I. Kousaka, and K. Takeuchi, 2001: Interannual Seesaw between the Aleutian and Icelandic Lows. Part I: Seasonal Dependence and Life Cycle. *Journal of Climate*, **14**, 1029–1042, doi:10.1175/1520-0442(2001)014⟨1029:ISBTAA⟩2.0.CO;2.

Hoskins, B. J., and T. Ambrizzi, 1993: Rossby Wave Propagation on a Realistic Longitudinally Varying Flow. *Journal of Atmospheric Sciences*, **50**, 1661–1671, doi:10.1175/1520-0469(1993)050⟨1661:RWPOAR⟩2.0.CO;2.

Hoskins, B. J., and D. J. Karoly, 1981: The Steady Linear Response of a Spherical Atmosphere to Thermal and Orographic Forcing. *Journal of Atmospheric Sciences*, **38**, 1179–1196, doi:10.1175/1520-0469(1981)038⟨1179:TSLROA⟩2.0.CO;2.

Kang, I.-S., I. U. Rashid, F. Kucharski, M. Almazroui, and A. K. Alkhalaf, 2015: Multidecadal Changes in the Relationship between ENSO and Wet-Season Precipitation in the Arabian Peninsula. *Journal of Climate*, **28**, 4743–4752, doi:10.1175/JCLI-D-14-00388.1.

Knippertz, P., U. Ulbrich, F. Marques, and J. Corte-Real, 2003: Decadal changes in the link between El Niño and springtime North Atlantic oscillation and European-North African rainfall. *International Journal of Climatology*, **23**, 1293–1311, doi:10.1002/joc.944.

Latif, M., and T. P. Barnett, 1996: Decadal Climate Variability over the North Pacific and North America: Dynamics and Predictability. *Journal of Climate*, **9**, 2407–2423, doi:10.1175/1520-0442(1996)009⟨2407:DCVOTN⟩2.0.CO;2.

Lloyd, S. P., 1982: Least squares quantization in PCM. *Information Theory, IEEE Transactions on*, **28 (2)**, 129–137.

López-Parages, J., and B. Rodríguez-Fonseca, 2012: Multidecadal modulation of El Niño influence on the Euro-Mediterranean rainfall. *GRL*, **39**, L02704, doi:10.1029/2011GL050049.

López-Parages, J., B. Rodríguez-Fonseca, and L. Terray, 2015: A mechanism for the multidecadal modulation of ENSO teleconnection with Europe. *Climate Dynamics*, **45 (3-4)**, 867–880, doi:10.1007/s00382-014-2319-x, URL http://dx.doi.org/10.1007/s00382-014-2319-x.

Mantua, N. J., S. R. Hare, Y. Zhang, J. M. Wallace, and R. C. Francis, 1997: A Pacific Interdecadal Climate Oscillation with Impacts on Salmon Production. *Bulletin of the American Meteorological Society*, **78**, 1069–1079, doi:10.1175/1520-0477(1997)078⟨1069:APICOW⟩2.0.CO;2.

Mariotti, A., N. Zeng, and K.-M. Lau, 2002: Euro-Mediterranean rainfall and ENSO-a seasonally varying relationship. *GRL*, **29**, 1621, doi:10.1029/2001GL014248.

Martin, G., and Coauthors, 2011: The HadGEM2 family of met office unified model climate configurations. *Geoscientific Model Development Discussions*, **4**, 765–841.

Mo, K. C., and R. E. Livezey, 1986: Tropical-Extratropical Geopotential Height Teleconnections during the Northern Hemisphere Winter. *Monthly Weather Review*, **114**, 2488, doi:10.1175/1520-0493(1986)114⟨2488:TEGHTD⟩2.0.CO;2.

Moron, V., and I. Gouirand, 2003: Seasonal modulation of the El Niño-southern oscillation relationship with sea level pressure anomalies over the North Atlantic in October-March 1873-1996. *International Journal of Climatology*, **23**, 143–155, doi:10.1002/joc.868.

Moron, V., and G. Plaut, 2003: The impact of El Niño-southern oscillation upon weather regimes over Europe and the North Atlantic during boreal winter. *International Journal of Climatology*, **23**, 363–379, doi:10.1002/joc.890.

North, G. R., T. L. Bell, R. F. Cahalan, and F. J. Moeng, 1982: Sampling Errors in the Estimation of Empirical Orthogonal Functions. *Monthly Weather Review*, **110**, 699, doi:10.1175/1520-0493(1982)110⟨0699:SEITEO⟩2.0.CO;2.

Quadrelli, R., and J. M. Wallace, 2002: Dependence of the structure of the Northern Hemisphere annular mode on the polarity of ENSO. *GRL*, **29**, 2132, doi:10.1029/2002GL015807.

Reverdin, G., 2010: North Atlantic Subpolar Gyre Surface Variability (1895-2009). *Journal of Climate*, **23**, 4571–4584, doi:10.1175/2010JCLI3493.1.

Ropelewski, C. F., and M. S. Halpert, 1987: Global and Regional Scale Precipitation Patterns Associated with the El Niño/Southern Oscillation. *Monthly Weather Review*, **115**, 1606, doi:10.1175/1520-0493(1987)115⟨1606:GARSPP⟩2.0.CO;2.

Rotstayn, L. D., M. A. Collier, M. R. Dix, Y. Feng, H. B. Gordon, S. P. O'Farrell, I. N. Smith, and J. Syktus, 2010: Improved simulation of Australian climate and ENSO-related rainfall variability in a global climate model with an interactive aerosol treatment. *International Journal of Climatology*, **30 (7)**, 1067–1088.

Sakamoto, T., and Coauthors, 2012: MIROC4ha new high-resolution atmosphere-ocean coupled general circulation model. *Journal of the Meteorological Society of Japan*, **90 (3)**, 325–359.

Sardeshmukh, P. D., and B. J. Hoskins, 1988: The Generation of Global Rotational Flow by Steady Idealized Tropical Divergence. *Journal of Atmospheric Sciences*, **45**, 1228–1251, doi:10.1175/1520-0469(1988)045⟨1228:TGOGRF⟩2.0.CO;2.

Schmidt, G. A., and Coauthors, 2014: Configuration and assessment of the GISS ModelE2 contributions to the CMIP5 archive. *Journal of Advances in Modeling Earth Systems*, **6 (1)**, 141–184.

Sutton, R. T., and D. L. R. Hodson, 2003: Influence of the Ocean on North Atlantic Climate Variability 1871-1999. *Journal of Climate*, **16**, 3296–3313, doi:10.1175/1520-0442(2003)016⟨3296:IOTOON⟩2.0.CO;2.

Taylor, K. E., R. J. Stouffer, and G. A. Meehl, 2012: An Overview of CMIP5 and the Experiment Design. *Bulletin of the American Meteorological Society*, **93**, 485–498, doi:10.1175/BAMS-D-11-00094.1.

Torrence, C., and P. J. Webster, 1998: The annual cycle of persistence in the El Nño/Southern Oscillation. *Quarterly Journal of the Royal Meteorological Society*, **124**, 1985–2004, doi:10.1002/qj.49712455010.

Tourre, Y. M., B. Rajagopalan, Y. Kushnir, M. Barlow, and W. B. White, 2001: Patterns of coherent decadal and interdecadal climate signals in the Pacific Basin during the 20^{th} century. *GRL*, **28**, 2069–2072, doi:10.1029/2000GL012780.

Van Oldenborgh, G. J., and G. Burgers, 2005: Searching for decadal variations in ENSO precipitation teleconnections. *GRL*, **32**, L15701, doi:10.1029/2005GL023110.

Villamayor, J., and E. Mohino, 2015: Robust Sahel drought due to the Interdecadal Pacific Oscillation in CMIP5 simulations. *GRL*, **42**, 1214–1222, doi:10.1002/2014GL062473.

Voldoire, A., and Coauthors, 2013: The CNRM-CM5.1 global climate model: description and basic evaluation. *Climate Dynamics*, **40**, 2091–2121, doi:10.1007/s00382-011-1259-y.

Volodin, E., N. Dianskii, and A. Gusev, 2010: Simulating present-day climate with the INMCM4. 0 coupled model of the atmospheric and oceanic general circulations. *Izvestiya, Atmospheric and Oceanic Physics*, **46 (4)**, 414–431.

Watanabe, M., and Coauthors, 2010: Improved climate simulation by MIROC5: mean states, variability, and climate sensitivity. *Journal of Climate*, **23 (23)**, 6312–6335.

Watanabe, S., and Coauthors, 2011: MIROC-ESM: model description and basic results of CMIP5-20c3m experiments. *Geosci Model Dev Discuss*, **4 (2)**, 1063–1128.

Xiao-Ge, X., W. Tong-Wen, and Z. Jie, 2013: Introduction of CMIP5 experiments carried out with the climate system models of Beijing Climate Center. *Advances in Climate Change Research*, **4 (1)**, 41–49.

Yukimoto, S., 2011: *Meteorological research institute earth system model version 1 (MRI-ESM1): model description*.

Supplementary Material

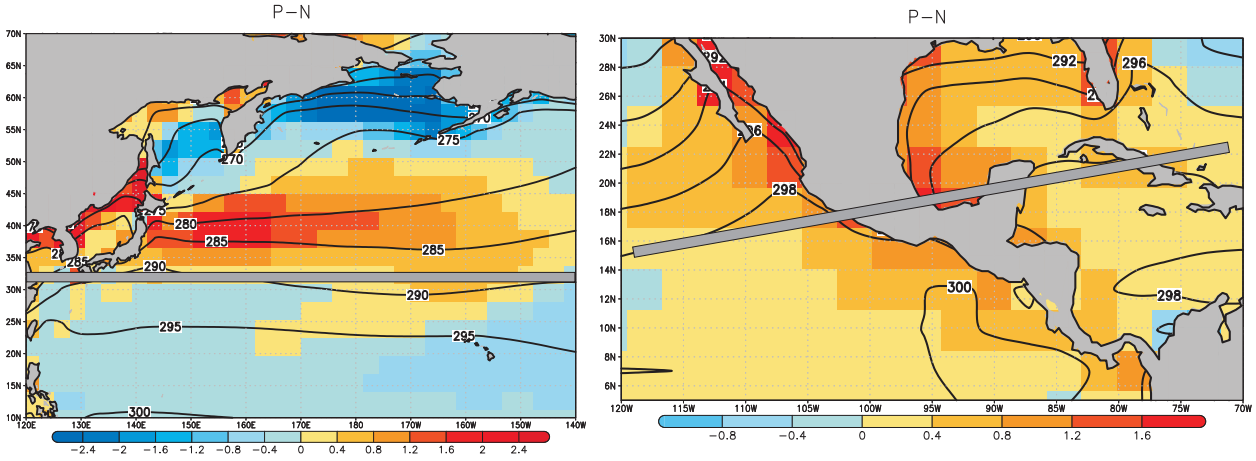

Figure A1: Regional SST anomalous patterns, over the North Pacific and Central America, obtained as P-N difference from Figures 5c,d (K; shaded). In contours the climatological SST temperature. Grey bar indicates, approximately, the position of the main U200 centre of action identified in Figures 5a,b over these regions.

In Figure A1 it is possible to note how in those areas where the gray bars are, the anomalous meridional temperature gradient (see shaded areas) appears in a way that diminishes (strength) the climatological SST meridional gradient (see contours). And it coincides, approximately, with those regions where multidecadal anomalous U200 weakens (enhances) in P (N) (see Figure 5).

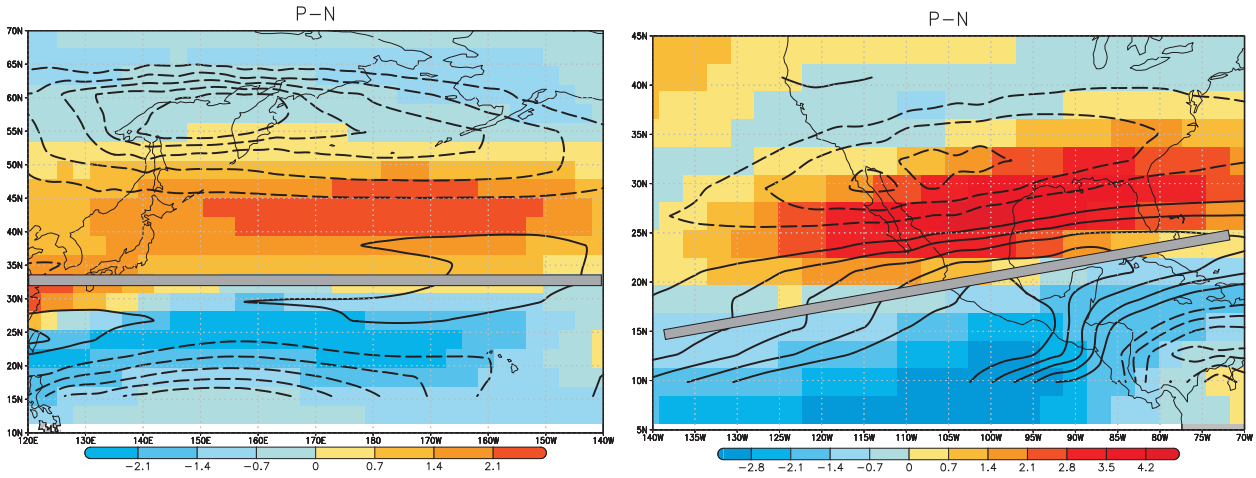

Figure A2: As Figure A1 (P-N difference) but for the first (shaded) and second (contoured, being solid lines positive values and dashed lines negative ones) order derivatives of U200 with respect to the latitude.

Gray bars previously plotted in Figure A1 are added in Figure A2 together with the first (shaded) and second (contoured, being solid lines positive values and dashed lines negative ones) order derivatives of U200. According to this figure the location of the negative centers of this second order derivative over the North Pacific and the North American Continent coincides with the reinforced waveguides found over these regions (Figure 6; bottom) in P periods. Taking into

account the Equation 5 it seems therefore to be clear how the changes identified in the Stationary Rossby waveguides (Figure 6; bottom) respond to the low frequency variability of the jet-streams (Figures 5a,b, and Figure A2) associated with the underlying SST (Figure A1).

6.3 ENSO - NAE Sector: A non-linear and non-stationary teleconnection

In this part of the results section, a set of experiments in which diverse idealised SST El Niño signals are superimposed over different SST mean states, are performed with the ACCESS model.

These results are presented in the following publication:

6.3.1 López-Parages, J., Rodríguez-Fonseca, B., Dommenget, D., and Frauen, C.: ENSO influence on the North Atlantic European climate: A non-linear and non-stationary approach, Clim. Dyn., *under review (CLDY-D-15-00443R1)*, 2015.

6.3.1 López-Parages, J. et al. 2015b

ENSO influence on the North Atlantic European climate: A non-linear and non-stationary approach

Jorge López Parages · Belén Rodríguez-Fonseca · Dietmar Dommenget · Claudia Frauen

Received: 2 August 2015

Abstract El Niño Southern Oscillation (ENSO) impact on the North Atlantic European sector (NAE) is still under discussion. Recent studies have found a non stationary feature of this teleconnection, suggesting an effective modulating role of the ocean mean state. Nevertheless, physical explanations about the underlying mechanisms have been little studied in the available literature. In addition, ENSO events shows different SST spatial patterns, phases, and amplitudes, which can also influence on the related remote impacts. In view of all this, in the present study a set of partially coupled experiments have been performed with a global atmospheric general circulation model, in which different SST ENSO patterns are superimposed over distinct Pacific and Atlantic SST mean states. The SST background conditions are constructed according to the observational difference between periods with a distinct impact of ENSO on the leading Euro-Mediterranean rainfall mode in late winter-early spring. Our results point to two distinct mechanisms associated with ENSO that can be modulated by the SST mean state: 1) the thermally driven direct circulation (Walker and Hadley cells) connecting the Atlantic and Pacific basins, and 2) the Rossby wave propagation from the tropical Pacific to the North Atlantic. The former elucidates that the positive NAO-like pattern usually related to La Niña events could be only valid for selected decades. The latter explains a reinforced signature of Eastern Niños on the Euro-Mediterranean rainfall when the tropical Pacific is warmer than usual and the North Atlantic is colder than usual. This feature is consistent with the changing ENSO impact identified in previous studies and demonstrates how the ENSO teleconnection with the NAE climate at interannual timecales could be modulated by multidecadal changes in the SST. According to our results, the assumption of stationarity which is still common to many studies of ENSO teleconnections clearly has to be questioned.

J. López-Parages
Departamento de Física de la Tierra, Astronomía y Astrofśica I (Geofísica y Meteorología). Instituto de Geociencias UCM-CSIC, Facultad de C.C. Físicas , Universidad Complutense de Madrid (UCM), Pza de las Ciencias, 28040, Spain
Tel.: +0034-91-3944513
E-mail: jlopezpa@ucm.es

1 Introduction

El Niño-Southern Oscillation (ENSO) is the coupled ocean-atmosphere mode that is considered as the main driver of global atmospheric teleconnections at interannual timescales. Its oceanic component (El Niño), which is characterized by anomalous Sea Surface Temperatures (SSTs) over the equatorial Pacific Ocean, alters the sources of atmospheric heating and, as a consequence, affects remote regions around the globe. During El Niño (La Niña) events the central-eastern tropical Pacific becomes warmer (colder) and the related atmospheric convection and rainfall are shifting along with the anomalous temperature. ENSO related changes in the local divergent flow induce further changes in the divergent and non-divergent (or rotational) flow, therefore impacting distant areas through different teleconnection mechanisms. In the last decades a series of publications have found a non-linear response of zonal winds in the central Pacific to SST anomalies (Kang and Kug, 2002; Philip and van Oldenborgh, 2009; Frauen and Dommenget, 2010). This feature could be associated with two distinct and documented El Niño patterns, Eastern Pacific (EP) and Central Pacific (CP), which have discernibly different impacts on remote regions (Kug et al., 2009; Kao and Yu, 2009; Choi et al., 2011; Frauen et al., 2014). However, whilst the ENSO signature over the Pacific and the tropics has been highly analyzed, ENSO response over extratropical regions requires further investigation. One of the less understood teleconnec-

tions is the one associated with the North Atlantic European Sector (NAE), which even is far from being unequivocally accepted (Brönnimann (2007) and paper therein).

The divergent flow response associated with ENSO involves 1) changes in the Hadley and Walker cells in relation to variations in the convection (Wang, 2002b; Wang and Enfield, 2003; Wang and Picaut, 2004; Ruiz-Barradas et al., 2003) but also 2) changes in the rotational flow by the modification of the planetary vorticity and hence, the triggering of Rossby waves (Cassou and Terray, 2001; Honda et al., 2001).

Regarding the changes in the direct circulation, six centers of action of velocity potential appear when an ENSO episode occurs: three over the equator (western Pacific, eastern Pacific, and Atlantic) and three over mid-latitude regions (west Pacific, near Caribbean Sea, and Europe). These divergent and convergent centers along the globe represent a weakening (for El Niño; strengthening for La Niña) of the Pacific and Atlantic Walker circulations (equatorial centers), and its related Hadley cells in the subtropics (Wang, 2002a; Wang and Picaut, 2004). Thus, climate variability over the NAE could be significantly linked (or not) with tropical Pacific SSTs depending on the intensity and spatial configuration of the previously mentioned anomalous circulations.

Regarding the changes in the rotational flow, the most accepted dynamical mechanism explaining the ENSO-NAE teleconnection via the troposphere implies the disturbance of the Aleutian low through variations in the Pacific Hadley circulation in early and mid winter, and then the downstream propagation of Rossby wavetrains across North America from January (Honda et al., 2001; Moron and Gouirand, 2003). From this month the canonical Tropical Northern Hemisphere Pattern (TNH), which is organized in three centers of actions along the North Pacific-American sector (Mo and Livezey, 1986; Barnston and Livezey, 1987; Livezey and Mo, 1987; Trenberth et al., 1998), is completely established (Bladé et al., 2008), together with a split of the Rossby wavetrain impacting Eurasia (Karoly et al., 1989). The resultant rotational atmospheric response to ENSO is formed by a TNH-like pattern and the abovementioned split of the wavetrain, revealing a quasi barotropic structure, and representing the leading rotational mode of upper level streamfunction in the NAE (García-Serrano et al., 2011).

It is worth noting that the ENSO atmospheric signal detection in NAE is difficult due to the fact that the atmospheric interannual variability over this region is highly dominated by internal processes (Trenberth et al., 1998; Quadrelli and Wallace, 2002). Nevertheless, the above mentioned studies together with other statistical analyses point to a robust ENSO response (Brönnimann, 2007), which is seasonal dependant (Moron and Gouirand, 2003; Mariotti et al., 2002), maybe nonlinear (Wu and Hsieh, 2004; Pozo-Vázquez et al., 2005a), and possibly nonstationary in time (Knippertz et al., 2003; Sutton and Hodson, 2003; Gouirand and Moron, 2003; Greatbatch et al., 2004), with the late winter being the more appropriate season for finding a robust signal (Brönnimann, 2007). However, a better understanding of how this link is affected by different phases, spatial patterns, and strengths of ENSO events, is necessary.

Concerning the non-stationary behavior of the response, several studies have found a strong impact of ENSO over the Euro-Mediterranean rainfall in late winter and early spring during the beginning of the 20th century (1900s-1920s) and after the sixties (1970s-1980s), compared to a weak signal in the decades in between (Mariotti et al., 2002; López-Parages and Rodríguez-Fonseca, 2012). Nevertheless, this changing response is not completely accepted and a clear agreement about the possible underlying mechanism is still needed. Several studies have indicated the importance of a realistic representation of the SST mean state in order to properly reproduce the atmospheric response to SST anomalies (Peng and Whitaker, 1999; Cassou and Terray, 2001). Related to this, in a recent paper López-Parages et al. (2014) have attributed the variable ENSO-EuroMediterranean rainfall link to changes in the upper mean flow associated with the multidecadal variability of the SST. Thus, new challenges related to a possible modulation of the already not-completely understood ENSO-NAE teleconnection, appear.

With the aim to shed light on these questions, an atmospheric general circulation model (AGCM) is forced in this work with idealized ENSO SST patterns (of different spatial configurations, strengths, and signs) under distinct ocean background states to test, which of the aforementioned features are determinant to better achieve the changing impact of ENSO events on the European region.

The article is organized as follows. We begin by presenting the data and model simulation used for this study (Section 2). The remote impact of ENSO on the NAE is analyzed in Section 3 for different types of El Niño and La Niña events, paying special attention to the non-linear features. Finally, in Section 4, a brief summary and a discussion are presented.

2 Data and Model

In this work a low resolution version (3.75° x 2.5°) of the atmospheric component of the Australian Community Climate and Earth System Simulator (ACCESS) model (Bi et al., 2013) is used to analyze the role of the ocean mean state as modulator of ENSO teleconnections with the NAE climate in February-March-April after the mature phase of ENSO events, according to López-Parages and Rodríguez-Fonseca (2012) and López-Parages et al. (2014).

ACCESS Model is made up of the Met Office (UKMO) Unified Model AGCM with Hadley Centre Global Environment Model version 2 (HadGEM2) physics (Davies et al.,

2005; Martin et al., 2010; Martin et al., 2011). In the present study this model is coupled in some specific regions to a simple slab ocean model (Washington and Meehl, 1984; Dommenget and Latif, 2002; Murphy et al., 2004; Dommenget, 2010) letting the SSTs over these regions to respond to the different spatial patterns of SST forcing, which in turn are defined from HadISSTs data (Rayner et al., 2003). A flux correction, however, is required to force the model SSTs to closely follow a reference SST climatology (1950-2010). The sea ice climatology is also prescribed here from HadISST dataset.

First of all, a set of control simulations, for which the aforementioned reference SST climatology is modified over the Atlantic (40S-80N) and the tropical Pacific (30S-30N) basins, are performed. To this aim, an anomalous SST pattern (Figure 1a) corresponding to the difference between periods with a distinct impact of ENSO on the European and Mediterranean rainfall in late winter-early spring (Mariotti et al., 2002; López-Parages and Rodríguez-Fonseca, 2012), is added or subtracted to the reference SST climatology. This pattern (1a), which resembles an Atlantic Multidecadal Oscillation structure (AMO; Knight et al. (2005); Kang et al. (2014)), has been only prescribed here over the Atlantic and the tropical Pacific. This has been done in order to take into account, not only the Atlantic SSTs associated with the AMO, but also the AMO signature on the tropical Pacific (Kucharski et al., 2015; Dong et al., 2006), which could influence the processes involved during the ENSO event. Furthermore, to better analyze the influence of the changing SST background state on the ENSO-NAE teleconnection the amplitude of this anomalous SST pattern, has been doubled. The resultant "modified climatologies" (obtained by adding or subtracting Figure 1a with double amplitude to the reference 1950-2010 climatology) are hereinafter referred as P and N, respectively, in accordance to the positive (P) and negative (N) links, between El Niño and rainfall variability in central Europe, identified in López-Parages et al. (2014).

Secondly, for these modified climatologies, a series of sensitivity experiments (see Table 1) are performed superimposing different idealized ENSO patterns as defined in Dommenget et al. (2013). These patterns (Figures 1b and c), which represent the non-linear spatial structure of ENSO events in an optimal way, have been normalized to have a Niño-3.4 (5S-5N, 120-170W) mean SST anomaly of +1K (for El Niño events) or -1K (for La Niña events), as in Frauen et al. (2014). Hereinafter these spatial patterns will be referred as Eastern (EP) and Central (CP) ENSO. Note, however, that in these sensitivity experiments performed with an AGCM only the oceanic component of ENSO (El Niño) is prescribed. Outside the Atlantic and the tropical Pacific, the AGCM model is coupled to the simple slab ocean model. All the experiments are performed considering different signs (El Niño and La Niña) and amplitudes (100% and 200%) of ENSO forcing.

Table 1 Overview of the simulations performed in this study. All of them are 50 years long

ENSO amplitude	**SST mean state**			
	P		**N**	
+200%	EP200 P	CP200 P	EP200 N	CP200 N
+100%	EP100 P	CP100 P	EP100 N	CP100 N
Control	P		N	
-100%	-EP100 P	-CP100 P	-EP100 N	-CP100 N
-200%	-EP200 P	-CP200 P	-EP200 N	-CP200 N

The mean response of each sensitivity experiment has been calculated and compared with the other experiments in order to answer different open questions regarding the influence of distinct types of ENSO phases and patterns (El Niño and La Niña; EP and CP) under different ocean mean states (P and N). The significant differences have been evaluated through the non-parametric Wilcoxon-Mann-Whitney test (Wilks, 2011).

It is worth to note how the experimental design applied here only allows us to investigate the direct global impacts of tropical Pacific SSTs during ENSO events and does not capture the entire global impact of ENSO. For instance, the ENSO signature over the Tropical North Atlantic, which also influences the ENSO-related atmospheric response over the North Atlantic and Europe (Mathieu et al., 2004; Ham et al., 2014), is not captured here (taking into account that the AGCM is not coupled to the slab ocean model over the Atlantic basin). Thus, the present study is designed only in order to isolate the direct link between tropical Pacific SSTs during ENSO events and the NAE climate.

A basic observational validation of our experimental results has been also presented in this study. For this purpose, SLP data from NCAR (Trenberth and Paolino, 1980) and from the 20th century reanalysis V2 (20CR; Compo et al. (2011)) provided by the NOAA, have been used. The significance of the observational patterns has been also determined by the Wilcoxon-Mann-Whitney test.

3 Results

3.1 ENSO responses under different background climatologies

In this section the anomalous responses, in February-March-April, to distinct ENSO SST patterns (with different signs, amplitudes and spatial patterns) under P and N climatologies, are obtained. The impact is analyzed, for each case, at upper and surface levels, normalizing the ENSO-related

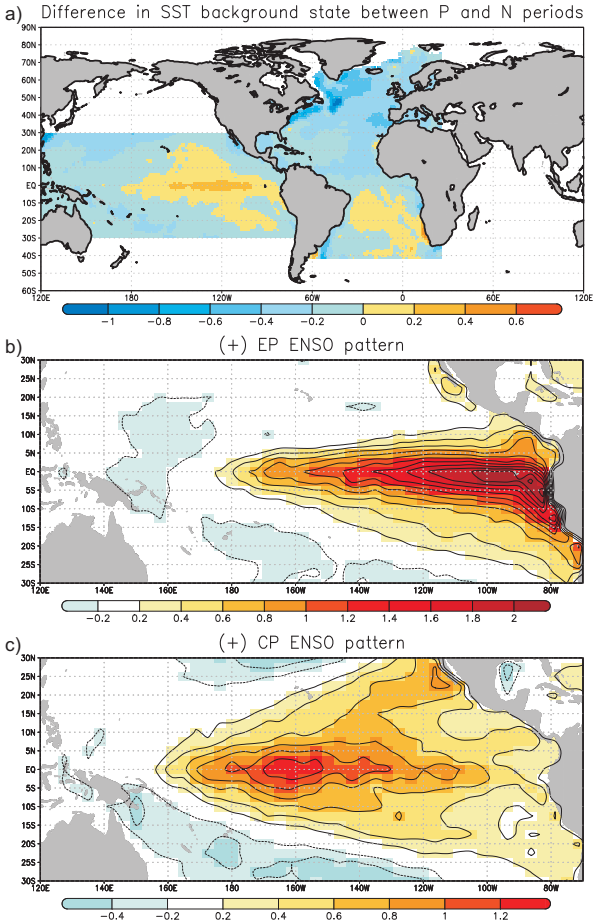

Fig. 1 a) P (1910-1940 + 1965-1990) minus N (1941-1955 + 1995-2009) Sea Surface Temperature annual mean state obtained from HadISST. Units are $[K]$ b) Standardised EP 100% ENSO pattern c) Standardised CP 100% ENSO patterns. ENSO patterns (the same as in Dommenget et al. (2013)) are normalised by their corresponding SST anomalies over the El Niño34 region $[K/(KNino34)^{-1}]$. The simple slab ocean model is active outside the Atlantic and the tropical Pacific (white areas in figure above).

patterns by the mean Niño-3.4 SST anomaly values. In order to distinguish the rotational and divergent signals in the upper troposphere, the atmospheric streamfunction and the velocity potential at 200hPa have been presented.

Additionally, the wave activity flux (WAF), which is a vector approximately parallel to the local group velocity of Rossby waves, has been computed directly from the zonally asymmetric part of the anomalous streamfunction regression maps (assuming stationary Rossby waves and neglecting vertical movements; see equation 38 of Takaya and Nakamura (2001) for further details).

3.1.1 EP El Niños

For Eastern Pacific El Niños (EP), the atmospheric response appears stronger in P than in N at upper (Figure 2) and surface (Figure 3) levels. In both cases, the model is able to reproduce the ENSO-related rotational impact over the NAE in late winter and early spring (Gouirand and Moron, 2003; Moron and Plaut, 2003; García-Serrano et al., 2011), that is, a well established TNH pattern together with a significant center located downstream over the European continent. This enhanced signal in P with respect to N is less noticeable when the EP forcing is doubled (Figures 2b,d and 3b,d).

For EP100 El Niños, the intense rotational response in P (Figure 2a) contrasts with the weaker wave activity in N (Figure 2c). This seems to be due to the stronger divergence identified over the tropical Pacific in the former case (see contours in Figures 2a,c), for which the two twin anticyclones straddling the equator and related to the typical Gill-type atmospheric response to equatorial anomalous heating (Gill, 1980), appear also reinforced. Considering that remote impacts associated with tropical convection are sensitive to absolute rather than anomalous values of SST, temperatures required for deep convection (preferentially exceeding a threshold of 26°-28°; see Graham and Barnett (1987)) are favored in P mean state, in which the underlying tropical Pacific is warmer (Figure 1a; see also Figure A1 of supplementary material). If EP El Niños are strong (200%) this threshold is exceeded in both, P and N, and so, their related upper level perturbations look similar (Figures 2b,d). Two distinct wavetrains can be clearly identified over the northern hemisphere in those cases in which a strong rotational response is found (in P for normal El EP Niños and in both, P and N, for strong EP El Niños). One is generated from the west Pacific extending east across the North Pacific and then south over North America. A second wavetrain originates from the east tropical Pacific and crosses the North Atlantic northward until the British Islands, where it is reflected towards lower latitudes over the Euro-Mediterranean region. The resultant SLP patterns highlights the barotropic nature of the anomalous perturbation (contours in Figures 3a,b,d). As a consequence, a deep low pressure system appears over the British Islands, and a significant impact on European rainfall is found (shaded in Figures 3a,b,d), being similar to the ENSO-related impact identified in previous studies (Moron and Gouirand, 2003; Bulić and Kucharski, 2012). It is interesting to note that, for EP100 in N, the three centres over Florida, the Labrador Strait and, in particular, over the British Islands appear noticeably weakened (Figure 3c). Hence, the significant Euro-Mediterranean rainfall pattern associated with ENSO is not found (Figure 3c). The aforementioned responses are coherent with the distinct ENSO signature on Euro-Mediterranean

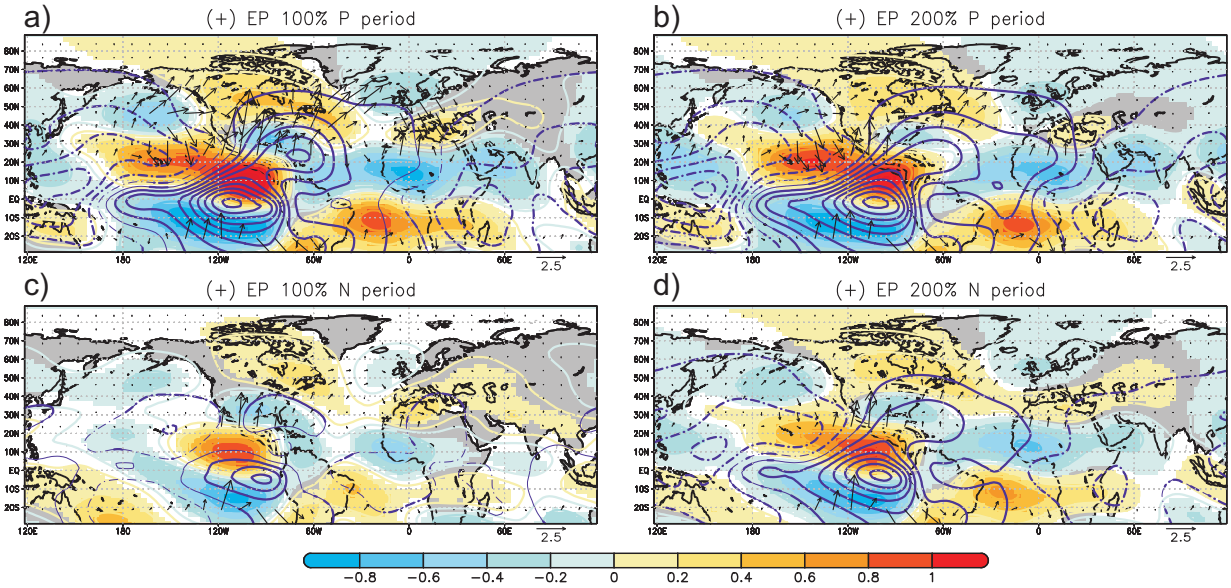

Fig. 2 EP El Niños. Streamfunction (units in $10^7 m2/s$), velocity potential (with opposite sign; $10^7 m2/s$), and wave activity flux (arrows; m^2/s^2), at upper troposphere (200hPa) under P (top) and N (bottom) mean states. On the left side, results for 100% EP ENSO amplitude. On the right side, for EP 200% amplitude. The patterns are February-March-April seasonal means normalized by the corresponding SST mean anomalies over the El Niño3.4 region (Units in K^{-1}). Only the 95% significant regions are shown for streamfunction (shaded areas). For velocity potential (purple contours) the whole signal is plotted but only the 95% significant response is bolded. The minimum (maximum) contour represented, for positive (negative) values, is $0.05 \cdot 10^7$ ($-0.05 \cdot 10^7$), with ci= $0.05 \cdot 10^7$. Only the WAF values larger than 1 m^2/s^2 are shown, being removed the values for equatorial latitudes (lower than 10).

rainfall identified, for late winter and early spring, before (under a P-like SST mean state configuration) and after (under a N-like SST mean state configuration) the 1920's, and before (under a N-like SST mean state configuration) and after (under a P-like SST mean state configuration) the 1960's (Mariotti et al., 2002; López-Parages and Rodríguez-Fonseca, 2012; López-Parages et al., 2014). It is worth, however, to quantify the amplitude in the response between observational and model impacts. According to López-Parages et al. (2014), an anomaly of 8 mm/month is detected for central European rainfall in relation to $1K$ anomalous warming over the tropical Pacific (see Figures 2b and 2d of that paper). By carefully looking at the EP100 ENSO signature on European rainfall in our idealised experiments (Figure 3a), between 0.4 and $0.5 \cdot 10^{-5} Kg/m^2 s$ anomalous rainfall is obtained on central Europe for $1.3K$ warming in the Niño 3 region (Figure 1b). This implies between 8 and 10 mm/month/K Nino3, which reflects a slight overestimation of rainfall in the model with respect to the observations. Let us consider, in order to illustrate these magnitudes, the averaged rainfall in FMA for La Coruña (north-western Iberia; data from the Spanish Meteorological Agency) and Paris (data from Météo-France), which corresponds to 83 and 47 mm/month, respectively. According to this, an anomalous EP El Niño episode of $1K$ amplitude is related to an enhanced rainfall in these locations of around $10\% - 12\%$ (La Coruña) and $17\% - 21\%$ (Paris).

A closer inspection also reveals a changing response of surface rainfall over the tropical North Atlantic (Figure 3), which seems to be associated with the distinct eastward extension of the divergence flow signal forced by ENSO (contours in Figure 2). Related to this, for EP200 events a significant rainfall impact is found over the whole TNA and the Sahelian region in P (Figure 3b), while the areas with a significant signature are reduced in N (Figure 3d). A similar difference can be observed between EP100P (Figure 3a) and EP100N (Figure 3c). As it was previously noted, the remote impacts associated with tropical convection depend on absolute values of SST. Hence, the aforementioned extension of the divergent flow towards the TNA depends on both, the Pacific SST mean state (P or N), and the intensity of the EP El Niño event. Thus, when a strong EP El Niño happens under a warm Pacific background state (P), the divergent flow over the TNA is highly perturbed (Figure 2b), and a significant impact is found in rainfall (Figure 3b). On the contrary, if a weak EP El Niño happens over a cold Pacific background state (N), the perturbation at upper levels is clearly reduced (Figure 2c), and the rainfall signature over the TNA weakens (Figure 3c). According to this, EP100P (weak EP El Niño plus warm Pacific mean state; see Figures

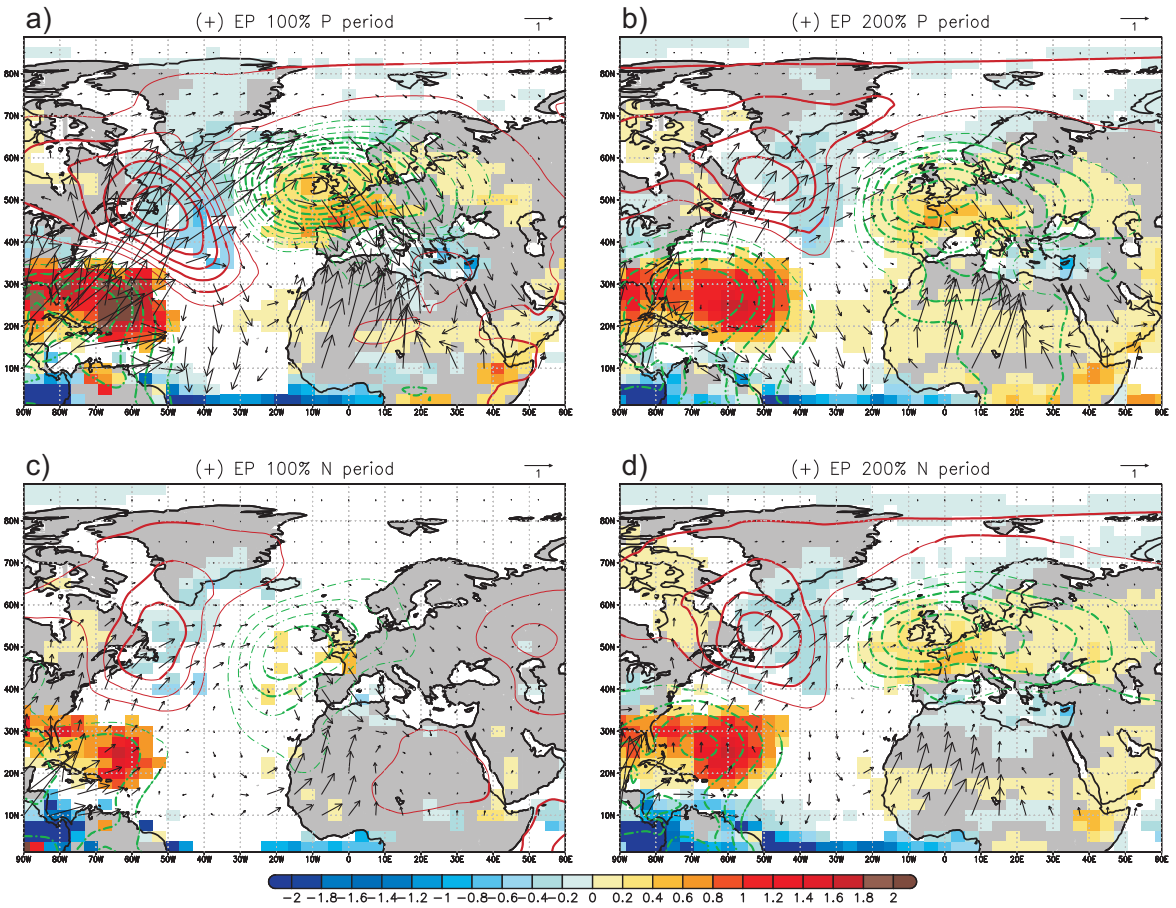

Fig. 3 EP El Niños. Rainfall (shaded; $10^{-5} Kg/m^2 s$), SLP (red and green contours for positive and negative values, respectively; Pa), and WAF (arrows; m^2/s^2), over the NAE sector under P (top) and N (bottom) mean states. On the left side, results for 100% EP ENSO amplitude. On the right side, for EP 200% amplitude. The patterns are February-March-April seasonal means normalized by the corresponding Niño3.4 mean anomalies (Units in K^{-1}). Only the 95% significant regions are shown for rainfall. For SLP (purple contours) the whole signal is plotted but only the 95% significant response is bolded. The minimum (maximum) contour represented, for positive (negative) values, is 30 (−30), with ci= 30. Only the WAF values larger than 1 m^2/s^2 are shown, being removed the values for equatorial latitudes (lower than 10).

2a and 3a) and EP200N (strong EP El Niño plus cold Pacific mean state; Figures 2d and 3d) reflect intermediate cases.

3.1.2 CP El Niños

As for EP El Niños, atmospheric response to the Central Pacific El Niños (CP) appears stronger in P than in N (see Figure 4). The main wavetrain associated with the well-known TNH pattern is obtained for both intensities (CP100 and CP200) and ocean mean states (P and N), finding a similar response as for EP events. Nevertheless, the rotational impact over Europe appears weaker and more northerly located than for EP El Niños. At surface, a negative NAO-like pattern emerges (Figure 5), showing different intensities depending on the mean state and, most specially, on the amplitude of the El Niño forcing.

The intensified rotational response of CP Niños in P is explained, as for EP Niños, by the stronger divergence signal over the tropical Pacific (contoured in Figure 4). The divergent response for CP100N (Figure 4c) is, however, not as weak as for EP100N (Figure 2c). This feature is explained by the fact that, in N, the climatological SSTs in the western tropical Pacific (Figure 1a, opposite sign for N periods) are warmer than on the eastern side, which allows the development of deep convection easily in this region if an anomalous warming is superimposed. As a consequence, the rotational signal over the Pacific North American sector is slightly stronger for CP than for EP events (note the stronger Aleutian low in Figure 4 with respect to Figure 2). Over the North Atlantic, on the contrary, a weakening of the WAF is found for CP in both, P and N. Related to this, the centre of streamfunction over Canada (positive) appears weaker and more zonally elongated than for EP El Niños and so, a

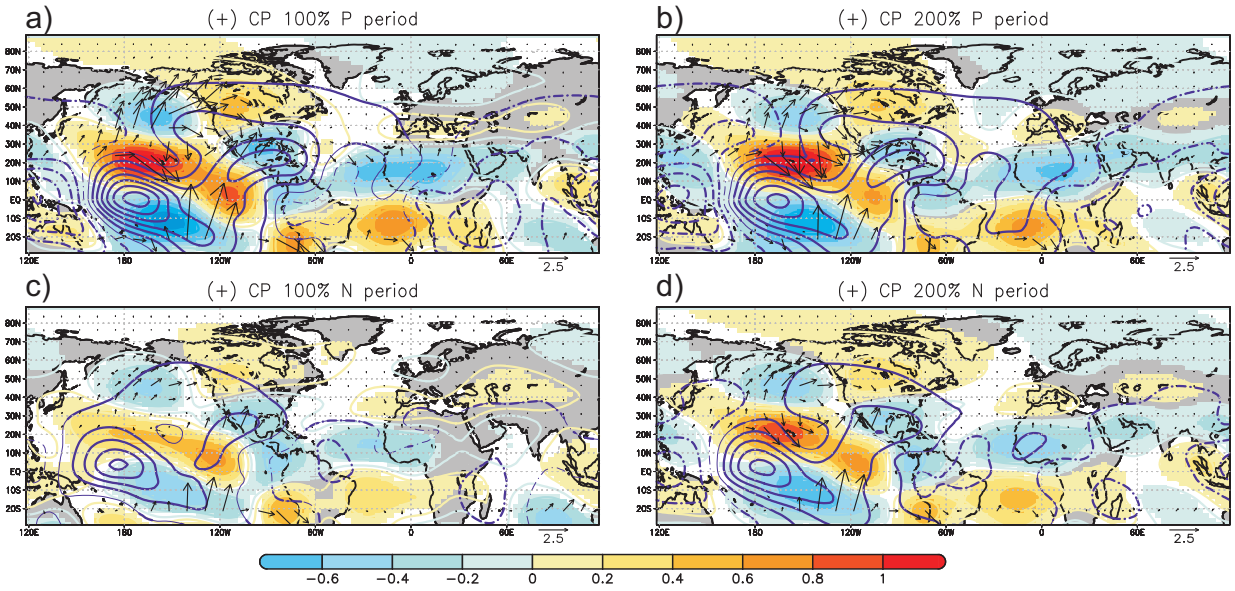

Fig. 4 CP El Niños. Same as Figure 2 but for CP El Niños.

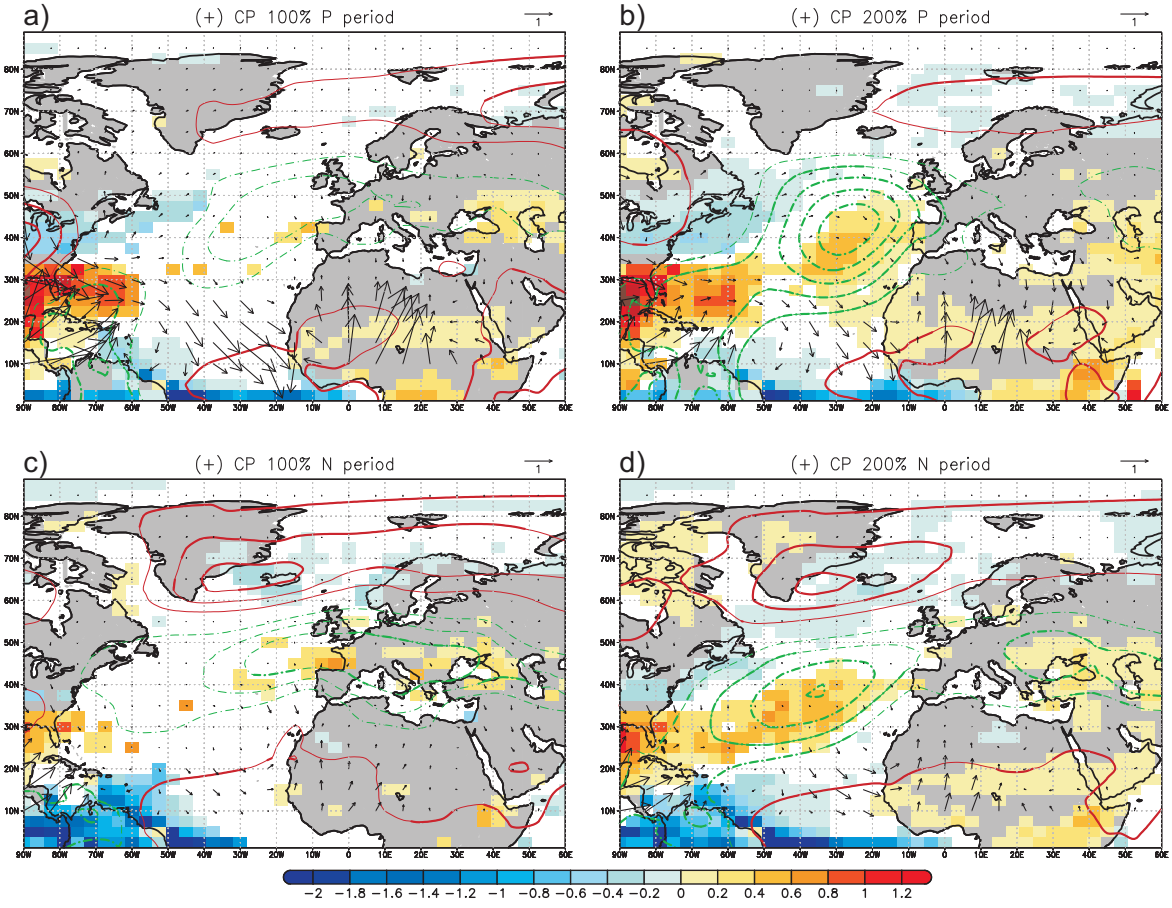

Fig. 5 CP El Niños. Same as Figure 3 but for CP El Niños.

totally positive SLP signal is found at high latitudes (Figure 5). This feature is specially marked in N, for which the positive SLP signal is statistically significant (Figure 5c,d). Regarding the divergent flow response (contours in Figure 4), it seems that the eastward extension over the subtropical North Atlantic appears reinforced in P. At surface (Figure 5), however, no clear differences are identified between P and N at subtropical latitudes. On the contrary, the most distinguishable response is obtained in relation to the intensity of the CP event instead of in relation to the background state, finding a significant impact over the Azores region for strong CP El Niños in both, P and N (Figure 5b,d).

A joint analysis of the rotational and the divergent flow is needed to understand this impact at surface levels. According to the results obtained here the shape of the aforementioned centre of streamfunction over Canada (positive), not only produces the high SLPs over the North Atlantic, but also influences the impact over the Azores region through the divergent flow: If this centre appears slightly southeastward elongated towards the subtropical Atlantic (as in P) the Azores high is significantly perturbed only if the divergent impact associated with ENSO is really strong (Figures 4b and 5b); whilst, if this centre is weaker and zonally distributed (as in N), a slight increase of the divergent flow is enough to significantly change the Azores high (Figures 4d and 5d).

Thus, the changing dipole SLP configuration obtained for CP El Niños is broadly explained by: 1) a distinct propagation of stationary Rossby waves and 2) a different eastward extension towards the North Atlantic of the divergent flow signal associated with ENSO.

The aforementioned signatures over the NAE related to CP and EP El Niños resemble the documented responses in relation to "moderate" and "strong" El Niños (Toniazzo and Scaife, 2006), which responds to the fact that the latter are closely associated with the EP pattern prescribed here (see Figure 2 from Frauen et al. (2014)).

3.1.3 La Niñas

A first view of the La Niña experiments reveals a weaker response than for El Niño episodes in both, the rotational and the divergent flow (see Figure 6).

A reinforced TNH pattern associated with CP La Niña events is identified in P (Figures 6a,b) compared to N (Figures 6c,d). This fact, which occurs as a consequence of the stronger convergence in the upper troposphere over the tropical Pacific in P, is in agreement with Frauen et al. (2014), who found a stronger atmospheric response for the same SST anomalies under a warmer background tropical Pacific (as occurs here in P). The downstream signal over the NAE is much weaker than for El Niño episodes. A significant center of negative streamfunction is found at upper levels over Western Europe (Figures 6a,c), spreading eastward when La Niña amplitude is doubled (Figures 6b,d). A positive center is also obtained at higher latitudes, being situated over the North Atlantic in N (Figures 6c,d), and further east over the Northern Eurasia in P (Figures 6a,b). This feature seems to explain the positive SLP signal identified in N over Iceland and its surrounding areas (Figures 7c,d), differently from P, for which the SLP anomalies obtained over the same region are negative (Figures 7a,b).

At lower latitudes the stronger convergence detected over the tropical Pacific in P (Figures 6a,b) with respect to N (Figures 6c,d) reinforces the climatological Walker cell connecting the tropical Pacific with the tropical Atlantic. As a consequence, an anomalous divergence is found over the tropical Atlantic in P, which is related to the enhancement of the two twin anticyclones straddling the equator (Figures 6a,b). This stronger inter-basin connection strengthens, in turn, the meridional Hadley cell over the Atlantic basin (Wang, 2002b), favouring therefore the intensification of the Azores high pressure system (Figures 7a,b). In N, on the contrary, the inter-basin connection is much less intense, and the aforementioned perturbation over the Azores is not found (Figures 7c,d).

The aforementioned characteristics are broadly reproduced for EP La Niñas, finding however a weaker impact over the NAE sector than for CP La Niñas (see Figures A2 and A3 of supplementary material).

4 Summary and Discussion

In this study the role of the ocean mean state as a modulator of the ENSO-NAE teleconnection in late winter and early spring (February-March-April) is explored. To this aim, a set of sensitivity experiments, in which a full complexity AGCM is forced with standardised ENSO patterns of different signs and strengths, are performed. These ENSO patterns are, in turn, superimposed over distinct SST background states over the Atlantic and the tropical Pacific basins. These background SST patterns are obtained by adding the difference between the climatologies in those periods, in which the impact of ENSO over the Euro-Mediterranean rainfall is different, to a control climatology (1950-2010).

Regarding El Niño events it has been found that, a wavetrain crossing the North Atlantic north-eastward reaches the European Continent and a significant impact on the Euro-Mediterranean rainfall is obtained, if the anomalous heating occurs in the eastern side of the tropical Pacific (EP Niños). This feature is dependent on the ocean mean state (P or N), specially if the El Niño amplitude is "normal" (100% EP events). According to this, the aforementioned wavetrain associated with normal EP Niños is clearly enhanced when the tropical Pacific SST mean state is warmer than usual and the North Atlantic SST mean state is colder than usual.

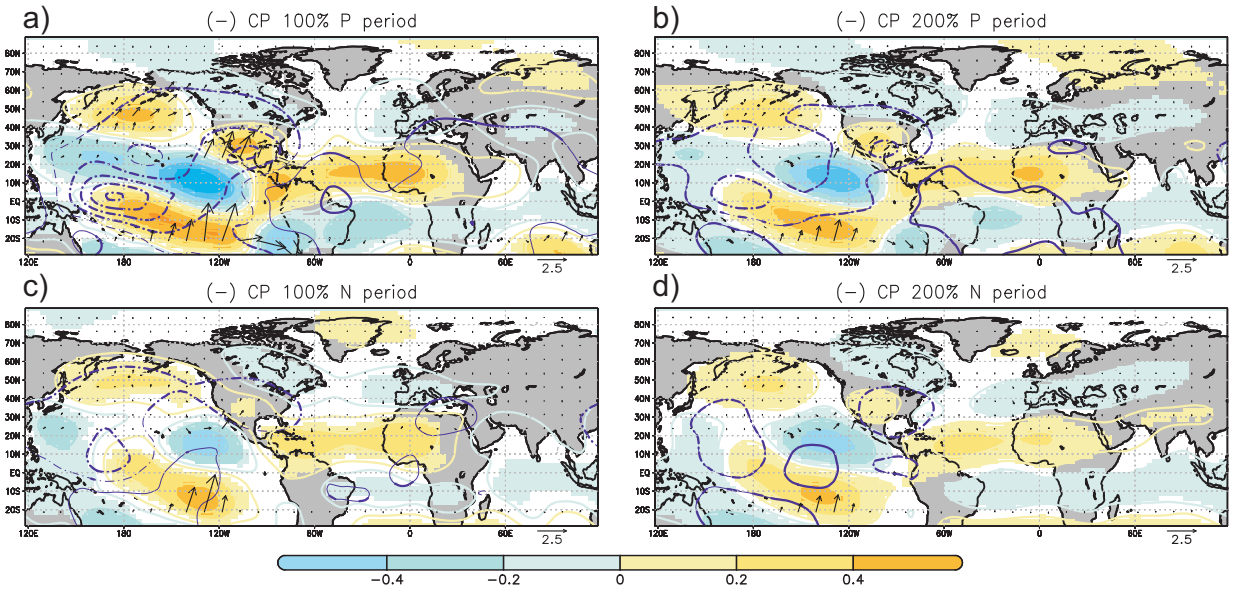

Fig. 6 CP La Niñas. Same as Figure 2 but for CP La Niñas.

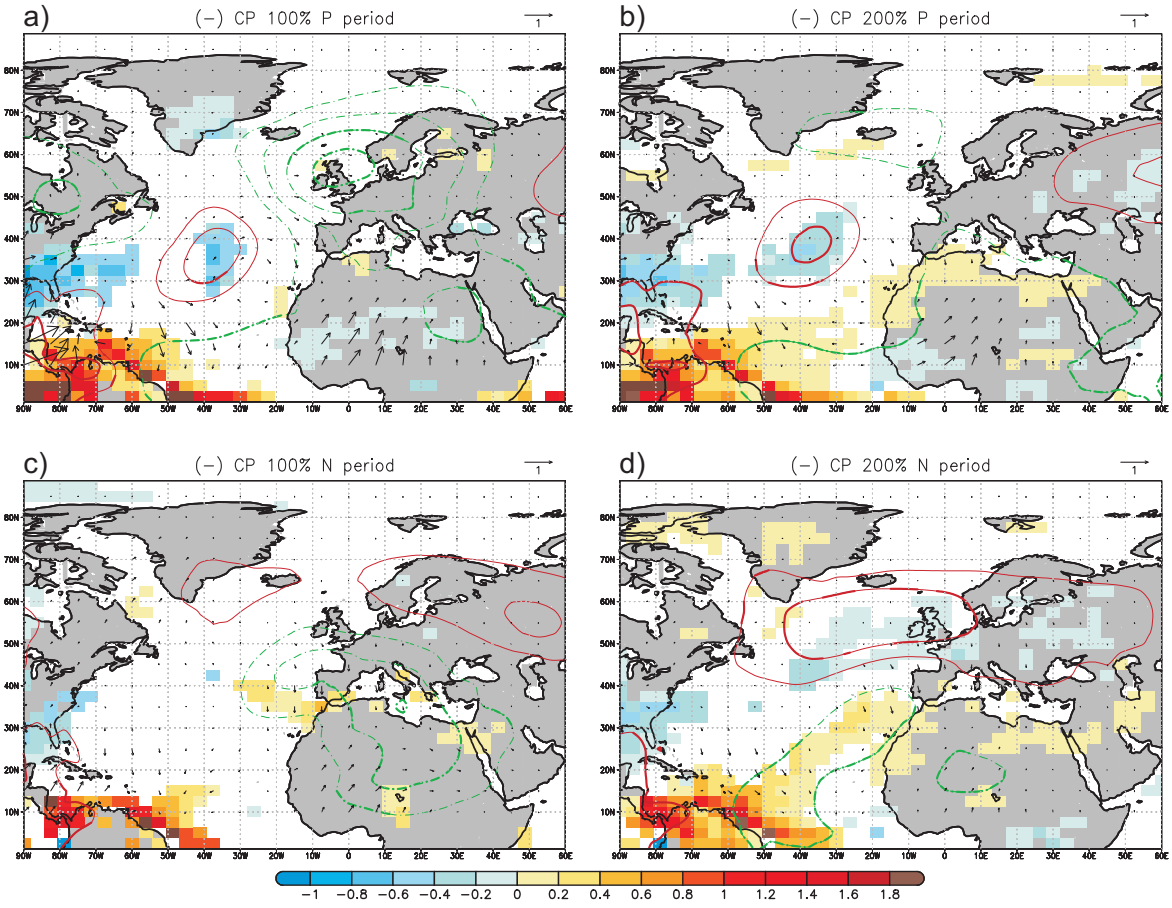

Fig. 7 CP La Niñas. Same as Figure 3 but for CP La Niñas.

If the heating associated with El Niño occurs in the central tropical Pacific (CP El Niños) the wavetrain towards the North Atlantic is more zonally guided, which favours a weakening of the Iceland low pressure system. Under these circumstances, a significant weakening of the Azores high is also found if the CP El Niño is "strong" (200% CP events). In these cases, an anomalous negative NAO-like pattern is identified.

Regarding La Niña events a weaker impact, compared to that of El Niño events, is detected over the NAE sector. Opposite SLP signatures, at high and subtropical latitudes, are found for the same La Niña pattern over the North Atlantic depending on the SST background state. If the tropical Pacific SST background conditions are warmer than usual, a stronger anomalous convergence is detected in the upper troposphere when a La Niña pattern is superimposed. Under these circumstances the Rossby wavetrain associated with the La Niña forcing is modified, and the zonal and thermally driven Walker cell connecting the Pacific and the Atlantic basins is enhanced. These characteristics associated with CP La Niñas are broadly reproduced for EP La Niñas, just finding slight differences in the intensity and spatial location of some centers of action (see Figure A2 of supplementary material). According to the results presented here, the positive NAO-like pattern usually related to La Niña events (Fraedrich and Müller, 1992; Gouirand and Moron, 2003; Moron and Plaut, 2003; Moron and Gouirand, 2003; Pozo-Vázquez et al., 2001, 2005b) could take place only during selected decades.

As this study is based on idealised experiments, a basic validation of the distinct model mean responses obtained is recommended in order to put our results in context with the observations. To this aim, SLP composites maps over the NAE sector are calculated in the observational period for each ENSO forcing and ocean mean states (Figure 8). This composite analysis is based on composites of anomalies calculated for warm and cold ENSO events, being characterised the EP and CP episodes by the Niño3 and Niño4 indices, respectively. For EP Niños, the three centres of action identified in our simulations over Florida, the Labrador Strait, and the British Islands in relation to a wavetrain coming from the Eastern Pacific under a P SST mean state (Figure 3a), are also obtained in observations for those decades under a P-like SST mean state configuration (Figure 8a). Under N SST mean conditions this SLP structure is weakened for both, model (Figure 3c) and observation (Figure 8d). For CP Niños, a dipolar pattern resembling a negative NAO-like structure is found, but with different amplitudes, in P and N (Figure 8b and 8e). This feature is also coherent with the model response to CP Niños (Figures 5a and 5c). Finally, for CP Niñas, a positive NAO-like signature is detected in P for both, observations (Figure 7a) and model (Figure 8c); whilst the same is not found in N for any of them (Figures 7c and 8f). It is necessary to note that the comparison between observational and model results is far to be direct, as in the former case significant differences in ENSO forcing appears between P and N (see Figure A4 of supplementary material) and hence, to associate a distinct response over the NAE sector with an effective modulation by the SST mean state rather than with the differences in the forcing itself, is highly complicated. In spite of this aspect, as it is shown in Figure 8, the main observational characteristics identified in the ENSO-related responses in P and N mean states are consistent with those detected in model results. Two different observational SLP databases are used, finding for both of them consistent results with our experimental responses. We can conclude that the observational dependence of ENSO response over the NAE sector on the SST background conditions is, therefore, properly reproduced by the ACCESS model.

Regarding rainfall, it has been demonstrated how the dependence of ENSO signature in European rainfall on the ocean mean state is evident for EP El Niños, in agreement with previous observational studies (Mariotti et al., 2002; Knippertz et al., 2003; López-Parages and Rodríguez-Fonseca 2012; López-Parages et al., 2014). This feature takes place even though 1) no SST anomalies over the TNA are prescribed in our simulations, and 2) the ocean-atmosphere feedbacks over the TNA, which could enhance the ENSO-related atmospheric response over the NAE (Mathieu et al., 2004), are absent in our experimental design. The other ENSO events (CP El Niños, EP La Niñas, and CP La Niñas) present a less evident dependence of European and mediterranean rainfall response to ENSO on the SST mean state than EP El Niños. This fact could be partially explained by the aforementioned decoupling over the TNA region in our experimental design. Indeed, an eastward displacement of the centres of action associated with ENSO towards the European continent is expected if the influence associated with the TNA SSTs would be considered (Sung et al., 2013; Ham et al., 2014). Thus, further experiments, in which the anomalous SSTs over the TNA are prescribed, or in which the slab ocean model is also applied over the Atlantic basin, could shed light on new changing processes related to the non-stationary ENSO-NAE teleconnection identified in observations.

Along this study the importance of having a changing propagation of Rossby wavetrains associated with ENSO for a non-stationary impact downstream over the North Atlantic, has been highlighted. Related to this it is necessary to note the relevance of the eastern North American region for North Atlantic storm track development. According to this, the slight differences detected here in the propagation of Rossby wavetrains could induce strong changes in baroclinicity and low level heat fluxes over Newfoundland and its surrounding areas. As a consequence, the growth condi-

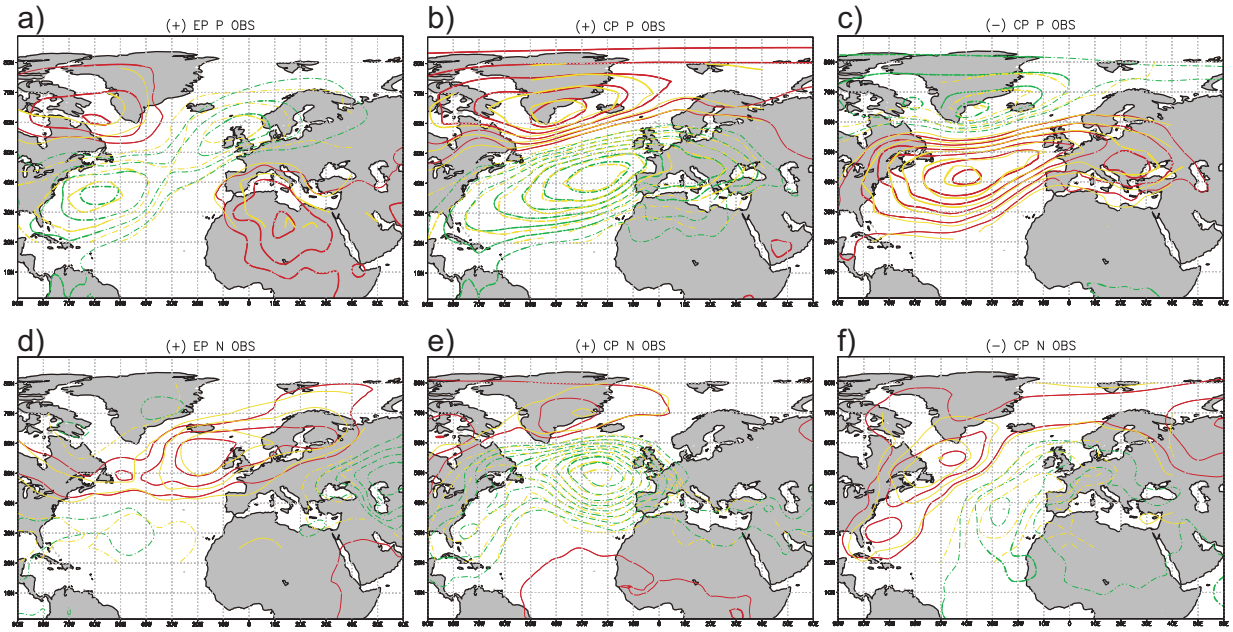

Fig. 8 Observational ENSO impact. SLP response of EP and CP ENSO over the NAE sector in P (1910-1940 and 1965-1990; top) and N (1941-1955 and 1995-2009; bottom) observational periods. They are constructed by calculating the composite maps based on those years in which the Niño3 (EP) and Niño4 (CP) indices, respectively, exceeds 0.5 (-0.5 for La Niña events) standard deviations. Red (solid yellow) and green (dashed yellow) contours represent positive and negative values from 20CR (NCAR) database. The 95% significant responses are bolded. Contours lines are the same as in figures 3, 5, and 7.

tions of tropospheric eddies could be remarkably different and so, the storm track activity over the whole North Atlantic.

The present study demonstrates how the remote impact of both warm and cold ENSO events, on the NAE climate could be noticeable different depending on the low frequency variability of the SST. According to our results a warmer than usual SST background of the tropical Pacific, together with a colder than usual SST background over the North Atlantic, favours the link between ENSO and the NAE sector in twofold: 1) changing the thermally driven direct circulation (Walker and Hadley cells), and 2) varying the Rossby waves pathway in their propagation from the tropical Pacific to the North Atlantic. However, the underlying mechanism in the latter case is still unclear, needing further analysis to completely understand by which way the ocean mean state could alter the propagation of the planetary waves triggered by ENSO, in the upper troposphere. It is important to note how most of the available studies consider the jet streams as important agents controlling the propagation of Rossby waves from tropical to extratropical latitudes (Hoskins and Karoly, 1981; Hoskins and Ambrizzi, 1993; Ambrizzi et al., 1995; Branstator, 2002). Hence, the influence that changes in the ocean mean state exert on the zonal mean flow at upper levels is a matter which should be examined in detail in the future. Another interesting question emerging from this modelling study is the important role that tropical Pacific SST background state seems to play in remote ENSO responses. It should be pointed out that the SST mean state pattern prescribed in our sensitivity experiments, which is based on the changing impact of ENSO on the leading Euro-Mediterranean rainfall mode in the observational record, has strong similarities with the AMO spatial signature over both, the Atlantic and the tropical Pacific basins. According to this, one might well wonder why the non-stationary teleconnection identified in observations evolve in phase with the AMO instead of with other multidecadal variability modes associated with the Pacific SSTs such as the Pacific Decadal Oscillation (Mantua et al., 1997) or the Interdecadal Pacific Oscillation (Zhang et al., 1997). Future studies should investigate this issue and its possible relation to the model bias. Furthermore, it should be also pointed out that the distinct SST mean states prescribed in our sensitivity experiments could interact in different ways with the ENSO forcing. Which specific ENSO-related processes depend on the ocean mean state? To address this question the non-linear interaction between the background state and the forcing must be also thoroughly analysed in forthcoming studies.

The main conclusion of our work is that the assumption of stationarity that is common to many studies of ENSO teleconnections must be clearly questioned. According to our results, impacts over the NAE sector associated with ENSO

events (with different signs, patterns, and amplitudes) could be significantly different if they take place under distinct background conditions. As a consequence, the comparability between those studies considering different climatologies is limited, which could explain the apparent disagreement among them in the available literature.

Acknowledgements This work was supported by the National Spanish projects: TRACS (CGL2009-10285) and MULCLIVAR (CGL2012-38923-C02-01). In particular, JLP thanks the FPI grant (BES-2010-042234) associated with TRACS project. JLP also thanks the Monash Weather and Climate group of Monash University (Melbourne) for scientific discussions and incredible hospitality. The sensitivity experiments described in this paper were performed on Monash University.

References

Ambrizzi, T., Hoskins, B. J., and Hsu, H.-H.: Rossby Wave Propagation and Teleconnection Patterns in the Austral Winter., J. Atmos. Sci., 52, 3661–3672, doi:10.1175/1520-0469(1995)0523661:RWPATP 2.0.CO;2, 1995.

Barnston, A. and Livezey, R.: Classification, Seasonality and Persistence of Low-Frequency Atmospheric Circulation Patterns, Mon. Wea. Rev., 115, 1083, doi:10.1175/1520-0493(1987)1151083:CSAPOL 2.0.CO;2, 1987.

Bi, D., Dix, M., Marsland, S. J., OFarrell, S., Rashid, H., Uotila, P., Hirst, A., Kowalczyk, E., Golebiewski, M., Sullivan, A., et al.: The ACCESS coupled model: description, control climate and evaluation, Aust. Meteorol. Oceanogr. J, 63, 41–64, 2013.

Bladé, I., Newman, M., Alexander, M. A., and Scott, J. D.: The Late Fall Extratropical Response to ENSO: Sensitivity to Coupling and Convection in the Tropical West Pacific, J. Climate, 21, 6101, doi:10.1175/2008JCLI1612.1, 2008.

Branstator, G.: Circumglobal Teleconnections, the Jet Stream Waveguide, and the North Atlantic Oscillation., J. Climate, 15, 1893–1910, doi:10.1175/1520-0442(2002)0151893:CTTJSW 2.0.CO;2, 2002.

Brönnimann, S.: Impact of El Niño-Southern Oscillation on European climate, Rev. Geophys., 45, RG3003, doi:10.1029/2006RG000199, 2007.

Bulić, I. H. and Kucharski, F.: Delayed ENSO impact on spring precipitation over North/Atlantic European region, Climate Dyn., 38, 2593–2612, 2012.

Cassou, C. and Terray, L.: Oceanic Forcing of the Wintertime Low-Frequency Atmospheric Variability in the North Atlantic European Sector: A Study with the ARPEGE Model., J. Climate, 14, 4266–4291, doi:10.1175/1520-0442(2001)0144266:OFOTWL 2.0.CO;2, 2001.

Choi, J., An, S.-I., Kug, J.-S., and Yeh, S.-W.: The role of mean state on changes in El Niño's flavor, Climate Dyn., 37, 1205–1215, doi:10.1007/s00382-010-0912-1, 2011.

Compo, G. P., Whitaker, J. S., Sardeshmukh, P. D., Matsui, N., Allan, R. J., Yin, X., Gleason, B. E., Vose, R. S., Rutledge, G., Bessemoulin, P., Brönnimann, S., Brunet, M., Crouthamel, R. I., Grant, A. N., Groisman, P. Y., Jones, P. D., Kruk, M. C., Kruger, A. C., Marshall, G. J., Maugeri, M., Mok, H. Y., Nordli, Ø., Ross, T. F., Trigo, R. M., Wang, X. L., Woodruff, S. D., and Worley, S. J.: The Twentieth Century Reanalysis Project, Quart. J. Roy. Meteor. Soc., 137, 1–28, doi:10.1002/qj.776, 2011.

Davies, T., Cullen, M., Malcolm, A., Mawson, M., Staniforth, A., White, A., and Wood, N.: A new dynamical core for the Met Office's global and regional modelling of the atmosphere, Quart. J. Roy. Meteor. Soc., 131, 1759–1782, 2005.

Dommenget, D.: The slab ocean El Niño, Geophys. Res. Lett., 37, L20701, doi:10.1029/2010GL044888, 2010.

Dommenget, D. and Latif, M.: Analysis of observed and simulated SST spectra in the midlatitudes, Climate Dyn., 19, 277–288, doi:10.1007/s00382-002-0229-9, 2002.

Dommenget, D., Bayr, T., and Frauen, C.: Analysis of the non-linearity in the pattern and time evolution of El Niño southern oscillation, Climate Dyn., 40, 2825–2847, doi:10.1007/s00382-012-1475-0, 2013.

Dong, B., Sutton, R. T., and Scaife, A. A.: Multidecadal modulation of El Niño-Southern Oscillation (ENSO) variance by Atlantic Ocean sea surface temperatures, Geophys. Res. Lett., 33, L08705, doi:10.1029/2006GL025766, 2006.

Fraedrich, K. and Müller, K.: Climate anomalies in Europe associated with ENSO extremes, Int. J. Climatol., 12, 25–31, doi:10.1002/joc.3370120104, 1992.

Frauen, C. and Dommenget, D.: El Niño and La Niña amplitude asymmetry caused by atmospheric feedbacks, Geophys. Res. Lett., 37, L18801, doi:10.1029/2010GL044444, 2010.

Frauen, C., Dommenget, D., Tyrrell, N., Rezny, M., and Wales, S.: Analysis of the Nonlinearity of El Niño-Southern Oscillation Teleconnection, J. Climate, 27, 6225, doi:10.1175/JCLI-D-13-00757.1, 2014.

García-Serrano, J., Rodríguez-Fonseca, B., Bladé, I., Zurita-Gotor, P., and de La Cámara, A.: Rotational atmospheric circulation during North Atlantic-European winter: the influence of ENSO, Climate Dyn., 37, 1727–1743, doi:10.1007/s00382-010-0968-y, 2011.

Gill, A. E.: Some simple solutions for heat-induced tropical circulation, Quart. J. Roy. Meteor. Soc., 106, 447–462, doi:10.1002/qj.49710644905, 1980.

Gouirand, I. and Moron, V.: Variability of the impact of El Niño-Southern Oscillation on sea-level pressure anomalies over the North Atlantic in January to March(1874-1996), Int. J. Climatol., 23, 1549–1566, doi:10.1002/joc.963, 2003.

Graham, N. E. and Barnett, T. P.: Sea Surface Temperature, Surface Wind Divergence, and Convection over Tropical Oceans, Science, 238, 657–659, doi:10.1126/science.238.4827.657, 1987.

Greatbatch, R. J., Lu, J., and Peterson, K. A.: Nonstationary impact of ENSO on Euro-Atlantic winter climate, Geophys. Res. Lett., 31, L02208, doi:10.1029/2003GL018542, 2004.

Ham, Y.-G., Sung, M.-K., An, S.-I., Schubert, S. D., and Kug, J.-S.: Role of tropical atlantic SST variability as a modulator of El Niño teleconnections, Asia. Pac. J. Atmos. Sci., 50, 247–261, doi:10.1007/s13143-014-0013-x, 2014.

Honda, M., Nakamura, H., Ukita, J., Kousaka, I., and Takeuchi, K.: Interannual Seesaw between the Aleutian and Icelandic Lows. Part I: Seasonal Dependence and Life Cycle., J. Climate, 14, 1029–1042, doi:10.1175/1520-0442(2001)0141029:ISBTAA 2.0.CO;2, 2001.

Hoskins, B. J. and Ambrizzi, T.: Rossby Wave Propagation on a Realistic Longitudinally Varying Flow., J. Atmos. Sci., 50, 1661–1671, doi:10.1175/1520-0469(1993)0501661:RWPOAR 2.0.CO;2, 1993.

Hoskins, B. J. and Karoly, D. J.: The Steady Linear Response of a Spherical Atmosphere to Thermal and Orographic Forcing., J. Atmos. Sci., 38, 1179–1196, doi:10.1175/1520-0469(1981)0381179:TSLROA 2.0.CO;2, 1981.

Kang, I.-S. and Kug, J.-S.: El Niño and La Niña sea surface temperature anomalies: Asymmetry characteristics associated with their wind stress anomalies, J. Geophys. Res. Atmos., 107, 4372, doi:10.1029/2001JD000393, 2002.

Kang, I.-S., No, H.-h., and Kucharski, F.: ENSO Amplitude Modulation Associated with the Mean SST Changes in the Tropical Central Pacific Induced by Atlantic Multidecadal Oscillation, J. Climate, 27, 7911–7920, doi:10.1175/JCLI-D-14-00018.1, 2014.

Kao, H.-Y. and Yu, J.-Y.: Contrasting Eastern-Pacific and Central-Pacific Types of ENSO, J. Climate, 22, 615, doi:10.1175/2008JCLI2309.1, 2009.

Karoly, D. J., Plumb, R. A., and Ting, M.: Examples of the Horizontal Propagation of Quasi-stationary Waves., J. Atmos. Sci., 46, 2802–2811, doi:10.1175/1520-0469(1989)0462802:EOTHPO 2.0.CO;2, 1989.

Knight, J. R., Allan, R. J., Folland, C. K., Vellinga, M., and Mann, M. E.: A signature of persistent natural thermohaline circulation cycles in observed climate, Geophys. Res. Lett., 32, L20708, doi:10.1029/2005GL024233, 2005.

Knippertz, P., Ulbrich, U., Marques, F., and Corte-Real, J.: Decadal changes in the link between El Niño and springtime North Atlantic oscillation and European-North African rainfall, Int. J. Climatol., 23, 1293–1311, doi:10.1002/joc.944, 2003.

Kucharski, F., Ikram, F., Molteni, F., Farneti, R., Kang, I.-S., No, H.-H., King, M., Giuliani, G., and Mogensen, K.: Atlantic forcing of Pacific decadal variability, Climate Dyn., pp. 1–15, doi:10.1007/s00382-015-2705-z, 2015.

Kug, J.-S., Jin, F.-F., and An, S.-I.: Two Types of El Niño Events: Cold Tongue El Niño and Warm Pool El Niño, J. Climate, 22, 1499, doi:10.1175/2008JCLI2624.1, 2009.

Livezey, R. E. and Mo, K. C.: Tropical-Extratropical Teleconnections during the Northern Hemisphere Winter. Part II: Relationships between Monthly Mean Northern Hemisphere Circulation Patterns and Proxies for Tropical Convection, Mon. Wea. Rev., 115, 3115, doi:10.1175/1520-0493(1987)1153115:TETDTN 2.0.CO;2, 1987.

López-Parages, J. and Rodríguez-Fonseca, B.: Multidecadal modulation of El Niño influence on the Euro-Mediterranean rainfall, Geophys. Res. Lett., 39, L02704, doi:10.1029/2011GL050049, 2012.

López-Parages, J., Rodríguez-Fonseca, B., and Terray, L.: A mechanism for the multidecadal modulation of ENSO teleconnection with Europe, Climate Dyn., 45, 867–880, doi:10.1007/s00382-014-2319-x, 2014.

Mantua, N. J., Hare, S. R., Zhang, Y., Wallace, J. M., and Francis, R. C.: A Pacific Interdecadal Climate Oscillation with Impacts on Salmon Production., Bull. Amer. Meteor. Soc., 78, 1069–1079, doi:10.1175/1520-0477(1997)0781069:APICOW 2.0.CO;2, 1997.

Mariotti, A., Zeng, N., and Lau, K.-M.: Euro-Mediterranean rainfall and ENSO-a seasonally varying relationship, Geophys. Res. Lett., 29, 1621, doi:10.1029/2001GL014248, 2002.

Martin, G., Bellouin, N., Collins, W., Culverwell, I., Halloran, P., Hardiman, S., Hinton, T., Jones, C., McDonald, R., McLaren, A., et al.: The HadGEM2 family of met office unified model climate configurations, Geosci. Model. Dev. Discuss., 4, 765–841, 2011.

Martin, G. M., Milton, S. F., Senior, C. A., Brooks, M. E., Ineson, S., Reichler, T., and Kim, J.: Analysis and Reduction of Systematic Errors through a Seamless Approach to Modeling Weather and Climate, J. Climate, 23, 5933–5957, doi:10.1175/2010JCLI3541.1, 2010.

Mathieu, P.-P., Sutton, R. T., Dong, B., and Collins, M.: Predictability of Winter Climate over the North Atlantic European Region during ENSO Events., J. Climate, 17, 1953–1974, doi:10.1175/1520-0442(2004)0171953:POWCOT 2.0.CO;2, 2004.

Mo, K. C. and Livezey, R. E.: Tropical-Extratropical Geopotential Height Teleconnections during the Northern Hemisphere Winter, Mon. Wea. Rev., 114, 2488, doi:10.1175/1520-0493(1986)1142488:TEGHTD 2.0.CO;2, 1986.

Moron, V. and Gouirand, I.: Seasonal modulation of the El Niño-southern oscillation relationship with sea level pressure anomalies over the North Atlantic in October-March 1873-1996, Int. J. Climatol., 23, 143–155, doi:10.1002/joc.868, 2003.

Moron, V. and Plaut, G.: The impact of El Niño-southern oscillation upon weather regimes over Europe and the North Atlantic during boreal winter, Int. J. Climatol., 23, 363–379, doi:10.1002/joc.890, 2003.

Murphy, J. M., Sexton, D. M. H., Barnett, D. N., Jones, G. S., Webb, M. J., Collins, M., and Stainforth, D. A.: Quantification of modelling uncertainties in a large ensemble of climate change simulations, Nature, 430, 768–772, doi:10.1038/nature02771, 2004.

Peng, S. and Whitaker, J. S.: Mechanisms Determining the Atmospheric Response to Midlatitude SST Anomalies., J. Climate, 12, 1393–1408, doi:10.1175/1520-0442(1999)0121393:MDTART 2.0.CO;2, 1999.

Philip, S. and van Oldenborgh, G. J.: Significant Atmospheric Nonlinearities in the ENSO Cycle, J. Climate, 22, 4014, doi:10.1175/2009JCLI2716.1, 2009.

Pozo-Vázquez, D., Esteban-Parra, M. J., Rodrigo, F. S., and Castro-Díez, Y.: The Association between ENSO and Winter Atmospheric Circulation and Temperature in the North Atlantic Region., J. Climate, 14, 3408–3420, doi:10.1175/1520-0442(2001)0143408:TABEAW 2.0.CO;2, 2001.

Pozo-Vázquez, D., Gámiz-Fortis, S. R., Tovar-Pescador, J., Esteban-Parra, M. J., and Castro-Díez, Y.: El Niño-southern oscillation events and associated European winter precipitation anomalies, Int. J. Climatol., 25, 17–31, doi:10.1002/joc.1097, 2005a.

Pozo-Vázquez, D., Gámiz-Fortis, S. R., Tovar-Pescador, J., Esteban-Parra, M. J., and Castro-Díez, Y.: North Atlantic Winter SLP Anomalies Based on the Autumn ENSO State., J. Climate, 18, 97–103, doi:10.1175/JCLI-3210.1, 2005b.

Quadrelli, R. and Wallace, J. M.: Dependence of the structure of the Northern Hemisphere annular mode on the polarity of ENSO, Geophys. Res. Lett., 29, 2132, doi:10.1029/2002GL015807, 2002.

Rayner, N. A., Parker, D. E., Horton, E. B., Folland, C. K., Alexander, L. V., Rowell, D. P., Kent, E. C., and Kaplan, A.: Global analyses of sea surface temperature, sea ice, and night marine air temperature since the late nineteenth century, J. Geophys. Res. Atmos., 108, 4407, doi:10.1029/2002JD002670, 2003.

Ruiz-Barradas, A., Carton, J. A., and Nigam, S.: Role of the Atmosphere in Climate Variability of the Tropical Atlantic., J. Climate, 16, 2052–2065, doi:10.1175/1520-0442(2003)016 2052:ROTAIC 2.0.CO;2, 2003.

Sung, M.-K., Ham, Y.-G., Kug, J.-S., and An, S.-I.: An alterative effect by the tropical North Atlantic SST in intraseasonally varying El Nino teleconnection over the North Atlantic, Tellus, 65, 2013.

Sutton, R. T. and Hodson, D. L. R.: Influence of the Ocean on North Atlantic Climate Variability 1871-1999., J. Climate, 16, 3296–3313, doi:10.1175/1520-0442(2003)0163296:IOTOON 2.0.CO;2, 2003.

Takaya, K. and Nakamura, H.: A Formulation of a Phase-Independent Wave-Activity Flux for Stationary and Migratory Quasigeostrophic Eddies on a Zonally Varying Basic Flow., J. Atmos. Sci., 58, 608–627, doi:10.1175/1520-0469(2001)0580608:AFOAPI 2.0.CO;2, 2001.

Toniazzo, T. and Scaife, A.: The influence of ENSO on winter North Atlantic climate, Geophys. Res. Lett., 33, L24704, doi:10.1029/2006GL027881, 2006.

Trenberth, K. E. and Paolino, D. A.: The Northern Hemisphere Sea-Level Pressure Data Set: Trends, Errors and Discontinuities, Mon. Wea. Rev., 108, 855, doi:10.1175/1520-0493(1980)1080855:TNHSLP 2.0.CO;2, 1980.

Trenberth, K. E., Branstator, G. W., Karoly, D., Kumar, A., Lau, N.-C., and Ropelewski, C.: Progress during TOGA in understanding and modeling global teleconnections associated with tropical sea surface temperatures, J. Geophys. Res., 103, 14 291, doi:10.1029/97JC01444, 1998.

Wang, C.: Atlantic Climate Variability and Its Associated Atmospheric Circulation Cells., J. Climate, 15, 1516–1536, doi:10.1175/1520-0442(2002)0151516:ACVAIA 2.0.CO;2, 2002a.

Wang, C.: Atmospheric Circulation Cells Associated with the El Niño-Southern Oscillation., J. Climate, 15, 399–419, doi:10.1175/1520-0442(2002)0150399:ACCAWT 2.0.CO;2, 2002b.

Wang, C. and Enfield, D. B.: A Further Study of the Tropical Western Hemisphere Warm Pool., J. Climate, 16, 1476–1493, doi:10.1175/1520-0442-16.10.1476, 2003.

Wang, C. and Picaut, J.: Understanding ENSO physics: a review, AGU Geophysical Monograph Series, 147, 21–48, doi: 10.1029/147GM02, 2004.

Washington, W. M. and Meehl, G. A.: Seasonal Cycle Experiment on the Climate Sensitivity Due to a Doubling of CO_2 with an atmospheric general circulation model coupled to a simple mixed-layer ocean model, J. Geophys. Res., 89, 9475–9503, doi: 10.1029/JD089iD06p09475, 1984.

Wilks, D. S.: Statistical methods in the atmospheric sciences, vol. 100, Academic press, 2011.

Wu, A. and Hsieh, W. W.: The nonlinear association between ENSO and the Euro-Atlantic winter sea level pressure, Climate Dyn., 23, 859–868, doi:10.1007/s00382-004-0470-5, 2004.

Zhang, Y., Wallace, J. M., and Battisti, D. S.: ENSO-like Interdecadal Variability: 1900-93., J. Climate, 10, 1004–1020, doi: 10.1175/1520-0442(1997)0101004:ELIV 2.0.CO;2, 1997.

Supplementary Material

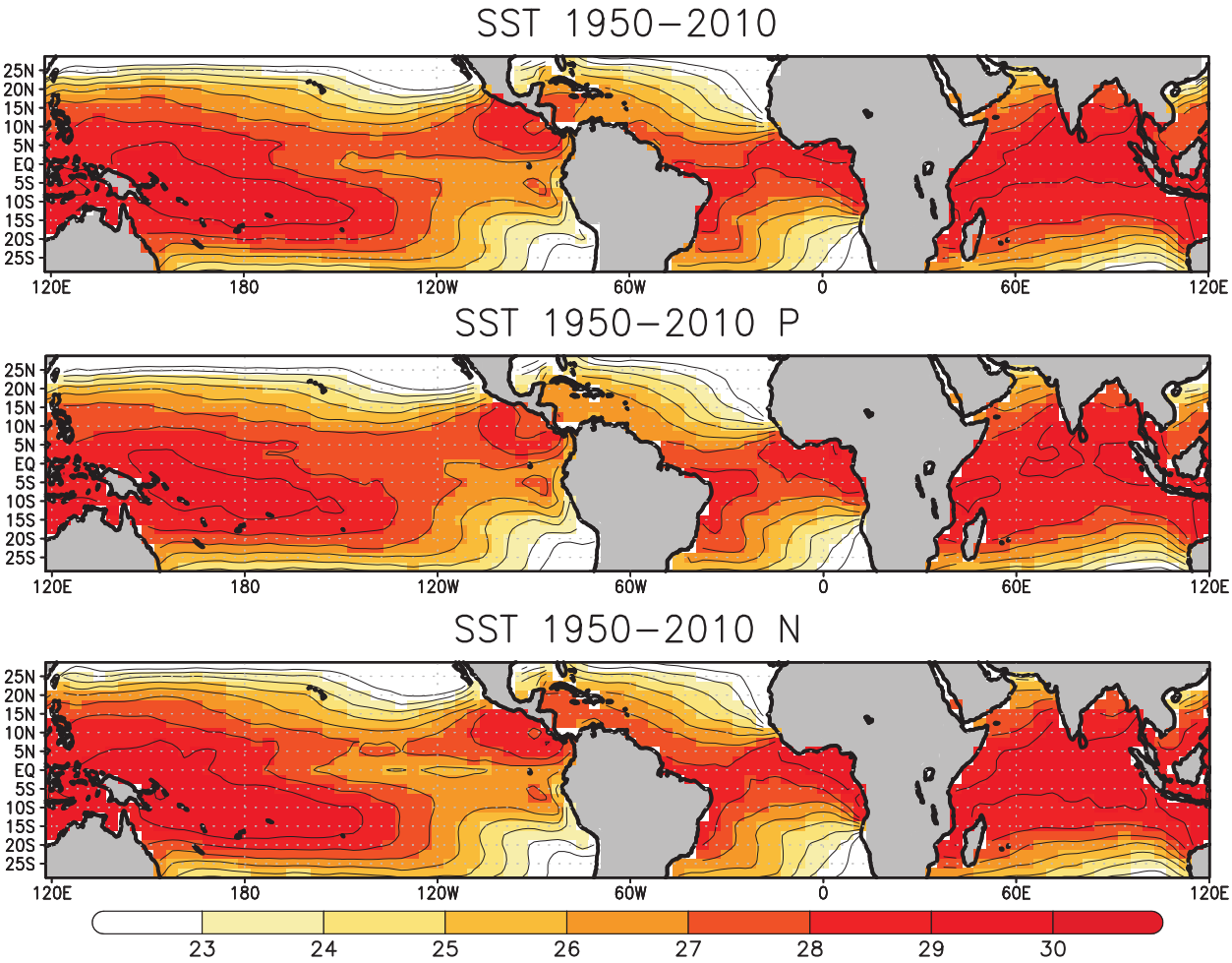

Figure A1: SST Climatology in February-March-April (seasonal mean) for a) (1950-2010), b) (1950-2010) plus the doubled anomalous pattern from Figure 1a (P mean state), and c) (1950-2010) minus doubled anomalous pattern from Figure 1a (N mean state).

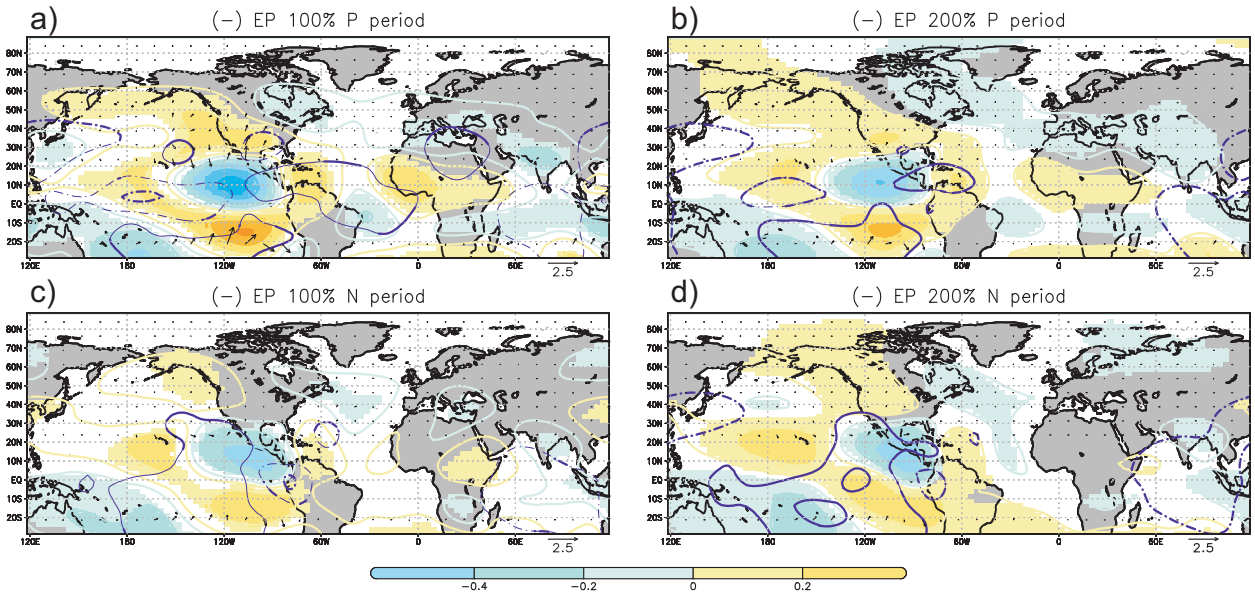

Figure A2: EP La Niñas. Same as Figure 2 but for EP La Niñas.

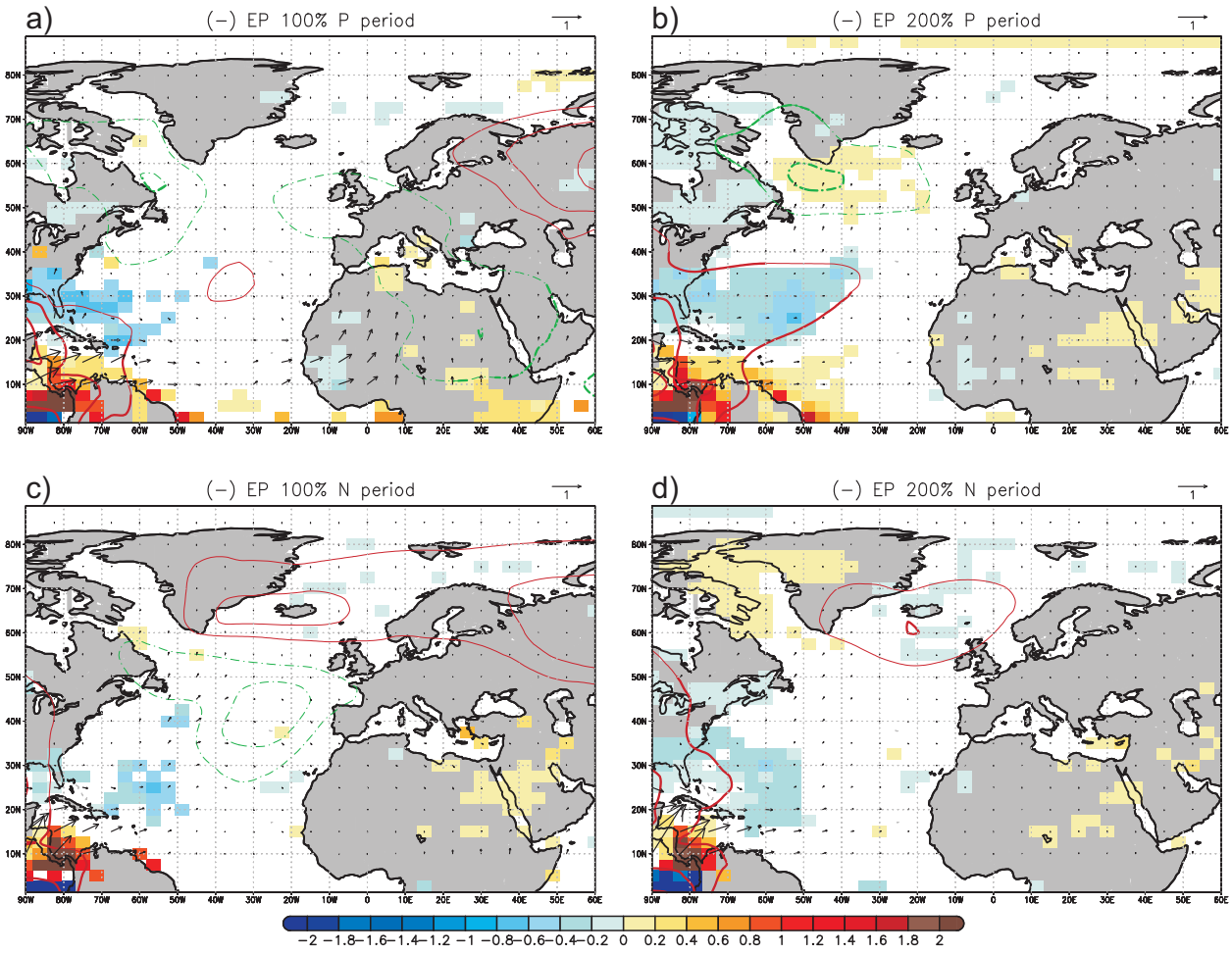

Figure A3: EP La Niñas. Same as Figure 3 but for EP La Niñas.

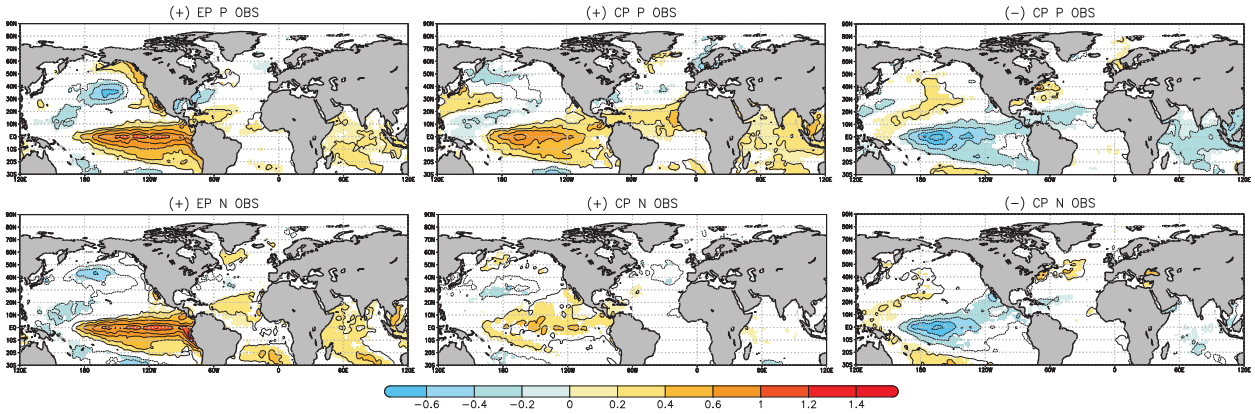

Figure A4: Non-stationary forcings. EP and CP SST patterns for P (1910-1940 and 1965-1990; top) and N (1941-1955 and 1995-2009; bottom) observational periods. They are based on HadISST data and constructed by calculating the composite maps of those years in which the Niño3 (EP) and Niño4 (CP) indices exceeds 0.5 (-0.5 for La Niña events) standard deviations. Only the 95% significant anomalies are shaded.

7

Integrated Discussion

Contradiction is the power for scientific progress.
If a scientist see "A" and he/she thought "Not A",
he/she changes the way of looking or the way of thinking.
The incoherence can not be maintained.

La contradicción es el motor del avance científico.
Si un científico ve "A" y creía "No A", o cambia la
manera de mirar, o cambia la manera de pensar.
No puede mantener la incoherencia

Jorge Wagensberg Lubinski,
IV seminario de Creatividad e Inclusión social

The main purpose of this thesis is to shed light on the non-stationary behavior of ENSO teleconnection with European and Mediterranean rainfall (denoted along the thesis as EMedR). To this aim, a compilation of papers in which different aspects associated with the aforementioned main objective are analysed, is presented. In this chapter, a reflection and a general discussion is exposed in order to integrate the distinct results that emerge from this thesis and, also, to discuss some open questions that arise from it.

As it is shown in the State of the Art (Section 2.4), ENSO teleconnection with the NAE sector is a matter which arouses diverging views. Hence, while some authors point to a robust impact, others are really sceptic on it (see Brönnimann (2007) and paper therein). In this thesis this controversy addressed. To this aim, a strong effort is done in order to better understand the underlying dynamics of the teleconnection, to clarify its stationarity, and to open a window of opportunity for the enhancement of current seasonal prediction system of European and Mediterranean climate variability.

First of all, different EOF analyses are applied in order to examine how the variability of the European and the Mediterranean rainfall is organised from 1900 onwards (López-Parages

and Rodríguez-Fonseca, 2012). The resultant leading EOFs, in October-November-December (OND) and February-March-April (FMA), present significant scores in central Europe, including the British Islands, opposite in sign to those over the Mediterranean region and the northwestern Africa. Sliding correlations between the associated principal component and El Niño3.4 index are then made with a 21-yr window. We find a non-stationary link in both, OND and FMA (López-Parages and Rodríguez-Fonseca, 2012). In fall and early winter (OND) the changing teleconnection appears in phase with the Pacific Decadal Oscillation (or the Interdecadal Pacific Oscillation), displaying significant correlations for extreme PDO phases (positives and negatives). In late winter and early spring (FMA), however, a non-stationary link evolving in phase with the Atlantic Multidecadal Oscillation (AMO) is detected, which is consistent with the variable signature of ENSO over the NAE sector identified in previous studies (Mariotti et al., 2002; Sutton and Hodson, 2003; Knippertz et al., 2003). This season (late winter-early spring) is considered as the most appropriated for finding a robust signal of ENSO over Europe (Brönnimann, 2007) and hence, this thesis is focused on it. Thus, under negative AMO phases, an increase of rainfall over central Europe and a decrease of rainfall over northern Scandinavia and the Mediterranean region in relation to anomalous positive SSTs over the tropical Pacific, is detected. These periods are denoted along this thesis as *P periods*. Under positive AMO phases the aforementioned link is almost the opposite, but noticeably weaker and not statistically significant. These periods are denoted as *N periods*. Related to this, Rodó et al. (1997) published an observational study based on the level of Lake Gallocanta, which is located in the north-east Spain, and on rainfall measurements from nearby stations. From this work, an unstable relationship with ENSO is also inferred: an opposite behaviour is found in the 1940's and 1950's, with negative correlations between rainfall (and lake level) and SOI index, in comparison to the preceding and following decades, for which positive correlations are found. This changing link is coherent with the aforementioned P and N periods identified in this thesis, and reinforces therefore the idea of a non-stationary impact of ENSO on the leading EMedR mode.

These results detected for the 20th century buttress the hypothesis of a changing El Niño - EMedR teleconnection, and suggest a modulating role of the natural variability (internal of the ocean-atmosphere coupled system). In order to address this issue an unforced long-term preindustrial control simulation (piControl) from the CNRM-CM5 model (López-Parages et al., 2014), is thoroughly explored. The results obtained point to a key role of the multidecadal variability of the zonal flow at upper troposphere forced by the ocean in the modulation of El Niño impact on European and Mediterranean rainfall. This finding is consistent with most of the theoretical studies that demonstrate the importance of jet streams for tropical-extratropical teleconnections (Hoskins and Karoly, 1981; Hoskins and Ambrizzi, 1993; Ambrizzi et al., 1995; Branstator, 2002). As it is theoretically argued in subsection 4, this fact is explained by the influence that zonal mean flow at upper troposphere exerts on Rossby wavetrains. Hence, it is known that the meridional

propagation of Rossby waves from tropical to extratropical latitudes is favoured in those regions where the jet streams get weaker. In those cases the waves can reach high latitudes describing an arching pattern. However, at those regions where jet streams are intense Rossby waves tend to be zonally propagated. Related to this, any scientific study aiming at a better understanding of a non-stationary tropical-extratropical teleconnection must necessarily analyse the related changes in the background of jet streams.

The aforementioned study carried out with the CNRM-CM5 model is subsequently extended for other 17 CMIP5 models (López-Parages et al., 2015a). We detect a very similar changing impact of ENSO on the leading EMedR mode to the one identified in observations. Therefore, this reinforces the hypothesis of a non-stationary teleconnection modulated by internal variability modes (such as AMO or IPO) of the coupled system. According to our results, the non-stationary teleconnection identified in piControl CMIP5 models responds to statistically significant variations in the intensity and spatial configuration of the jet streams, which in turn seem to be forced by the underlying SST meridional gradient. As it is shown in this thesis (López-Parages et al., 2015a), these variations can alter the efficiency of the mean flow to propagate Rossby waves. As a consequence, only for certain decades (the so-called P periods in CMIP5 models) the rotational response associated with ENSO impacts over the NAE sector. This feature is highly coherent with the observational results. Thus, the changing link between ENSO and the leading EMedR mode can be ultimately explained by multidecadal variability of the SST associated with the ocean-atmosphere coupled system.

From the aforementioned results a hypothesis is posed: *a common SST ENSO forcing produces distinct responses over the NAE sector depending on the ocean background state*. To test this hypothesis a set of experiments in which diverse SST ENSO forcings are prescribed under different SST mean states, are performed with the ACCESS model. This is done by prescribing the SST ENSO signature with distinct amplitudes, phases, and spatial patterns, taking therefore into account the documented non-linearity of ENSO teleconnections (Frauen et al., 2014). In this way, the different impact on EMedR of weak and strong Niñas and Niños, with distinct spatial patterns (Eastern or Central events), and under opposite SST mean states (P and N), can be explored. The canonical ENSO signature identified in previous studies is characterized by a negative NAO-like pattern in relation to El Niño episodes and a positive NAO-like pattern in relation to La Niña episodes (Fraedrich and Müller, 1992; Gouirand and Moron, 2003; Moron and Gouirand, 2003; Moron and Plaut, 2003; Brönnimann et al., 2007). However, this canonical response is not unequivocally accepted and non-symmetric signatures are also found, in agreement with Toniazzo and Scaife (2006). Furthermore, to our knowledge, there is no study in which sensitivity experiments are designed in order to explore both, the stationarity and the linearity, of the ENSO-

EMedR teleconnection. Thus, the results obtained here shed light on this issue. The SST mean state pattern prescribed in our experiments is constructed as the difference in monthly mean SST between periods with distinct impact of ENSO on the leading EMedR mode in late winter and early spring along the 20th century (the so-called P and N periods). As it is repeatedly mentioned, these *modified climatologies* approximately correspond to extreme AMO phases. Nevertheless, in our experiments it is not assumed *a priori* that the modulating factor is constrained over the Atlantic basin and hence, in agreement with previous studies, the SST mean state signature over the tropical Pacific is also prescribed (Dong et al., 2006; Kucharski et al., 2015). Results obtained from these experiments demonstrate how the remote impact of both, warm and cold ENSO events, on the NAE climate could be noticeably different depending on the low frequency variability of the SST. In particular, SST mean state can modulate two distinct mechanisms associated with ENSO events: (1) the thermally driven direct circulation (Waker and Hadley cells) connecting the Atlantic and Pacific basins, and (2) the Rossby wave propagation from the tropical Pacific to the North Atlantic. The former explains a distinct impact of Central Niñas on the Azores high pressure depending on the SST mean state. Related to this, a positive or a negative NAO-like pattern can be identified in relation to the same La Niña episode depending on whether it takes place under a P-like or a N-like SST mean state configuration. The latter mechanism explains a reinforced impact of Eastern Niños on European and Mediterranean rainfall under P conditions. This feature is consistent with the changing ENSO signal identified in observations and CMIP5 models, and demonstrates how it can be modulated by the SST mean state. A schematic synapse of these results can be found at the end of the present discussion (Figure 7).

Nevertheless, from the findings obtained along this thesis new and interesting open questions, which require further discussion, emerge. Some of them are explored within the following subsections.

Models reliability

An apparent contradiction of our results may be noted: the modulating factor found in CMIP5 models seems not to be consistent with the one identified in observations. In the latter, the moving window correlation timeseries associated with the non-stationary link in FMA projects on a pattern resembling an AMO-like structure over the Atlantic basin; whilst in CMIP5 models the analogous timeseries projects on a spatial pattern closer with the well-known PDO/IPO configuration. As it is expected, these distinct SST patterns are related to different multidecadal changes in the atmospheric mean state. In particular, the multidecadal changes identified for extratropical jet streams in observations and CMIP5 models are noticeably different. Paradoxically, the changing impact

of ENSO on the leading EMedR mode is, in both cases, quite similar. Why the non-stationary teleconnection identified in observations and CMIP5 models is consistent if their corresponding modulating factors are not?

To address this question it is necessary to take into account the *model bias*, which refers to the systematic (and stationary) error of climate models. It is quantified as the difference between the ensemble simulation of a variable from a specific model with respect to the corresponding one in the observational data, which in principle, is assumed closer to the real value. In Figure 7.1a the climatological U200 in FMA (observations) is plotted together with the bias of those CMIP5 models analysed along this thesis (U200 for CMIP5 models minus U200 for observations). We identify an overestimation of U200 in CMIP5 models (on average) over the subtropics (latitudes below 30º approximately) and a subestimation in mid and high latitudes (latitudes greater than 30º approximately). A shift of jet streams towards the equator is, therefore, found in our pi-Control CMIP5 simulations. It is worth also mentioning that the bias in the subtropics is maximum over the Pacific basins between 180º and 120ºW longitudes, which broadly coincides with the region of weak climatological U200 located between the exit of the EA-jet and the entrance of the NA-jet. Hence, due to this bias one would think that ENSO impact on extratropical latitudes associated with Rossby waves should be hindered in CMIP5 models with respect to the observations. Indeed, in observations the percentage of positive and statistically significant moving window correlations between the PC associated with the leading EMedR mode and El Niño34 index (the so-called P periods in which the teleconnection is stronger) with respect to the total number of windows is 30.0% (averaged for different observational datasets; see Figure 2 from López-Parages and Rodríguez-Fonseca (2012)); whilst in CMIP5 models the equivalent percentage is reduced to 18.0%.

It is also interesting how the CMIP5-models bias differ from P to N periods, being globally reduced in P (Figure 7.1b) and globally increased in N (Figure 7.1c). Note for example how the aforementioned bias located between the EA-jet and the NA-jet appears weakened under P conditions. Thus, for those periods in which the extratropical ENSO response is strong and similar in CMIP5 and observations (the so-called P periods), the jet streams are better represented (reduced bias). The striking point is that these approximately similar jet streams in CMIP5 and observations occurs in P under distinct SST patterns (resembling a negative IPO-like pattern in the former case and negative AMO-like pattern in the latter case). This feature could be explained by the amplitude of bias, which clearly excess the differences identified under P and N ocean mean states. The extratropical jet streams, which are crucial to suitably reproduce the non-stationary impact of ENSO on extratropical latitudes, are not well reproduced in the model (strong bias) and hence, the changing downstream impact of anomalous Rossby waves forced by ENSO on the NAE sector can be mo-dulated by a distinct ocean multidecadal variability mode than in the real climate. In other

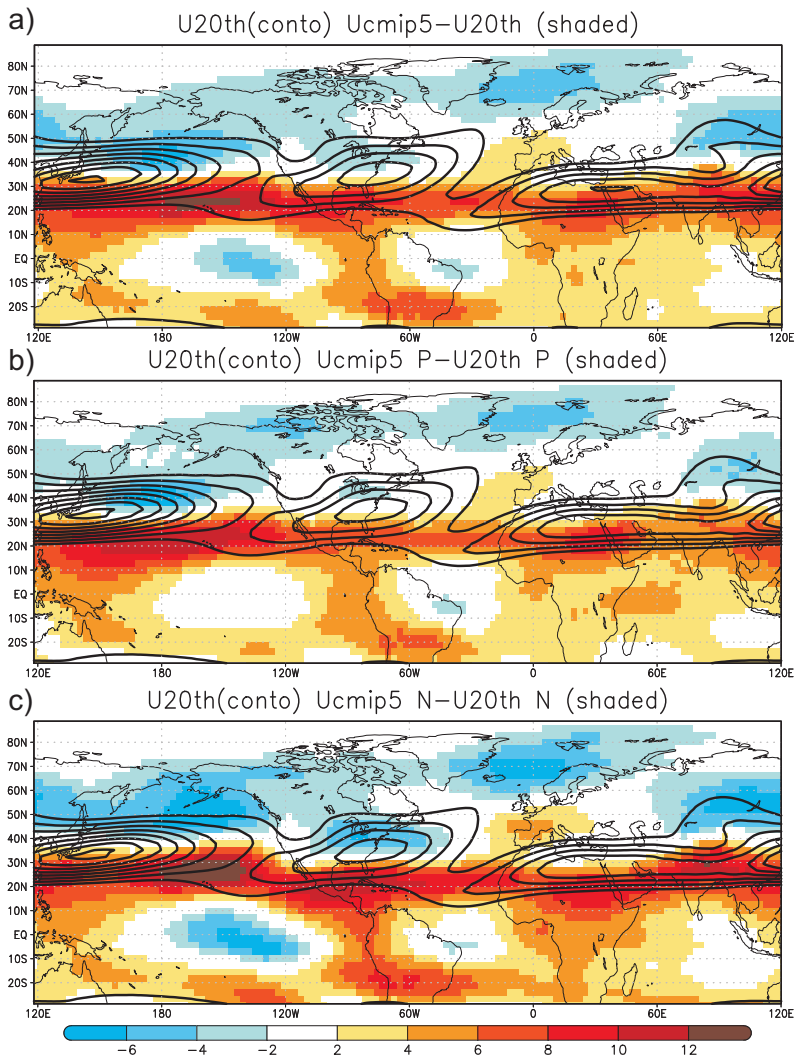

Figure 7.1: Bias of CMIP5 models (shaded) in FMA for: a) entire mean state (prescribing the SSTs for 1950-2010 time period), b) P mean state (prescribing a negative AMO-like SST pattern), and c) N mean state (prescribing a positive AMO-like SST pattern). Units in m/s. The climatological values of U200 are contoured (averaged from 20CR dataset for the 1900-2010 time period). The minimum value represented is 20 m/s (ci=5 m/s).

words, the modulating factor in the model (resembling an IPO pattern over the Pacific) is the one which alters the modeled jet stream in the convenient way to favour the impact of the simulated ENSO on extratropical latitudes. However, this way can be very different from the one needed by the real jet streams. As a consequence, the resultant modulating agent (resembling an AMO pattern over the Atlantic) is different as well.

Another remarkable feature associated with our sensitivity experiments is that the extratropical Rossby wavetrain linked to the Eastern Niños is roughly obtained (but with different amplitudes) under both, P and N SST mean states (Figure 2 in López-Parages et al. (2015b)). This

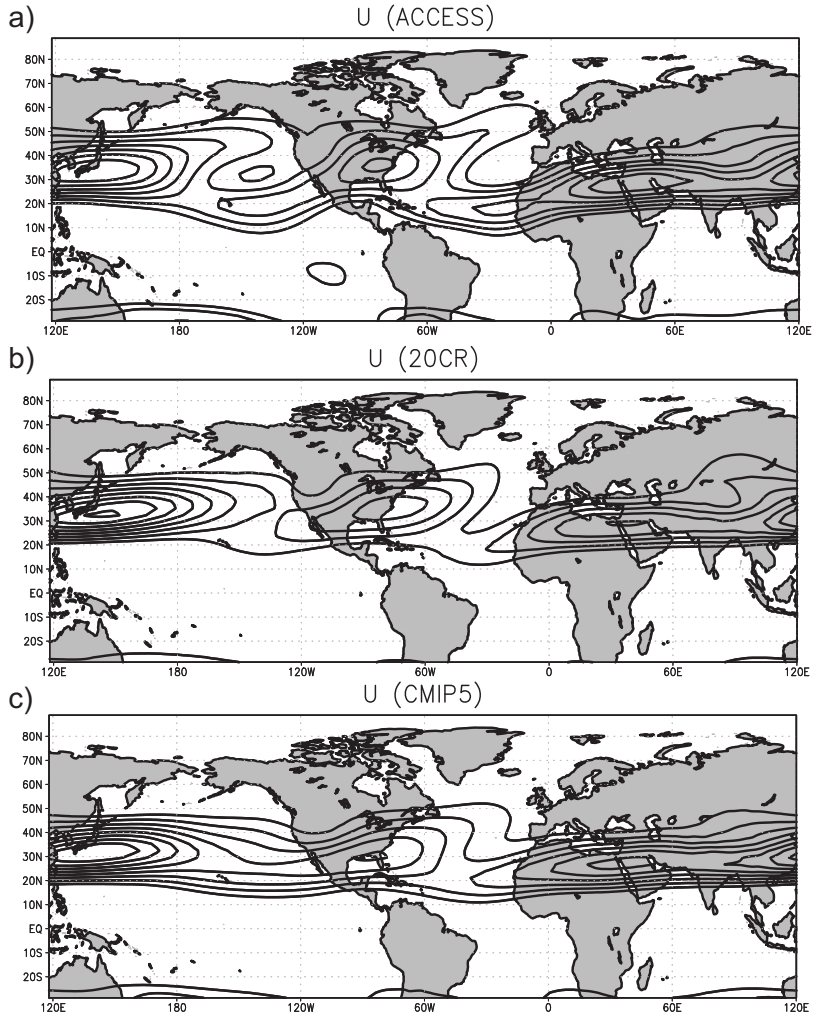

Figure 7.2: Climatological values of U200 in FMA for: a) ACCESS model (prescribing the SSTs for 1950-2010 time period), b) 20CR (averaged for the 1900-2010 time period), and c) CMIP5 models. The minimum value represented is 20 m/s (ci=5 m/s).

fact, different from observations and CMIP5 models for which very distinct responses in relation to ENSO are found in P and N periods, can be also explained by the bias of the extratropical jet streams in ACCESS model. Contrary to the excessively zonal jets in CMIP5 models (Figure 7.2c), in ACCESS model the jets seem to be excessively meridional, with a clear discontinuity over the subtropical Pacific and a marked entrainment of the NA-jet on the NAE sector (Figure 7.2a). These characteristics could favour the propagation of the ENSO-related disturbances from the tropical Pacific to the extratropics and, as a consequence, Eastern Niños related signature is found at mid latitudes in both, P and N periods. The role of the changing mean state in ACCESS model is, therefore, to vary this jet streams configuration in order to either favour or disfavour the downstream impact over the NAE sector. In this way, only a statistically significant impact of Eastern Niños on the EMedR (highly consistent with observations) is found under P conditions. These

results underscore, therefore, the importance of a realistic representation of jet streams in current coupled models (weak bias) in order to properly reproduce the non-stationary features of tropical-extratropical teleconnections, specially those involving very distant regions such as the tropical Pacific and the NAE sector.

Non-linear processes

A question regarding the AGCM sensitivity experiments carried out in this thesis is still unresolved. In these experiments an El Niño or La Niña forcing (with a particular phase, amplitude, and pattern) is superimposed over two different SST mean states (P and N). The difference between the responses in P and N is not only the distinct SST background state itself (linear response), but also the different processes triggered by the same forcing on both mean states (non-linear response). How to isolate these two different contributions?

Assuming the climate as a non-linear system, the response R of a forcing F (El Niño/La Niña) applied under different climatologies P and N (defined in our experiments over the Atlantic and Pacific basins; see Figure 1a in López-Parages et al. (2015b)) can be expressed as:

$$R(F+P) = R(P) + R(F) + NL(P,F) \tag{7.1}$$

$$R(F+N) = R(N) + R(F) + NL(N,F) \tag{7.2}$$

where, on the one hand, $R(P)$, $R(N)$ and $R(F)$ represent the linear responses associated with the prescribed SST climatology P, the prescribed SST climatology N, and the anomalous forcing F, respectively. On the other hand, the terms $NL(P,F)$ and $NL(N,F)$ represent the non-linear responses of F under P and N. Hence, the anomalous response of F with respect to each climatology (P and N) is given by:

$$R(F+P) - R(P) = R(F) + NL(F,P) \tag{7.3}$$

$$R(F+N) - R(N) = R(F) + NL(F,N) \tag{7.4}$$

By subtraction of Equation 7.1 and Equation 7.2, the whole change in the response of F in P and N is:

$$R(F+P) - R(F+N) = \Big(R(P) - R(N)\Big) + \Big(NL(F,P) - NL(F,N)\Big) \tag{7.5}$$

which can be regrouped, for simplicity, as:

$$R(F+P) - R(F+N) = \Big(L(P,N)\Big) + \Big(NL(F,P,N)\Big) \tag{7.6}$$

where $L(P, N)$ and $NL(F, P, N)$ group together the *linear* and *non-linear* terms of expression 7.5, respectively. Thus, the total change (or non-stationary behavior) of F when it is superimposed on different background states (P or N) can be organised in a linear term, which represents the different responses to distinct climatologies, and in a non-linear term, which represents the processes triggered by the forcing F in P but not in N, and viceversa.

We represent these different terms in Equation 7.6 for distinct forcings F (EP Niño, CP Niño, and CP Niña) in Figure 7.3. The common L term is shown in Figure 7.3a. According to it, an enhanced upper level divergence over the tropical Pacific together with an enhanced convergence over Central America and the tropical Atlantic, take place in P due to the diabatic heating in the equatorial Pacific (Figure 2a in López-Parages et al. (2015b)). As a consequence, the rotational flow changes as well (shaded in Figure 7.3), which reflects the variation in the climatological jet streams (Figure 7.4a). In a linear context, for each pattern (EP and CP) and phase (El Niño and La Niña) of the forcing F, the difference in the response in P and N periods (e.g. EP in P minus EP in N; see Equations 7.5 and 7.6) should be dominated by the difference in the climatologies, or L term (Figure 7.3a). However, our experiments reflect how this linear approach is not valid, as the NL terms are comparable with L (Figure 7.3b, Figure 7.3d, and Figure 7.3f). Therefore, these NL terms are analysed in detail in the following paragraphs.

For Eastern (Figure 7.3b) and Central (Figure 7.3d) Niños, the NL response reveals a wavetrain generated from the western Pacific extending across the Pacific North American region. This wavetrain is guided by the jets, whose spatial configuration favours their wave-guiding effect towards extratropical latitudes (note the red shaded values over the North Pacific in Figure 7.4b), according to the values of the stationary Rossby wavenumber Ks (Hoskins and Ambrizzi, 1993). This wavetrain is produced by the strong equatorial diabatic heating that perturbs the upper troposphere when El Niño event occurs under a warm Pacific SST background state (see contours in Figure 7.3b and Figure 7.3d). Indeed, the rotational patterns associated with L (shaded in Figure 7.3a) and NL (shaded in Figure 7.3b and Figure 7.3d) are similar over the North Pacific American sector, both resembling a negative TNH pattern, since the heating imposed by the interannual EP (or CP) Niños and by the P-N mean state difference over the tropical Pacific are similar among them (see Figure 1 from López-Parages et al. (2015b)). In particular, for EP events, a second north-eastward wavetrain from the eastern Pacific to the North Atlantic is enhanced in P (note the arrows associated with the WAF in Figure 7.3b), being also favoured by the reinforced waveguide associated with the NA-jet (Figure 7.4b). This Rossby wavetrain excited from the eastern equatorial Pacific and crossing the North Atlantic has been already documented in the past (e.g. Shaman (2014)). Its non-stationary impact downward over Europe (Figure 7.3c) associated with a NL interaction between the ENSO forcing and the changing climatology (Figure 7.3b) represents,

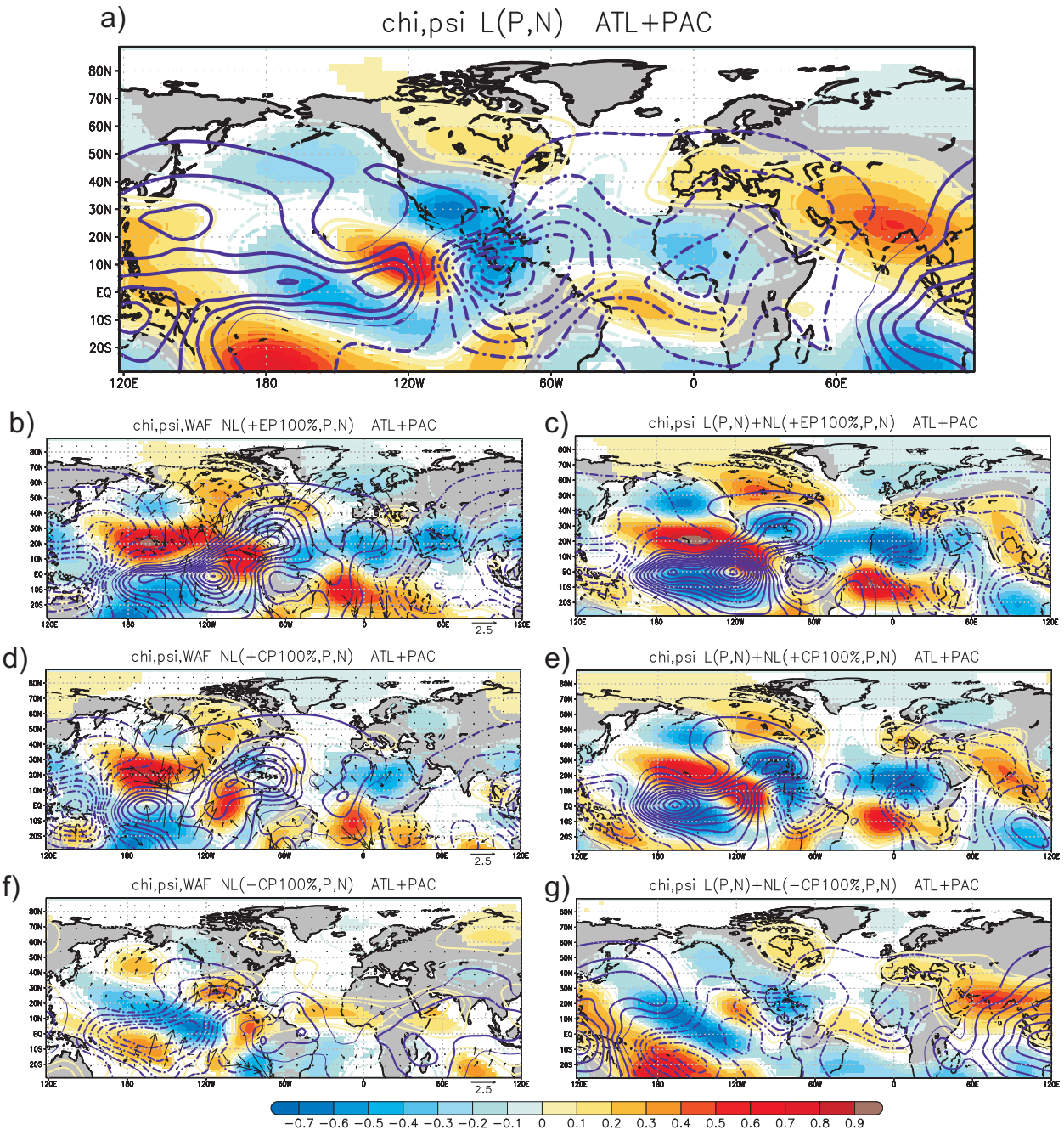

Figure 7.3: Addends described in Equation 7.6 for streamfunction (shaded) and velocity potential (contoured) at 200hPa. On top the L term. At the bottom the NL term (b, d, and f) and the sum (L + NL terms; c, e, g) for EP Niños, CP Niños, and CP Niñas, respectively. The wave activity flux (WAF; in arrows) is also plotted for the NL term. Units in $10^7 m^2/s$ (streamfunction and velocity potential) and m^2/s^2 (WAF). Shaded areas represent 90% significant responses (Wilcoxon-Mann-Whitney test). For velocity potential the whole signal is plotted, but only the 90% significant response is bolded (Wilcoxon-Mann-Whitney test). The minimum values represented for velocity potential is $0.05 \cdot 10^7$ (ci= $0.05 \cdot 10^7$). Only the WAF values larger than $1 m^2/s^2$ are shown, being removed the values over equatorial latitudes (lower than 10^o).

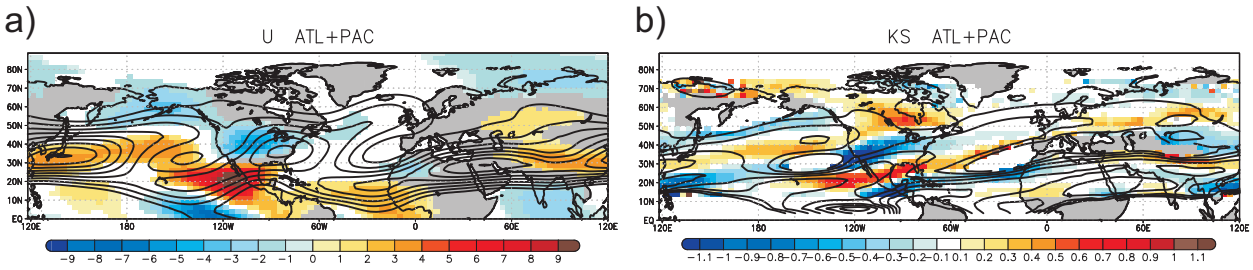

Figure 7.4: Changes in U200 (a) and Ks (b) background states. Contoured the climatological values (prescribing the SSTs for 1950-2010 time period). Shaded the 90% significant differences (according to a Wilcoxon-Mann-Whitney test) in P and N background states. The minimum value represented is 15 m/s (ci=10 m/s) and 3 (ci=1) for U200 and Ks, respectively.

however, a step forward in the understanding of the role of the ocean mean state as modulator of the ENSO teleconnection with the European climate.

Regarding La Niña events, an anomalous wavetrain is also found at upper troposphere in the NL term associated with Central Niñas (Figure 7.3f). The related wave activity is, however, restricted to the North Pacific, being its downstream impact over the NAE sector weaker than for El Niño events. At tropical latitudes, a significant convergence over the Pacific appears in relation to a significant divergence over South America (Figure 7.3f). This feature reflects a change in the Pacific-Atlantic connection through the zonal walker circulation, which in turns could influence the Meridional Hadley cell over the subtropical North Atlantic (Ruiz-Barradas et al., 2003; Wang and Picaut, 2004) and so, the Azores high pressures system (see Figures 6a, 6c, 7a, and 7c in López-Parages et al. (2015b)). Hence, the contribution of this NL term in P could explain the distinct surface signature obtained over the North Atlantic under P (Figure 7a in López-Parages et al. (2015b)) and N (Figure 7c in López-Parages et al. (2015b)) climatologies. The non-stationary response of Eastern Niñas is weaker.

Summarizing, it has been demonstrated that the NL terms from Equation 7.6 can explain the changing downstream impact of ENSO over the NAE sector for both, El Niño and La Niña episodes. La Niña response (mainly for Central events) is associated with variations in the Walker and Hadley circulations, and El Niño response (mainly for Eastern events) with variations in the ENSO-related Rossby wavetrain propagation. This dependence of the NAE sector response on the ENSO SST structure is consistent with previous works (Toniazzo and Scaife, 2006; Shaman, 2014). Regarding the changing rotational response associated with Eastern Pacific Niños, and considering that P and N experiments are designed here by prescribing the SST mean states over the Atlantic and Pacific basins, a couple of questions emerge: what is the response of the climatological jet

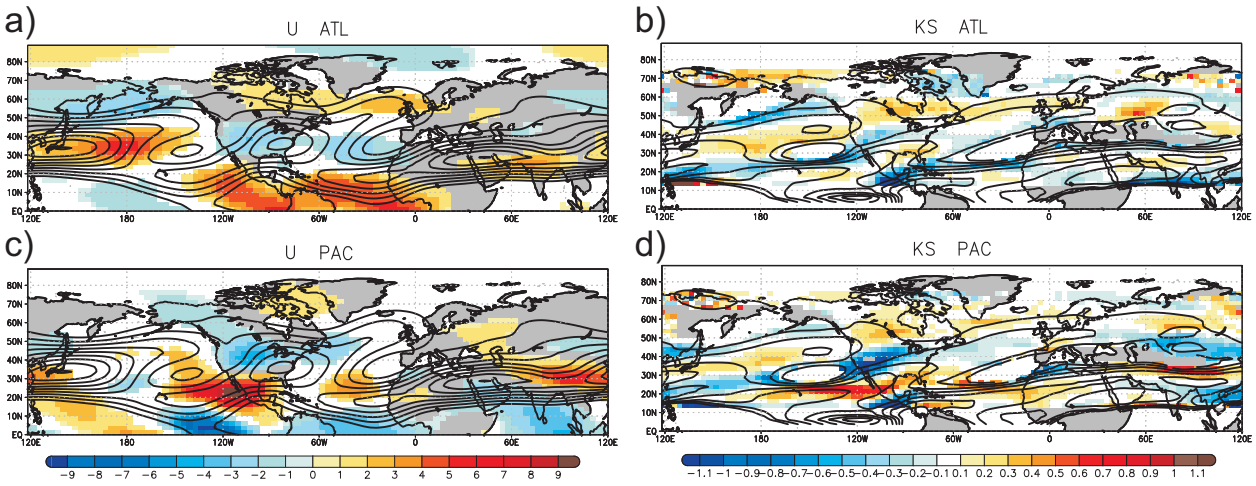

Figure 7.5: Same as Figure 7.4 but for ATL (prescribing Patl or Natl mean states; on top) and PAC (prescribing Ppac or Npac mean states; at the bottom) experiments.

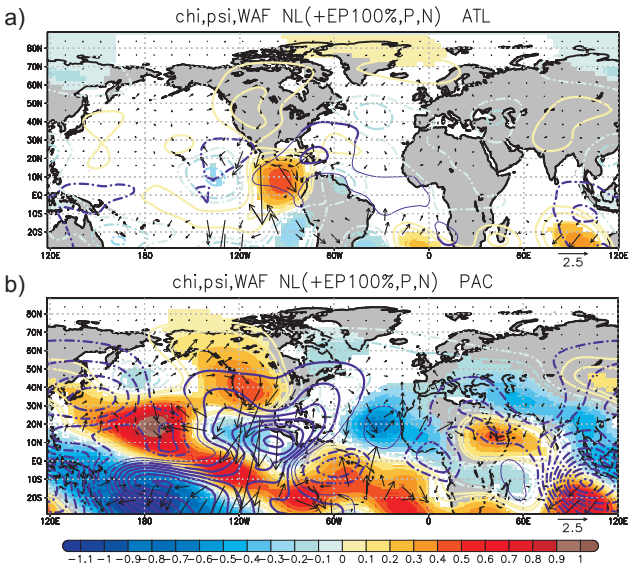

Figure 7.6: NL term for Eastern Niños. Same as Figure 7.3b but for a) ATL (prescribing Patl or Natl mean states) and b) PAC (prescribing Ppac or Npac mean states) experiments.

streams if the SST mean states are just prescribed over the Atlantic or the Pacific basin? and, which is the response associated with Eastern Niños in these cases? To answer these questions the changes in U200 mean state (and Ks mean state; Figure 7.5) and the interannual response associated with Eastern Niños (Figure 7.6) are plotted for those experiments in which the SST background state is prescribed over the Atlantic or the Pacific only. These experiments are denoted as ATL (prescribing Patl or Natl mean states) and PAC (prescribing Ppac or Npac mean states) experiments.

The previously commented P minus N difference (in U200 and Ks; see Figure 7.4), is broadly reproduced for Patl minus Natl (Figure 7.5a,b) and Ppac minus Npac (Figure 7.5c,d), but with some interesting variations. On the one hand, a weaker alteration of Ks over the North Pacific is found for both, ATL and PAC experiments. On the other hand the changes associated with the NA-jet appears slightly weakened in PAC, but not as dramatically as they appear in ATL. The NL response of Eastern Niños is well-established in the former case (Figure 7.6b) but not in the latter case (Figure 7.6a). This fact is explained by the unaltered SST mean state over the tropical Pacific in ATL experiments, which produces very weak differences in convection when the same Eastern Niño is prescribed under Patl and Natl mean states. For PAC experiments, however, a clear stronger convergence is found over the tropical Pacific in Ppac with respect to Npac. This behaviour responds to the warmer tropical Pacific in Ppac than in Npac (see Figure 1a in López-Parages et al. (2015b)), which favours the occurrence of the required temperatures for deep convection development in the former case. As a consequence, a clockwise rotational circulation reinforcing a TNH pattern is found in Ppac over the Pacific North American sector (Figure 7.6b). However, the signature over the North Atlantic is almost the same under Ppac and Npac background states. By carefully comparing Figure 7.3b and Figure 7.6b it is possible to note that the downstream impact over the North Atlantic, specifically the negative centre over Northern Europe, is clearly stronger in the former case. This feature demonstrates how a combined influence of Atlantic and Pacific SSTs is needed to efficiently alter the jet streams in order to reproduce the non-stationary impact of Eastern Niños over the NAE sector.

Implications for seasonal predictability

As it is described in Chapter 4, atmospheric teleconnections associated with SST processes are of special importance due to the ocean's thermal inertia, which provides an important tool for seasonal predictability. Our predictive skill is, however, scarce for some regions along the globe. At extratropical latitudes the potential predictability is lower than in the tropics, but some studies have recently found a certain ability for some regions (e.g., in North America) in relation to ENSO (Quan et al., 2006). Nevertheless, the skill is still poor for Europe (Van Oldenborgh, 2005). One of the factors which could influence this low ability of current seasonal forecast system over Europe is the assumption of stationary predictor-predictand teleconnections. In particular, as it is widely analysed along this thesis, the link between ENSO and the leading EMedR mode is modulated by the ocean multidecadal variability. Hence, the seasonal predictive skill of rainfall based on ENSO-related SSTs might be variable and much greater than expected, at least, for specific time periods. Although the study of predictability is out of the scope of the present thesis, it has been briefly explored the potential improvement in seasonal forecasting of European and Mediterranean rainfall

that a non-stationary assumption of the teleconnection with ENSO represents. To this aim, the Sea Surface Temperature based Statistical Seasonal foreCAST model (S4CAST model;Suárez-Moreno and Rodríguez-Fonseca (2015)), is used. S4CAST is based on MCAs and has been developed in order to asses the predictability of climate-related variables based on the predictive nature of the SST, with special attention to possible non-stationary predictor-predictand relationships.

In particular, the S4CAST model is used to evaluate the predictive skill of tropical SSTs in fall-early winter (OND) on the EMedR in late winter-early spring (FMA) if an invariant (stationary) or a changing (non-stationary) teleconnection among them is considered. We detect significant correlations between the predictant (EMedR) and the predictor (SSTs between 30ºS and 30ºN) just for some periods (Figure 7.7), identifying an AMO-like evolution, as for the link in lag-0 between ENSO and the leading EMedR mode (see Figure 2 in López-Parages and Rodríguez-Fonseca (2012)). At this point, two distinct approaches can be considered: (1) to analyse the predictive skill for the entire available period, or (2) to restrict the study to those periods for which a significant correlation between the predictor and the predictant related expansion coefficients (from the MCAs) is found. Both procedures are explored here, being denoted as STAT and NSTAT, respectively. For each year of the selected period the model calculates a MCA without considering the year to predict, performing in this way a so-called one-year *leave out* cross-validated hindcast for both, STAT and NSTAT. The hindcast of the predictand field is obtained, for each year and gridpoint, by comparing the observed and simulated fields in time and space domain. For a more detailed description of S4CAST model please refer to Suárez-Moreno and Rodríguez-Fonseca (2015).

The leading mode explains 34.5% of co-variability for STAT, while the percentage increases to 43.0% for NSTAT. Comparing the corresponding heterogeneous regression map of rainfall it is possible to note how the anomalies are clearly higher in NSTAT (Figure 7.8). The most interesting point is, not only this stronger impact, but also the enhanced skill for seasonal predictability (four months in advance). Pearson correlation coefficients and Root Mean Squared Errors are used as skill-scores, finding for both of them stronger values over central Europe and the western Mediterranean in NSTAT with respect to STAT (Figure 7.9). The former means that, in this specific case and over the aforementioned regions, the NSTAT approach allows for a better prediction of the sign (more or less rainfall). The latter means that the uncertainties of the amplitudes predicted are larger in the NSTAT approach (the impact is overestimated or underestimated). This dependence on the time period considered invite us to question ourselves about the usual assumption in the available literature of a stationary teleconnection between ENSO and European and Mediterranean climate, which could in part explain the limited surface impact identified in previous works, even though the signature at upper troposphere was intense (García-Serrano et al., 2011). Therefore, our results

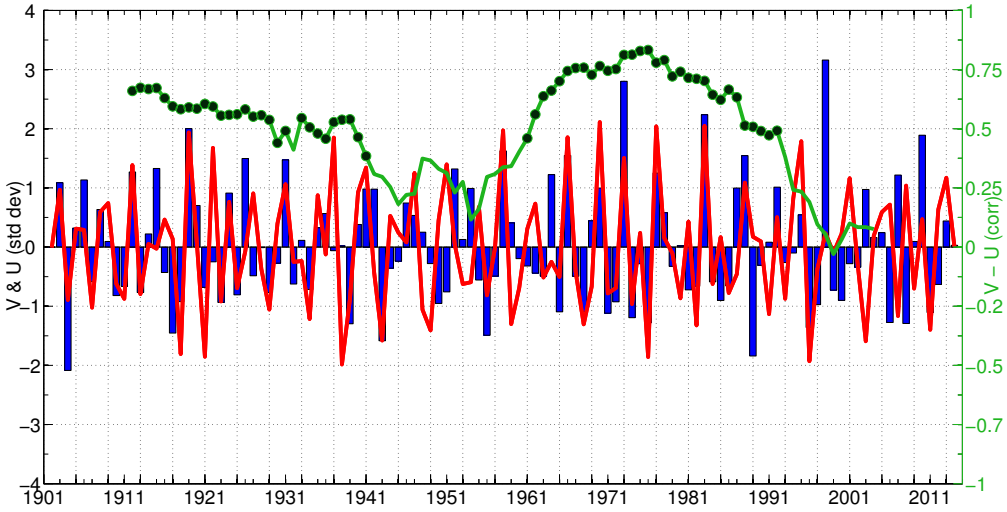

Figure 7.7: 21 years moving correlation windows (green line) between the expansion coefficients U corresponding to the predictor field (anomalous tropical SSTs in OND, blue bars) and V corresponding to the predictant field (anomalous EMedR in FMA, red line) obtained from the leading mode of co-variability from MCA analysis between both fields. Shaded circles represent 95% statistical significant correlation under a Monte-Carlo test.

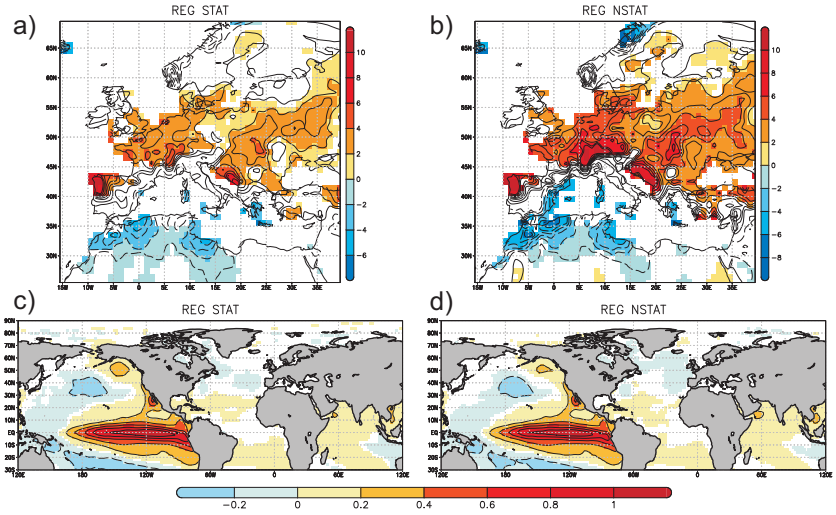

Figure 7.8: Regression maps for STAT (left) and NSTAT (right) approaches. On top the projection of U onto global SSTs (homogeneous map; $Kstd^{-1}$). At the bottom the projection of U onto the EMedR (heterogeneous map; $mmday^{-1}std^{-1}$). Statistical significant areas, according to a Monte-Carlo test at the 90% level, are shaded.

point to a potential improvement in the predictive skill of the leading EMedR rainfall mode by tropical SSTs if the non-stationary features are considered. This issue, however, must be further analysed in future works by the use of, not only statistical models but also dynamical ones.

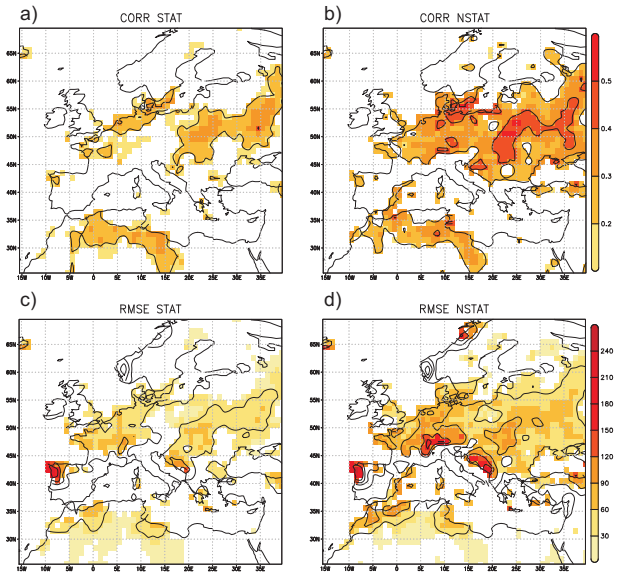

Figure 7.9: Skill-score validation in terms of Pearson correlation coefficients (top) and Root Mean Square Error (bottom) between observed (from Univ. of Delaware database) and simulated maps (hindcast). On the left STAT approach and on the right NSTAT approach. Statistical significant areas, according to a Monte-Carlo test at the 90% level, are shaded.

What about other seasons?

Up to now the research of this thesis has been focused on the teleconnection between ENSO and the leading EMedR mode in later winter and early spring, which as has been noted, corresponds with the season in which the ENSO signature on European continent has been found stronger in previous works (Brönnimann, 2007). It also seems interesting to explore, however, to what extend and in which way, the teleconnection evolve in time in others seasons of the year. This issue is briefly studied in López-Parages and Rodríguez-Fonseca (2012) (see Figure 2 of this paper) by the analysis of independent anomalous rainfall EOFs for different seasons. However, climate variability can be distributed in different ways in each of the aforementioned EOFs and hence, the resultant modes could represent very distinct dynamical mechanisms. In order to capture a common mode of variability among the different months, an extended-EOF (see Section 5.2.2.1) of the EMedR spanning the whole year (from January to December), is applied. The leading extended-EOF (Figure 7.10), which explains the 14.0% of the total variance, is characterized by positive anomalies in central Europe, and negative ones over the northern Scandinavia and the Mediterranean region. This spatial structure is highly similar to the leading EOFs analysed in FMA and OND (López-Parages et al. (2014)), but with slight differences in the amplitude over some areas.

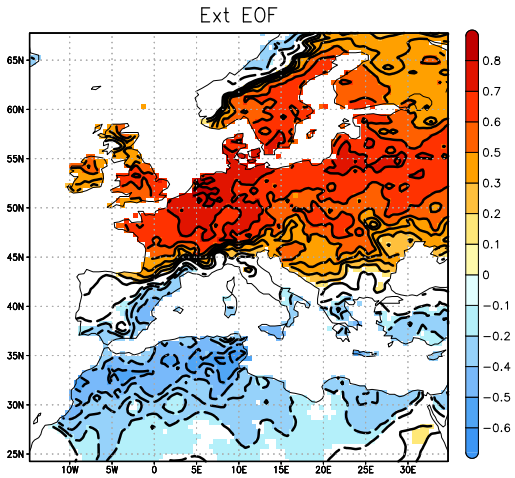

Figure 7.10: Leading Extended EOF (from January to December) of EMedR. Units are in standarized rainfall per standard deviation in the leading PC. Statistical significant areas, according to a Monte-Carlo test at the 95% level, are shaded.

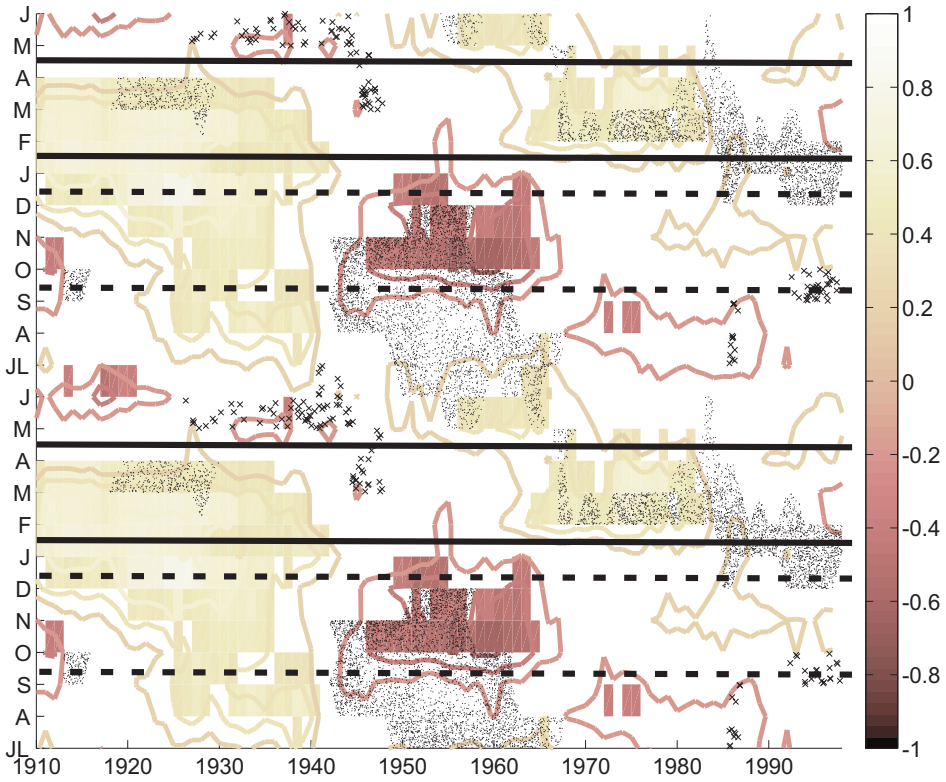

Figure 7.11: 21-years sliding window correlations between the leading PC from the Extended-EOF and El Niño3.4 index for each corresponding month. Only the 95% significant correlations according a Monte-Carlo test are shaded. 21-years sliding window standard deviation at 95% significant level are also plotted, being the positive values marked with dots and the negative values marked with crosses. Highlighted between the solid lines February-March-April. Highlighted between the dashed lines October-November-December. The pattern has been duplicated (2 years) for an easier interpretation.

For consistency with previous analysis of this thesis, the link with El Niño is obtained by computing 21 year sliding window correlations between the leading principal component from the extended EOF and El Niño3.4 index of the corresponding month (Figure 7.11) . According to this, the AMO-like evolution detected in FMA (highlighted between the solid lines in Figure 7.11) and the PDO-like evolution found in OND (highlighted between the dashed lines in Figure 7.11), seem to be part of a more global pattern in which the correlation (positive or negative) between the PC associated with the leading EMedR mode and El Niño3.4 index occurs, either few months earlier or few months later, depending on the decade considered. Furthermore, in accordance to the variance of the PC, a lack of stationarity in the related EMedR variability mode is detected. Hence, in some decades rainfall variability is enhanced (marked with dots in Figure 7.11) while in others it is weakened (marked with crosses in Figure 7.11). In particular, the periods with an enhanced rainfall variability in FMA broadly coincides with those in which the correlations are significant, reinforcing the hypothesis of a changing impact of ENSO.

As it is mentioned in the previous paragraph, significant changes are also found for other seasons, being specially clear in autumn during the central decades of the 20th century. Related to this, an interesting issue to be explored in the future would be whether the non-stationary behavior of the teleconnection between the EMedR and El Niño appears as a result of either (1) a time displacement of the season in which the link occurs beyond the seasonal interval we consider or (2) a *real* intermittent nature. In the former case, the consideration of late winter early spring as the most properly season for detecting a robust signal of ENSO over Europe and the Mediterranean region must be clearly questioned, at least, for certain decades.

Synapses of the research: one page thesis

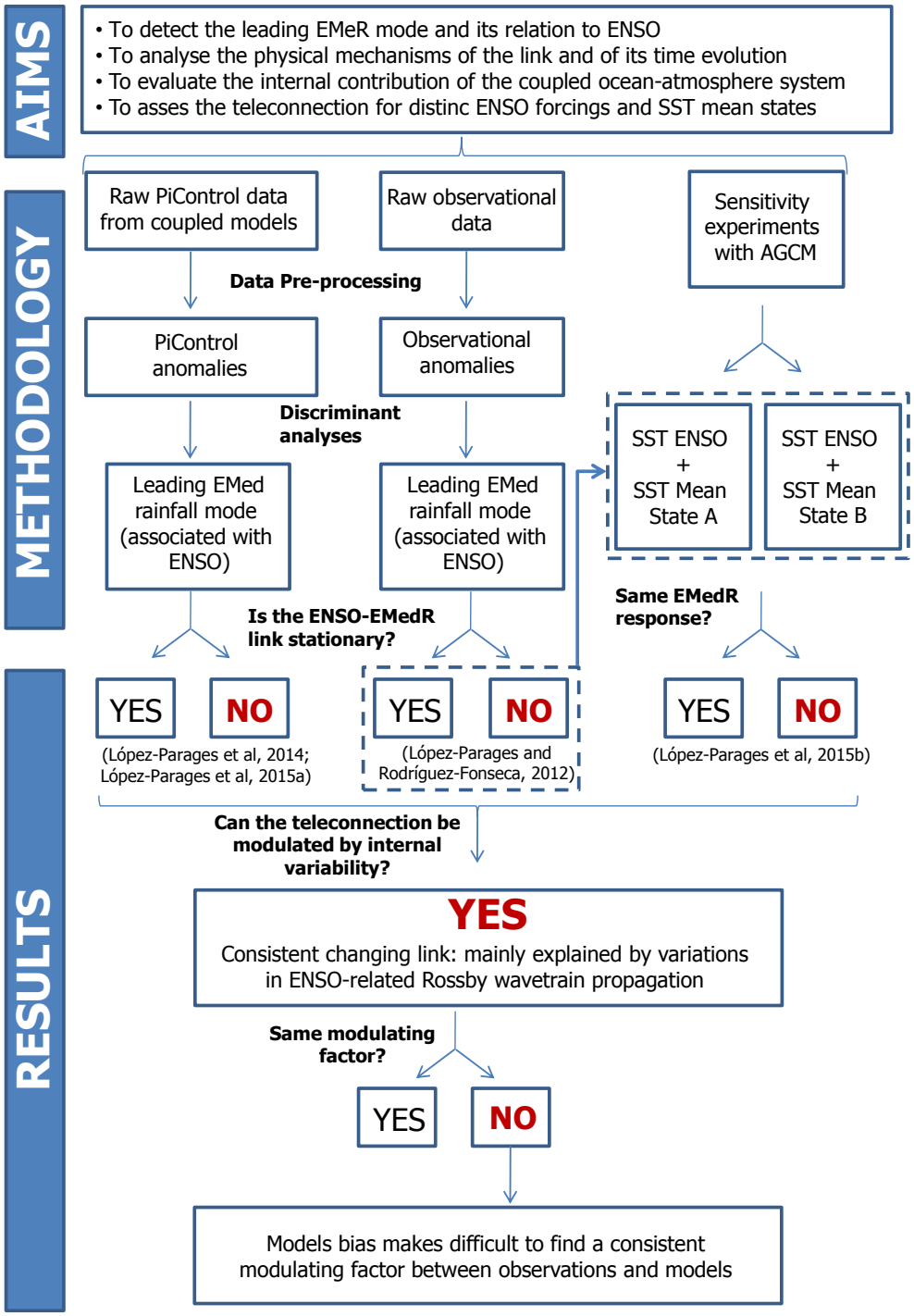

Figure 7.12: Very simplified synapses of the research undertaken. It includes the main objectives, data, and methodology considered in this thesis. Please compare to Figure 5.4.

8

Conclusions

The main conclusions of this PhD thesis are:

1. **The leading EMedR variability mode, at interannual timescales, in fall-early winter and in late winter-early spring, is related to El Niño in a non-stationary way in the observational record (López-Parages and Rodríguez-Fonseca, 2012).**

   According to the leading EOF, an increase (decrease) of rainfall over central Europe and a decrease (increase) of rainfall over the northern Scandinavia and the Mediterranean rainfall is detected, for both seasons, in relation to anomalous positive (negative) SSTs over the tropical Pacific. A changing link between the corresponding Principal Component and El Niño3.4 index is found.

   - In fall-early winter (October-November-December; OND) this link evolves in phase with the Pacific Decadal Oscillation (PDO). Statistically significant positive (negative) correlations appears for positive (negative) PDO phases.

   - In late winter-early spring (February-March-April; FMA) this link evolves in phase with the Atlantic Multidecadal Oscillation (AMO). Statistically significant positive correlations appears during negative AMO phases.

   The spatial projections of anomalous SLP and SST onto these leading PCs present different structures depending on the period considered. They suggest the influence of tropical SSTs associated with ENSO over the NAE sector in some decades; whilst in others, the patterns appears in absence of oceanic signatures and resemble spatial configurations usually related to internal variability of the atmosphere.

2. **The non-stationary teleconnectiom between ENSO and the leading EMedR mode, in FMA, can be reproduced by internal variability of the ocean-atmosphere coupled system (López-Parages et al., 2014, 2015a).**

   Long-term preindustrial control simulations (pi-Control) from different 18 CMIP5 models are able to reproduce the observed changing impact of ENSO on the leading EMedR mode.

   - For those periods in which the observational signature of ENSO on EMedR is found, a Rossby wavetrain structure associated with an anomalous warming over the tropical Pacific reaches the NAE sector. As a consequence, a low pressure center appears over northern Europe and a significant impact on rainfall is detected.

   - In others periods, however, the anomalous Rossby wavetrain associated with ENSO is constrained over the Pacific North American sector and a very different EMedR pattern (broadly the opposite) is identified.

3. **The absence of stationarity in the teleconnection between ENSO and the leading EMedR mode can be explained by multidecadal changes of jet streams forced by the ocean (López-Parages et al., 2014, 2015a).**

   This feature is explained, in pi-Control CMIP5 simulations, as follows:

   a) SST variability associated with an IPO-like pattern alters the climatological meridional temperature gradient over the North Pacific and over the vicinity of the Central American continent.

   b) These changes modify the vertical shear of the horizontal wind (thermal wind) and hence, the intensity and spatial configuration of the EA-jet and the NA-jet above.

   c) As a consequence, the stationary Rossby waveguides associated with these jets vary in a way that the propagation of the ENSO-related wavetrains from tropical to extratropical latitudes is either enhanced or weakened.

   d) When the aforementioned propagation is enhanced, the related wave activity reaches the NAE sector and hence, a significant signature of ENSO on European and Mediterranean rainfall (consistent with the observational one) is found.

4. **Sensitivity experiments with the ACCESS model (AGCM) demonstrate how the ENSO impact on the leading EMedR mode in FMA can be modulated by the SST mean state variability. This modulation occurs, however, in a distinct way depending on the phase, amplitude, and spatial pattern of the SST ENSO forcing (López-Parages et al., 2015b).**

   The main specific outcomes obtained from these experiments are:

   - The non-stationary impact of La Niña events (mainly the Central episodes) over the NAE sector is explained by changes in the divergent flow. In particular, under a negative AMO-like SST mean state, the thermally driven Walker cell connecting the Pacific and Atlantic basins, and Hadley cell linking the equatorial and subtropical Atlantic, are weakened during La Niña events. As a consequence, the Azores high pressures system is also weakened.

   - The non-stationary impact of El Niño events (mainly the Eastern episodes) over the NAE sector is explained by changes in the rotational flow. In particular, under a negative AMO-like SST mean state, the El Niño-related Rossby wavetrains are guided by the EA-jet and the NA-jet from the tropical Pacific to the NAE sector. Under a positive AMO-like mean state, however, the wave activity associated with El Niño is restricted to the Pacific North-American sector. This feature is coherent with the changing signature of ENSO identified in observations. For strong Eastern Pacific Niños this dependence with the ocean background state is not found.

   - The aforementioned changes in Rossby waveguides reflect a combined influence of both, the Atlantic and Pacific basins, on the EA-jet and the NP-jet. Thus, only when the AMO-like signature over the Pacific is considered the waveguides vary in a way that efficiently propagate the anomalous disturbances associated with ENSO towards the NAE sector.

5. **Extratropical jet streams play a key role for tropical-extratropical teleconnections.**

   The comparison of the ENSO-EMedR teleconnection found in (1) observations, (2) pi-Control CMIP5 simulations, and (3) sensitivity experiments carried out with the ACCESS model, leads to the conclusion that the intensity and spatial configuration of the jet streams play a key role in representing the non-stationary features of ENSO teleconnections with remote extratropical regions. According to our results, if the jets (and their related Rossby waveguides) are poorly represented by climate models (strong bias), a common changing impact of ENSO on EMedR, in observations and models, can be modulated by very different SST multidecadal patterns.

A

Future Work

The results of the present thesis have shed light on a non-stationary teleconnection between ENSO and the leading EMedR mode. This changing link can be modulated by variations in the upper tropospheric mean flow associated with multidecadal variability of the underlying SST. Some interesting issues, which are outside the scope of this work, also arise from the present study. To address them in the future we identify the following particular tasks:

- **To deeper analyse the role of the TNA.** To this aim new sensitivity experiments, in which the influence of ENSO on TNA SSTs is considered, must be carried out. This task could be performed by: (1) prescribing the TNA SST pattern associated with ENSO in an AGCM, or (2) coupling the ocean and the atmosphere over the TNA region using a CGCM.

- **To quantify the improvement in the predictive skill** of EMedR through ENSO-related SSTs when the non-stationary behavior of the teleconnection is considered. This task requires further analyses in future works by using of statistical and dynamical models.

- **To explore a possible change of the season in which the tropospheric teleconnection between ENSO and the leading EMedR mode occurs, as well as the role of the SST background state.** In the case that this change exists, the assumption of late winter and early spring as the most properly season for detecting a robust signal of ENSO over Europe must be clearly questioned.

- **To investigate the stratospheric link and its possible non-stationary feature**. Considering the strong influence of ENSO over the NAE sector via the stratosphere (Butler et al., 2014), it would be of great interest to distinguish between the tropospheric and stratospheric pathways. The study of both is convenient, not only for an integral vision of the teleconnection, but also to be able to isolate their related possible modulating factors.

B

List of Acronyms

20CR 20th Century Reanalysis.

ACCESS Australian Community Climate and Earth System Simulator.

AGCM Atmospheric General Circulation Model.

AMO Atlantic Multi-decadal Oscillation.

AMOC Atlantic Multi-decadal Overturning Circulation.

AO Arctic Oscillation.

COADS Comprehensive Ocean-Atmosphere Data Set.

CGCM Coupled General Circulation Model.

CMIP Coupled Model Intercomparison Project.

CP Central Pacific.

EMedR European and Mediterranean Rainfall.

ENSO El Niño and the Southern Oscillation.

EOF Empirical Orthogonal Function.

EP Eastern Pacific.

ECMWF European Centre for Medium-Range Weather Forecast.

ERSST Extended Reconstructed Sea Surface Temperature.

FT Fourier Transform.

GCM General Circulation Model.

GPCC Global Precipitation Climatology Centre.

HadISST Hadley Center Sea Ice and Sea Surface Temperature.

ICOADS International Comprehensive Ocean-Atmosphere Data Set.

IPCC Intergovernmental Panel on Climate Change.

IPO Inte-decadal Pacific Oscillation.

ITCZ Inter-Tropical Convergence Zone.

MCA Maximum Covariance Analysis.

MOC Meridional Overturning Circulation.

NAE North Atlantic European.

NAM Northern Annular Mode.

NAO North Atlantic Oscillation.

NCAR National Center for Atmospheric Research.

NCEP National Center for Environmental Prediction.

NOAA National Oceanic and Atmospheric Administration.

OGCM Ocean General Circulation Model.

PC Principal Component.

PCA Principal Component Analysis.

PDO Pacific Decadal Oscillation.

PNA Pacific North American Pattern.

S4CAST Sea Surface Temperature based Statistical Seasonal foreCAST.

SLP Sea Level Pressure.

SO Southern Oscillation.

SOI Southern Oscillation Index.

SST Sea Surface Temperature.

SVD Singular Value Decomposition.

TNA Tropical North Atlantic.

TNH Tropical Northern Hemisphere.

C

List of Publications

Within the context of this thesis, the following papers have been published:

- López-Parages, J. and Rodríguez-Fonseca, B.: Multidecadal modulation of El Niño influence on the Euro-Mediterranean rainfall, Geophys. Res. Lett., 39, L02704, doi:10.1029 2011GL050049, 2012.
- López-Parages, J., Rodríguez-Fonseca, B., and Terray, L.: A mechanism for the multidecadal modulation of ENSO teleconnection with Europe, Clim. Dyn., 45, 867–880, doi:10.1007/ s00382-014-2319-x, 2014.
- López-Parages, J., Rodríguez-Fonseca, B., Mohino, E., and Losada, T. : Multidecadal modulation of ENSO teleconnection with Europe in CMIP5 models, J. Climate, *under review (JCLI-S-15-00678)*, 2015.
- López-Parages, J., Rodríguez-Fonseca, B., Dommenget, D., and Frauen, C.: ENSO influence on the North Atlantic European climate: A non-linear and non-stationary approach, Clim. Dyn., *under review (CLDY-D-15-00443R1)*, 2015.

Other publications during the PhD period:

- López-Parages, J., Villamayor, J., Losada, T., Martín-Rey, M., Mohino, E., Polo, I., Rodríguez-Fonseca, B., Suárez, R.: Nonstationary interannual teleconnections modulated by multidecadal variability, Física de la Tierra, 25, 11-39, ISSN 0214-4557, 2013.

Bibliography

Abatzoglou, J. T. and Magnusdottir, G.: Planetary Wave Breaking and Nonlinear Reflection: Seasonal Cycle and Interannual Variability, J. Climate, 19, 6139, doi:10.1175/JCLI3968.1, 2006.

Alexander, M. A., Bladé, I., Newman, M., Lanzante, J. R., Lau, N.-C., and Scott, J. D.: The Atmospheric Bridge: The Influence of ENSO Teleconnections on Air-Sea Interaction over the Global Oceans., J. Climate, 15, 2205–2231, doi:10.1175/1520-0442(2002)015<2205:TABTIO>2.0.CO;2, 2002.

Allan, R., Lindesay, J., Parker, D., et al.: El Nino Southern oscillation and climatic variability, CSIRO, Collingwood, Victoria, Australia, p. 416, 1996.

Allan, R. J. and D'Arrigo, R. D.: 'Persistent' ENSO sequences: how unusual was the 1990-1995 El Niño?, Holocene, 9, 101–118, doi:10.1191/095968399669125102, 1999.

Alpert, P., Baldi, M., Ilani, R., Krichak, S., Price, C., Rodo, X., Saaroni, H., Ziv, B., Kishcha, P., Barkan, J., et al.: Relations between climate variability in the Mediterranean region and the tropics: ENSO, South Asian and African monsoons, hurricanes and Saharan dust, Mediterranean climate variability. Elsevier, Amsterdam, pp. 149–177, 2006.

Ambrizzi, T., Hoskins, B. J., and Hsu, H.-H.: Rossby Wave Propagation and Teleconnection Patterns in the Austral Winter., J. Atmos. Sci., 52, 3661–3672, doi:10.1175/1520-0469(1995)052<3661:RWPATP>2.0.CO;2, 1995.

AMS Glossary, A. M.: American Meteorological Society; 2015, Web, 2015.

An, S.: A review of interdecadal changes in the nonlinearity of the El Niño-Southern Oscillation, Theor. Appl. Climatol., 97, 29–40, doi:10.1007/s00704-008-0071-z, 2009.

An, S. and Wang, B.: Interdecadal Change of the Structure of the ENSO Mode and Its Impact on the ENSO Frequency., J. Climate, 13, 2044–2055, doi:10.1175/1520-0442(2000)013<2044:ICOTSO>2.0.CO;2, 2000.

An, S.-I., Ye, Z., and Hsieh, W. W.: Changes in the leading ENSO modes associated with the late 1970s climate shift: Role of surface zonal current, Geophys. Res. Lett., 33, L14609, doi:10.1029/2006GL026604, 2006.

Arthur, D. and Vassilvitskii, S.: k-means++: The advantages of careful seeding, in: Proceedings of the eighteenth annual ACM-SIAM symposium on Discrete algorithms, pp. 1027–1035, SIAM, 2007.

Ashok, K., Behera, S. K., Rao, S. A., Weng, H., and Yamagata, T.: El Niño Modoki and its possible teleconnection, J. Geophys. Res. Oceans, 112, 2007.

Baldwin, M. P. and Dunkerton, T. J.: Stratospheric Harbingers of Anomalous Weather Regimes, Science, 294, 581–584, doi:10.1126/science.1063315, 2001.

Bao, Q., Lin, P., Zhou, T., Liu, Y., Yu, Y., Wu, G., He, B., He, J., Li, L., Li, J., et al.: The flexible global ocean-atmosphere-land system model, spectral version 2: FGOALS-s2, Adv. Atmos. Sci., 30, 561–576, 2013.

Barnston, A. and Livezey, R.: Classification, Seasonality and Persistence of Low-Frequency Atmospheric Circulation Patterns, Mon. Wea. Rev., 115, 1083, doi:10.1175/1520-0493(1987)115<1083:CSAPOL>2.0.CO;2, 1987.

Bell, C. J., Gray, L. J., Charlton-Perez, A. J., Joshi, M. M., and Scaife, A. A.: Stratospheric Communication of El Niño Teleconnections to European Winter, J. Climate, 22, 4083, doi:10.1175/2009JCLI2717.1, 2009.

Bentsen, M., Bethke, I., Debernard, J., Iversen, T., Kirkevåg, A., Seland, Ø., Drange, H., Roelandt, C., Seierstad, I., Hoose, C., et al.: The Norwegian earth system model, NorESM1-M—Part 1: description and basic evaluation of the physical climate, Geosci. Model Dev., 6, 687–720, 2013.

Bi, D., Dix, M., Marsland, S. J., O'Farrell, S., Rashid, H., Uotila, P., Hirst, A., Kowalczyk, E., Golebiewski, M., Sullivan, A., et al.: The ACCESS coupled model: description, control climate and evaluation, Aust. Meteorol. Oceanogr. J, 63, 41–64, 2013.

Bjerknes, J.: Atmospheric Teleconnections from the Equatorial PACIFIC, Mon. Wea. Rev., 97, 163, doi:10.1175/1520-0493(1969)097<0163:ATFTEP>2.3.CO;2, 1969.

Bladé, I., Newman, M., Alexander, M. A., and Scott, J. D.: The Late Fall Extratropical Response to ENSO: Sensitivity to Coupling and Convection in the Tropical West Pacific, J. Climate, 21, 6101, doi:10.1175/2008JCLI1612.1, 2008.

Bonsal, B. and Shabbar, A.: Large-scale climate oscillations influencing Canada, 1900-2008, Canadian Biodiversity: Ecosystem Status and Trends 2010, Technical Thematic Report No. 4, Canadian Councils of Resource Ministers, 2011.

Booth, B. B., Dunstone, N. J., Halloran, P. R., Andrews, T., and Bellouin, N.: Aerosols implicated as a prime driver of twentieth-century North Atlantic climate variability, Nature, 484, 228–232, 2012.

Box, G. E. and Jenkins, G.: Time Series Analysis: Forecasting and Control, Time Series and Digital Processing, 1976.

Branstator, G.: Horizontal Energy propagation in a Barotropic Atmosphere with Meridional and Zonal Structure., J. Atmos. Sci., 40, 1689–1708, doi:10.1175/1520-0469(1983)040<1689:HEPIAB>2.0.CO;2, 1983.

Branstator, G.: The Maintenance of Low-Frequency Atmospheric Anomalies., J. Atmos. Sci., 49, 1924–1946, doi:10.1175/1520-0469(1992)049<1924:TMOLFA>2.0.CO;2, 1992.

Branstator, G.: Circumglobal Teleconnections, the Jet Stream Waveguide, and the North Atlantic Oscillation., J. Climate, 15, 1893–1910, doi:10.1175/1520-0442(2002)015<1893:CTTJSW>2.0.CO;2, 2002.

Branstator, G.: Waveguides and the remote response to tropical SST anomalies., in: 13th Conference on Interactions of the Sea and Atmosphere, Midlatitude atmosphere-ocean interaction: Part I The North Pacific and its connection to the tropics, 2004.

Bretherton, C. S., Smith, C., and Wallace, J. M.: An Intercomparison of Methods for Finding Coupled Patterns in Climate Data., J. Climate, 5, 541–560, doi:10.1175/1520-0442(1992)005<0541:AIOMFF>2.0.CO;2, 1992.

Brönnimann, S.: Impact of El Niño-Southern Oscillation on European climate, Rev. Geophys., 45, RG3003, doi:10.1029/2006RG000199, 2007.

Brönnimann, S., Xoplaki, E., Casty, C., Pauling, A., and Luterbacher, J.: ENSO influence on Europe during the last centuries, Clim. Dyn., 28, 181–197, doi:10.1007/s00382-006-0175-z, 2007.

Brunet, G. and Haynes, P. H.: Low-Latitude Reflection of Rossby Wave Trains., J. Atmos. Sci., 53, 482–496, doi:10.1175/1520-0469(1996)053<0482:LLRORW>2.0.CO;2, 1996.

Bulić, I. H. and Kucharski, F.: Delayed ENSO impact on spring precipitation over North/Atlantic European region, Clim. Dyn., 38, 2593–2612, 2012.

Butler, A. H., Polvani, L. M., and Deser, C.: Separating the stratospheric and tropospheric pathways of El Niño-Southern Oscillation teleconnections, Environ. Res. Lett., 9, 024014, doi:10.1088/1748-9326/9/2/024014, 2014.

Cagnazzo, C. and Manzini, E.: Impact of the Stratosphere on the Winter Tropospheric Teleconnections between ENSO and the North Atlantic and European Region, J. Climate, 22, 1223, doi:10.1175/2008JCLI2549.1, 2009.

Calvo, N. and Marsh, D. R.: The combined effects of ENSO and the 11 year solar cycle on the Northern Hemisphere polar stratosphere, J. Geophys. Res. Atmos., 116, D23112, doi:10.1029/2010JD015226, 2011.

Cassou, C. and Terray, L.: Dual influence of Atlantic and Pacific SST anomalies on the North Atlantic/Europe winter climate, Geophys. Res. Lett., 28, 3195–3198, doi:10.1029/2000GL012510, 2001a.

Cassou, C. and Terray, L.: Oceanic Forcing of the Wintertime Low-Frequency Atmospheric Variability in the North Atlantic European Sector: A Study with the ARPEGE Model., J. Climate, 14, 4266–4291, doi:10.1175/1520-0442(2001)014<4266:OFOTWL>2.0.CO;2, 2001b.

Cassou, C., Terray, L., Hurrell, J. W., and Deser, C.: North Atlantic Winter Climate Regimes: Spatial Asymmetry, Stationarity with Time, and Oceanic Forcing., J. Climate, 17, 1055–1068, doi:10.1175/1520-0442(2004)017<1055:NAWCRS>2.0.CO;2, 2004.

Castanheira, J. M. and Graf, H.-F.: North Pacific-North Atlantic relationships under stratospheric control?, J. Geophys. Res. Atmos., 108, 4036, doi:10.1029/2002JD002754, 2003.

Castro-Díez, Y., Pozo-Vázquez, D., Rodrigo, F. S., and Esteban-Parra, M. J.: NAO and winter temperature variability in southern Europe, Geophys. Res. Lett., 29, 1160, doi:10.1029/2001GL014042, 2002.

Chen, S., Wu, R., and Chen, W.: The Changing Relationship between Interannual Variations of the North Atlantic Oscillation and Northern Tropical Atlantic SST, J. Climate, 28, 485–504, doi:10.1175/JCLI-D-14-00422.1, 2015.

Choi, J., An, S.-I., Kug, J.-S., and Yeh, S.-W.: The role of mean state on changes in El Niño's flavor, Clim. Dyn., 37, 1205–1215, doi:10.1007/s00382-010-0912-1, 2011.

Chung, P.-H. and Li, T.: Interdecadal Relationship between the Mean State and El Niño Types, J. Climate, 26, 361–379, doi:10.1175/JCLI-D-12-00106.1, 2013.

Chylek, P., Folland, C. K., Lesins, G., and Dubey, M. K.: Twentieth century bipolar seesaw of the Arctic and Antarctic surface air temperatures, Geophys. Res. Lett., 37, L08703, doi:10.1029/2010GL042793, 2010.

Chylek, P., Li, J., Dubey, M., Wang, M., and Lesins, G.: Observed and model simulated 20th century Arctic temperature variability: Canadian earth system model CanESM2, Atmospheric Chemistry and Physics Discussions, 11, 22 893–22 907, 2011.

Chylek, P., Folland, C., Frankcombe, L., Dijkstra, H., Lesins, G., and Dubey, M.: Greenland ice core evidence for spatial and temporal variability of the Atlantic Multidecadal Oscillation, Geophys. Res. Lett., 39, L09705, doi:10.1029/2012GL051241, 2012.

Chylek, P., Klett, J. D., Lesins, G., Dubey, M. K., and Hengartner, N.: The Atlantic Multidecadal Oscillation as a dominant factor of oceanic influence on climate, Geophys. Res. Lett., 41, 1689–1697, doi:10.1002/2014GL059274, 2014.

Compo, G. P., Whitaker, J. S., Sardeshmukh, P. D., Matsui, N., Allan, R. J., Yin, X., Gleason, B. E., Vose, R. S., Rutledge, G., Bessemoulin, P., Brönnimann, S., Brunet, M., Crouthamel, R. I., Grant, A. N., Groisman, P. Y., Jones, P. D., Kruk, M. C., Kruger, A. C., Marshall, G. J., Maugeri, M., Mok, H. Y., Nordli, Ø., Ross, T. F., Trigo, R. M., Wang, X. L., Woodruff, S. D., and Worley, S. J.: The Twentieth Century Reanalysis Project, Quart. J. Roy. Meteor. Soc., 137, 1–28, doi:10.1002/qj.776, 2011.

Corte-Real, J., Qian, B., and Xu, H.: Regional climate change in Portugal: precipitation variability associated with large-scale atmospheric circulation, Int. J. Climatol., 18, 619–635, doi:10.1002/(SICI)1097-0088(199805)18:6<619::AID-JOC271>3.0.CO;2-T, 1998.

Czaja, A. and Frankignoul, C.: Influence of the North Atlantic SST on the atmospheric circulation, Geophys. Res. Lett., 26, 2969–2972, doi:10.1029/1999GL900613, 1999.

Dai, A. and Wigley, T. M. L.: Global patterns of ENSO-induced precipitation, Geophys. Res. Lett., 27, 1283–1286, doi:10.1029/1999GL011140, 2000.

Dai, A., Fung, I. Y., and del Genio, A. D.: Surface Observed Global Land Precipitation Variations during 1900-88., J. Climate, 10, 2943–2962, doi:10.1175/1520-0442(1997)010<2943:SOGLPV>2.0.CO;2, 1997.

Davey, M. K. and Gill, A. E.: Experiments on tropical circulation with a simple moist model, Quart. J. Roy. Meteor. Soc., 113, 1237–1269, doi:10.1002/qj.49711347809, 1987.

Davies, T., Cullen, M., Malcolm, A., Mawson, M., Staniforth, A., White, A., and Wood, N.: A new dynamical core for the Met Office's global and regional modelling of the atmosphere, Quart. J. Roy. Meteor. Soc., 131, 1759–1782, 2005.

Delworth, T. L. and Mann, M. E.: Observed and simulated multidecadal variability in the Northern Hemisphere, Clim. Dyn., 16, 661–676, doi:10.1007/s003820000075, 2000.

Delworth, T. L. and Zeng, F.: Multicentennial variability of the Atlantic meridional overturning circulation and its climatic influence in a 4000 year simulation of the GFDL CM2.1 climate model, Geophys. Res. Lett., 39, L13702, doi:10.1029/2012GL052107, 2012.

Deser, C., Alexander, M. A., Xie, S.-P., and Phillips, A. S.: Sea Surface Temperature Variability: Patterns and Mechanisms, Annual Review of Marine Science, 2, 115–143, doi:10.1146/annurev-marine-120408-151453, 2010.

Desser, C., Phillips, A. S., and Hurrell, J. W.: Pacific Interdecadal Climate Variability: Linkages between the Tropics and the North Pacific during Boreal Winter since 1900., J. Climate, 17, 3109–3124, doi:10.1175/1520-0442(2004)017<3109:PICVLB>2.0.CO;2, 2004.

Deweaver, E. and Nigam, S.: Linearity in ENSO's Atmospheric Response, J. Climate, 15, 2446–2461, doi:10.1175/1520-0442(2002)015<2446:LIESAR>2.0.CO;2, 2002.

Di Lorenzo, E., Cobb, K. M., Furtado, J. C., Schneider, N., Anderson, B. T., Bracco, A., Alexander, M. A., and Vimont, D. J.: Central Pacific El Niño and decadal climate change in the North Pacific Ocean, Nat. Geosci., 3, 762–765, doi:10.1038/ngeo984, 2010.

Diaz, H. F. and Markgraf, V.: El Niño and the Southern Oscillation: multiscale variability and global and regional impacts, Cambridge University Press, 2000.

Dima, M. and Lohmann, G.: A Hemispheric Mechanism for the Atlantic Multidecadal Oscillation, J. Climate, 20, 2706, doi:10.1175/JCLI4174.1, 2007.

Ding, Q. and Wang, B.: Circumglobal Teleconnection in the Northern Hemisphere Summer, J. Climate, 18, 3483–3505, doi:10.1175/JCLI3473.1, 2005.

Dommenget, D.: The slab ocean El Niño, Geophys. Res. Lett., 37, L20701, doi:10.1029/2010GL044888, 2010.

Dommenget, D. and Latif, M.: Analysis of observed and simulated SST spectra in the midlatitudes, Clim. Dyn., 19, 277–288, doi:10.1007/s00382-002-0229-9, 2002.

Dommenget, D., Bayr, T., and Frauen, C.: Analysis of the non-linearity in the pattern and time evolution of El Niño southern oscillation, Clim. Dyn., 40, 2825–2847, doi:10.1007/s00382-012-1475-0, 2013.

Dong, B., Sutton, R. T., and Scaife, A. A.: Multidecadal modulation of El Niño-Southern Oscillation (ENSO) variance by Atlantic Ocean sea surface temperatures, Geophys. Res. Lett., 33, L08705, doi:10.1029/2006GL025766, 2006.

Dong, B. W. and Sutton, R. T.: Adjustment of the coupled ocean-atmosphere system to a sudden change in the Thermohaline Circulation, Geophys. Res. Lett., 29, 1728, doi:10.1029/2002GL015229, 2002.

Drévillon, M., Terray, L., Rogel, P., and Cassou, C.: Mid latitude Atlantic SST influence on European winter climate variability in the NCEP Reanalysis, Clim. Dyn., 18, 331–344, doi:10.1007/s003820100178, 2001.

Drouard, M., Rivière, G., and Arbogast, P.: The Link between the North Pacific Climate Variability and the North Atlantic Oscillation via Downstream Propagation of Synoptic Waves, J. Climate, 28, 3957–3976, doi:10.1175/JCLI-D-14-00552.1, 2015.

Dufresne, J.-L., Foujols, M.-A., Denvil, S., Caubel, A., Marti, O., Aumont, O., Balkanski, Y., Bekki, S., Bellenger, H., Benshila, R., Bony, S., Bopp, L., Braconnot, P., Brockmann, P., Cadule, P., Cheruy, F., Codron, F., Cozic, A., Cugnet, D., de Noblet, N., Duvel, J.-P., Ethé, C., Fairhead, L., Fichefet, T., Flavoni, S., Friedlingstein, P., Grandpeix, J.-Y., Guez, L., Guilyardi, E., Hauglustaine, D., Hourdin, F., Idelkadi, A., Ghattas, J., Joussaume, S., Kageyama, M., Krinner, G., Labetoulle, S., Lahellec, A., Lefebvre, M.-P., Lefevre, F., Levy, C., Li, Z. X., Lloyd, J., Lott, F., Madec, G., Mancip, M., Marchand, M., Masson, S., Meurdesoif, Y., Mignot, J., Musat, I., Parouty, S., Polcher, J., Rio, C., Schulz, M., Swingedouw, D., Szopa, S., Talandier, C., Terray, P., Viovy, N., and Vuichard, N.: Climate change

projections using the IPSL-CM5 Earth System Model: from CMIP3 to CMIP5, Clim. Dyn., 40, 2123–2165, doi:10.1007/s00382-012-1636-1, 2013.

Duhamel, P. and Vetterli, M.: Fast Fourier transforms: a tutorial review and a state of the art, Signal processing, 19, 259–299, 1990.

Durán, L., Rodríguez-Fonseca, B., Yagüe, C., and Sánchez, E.: Water vapour flux patterns and precipitation at Sierra de Guadarrama mountain range (Spain), Int. J. Climatol., 35, 1593–1610, doi:10.1002/joc.4079, 2015.

Enfield, D. B., Mestas-Nuñez, A. M., and Trimble, P. J.: The Atlantic Multidecadal Oscillation and its relation to rainfall and river flows in the continental U.S., Geophys. Res. Lett., 28, 2077–2080, doi:10.1029/2000GL012745, 2001.

Evan, A. T., Vimont, D. J., Heidinger, A. K., Kossin, J. P., and Bennartz, R.: The role of aerosols in the evolution of tropical North Atlantic Ocean temperature anomalies, Science, 324, 778–781, doi:10.1126/science.1167404, 2009.

Fedorov, A. V. and Philander, S. G.: Is El Niño Changing?, Science, 288, 1997–2002, doi:10.1126/science.288.5473.1997, 2000.

Fraedrich, K. and Müller, K.: Climate anomalies in Europe associated with ENSO extremes, Int. J. Climatol., 12, 25–31, doi:10.1002/joc.3370120104, 1992.

Frauen, C. and Dommenget, D.: El Niño and La Niña amplitude asymmetry caused by atmospheric feedbacks, Geophys. Res. Lett., 37, L18801, doi:10.1029/2010GL044444, 2010.

Frauen, C., Dommenget, D., Tyrrell, N., Rezny, M., and Wales, S.: Analysis of the Nonlinearity of El Niño-Southern Oscillation Teleconnection, J. Climate, 27, 6225, doi:10.1175/JCLI-D-13-00757.1, 2014.

Frigo, M. and Johnson, S. G.: FFTW: An adaptive software architecture for the FFT, in: Acoustics, Speech and Signal Processing, 1998. Proceedings of the 1998 IEEE International Conference on, vol. 3, pp. 1381–1384, IEEE, 1998.

Gámiz-Fortis, S. R., Pozo-Vázquez, D., Esteban-Parra, M. J., and Castro-Díez, Y.: Spectral characteristics and predictability of the NAO assessed through Singular Spectral Analysis, J. Geophys. Res. Atmos., 107, 4685, doi:10.1029/2001JD001436, 2002.

García-Serrano, J., Rodríguez-Fonseca, B., Bladé, I., Zurita-Gotor, P., and de La Cámara, A.: Rotational atmospheric circulation during North Atlantic-European winter: the influence of ENSO, Clim. Dyn., 37, 1727–1743, doi:10.1007/s00382-010-0968-y, 2011.

Garfinkel, C. I. and Hartmann, D. L.: Different ENSO teleconnections and their effects on the stratospheric polar vortex, J. Geophys. Res. Atmos., 113, D18114, doi:10.1029/2008JD009920, 2008.

Gent, P. R., Danabasoglu, G., Donner, L. J., Holland, M. M., Hunke, E. C., Jayne, S. R., Lawrence, D. M., Neale, R. B., Rasch, P. J., Vertenstein, M., et al.: The community climate system model version 4, J. Climate, 24, 4973–4991, 2011.

Gershunov, A. and Barnett, T. P.: Interdecadal Modulation of ENSO Teleconnections., Bull. Amer. Meteor. Soc., 79, 2715–2726, doi:10.1175/1520-0477(1998)079<2715:IMOET>2.0.CO;2, 1998.

Gill, A. E.: Some simple solutions for heat-induced tropical circulation, Quart. J. Roy. Meteor. Soc., 106, 447–462, doi:10.1002/qj.49710644905, 1980.

Giorgetta, M. A., Jungclaus, J., Reick, C. H., Legutke, S., Bader, J., Böttinger, M., Brovkin, V., Crueger, T., Esch, M., Fieg, K., Glushak, K., Gayler, V., Haak, H., Hollweg, H.-D., Ilyina, T., Kinne, S., Kornblueh, L., Matei, D., Mauritsen, T., Mikolajewicz, U., Mueller, W., Notz, D., Pithan, F., Raddatz, T., Rast, S., Redler, R., Roeckner, E., Schmidt, H., Schnur, R., Segschneider, J., Six, K. D., Stockhause, M., Timmreck, C., Wegner, J., Widmann, H., Wieners, K.-H., Claussen, M., Marotzke, J., and Stevens, B.: Climate and carbon cycle changes from 1850 to 2100 in MPI-ESM simulations for the Coupled Model Intercomparison Project phase 5, J. Adv. Model. Earth Sy., 5, 572–597, doi:10.1002/jame.20038, 2013.

Glantz, M. H.: Currents of change: impacts of El Niño and La Niña on climate and society, Cambridge University Press, 2001.

Gouirand, I. and Moron, V.: Variability of the impact of El Niño-Southern Oscillation on sea-level pressure anomalies over the North Atlantic in January to March(1874-1996), Int. J. Climatol., 23, 1549–1566, doi:10.1002/joc.963, 2003.

Gouirand, I., Moron, V., and Zorita, E.: Teleconnections between ENSO and North Atlantic in an ECHO-G simulation of the 1000-1990 period, Geophys. Res. Lett., 34, L06705, doi:10.1029/2006GL028852, 2007.

Graf, H.-F. and Zanchettin, D.: Central Pacific El Niño, the subtropical bridge, and Eurasian climate, J. Geophys. Res. Atmos., 117, D01102, doi:10.1029/2011JD016493, 2012.

Graham, N. E.: Decadal-scale climate variability in the tropical and North Pacific during the 1970s and 1980s: observations and model results, Clim. Dyn., 10, 135–162, doi:10.1007/BF00210626, 1994.

Graham, N. E. and Barnett, T. P.: Sea Surface Temperature, Surface Wind Divergence, and Convection over Tropical Oceans, Science, 238, 657–659, doi:10.1126/science.238.4827.657, 1987.

Gray, S. T., Graumlich, L. J., Betancourt, J. L., and Pederson, G. T.: A tree-ring based reconstruction of the Atlantic Multidecadal Oscillation since 1567 A.D., Geophys. Res. Lett., 31, L12205, doi:10.1029/2004GL019932, 2004.

Greatbatch, R. J., Lu, J., and Peterson, K. A.: Nonstationary impact of ENSO on Euro-Atlantic winter climate, Geophys. Res. Lett., 31, L02208, doi:10.1029/2003GL018542, 2004.

Gulev, S. K., Latif, M., Keenlyside, N., Park, W., and Koltermann, K. P.: North Atlantic Ocean control on surface heat flux on multidecadal timescales, Nature, 499, 464–467, 2013.

Häkkinen, S., Rhines, P. B., and Worthen, D. L.: Atmospheric Blocking and Atlantic Multidecadal Ocean Variability, Science, 334, 655–, doi:10.1126/science.1205683, 2011.

Ham, Y.-G., Sung, M.-K., An, S.-I., Schubert, S. D., and Kug, J.-S.: Role of tropical atlantic SST variability as a modulator of El Niño teleconnections, Asia. Pac. J. Atmos. Sci., 50, 247–261, doi: 10.1007/s13143-014-0013-x, 2014.

Hare, S. and Francis, R.: Climate change and salmon production in the Northeast Pacific Ocean, Canadian Special Publication of Fisheries and Aquatic Sciences, pp. 357–372, 1995.

Harrison, D. E. and Larkin, N. K.: El Niño-Southern Oscillation sea surface temperature and wind anomalies, 1946-1993, Rev. Geophys., 36, 353–399, doi:10.1029/98RG00715, 1998.

Hastenrath, S.: Upper-air circulation of the Southern Oscillation from the NCEP-NCAR Reanalysis, Meteorol. Atmos. Phys., 83, 51–65, doi:10.1007/s00703-002-0562-x, 2003.

Hegyi, B. M. and Deng, Y.: A dynamical fingerprint of tropical Pacific sea surface temperatures on the decadal-scale variability of cool-season Arctic precipitation, J. Geophys. Res. Atmos., 116, D20121, doi: 10.1029/2011JD016001, 2011.

Hibbard, K. A., Meehl, G. A., Cox, P. M., and Friedlingstein, P.: A strategy for climate change stabilization experiments, EOS, Transactions American Geophysical Union, 88, 217–221, 2007.

Hilmer, M. and Jung, T.: Evidence for a recent change in the link between the North Atlantic Oscillation and Arctic Sea ice export, Geophys. Res. Lett., 27, 989–992, doi:10.1029/1999GL010944, 2000.

Holton, J.: An introduction to dynamic meteorology (International geophysics series), San Diego, New York, 1992.

Honda, M. and Nakamura, H.: Interannual Seesaw between the Aleutian and Icelandic Lows. Part II: Its Significance in the Interannual Variability over the Wintertime Northern Hemisphere., J. Climate, 14, 4512–4529, doi:10.1175/1520-0442(2001)014<4512:ISBTAA>2.0.CO;2, 2001.

Honda, M., Nakamura, H., Ukita, J., Kousaka, I., and Takeuchi, K.: Interannual Seesaw between the Aleutian and Icelandic Lows. Part I: Seasonal Dependence and Life Cycle., J. Climate, 14, 1029–1042, doi: 10.1175/1520-0442(2001)014<1029:ISBTAA>2.0.CO;2, 2001.

Horel, J. D. and Wallace, J. M.: Planetary-Scale Atmospheric Phenomena Associated with the Southern Oscillation, Mon. Wea. Rev., 109, 813, doi:10.1175/1520-0493(1981)109<0813:PSAPAW>2.0.CO;2, 1981.

Hoskins, B. J. and Ambrizzi, T.: Rossby Wave Propagation on a Realistic Longitudinally Varying Flow., J. Atmos. Sci., 50, 1661–1671, doi:10.1175/1520-0469(1993)050<1661:RWPOAR>2.0.CO;2, 1993.

Hoskins, B. J. and Karoly, D. J.: The Steady Linear Response of a Spherical Atmosphere to Thermal and Orographic Forcing., J. Atmos. Sci., 38, 1179–1196, doi:10.1175/1520-0469(1981)038<1179:TSLROA>2.0.CO;2, 1981.

Hoskins, B. J. and Valdes, P. J.: On the Existence of Storm-Tracks., J. Atmos. Sci., 47, 1854–1864, doi:10.1175/1520-0469(1990)047<1854:OTEOST>2.0.CO;2, 1990.

Hotelling, H.: The most predictable criterion., J. Educ. Phys., 26, 139, 1935.

Hsu, H.-H. and Lin, S.-H.: Global Teleconnections in the 250-mb Streamfunction Field during the Northern Hemisphere Winter, Mon. Wea. Rev., 120, 1169, doi:10.1175/1520-0493(1992)120<1169:GTITMS>2.0.CO;2, 1992.

Hurrell, J. W.: Decadal Trends in the North Atlantic Oscillation: Regional Temperatures and Precipitation, Science, 269, 676–679, doi:10.1126/science.269.5224.676, 1995.

Hurrell, J. W. and Deser, C.: Northern Hemisphere climate variability during winter: Looking back on the work of Felix Exner, Meteorol. Z., pp. 113–118, 2015.

Hurrell, J. W., Kushnir, Y., Ottersen, G., and Visbeck, M.: An overview of the North Atlantic Oscillation, AGU Geophysical Monograph Series, 134, 1–35, doi:10.1029/134GM01, 2003.

Ineson, S. and Scaife, A. A.: The role of the stratosphere in the European climate response to El Niño, Nat. Geosci., 2, 32–36, doi:10.1038/ngeo381, 2009.

Iza, M. and Calvo, N.: Role of Stratospheric Sudden Warmings on the response to Central Pacific El Niño, Geophys. Res. Lett., 42, 2482–2489, doi:10.1002/2014GL062935, 2015.

Kang, I.-S. and Kug, J.-S.: El Niño and La Niña sea surface temperature anomalies: Asymmetry characteristics associated with their wind stress anomalies, J. Geophys. Res. Atmos., 107, 4372, doi:10.1029/2001JD000393, 2002.

Kang, I.-S., No, H.-h., and Kucharski, F.: ENSO Amplitude Modulation Associated with the Mean SST Changes in the Tropical Central Pacific Induced by Atlantic Multidecadal Oscillation, J. Climate, 27, 7911–7920, doi:10.1175/JCLI-D-14-00018.1, 2014.

Kao, H.-Y. and Yu, J.-Y.: Contrasting Eastern-Pacific and Central-Pacific Types of ENSO, J. Climate, 22, 615, doi:10.1175/2008JCLI2309.1, 2009.

Karoly, D. J., Plumb, R. A., and Ting, M.: Examples of the Horizontal Propagation of Quasi-stationary Waves., J. Atmos. Sci., 46, 2802–2811, doi:10.1175/1520-0469(1989)046<2802:EOTHPO>2.0.CO;2, 1989.

Kerr, R. A.: A North Atlantic climate pacemaker for the centuries., Science, p. 1984, doi:10.1126/science.288.5473.1984, 2000.

Kiem, A. S., Franks, S. W., and Kuczera, G.: Multi-decadal variability of flood risk, Geophys. Res. Lett., 30, 1035, doi:10.1029/2002GL015992, 2003.

Kiladis, G. N. and Diaz, H. F.: Global Climatic Anomalies Associated with Extremes in the Southern Oscillation., J. Climate, 2, 1069–1090, doi:10.1175/1520-0442(1989)002<1069:GCAAWE>2.0.CO;2, 1989.

Klein, S. A., Soden, B. J., and Lau, N.-C.: Remote Sea Surface Temperature Variations during ENSO: Evidence for a Tropical Atmospheric Bridge., J. Climate, 12, 917–932, doi:10.1175/1520-0442(1999)012<0917:RSSTVD>2.0.CO;2, 1999.

Knight, J. R., Allan, R. J., Folland, C. K., Vellinga, M., and Mann, M. E.: A signature of persistent natural thermohaline circulation cycles in observed climate, Geophys. Res. Lett., 32, L20708, doi:10.1029/2005GL024233, 2005.

Knight, J. R., Folland, C. K., and Scaife, A. A.: Climate impacts of the Atlantic Multidecadal Oscillation, Geophys. Res. Lett., 33, L17706, doi:10.1029/2006GL026242, 2006.

Knippertz, P., Ulbrich, U., Marques, F., and Corte-Real, J.: Decadal changes in the link between El Niño and springtime North Atlantic oscillation and European-North African rainfall, Int. J. Climatol., 23, 1293–1311, doi:10.1002/joc.944, 2003.

Krishnamurti, T. N.: Tropical East-West Circulations During the Northern Summer., J. Atmos. Sci., 28, 1342–1347, doi:10.1175/1520-0469(1971)028<1342:TEWCDT>2.0.CO;2, 1971.

Krishnamurti, T. N., Kanamitsu, M., Koss, W. J., and Lee, J. D.: Tropical East-West Circulations During the Northern Winter., J. Atmos. Sci., 30, 780–787, doi:10.1175/1520-0469(1973)030<0780:TECDTN>2.0.CO;2, 1973.

Kucharski, F., Ikram, F., Molteni, F., Farneti, R., Kang, I.-S., No, H.-H., King, M., Giuliani, G., and Mogensen, K.: Atlantic forcing of Pacific decadal variability, Clim. Dyn., pp. 1–15, doi:10.1007/s00382-015-2705-z, 2015.

Kug, J.-S., Jin, F.-F., and An, S.-I.: Two Types of El Niño Events: Cold Tongue El Niño and Warm Pool El Niño, J. Climate, 22, 1499, doi:10.1175/2008JCLI2624.1, 2009.

Kuhlbrodt, T., Griesel, A., Montoya, M., Levermann, A., Hofmann, M., and Rahmstorf, S.: On the driving processes of the Atlantic meridional overturning circulation, Rev. Geophys., 45, RG2001, doi:10.1029/2004RG000166, 2007.

Larkin, N. K. and Harrison, D. E.: ENSO Warm (El Niño) and Cold (La Niña) Event Life Cycles: Ocean Surface Anomaly Patterns, Their Symmetries, Asymmetries, and Implications., J. Climate, 15, 1118–1140, doi:10.1175/1520-0442(2002)015<1118:EWENOA>2.0.CO;2, 2002.

Larkin, N. K. and Harrison, D. E.: Global seasonal temperature and precipitation anomalies during El Niño autumn and winter, Geophys. Res. Lett., 32, L16705, doi:10.1029/2005GL022860, 2005.

Latif, M. and Barnett, T. P.: Decadal Climate Variability over the North Pacific and North America: Dynamics and Predictability., J. Climate, 9, 2407–2423, doi:10.1175/1520-0442(1996)009<2407:DCVOTN>2.0.CO;2, 1996.

Latif, M., Roeckner, E., Botzet, M., Esch, M., Haak, H., Hagemann, S., Jungclaus, J., Legutke, S., Marsland, S., Mikolajewicz, U., and Mitchell, J.: Reconstructing, Monitoring, and Predicting Multidecadal-Scale Changes in the North Atlantic Thermohaline Circulation with Sea Surface Temperature., J. Climate, 17, 1605–1614, doi:10.1175/1520-0442(2004)017<1605:RMAPMC>2.0.CO;2, 2004.

Lau, N.-C. and Nath, M. J.: The Role of the 'Atmospheric Bridge' in Linking Tropical Pacific ENSO Events to Extratropical SST Anomalies., J. Climate, 9, 2036–2057, doi:10.1175/1520-0442(1996)009<2036:TROTBI>2.0.CO;2, 1996.

Lee, S.-K., Wang, C., and Mapes, B. E.: A Simple Atmospheric Model of the Local and Teleconnection Responses to Tropical Heating Anomalies, J. Climate, 22, 272, doi:10.1175/2008JCLI2303.1, 2009.

Li, Y. and Lau, N.-C.: Impact of ENSO on the Atmospheric Variability over the North Atlantic in Late Winter-Role of Transient Eddies, J. Climate, 25, 320–342, doi:10.1175/JCLI-D-11-00037.1, 2012.

Lin, H., Derome, J., and Brunet, G.: The Nonlinear Transient Atmospheric Response to Tropical Forcing, J. Climate, 20, 5642–5665, doi:10.1175/2007JCLI1383.1, 2007.

Livezey, R. E. and Mo, K. C.: Tropical-Extratropical Teleconnections during the Northern Hemisphere Winter. Part II: Relationships between Monthly Mean Northern Hemisphere Circulation Patterns and Proxies for Tropical Convection, Mon. Wea. Rev., 115, 3115, doi:10.1175/1520-0493(1987)115<3115:TETDTN>2.0.CO;2, 1987.

Lloyd, S. P.: Least squares quantization in PCM, Information Theory, IEEE Transactions on, 28, 129–137, doi:10.1109/TIT.1982.1056489, 1982.

López-Parages, J. and Rodríguez-Fonseca, B.: Multidecadal modulation of El Niño influence on the Euro-Mediterranean rainfall, Geophys. Res. Lett., 39, L02704, doi:10.1029/2011GL050049, 2012.

López-Parages, J., Rodríguez-Fonseca, B., and Terray, L.: A mechanism for the multidecadal modulation of ENSO teleconnection with Europe, Clim. Dyn., 45, 867–880, doi:10.1007/s00382-014-2319-x, 2014.

López-Parages, J., Rodríguez-Fonseca, B., Mohino, E., and Losada-Doval, T.: Multidecadal modulation of ENSO teleconnection with Europe in CMIP5 models, J. Climate, under review, 2015a.

López-Parages, J., Rodríguez-Fonseca, B., Dommenget, D., and Frauen, C.: ENSO influence on the North Atlantic European climate: A non-linear and non-stationary approach, Clim. Dyn., under review, 2015b.

Lorenz, E. N.: Empirical orthogonal functions and statistical weather prediction, Sci. Rep. 1, p. 49, 1956.

Lorenz, E. N.: Deterministic Nonperiodic Flow, J. Atmos. Sci., 20, 130–148, doi:10.1175/1520-0469(1963)020<0130:DNF>2.0.CO;2, 1963.

Lorenz, E. N. and Hilborn, R. C.: The Essence of Chaos, Am. J. Phys., 63, 862–863, doi:10.1119/1.17820, 1995.

Losada, T., Rodríguez-Fonseca, B., Polo, I., Janicot, S., Gervois, S., Chauvin, F., and Ruti, P.: Tropical response to the Atlantic Equatorial mode: AGCM multimodel approach, Clim. Dyn., 35, 45–52, doi:10.1007/s00382-009-0624-6, 2010.

Losada, T., Rodriguez-Fonseca, B., Mohino, E., Bader, J., Janicot, S., and Mechoso, C. R.: Tropical SST and Sahel rainfall: A non-stationary relationship, Geophys. Res. Lett., 39, L12705, doi:10.1029/2012GL052423, 2012.

Lu, J. and Greatbatch, R. J.: The changing relationship between the NAO and northern hemisphere climate variability, Geophys. Res. Lett., 29, 1148, doi:10.1029/2001GL014052, 2002.

Lutgens, F. and Tarbuck, E.: The Atmosphere: An Introduction to Meteorology, no. p. 3 in The Atmosphere: An Introduction to Meteorology, Prentice Hall, 2001.

Mahajan, S., Zhang, R., and Delworth, T. L.: Impact of the Atlantic Meridional Overturning Circulation (AMOC) on Arctic Surface Air Temperature and Sea Ice Variability, J. Climate, 24, 6573–6581, doi:10.1175/2011JCLI4002.1, 2011.

Mancuso, R. L.: A Numerical Procedure for Computing Fields of Stream Function and Velocity Potential., J. Appl. Meteor., 6, 994–1001, doi:10.1175/1520-0450(1967)006<0994:ANPFCF>2.0.CO;2, 1967.

Mantua, N. J. and Hare, S. R.: The Pacific decadal oscillation, Journal of Oceanography, 58, 35–44, 2002.

Mantua, N. J., Hare, S. R., Zhang, Y., Wallace, J. M., and Francis, R. C.: A Pacific Interdecadal Climate Oscillation with Impacts on Salmon Production., Bull. Amer. Meteor. Soc., 78, 1069–1079, doi:10.1175/1520-0477(1997)078<1069:APICOW>2.0.CO;2, 1997.

Manzini, E., Giorgetta, M. A., Esch, M., Kornblueh, L., and Roeckner, E.: The Influence of Sea Surface Temperatures on the Northern Winter Stratosphere: Ensemble Simulations with the MAECHAM5 Model, J. Climate, 19, 3863, doi:10.1175/JCLI3826.1, 2006.

Mariotti, A., Zeng, N., and Lau, K.-M.: Euro-Mediterranean rainfall and ENSO-a seasonally varying relationship, Geophys. Res. Lett., 29, 1621, doi:10.1029/2001GL014248, 2002.

Martin, G., Bellouin, N., Collins, W., Culverwell, I., Halloran, P., Hardiman, S., Hinton, T., Jones, C., McDonald, R., McLaren, A., et al.: The HadGEM2 family of met office unified model climate configurations, Geosci. Model. Dev. Discuss., 4, 765–841, 2011.

Martin, G. M., Milton, S. F., Senior, C. A., Brooks, M. E., Ineson, S., Reichler, T., and Kim, J.: Analysis and Reduction of Systematic Errors through a Seamless Approach to Modeling Weather and Climate, J. Climate, 23, 5933–5957, doi:10.1175/2010JCLI3541.1, 2010.

Martineu, C., Caneill, J.-Y., and Sadourny, R.: Potential Predictability of European Winters from the Analysis of Seasonal Simulations with an AGCM., J. Climate, 12, 3033–3061, doi:10.1175/1520-0442(1999)012<3033:PPOEWF>2.0.CO;2, 1999.

Mathieu, P.-P., Sutton, R. T., Dong, B., and Collins, M.: Predictability of Winter Climate over the North Atlantic European Region during ENSO Events., J. Climate, 17, 1953–1974, doi:10.1175/1520-0442(2004)017<1953:POWCOT>2.0.CO;2, 2004.

Matsuno, T.: Quasi-geostrophic motions in the equatorial area, J. Meteor. Soc. Japan, 44, 25–43, 1966.

Matsuura, K. and Willmott, C.-J.: Terrestrial Precipitation: 1900–2008 Gridded Monthly Time Series version 2.01, 2009.

McGuffie, K. and Henderson-Sellers, A.: A climate modelling primer, pp. 213–248, John Wiley & Sons, doi:10.1002/0470857617.ch6, 2005.

McPhaden, M. J., Zebiak, S. E., and Glantz, M. H.: ENSO as an Integrating Concept in Earth Science, Science, 314, 1740–, doi:10.1126/science.1132588, 2006.

Medhaug, I. and Furevik, T.: North Atlantic 20th century multidecadal variability in coupled climate models: sea surface temperature and ocean overturning circulation, Ocean Sci., 7, 389–404, doi:10.5194/os-7-389-2011, 2011.

Meehl, G. A. and Hu, A.: Megadroughts in the Indian Monsoon Region and Southwest North America and a Mechanism for Associated Multidecadal Pacific Sea Surface Temperature Anomalies, J. Climate, 19, 1605, doi:10.1175/JCLI3675.1, 2006.

Meehl, G. A., Hibbard, K., Committee, W. S., et al.: Summary Report: A Strategy for Climate Change Stabilization Experiments with AOGCMs and ESMs: Aspen Global Change Institute 2006 Session, Earth System Models: the Next Generation (Aspen, Colorado, July 30-August 5, 2006), World Climate Research Programme, 2007.

Meehl, G. A., Goddard, L., Murphy, J., Stouffer, R. J., Boer, G., Danabasoglu, G., Dixon, K., Giorgetta, M. A., Greene, A. M., Hawkins, E., et al.: Decadal prediction: can it be skilful?, 90, 1467–1485, doi:10.1175/2009BAMS2778.1, 2009.

Meehl, G. A., Hu, A., and Santer, B. D.: The Mid-1970s Climate Shift in the Pacific and the Relative Roles of Forced versus Inherent Decadal Variability, J. Climate, 22, 780, doi:10.1175/2008JCLI2552.1, 2009.

Mehta, V. M., Suarez, M. J., Manganello, J. V., and Delworth, T. L.: Oceanic influence on the North Atlantic Oscillation and associated northern hemisphere climate variations: 1959-1993, Geophys. Res. Lett., 27, 121–124, doi:10.1029/1999GL002381, 2000.

Meng, Q., Latif, M., Park, W., Keenlyside, N. S., Semenov, V. A., and Martin, T.: Twentieth century Walker Circulation change: data analysis and model experiments, Clim. Dyn., 38, 1757–1773, doi:10.1007/s00382-011-1047-8, 2012.

Merkel, U. and Latif, M.: A high resolution AGCM study of the El Niño impact on the North Atlantic/European sector, Geophys. Res. Lett., 29, 1291, doi:10.1029/2001GL013726, 2002.

Michelangeli, P.-A., Vautard, R., and Legras, B.: Weather Regimes: Recurrence and Quasi Stationarity., J. Atmos. Sci., 52, 1237–1256, doi:10.1175/1520-0469(1995)052<1237:WRRAQS>2.0.CO;2, 1995.

Miller, A. J., Cayan, D. R., Barnett, T. P., Graham, N. E., and Oberhuber, J. M.: Interdecadal variability of the Pacific Ocean: model response to observed heat flux and wind stress anomalies, Clim. Dyn., 9, 287–302, doi:10.1007/BF00204744, 1994.

Minobe, S.: A 50-70 year climatic oscillation over the North Pacific and North America, Geophys. Res. Lett., 24, 683–686, doi:10.1029/97GL00504, 1997.

Mo, K. C. and Livezey, R. E.: Tropical-Extratropical Geopotential Height Teleconnections during the Northern Hemisphere Winter, Mon. Wea. Rev., 114, 2488, doi:10.1175/1520-0493(1986)114<2488:TEGHTD>2.0.CO;2, 1986.

Moron, V. and Gouirand, I.: Seasonal modulation of the El Niño-southern oscillation relationship with sea level pressure anomalies over the North Atlantic in October-March 1873-1996, Int. J. Climatol., 23, 143–155, doi:10.1002/joc.868, 2003.

Moron, V. and Plaut, G.: The impact of El Niño-southern oscillation upon weather regimes over Europe and the North Atlantic during boreal winter, Int. J. Climatol., 23, 363–379, doi:10.1002/joc.890, 2003.

Moron, V., Robertson, A. W., Ward, M. N., and Ndiaye, O.: Weather Types and Rainfall over Senegal. Part I: Observational Analysis, J. Climate, 21, 266, doi:10.1175/2007JCLI1601.1, 2008.

Murphy, J. M., Sexton, D. M. H., Barnett, D. N., Jones, G. S., Webb, M. J., Collins, M., and Stainforth, D. A.: Quantification of modelling uncertainties in a large ensemble of climate change simulations, Nature, 430, 768–772, doi:10.1038/nature02771, 2004.

Nitta, T. and Yamada, S.: Recent Warming of Tropical Sea Surface Temperature and Its Relationship to the Northern Hemisphere Circulation, J. Meteorol. Soc. Jpn., 67, 375–383, 1989.

North, G. R., Bell, T. L., Cahalan, R. F., and Moeng, F. J.: Sampling Errors in the Estimation of Empirical Orthogonal Functions, Mon. Wea. Rev., 110, 699, doi:10.1175/1520-0493(1982)110<0699:SEITEO>2.0.CO;2, 1982.

Ohba, M., Nohara, D., and Ueda, H.: Simulation of Asymmetric ENSO Transition in WCRP CMIP3 Multimodel Experiments, J. Climate, 23, 6051–6067, doi:10.1175/2010JCLI3608.1, 2010.

Okumura, Y. M. and Deser, C.: Asymmetry in the Duration of El Niño and La Niña, J. Climate, 23, 5826–5843, doi:10.1175/2010JCLI3592.1, 2010.

Palmer, T. N.: Extended-Range Atmospheric Prediction and the Lorenz Model, Bull. Amer. Meteor. Soc., 74, 49–66, doi:10.1175/1520-0477(1993)074<0049:ERAPAT>2.0.CO;2, 1993.

Pearson, K.: On lines and planes of closest fit to systems of points in space, Philos. Mag., 2, 559–572, 1901.

Peixoto, J. P. and Oort, A. H.: Physics of climate, American institute of physics, New York, 1992.

Peng, S. and Whitaker, J. S.: Mechanisms Determining the Atmospheric Response to Midlatitude SST Anomalies., J. Climate, 12, 1393–1408, doi:10.1175/1520-0442(1999)012<1393:MDTART>2.0.CO;2, 1999.

Philander, S. G., Holton, J. R., and Dmowska, R.: El Niño, La Niña, and the southern oscillation, vol. 46, Academic press, 1989.

Philip, S. and van Oldenborgh, G. J.: Significant Atmospheric Nonlinearities in the ENSO Cycle, J. Climate, 22, 4014, doi:10.1175/2009JCLI2716.1, 2009.

Pinto, J. G. and Raible, C. C.: Past and recent changes in the North Atlantic oscillation, WIREs Clim. Change, 3, 79–90, 2012.

Pinto, J. G., Reyers, M., and Ulbrich, U.: The variable link between PNA and NAO in observations and in multi-century CGCM simulations, Clim. Dyn., 36, 337–354, doi:10.1007/s00382-010-0770-x, 2011.

Pohlmann, H. and Latif, M.: Atlantic versus Indo-Pacific influence on Atlantic-European climate, Geophys. Res. Lett., 32, L05707, doi:10.1029/2004GL021316, 2005.

Polo, I., Ullmann, A., Roucou, P., and Fontaine, B.: Weather regimes in the Euro-Atlantic and Mediterranean sector, and relationship with West African rainfall over the 1989-2008 period from a self-organizing maps approach, J. Climate, 24, 3423–3432, 2011.

Pozo-Vázquez, D., Esteban-Parra, M. J., Rodrigo, F. S., and Castro-Díez, Y.: An analysis of the variability of the North Atlantic Oscillation in the time and the frequency domains, Int. J. Climatol., 20, 1675–1692, doi:10.1002/1097-0088(20001130)20:14<1675::AID-JOC564>3.3.CO;2-3, 2000.

Pozo-Vázquez, D., Esteban-Parra, M. J., Rodrigo, F. S., and Castro-Díez, Y.: A study of NAO variability and its possible non-linear influences on European surface temperature, Clim. Dyn., 17, 701–715, doi:10.1007/s003820000137, 2001a.

Pozo-Vázquez, D., Esteban-Parra, M. J., Rodrigo, F. S., and Castro-Díez, Y.: The Association between ENSO and Winter Atmospheric Circulation and Temperature in the North Atlantic Region., J. Climate, 14, 3408–3420, doi:10.1175/1520-0442(2001)014<3408:TABEAW>2.0.CO;2, 2001b.

Pozo-Vázquez, D., Gámiz-Fortis, S. R., Tovar-Pescador, J., Esteban-Parra, M. J., and Castro-Díez, Y.: El Niño-southern oscillation events and associated European winter precipitation anomalies, Int. J. Climatol., 25, 17–31, doi:10.1002/joc.1097, 2005a.

Pozo-Vázquez, D., Gámiz-Fortis, S. R., Tovar-Pescador, J., Esteban-Parra, M. J., and Castro-Díez, Y.: North Atlantic Winter SLP Anomalies Based on the Autumn ENSO State., J. Climate, 18, 97–103, doi:10.1175/JCLI-3210.1, 2005b.

Qin, J. and Robinson, W. A.: On the Rossby Wave Source and the Steady Linear Response to Tropical Forcing., J. Atmos. Sci., 50, 1819–1823, doi:10.1175/1520-0469(1993)050<1819:OTRWSA>2.0.CO;2, 1993.

Quadrelli, R. and Wallace, J. M.: Dependence of the structure of the Northern Hemisphere annular mode on the polarity of ENSO, Geophys. Res. Lett., 29, 2132, doi:10.1029/2002GL015807, 2002.

Quan, X., Hoerling, M., Whitaker, J., Bates, G., and Xu, T.: Diagnosing Sources of U.S. Seasonal Forecast Skill, J. Climate, 19, 3279, doi:10.1175/JCLI3789.1, 2006.

Raible, C., Luksch, U., and Fraedrich, K.: Precipitation and Northern Hemisphere regimes, Atmos. Sci. Lett., 5, 43–55, doi:10.1016/j.atmoscilet.2003.12.001, 2004.

Raible, C. C., Luksch, U., Fraedrich, K., and Voss, R.: North Atlantic decadal regimes in a coupled GCM simulation, Clim. Dyn., 18, 321–330, doi:10.1007/s003820100176, 2001.

Rayner, N. A., Parker, D. E., Horton, E. B., Folland, C. K., Alexander, L. V., Rowell, D. P., Kent, E. C., and Kaplan, A.: Global analyses of sea surface temperature, sea ice, and night marine air temperature since the late nineteenth century, J. Geophys. Res. Atmos., 108, 4407, doi:10.1029/2002JD002670, 2003.

Reverdin, G.: North Atlantic Subpolar Gyre Surface Variability (1895-2009), J. Climate, 23, 4571–4584, doi:10.1175/2010JCLI3493.1, 2010.

Rodó, X., Baert, E., and Comín, F. A.: Variations in seasonal rainfall in Southern Europe during the present century: relationships with the North Atlantic Oscillation and the El Niño-Southern Oscillation, Clim. Dyn., 13, 275–284, doi:10.1007/s003820050165, 1997.

Rodríguez-Fonseca, B.: Relació entre el Régimen de precipitación anómalo en la Península Ibérica y la variabilidad de baja frecuencia del sistema climático en el Atlántico Norte, 2001.

Rodríguez-Fonseca, B. and de Castro, M.: On the connection between winter anomalous precipitation in the Iberian Peninsula and North West Africa and the summer subtropical Atlantic sea surface temperature, Geophys. Res. Lett., 29, 10–1, 2002.

Rodríguez-Fonseca, B. and Serrano, E.: Winter 10-day coupled patterns between geopotential height and Iberian Peninsula rainfall using the ECMWF precipitation reanalysis, J. Climate, 15, 1309–1321, 2002.

Rodríguez-Fonseca, B., Polo, I., Serrano, E., and Castro, M.: Evaluation of the North Atlantic SST forcing on the European and Northern African winter climate, Int. J. Climatol., 26, 179–191, doi:10.1002/joc.1234, 2006.

Rodwell, M. and Folland, C.: Atlantic air sea interaction and seasonal predictability, Quart. J. Roy. Meteor. Soc., 128, 1413–1443, doi:10.1256/00359000260247291, 2002.

Rodwell, M. J., Rowell, D. P., and Folland, C. K.: Oceanic forcing of the wintertime North Atlantic Oscillation and European climate, Nature, 398, 320–323, doi:10.1038/18648, 1999.

Rogers, J. C.: North Atlantic Storm Track Variability and Its Association to the North Atlantic Oscillation and Climate Variability of Northern Europe., J. Climate, 10, 1635–1647, doi:10.1175/1520-0442(1997)010<1635:NASTVA>2.0.CO;2, 1997.

Ropelewski, C. F. and Halpert, M. S.: Global and Regional Scale Precipitation Patterns Associated with the El Niño/Southern Oscillation, Mon. Wea. Rev., 115, 1606, doi:10.1175/1520-0493(1987)115<1606:GARSPP>2.0.CO;2, 1987.

Ropelewski, C. F. and Halpert, M. S.: Precipitation Patterns Associated with the High Index Phase of the Southern Oscillation., J. Climate, 2, 268–284, doi:10.1175/1520-0442(1989)002<0268:PPAWTH>2.0.CO;2, 1989.

Rotstayn, L. D., Collier, M. A., Dix, M. R., Feng, Y., Gordon, H. B., O'Farrell, S. P., Smith, I. N., and Syktus, J.: Improved simulation of Australian climate and ENSO-related rainfall variability in a global climate model with an interactive aerosol treatment, Int. J. Climatol., 30, 1067–1088, 2010.

Rowell, D. P.: Assessing potential seasonal predictability with an ensemble of multidecadal GCM simulations, J. Climate, 11, 109–120, 1998.

Ruiz-Barradas, A., Carton, J. A., and Nigam, S.: Role of the Atmosphere in Climate Variability of the Tropical Atlantic., J. Climate, 16, 2052–2065, doi:10.1175/1520-0442(2003)016<2052:ROTAIC>2.0.CO;2, 2003.

Sakamoto, T., Komuro, Y., Nishimura, T., Ishii, M., Tatebe, H., Shiogama, H., Hasegawa, A., Toyoda, T., Mori, M., Suzuki, T., et al.: MIROC4h—a new high-resolution atmosphere-ocean coupled general circulation model, J. Meteorol. Soc. Jpn., 90, 325–359, 2012.

Sanchez-Gomez, E., Alvarez Garcia, F., and Ortiz Bevia, M. J.: Empirical forecasts of 850 hPa air temperature anomalies over the North Atlantic, Quart. J. Roy. Meteor. Soc., 127, 2761–2786, doi:10.1256/smsqj.57812, 2001.

Santos, J. A., Corte-Real, J., and Leite, S. M.: Weather regimes and their connection to the winter rainfall in Portugal, Int. J. Climatol., 25, 33–50, doi:10.1002/joc.1101, 2005.

Sardeshmukh, P. D. and Hoskins, B. J.: Vorticity balances in the tropics during the 1982-83 El Niño-Southern Oscillation event, Quart. J. Roy. Meteor. Soc., 111, 261–278, doi:10.1002/qj.49711146802, 1985.

Sardeshmukh, P. D. and Hoskins, B. J.: On the derivation of the divergent flow from the rotational flow: the χ problem, Quart. J. Roy. Meteor. Soc., 113, 339–360, doi:10.1002/qj.49711347519, 1987.

Sardeshmukh, P. D. and Hoskins, B. J.: The Generation of Global Rotational Flow by Steady Idealized Tropical Divergence., J. Atmos. Sci., 45, 1228–1251, doi:10.1175/1520-0469(1988)045<1228:TGOGRF>2.0.CO;2, 1988.

Schmidt, G. A., Kelley, M., Nazarenko, L., Ruedy, R., Russell, G. L., Aleinov, I., Bauer, M., Bauer, S. E., Bhat, M. K., Bleck, R., et al.: Configuration and assessment of the GISS ModelE2 contributions to the CMIP5 archive, J. Adv. Model. Earth Sy., 6, 141–184, 2014.

Schneider, U., Fuchs, T., Meyer-Christoffer, A., and Rudolf, B.: Global precipitation analysis products of the GPCC, Global Precipitation Climatology Centre (GPCC), DWD, Internet Publication, pp. 1–12, 2008.

Shaman, J.: The Seasonal Effects of ENSO on Atmospheric Conditions Associated with European Precipitation: Model Simulations of Seasonal Teleconnections, J. Climate, 27, 1010 – 1028, doi:10.1175/JCLI-D-12-00734.1, 2014.

Shindell, D. T., Schmidt, G. A., Mann, M. E., Rind, D., and Waple, A.: Solar Forcing of Regional Climate Change During the Maunder Minimum, Science, 294, 2149–2152, doi:10.1126/science.1064363, 2001.

Slingo, J. M. and Annamalai, H.: 1997: The El Niño of the Century and the Response of the Indian Summer Monsoon, Mon. Wea. Rev., 128, 1778, doi:10.1175/1520-0493(2000)128<1778:TENOOT>2.0.CO;2, 2000.

Smith, S.: The Scientist and Engineer's Guide to Digital Signal Processing, California Technical Pub., 1997.

Smith, T. M., Reynolds, R. W., Peterson, T. C., and Lawrimore, J.: Improvements to NOAA's Historical Merged Land Ocean Surface Temperature Analysis (1880 2006), J. Climate, 21, 2283, doi:10.1175/2007JCLI2100.1, 2008.

Solomon, S.: Climate change 2007-the physical science basis: Working group I contribution to the fourth assessment report of the IPCC, vol. 4, Cambridge University Press, 2007.

Steffen, K., Box, J., and Abdalati, W.: Greenland climate network: GC-Net, US Army Cold Regions Reattach and Engineering (CRREL), CRREL Special Report, pp. 98–103, 1996.

Stephens, J. and Johnson, K.: Rotational and divergent wind potentials, Mon. Wea. Rev., 106, 1452–1457, 1978.

Stephenson, D. B., Pavan, V., and Bojariu, R.: Is the North Atlantic Oscillation a random walk?, Int. J. Climatol., 20, 1–18, doi:10.1002/(SICI)1097-0088(200001)20:1<1::AID-JOC456>3.3.CO;2-G, 2000.

Sterl, A., van Oldenborgh, G. J., Hazeleger, W., and Burgers, G.: On the robustness of ENSO teleconnections, Clim. Dyn., 29, 469–485, 2007.

Suárez-Moreno, R. and Rodríguez-Fonseca, B.: $S4CASTv2.0$: sea surface temperature based statistical seasonal forecast model, Geosci. Model. Dev. Discuss., 8, 3971–4018, doi:10.5194/gmdd-8-3971-2015, 2015.

Sung, M.-K., Ham, Y.-G., Kug, J.-S., and An, S.-I.: An alterative effect by the tropical North Atlantic SST in intraseasonally varying El Nino teleconnection over the North Atlantic, Tellus, 65, 2013.

Sutton, R. T. and Hodson, D. L. R.: Influence of the Ocean on North Atlantic Climate Variability 1871-1999., J. Climate, 16, 3296–3313, doi:10.1175/1520-0442(2003)016<3296:IOTOON>2.0.CO;2, 2003.

Sutton, R. T. and Hodson, D. L. R.: Atlantic Ocean Forcing of North American and European Summer Climate, Science, 309, 115–118, doi:10.1126/science.1109496, 2005.

Sutton, R. T. and Hodson, D. L. R.: Climate Response to Basin-Scale Warming and Cooling of the North Atlantic Ocean, J. Climate, 20, 891, doi:10.1175/JCLI4038.1, 2007.

Swarztrauber, P. and Sweet, R.: Efficient FORTRAN subprograms for the solution of elliptic partial differential equations, National Center for Atmospheric Research Boulder, Colorado, 1975.

Takaya, K. and Nakamura, H.: A Formulation of a Phase-Independent Wave-Activity Flux for Stationary and Migratory Quasigeostrophic Eddies on a Zonally Varying Basic Flow., J. Atmos. Sci., 58, 608–627, doi:10.1175/1520-0469(2001)058<0608:AFOAPI>2.0.CO;2, 2001.

Taylor, K. E., Stouffer, R. J., and Meehl, G. A.: An Overview of CMIP5 and the Experiment Design, Bull. Amer. Meteor. Soc., 93, 485–498, doi:10.1175/BAMS-D-11-00094.1, 2012.

Thompson, D. W. J. and Wallace, J. M.: The Arctic oscillation signature in the wintertime geopotential height and temperature fields, Geophys. Res. Lett., 25, 1297–1300, doi:10.1029/98GL00950, 1998.

Thompson, D. W. J., Lee, S., and Baldwin, M. P.: Atmospheric processes governing the Northern Hemisphere annular mode/North Atlantic Oscillation, AGU Geophysical Monograph Series, 134, 81–112, doi:10.1029/134GM05, 2003.

Ting, M. and Sardeshmukh, P. D.: Factors Determining the Extratropical Response to Equatorial Diabatic Heating Anomalies., J. Atmos. Sci., 50, 907–918, doi:10.1175/1520-0469(1993)050<0907:FDTERT>2.0.CO;2, 1993.

Ting, M., Hoerling, M. P., Xu, T., and Kumar, A.: Northern Hemisphere Teleconnection Patterns during Extreme Phases of the Zonal-Mean Circulation., J. Climate, 9, 2614–2640, doi:10.1175/1520-0442(1996)009<2614:NHTPDE>2.0.CO;2, 1996.

Toniazzo, T. and Scaife, A.: The influence of ENSO on winter North Atlantic climate, Geophys. Res. Lett., 33, L24704, doi:10.1029/2006GL027881, 2006.

Torrence, C. and Webster, P. J.: The annual cycle of persistence in the El Nño/Southern Oscillation, Quart. J. Roy. Meteor. Soc., 124, 1985–2004, doi:10.1002/qj.49712455010, 1998.

Tourre, Y. M., Rajagopalan, B., Kushnir, Y., Barlow, M., and White, W. B.: Patterns of coherent decadal and interdecadal climate signals in the Pacific Basin during the 20^{th} century, Geophys. Res. Lett., 28, 2069–2072, doi:10.1029/2000GL012780, 2001.

Trenberth, K. E.: Recent Observed Interdecadal Climate Changes in the Northern Hemisphere., Bull. Amer. Meteor. Soc., 71, 988–993, doi:10.1175/1520-0477(1990)071<0988:ROICCI>2.0.CO;2, 1990.

Trenberth, K. E.: The Definition of El Niño., Bull. Amer. Meteor. Soc., 78, 2771–2777, doi:10.1175/1520-0477(1997)078<2771:TDOENO>2.0.CO;2, 1997.

Trenberth, K. E. and Caron, J. M.: Estimates of Meridional Atmosphere and Ocean Heat Transports., J. Climate, 14, 3433–3443, doi:10.1175/1520-0442(2001)014<3433:EOMAAO>2.0.CO;2, 2001.

Trenberth, K. E. and Paolino, D. A.: The Northern Hemisphere Sea-Level Pressure Data Set: Trends, Errors and Discontinuities, Mon. Wea. Rev., 108, 855, doi:10.1175/1520-0493(1980)108<0855:TNHSLP>2.0.CO;2, 1980.

Trenberth, K. E. and Shea, D. J.: Atlantic hurricanes and natural variability in 2005, Geophys. Res. Lett., 33, L12704, doi:10.1029/2006GL026894, 2006.

Trenberth, K. E. and Stepaniak, D. P.: LETTERS: Indices of El Niño Evolution., J. Climate, 14, 1697–1701, doi:10.1175/1520-0442(2001)014<1697:LIOENO>2.0.CO;2, 2001.

Trenberth, K. E., Branstator, G. W., Karoly, D., Kumar, A., Lau, N.-C., and Ropelewski, C.: Progress during TOGA in understanding and modeling global teleconnections associated with tropical sea surface temperatures, J. Geophys. Res., 103, 14 291, doi:10.1029/97JC01444, 1998.

Trigo, R. M., Pozo-Vázquez, D., Osborn, T. J., Castro-Díez, Y., Gámiz-Fortis, S., and Esteban-Parra, M. J.: North Atlantic oscillation influence on precipitation, river flow and water resources in the Iberian Peninsula, Int. J. Climatol., 24, 925–944, doi:10.1002/joc.1048, 2004.

Van Loon, H. and Rogers, J. C.: The Seesaw in Winter Temperatures between Greenland and Northern Europe. Part I: General Description, Mon. Wea. Rev., 106, 296, doi:10.1175/1520-0493(1978)106<0296:TSIWTB>2.0.CO;2, 1978.

Van Oldenborgh, G. J.: Comments on Predictability of Winter Climate over the North Atlantic European Region during ENSO Events, J. Climate, 18, 2770–2772, doi:10.1175/JCLI3441.1, 2005.

Van Oldenborgh, G. J. and Burgers, G.: Searching for decadal variations in ENSO precipitation teleconnections, Geophys. Res. Lett., 32, L15701, doi:10.1029/2005GL023110, 2005.

Van Oldenborgh, G. J., Burgers, G., and Klein Tank, A.: On the El Niño teleconnection to spring precipitation in Europe, Int. J. Climatol., 20, 565–574, doi:10.1002/(SICI)1097-0088(200004)20:5<565::AID-JOC488>3.3.CO;2-X, 2000.

Venegas, S. A.: Statistical methods for signal detection in climate, Danish Center for Earth System Science Report, 2, 96, 2001.

Verdon, D. C. and Franks, S. W.: Long-term behaviour of ENSO: Interactions with the PDO over the past 400 years inferred from paleoclimate records, Geophys. Res. Lett., 33, L06712, doi:10.1029/2005GL025052, 2006.

Vicente-Serrano, S. M. and López-Moreno, J. I.: Nonstationary influence of the North Atlantic Oscillation on European precipitation, J. Geophys. Res. Atmos., 113, D20120, doi:10.1029/2008JD010382, 2008.

Villamayor, J. and Mohino, E.: Robust Sahel drought due to the Interdecadal Pacific Oscillation in CMIP5 simulations, Geophys. Res. Lett., 42, 1214–1222, doi:10.1002/2014GL062473, 2015.

Visbeck, M., Chassignet, E. P., Curry, R. G., Delworth, T. L., Dickson, R. R., and Krahmann, G.: The ocean's response to North Atlantic Oscillation variability, AGU Geophysical Monograph Series, 134, 113–145, doi:10.1029/134GM06, 2003.

Voldoire, A., Sanchez-Gomez, E., Salas y Mélia, D., Decharme, B., Cassou, C., Sénési, S., Valcke, S., Beau, I., Alias, A., Chevallier, M., Déqué, M., Deshayes, J., Douville, H., Fernandez, E., Madec, G., Maisonnave, E., Moine, M.-P., Planton, S., Saint-Martin, D., Szopa, S., Tyteca, S., Alkama, R., Belamari, S., Braun, A., Coquart, L., and Chauvin, F.: The CNRM-CM5.1 global climate model: description and basic evaluation, Clim. Dyn., 40, 2091–2121, doi:10.1007/s00382-011-1259-y, 2013.

Volodin, E., Dianskii, N., and Gusev, A.: Simulating present-day climate with the INMCM4. 0 coupled model of the atmospheric and oceanic general circulations, Izv. Atmos. Ocean Phy., 46, 414–431, 2010.

Von Storch, H. and Zwiers, F. W.: Statistical analysis in climate research, Cambridge university press, 2001.

Walker, G. T.: Correlation in Seasonal Variations of WEATHER:A Preliminary Study of World WEATHER, Mon. Wea. Rev., 24, 75–131, 1925a.

Walker, G. T.: Correlation in Seasonal Variations of WEATHER:A Further Study of World WEATHER, Mon. Wea. Rev., 53, 275–332, 1925b.

Walker, S. G. T. and Bliss, E.: World weather, III, Edward Stanford, 1928.

Wallace, J. M. and Gutzler, D. S.: Teleconnections in the Geopotential Height Field during the Northern Hemisphere Winter, Mon. Wea. Rev., 109, 784, doi:10.1175/1520-0493(1981)109<0784:TITGHF>2.0.CO;2, 1981.

Wallace, J. M. and Thompson, D. W. J.: The Pacific Center of Action of the Northern Hemisphere Annular Mode: Real or Artifact?., J. Climate, 15, 1987–1991, doi:10.1175/1520-0442(2002)015<1987:TPCOAO>2.0.CO;2, 2002.

Wang, B.: Interdecadal Changes in El Niño Onset in the Last Four Decades., J. Climate, 8, 267–285, doi:10.1175/1520-0442(1995)008<0267:ICIENO>2.0.CO;2, 1995.

Wang, B. and An, S. I.: A mechanism for decadal changes of ENSO behavior: roles of background wind changes, Clim. Dyn., 18, 475–486, doi:10.1007/s00382-001-0189-5, 2002.

Wang, C.: Atlantic Climate Variability and Its Associated Atmospheric Circulation Cells., J. Climate, 15, 1516–1536, doi:10.1175/1520-0442(2002)015<1516:ACVAIA>2.0.CO;2, 2002a.

Wang, C.: Atmospheric Circulation Cells Associated with the El Niño-Southern Oscillation., J. Climate, 15, 399–419, doi:10.1175/1520-0442(2002)015<0399:ACCAWT>2.0.CO;2, 2002b.

Wang, C.: ENSO, Atlantic climate variability, and the Walker and Hadley circulations, in: The Hadley circulation: Present, past and future, pp. 173–202, Springer, 2004.

Wang, C. and Picaut, J.: Understanding ENSO physics: a review, AGU Geophysical Monograph Series, 147, 21–48, doi:10.1029/147GM02, 2004.

Warn, T. and Warn, H.: The evolution of a nonlinear critical level, Stud. Apply. Math., 59, 37–71, doi:10.1002/sapm197859137, 1978.

Washington, W. M. and Meehl, G. A.: Seasonal Cycle Experiment on the Climate Sensitivity Due to a Doubling of CO_2 with an atmospheric general circulation model coupled to a simple mixed-layer ocean model, J. Geophys. Res., 89, 9475–9503, doi:10.1029/JD089iD06p09475, 1984.

Watanabe, M.: Asian Jet Waveguide and a Downstream Extension of the North Atlantic Oscillation., J. Climate, 17, 4674–4691, doi:10.1175/JCLI-3228.1, 2004.

Watanabe, M., Suzuki, T., O'ishi, R., Komuro, Y., Watanabe, S., Emori, S., Takemura, T., Chikira, M., Ogura, T., Sekiguchi, M., et al.: Improved climate simulation by MIROC5: mean states, variability, and climate sensitivity, J. Climate, 23, 6312–6335, 2010.

Watanabe, S., Hajima, T., Sudo, K., Nagashima, T., Takemura, T., Okajima, H., Nozawa, T., Kawase, H., Abe, M., Yokohata, T., et al.: MIROC-ESM: model description and basic results of CMIP5-20c3m experiments, Geosci. Model Dev. Discuss, 4, 1063–1128, doi:10.5194/gmd-4-845-2011, 2011.

Weare, B. C. and Nasstrom, J. S.: Examples of extended empirical orthogonal function analyses, Mon. Wea. Rev., 110, 481–485, doi:10.1175/1520-0493(1982)110<0481:EOEEOF>2.0.CO;2, 1982.

Webber, S. and Willmott, C.: South American precipitation: 1960-1990 gridded monthly time series (Version 1.02), Center for Climatic Research, Dept. of Geography, Univ. of Delaware, 1998.

Wei, W. and Lohmann, G.: Simulated Atlantic Multidecadal Oscillation during the Holocene, J. Climate, 25, 6989–7002, doi:10.1175/JCLI-D-11-00667.1, 2012.

Wilks, D. S.: Statistical methods in the atmospheric sciences, vol. 100, Academic press, 2011.

Woollings, T., Czuchnicki, C., and Franzke, C.: Twentieth century North Atlantic jet variability, Quart. J. Roy. Meteor. Soc., 140, 783–791, doi:10.1002/qj.2197, 2014.

Wright, P. B.: Relationships between Indices of the Southern Oscillation, Mon. Wea. Rev., 112, 1913, doi:10.1175/1520-0493(1984)112<1913:RBIOTS>2.0.CO;2, 1984.

Wu, A. and Hsieh, W. W.: The nonlinear association between ENSO and the Euro-Atlantic winter sea level pressure, Clim. Dyn., 23, 859–868, doi:10.1007/s00382-004-0470-5, 2004.

Xiao-Ge, X., Tong-Wen, W., and Jie, Z.: Introduction of CMIP5 experiments carried out with the climate system models of Beijing Climate Center, Adv. Climate Change Res., 4, 41–49, doi:10.3724/SP.J.1248.2013.041, 2013.

Xie, P. and Arkin, P. A.: Global Precipitation: A 17-Year Monthly Analysis Based on Gauge Observations, Satellite Estimates, and Numerical Model Outputs., Bull. Amer. Meteor. Soc., 78, 2539–2558, doi:10.1175/1520-0477(1997)078<2539:GPAYMA>2.0.CO;2, 1997.

Xoplaki, E., González-Rouco, J., Gyalistras, D., Luterbacher, J., Rickli, R., and Wanner, H.: Interannual summer air temperature variability over Greece and its connection to the large-scale atmospheric circulation and Mediterranean SSTs 1950–1999, Clim. Dyn., 20, 537–554, doi:10.1007/s00382-002-0291-3, 2003.

Yang, X., Rosati, A., Zhang, S., Delworth, T. L., Gudgel, R. G., Zhang, R., Vecchi, G., Anderson, W., Chang, Y.-S., DelSole, T., Dixon, K., Msadek, R., Stern, W. F., Wittenberg, A., and Zeng, F.: A Predictable AMO-Like Pattern in the GFDL Fully Coupled Ensemble Initialization and Decadal Forecasting System, J. Climate, 26, 650–661, doi:10.1175/JCLI-D-12-00231.1, 2013.

Yeh, S.-W., Kug, J.-S., Dewitte, B., Kwon, M.-H., Kirtman, B. P., and Jin, F.-F.: El Niño in a changing climate, Nature, 461, 511–514, doi:10.1038/nature08316, 2009.

Yeh, S.-W., Kirtman, B. P., Kug, J.-S., Park, W., and Latif, M.: Natural variability of the central Pacific El Niño event on multi-centennial timescales, Geophys. Res. Lett., 38, L02704, doi:10.1029/2010GL045886, 2011.

Yukimoto, S.: Meteorological research institute earth system model version 1 (MRI-ESM1): model description, doi:10.11483/mritechrepo.64, 2011.

Zanchettin, D., Franks, S. W., Traverso, P., and Tomasino, M.: On ENSO impacts on European wintertime rainfalls and their modulation by the NAO and the Pacific multi-decadal variability described through the PDO index, Int. J. Climatol., 28, 995–1006, doi:10.1002/joc.1601, 2008.

Zhang, L., Wang, C., and Wu, L.: Low-frequency modulation of the Atlantic warm pool by the Atlantic multidecadal oscillation, Clim. Dyn., 39, 1661–1671, doi:10.1007/s00382-011-1257-0, 2012.

Zhang, R. and Delworth, T. L.: Impact of Atlantic multidecadal oscillations on India/Sahel rainfall and Atlantic hurricanes, Geophys. Res. Lett., 33, L17712, doi:10.1029/2006GL026267, 2006.

Zhang, R., Delworth, T. L., Sutton, R., Hodson, D. L. R., Dixon, K. W., Held, I. M., Kushnir, Y., Marshall, J., Ming, Y., Msadek, R., Robson, J., Rosati, A. J., Ting, M., and Vecchi, G. A.: Have Aerosols Caused the Observed Atlantic Multidecadal Variability?, J. Atmos. Sci., 70, 1135–1144, doi:10.1175/JAS-D-12-0331.1, 2013.

Zhang, Y., Wallace, J. M., and Battisti, D. S.: ENSO-like Interdecadal Variability: 1900-93., J. Climate, 10, 1004–1020, doi:10.1175/1520-0442(1997)010<1004:ELIV>2.0.CO;2, 1997.